U. S. DEPARTMENT OF COMMERCE
Charles Sawyer, Secretary
NATIONAL BUREAU OF STANDARDS
E. U. Condon, Director

OCTOBER 1948
VOLUME 41
NUMBER 4

JOURNAL OF RESEARCH

of the

NATIONAL BUREAU OF STANDARDS

Contents

RP		Page
1922.	Color perceptions of deuteranopic and protanopic observers. Deane B. Judd (Price 15 cents)	247
1923.	Electrode function (pH response) of the soda-silica glasses. Gerald F. Rynders, Oscar H. Grauer, and Donald Hubbard. (Price 10 cents)	273
1924.	Effect of temperature on the volume of leather and collagen. Charles E. Weir. (Price 10 cents)	279
1925.	Image shifts caused by rotating a constant-deviation prism in divergent light. James B. Saunders. (Price 10 cents)	287
1926.	Thimble-chamber calibration on soft X-rays. Frank H. Day. (Price 10 cents)	295
1927.	Sources of error in and calibration of the *f*-number of photographic lenses. Francis E. Washer. (Price 10 cents)	301
1928.	Mass spectrometric investigation of the thermal decomposition of polymers. Leo A. Wall. (Price 10 cents)	315
1929.	Purification, purity, and freezing points of 30 hydrocarbons of the API-Standard and API-NBS series. Anton J. Streiff, Janice C. Zimmerman, Laurel F. Soule, Marie T. Butt, Vincent A. Sedlak, Charles B. Willingham, and Frederick D. Rossini. (Price 20 cents)	323

For sale by the Superintendent of Documents, U. S. Government Printing Office, Washington 25, D. C. - Price 60 cents
$4.50 per year on subscription

UNITED STATES GOVERNMENT PRINTING OFFICE, WASHINGTON : 1948

U. S. Department of Commerce
National Bureau of Standards

Research Paper RP1922
Volume 41, October 1948

Part of the Journal of Research of the National Bureau of Standards

Color Perceptions of Deuteranopic and Protanopic Observers

By Deane B. Judd

It is well established that about 2 percent of otherwise normal human males are confusers of red and green from birth. There is considerable interest in the question: What do red-green confusers see? From a knowledge of the normal color perceptions corresponding to deuteranopic and protanopic red and green, we may not only understand better why color-blindness tests sometimes fail, and so be in a position to develop improved tests, but also the color-deficient observer may understand better the nature of his color-confusions and be aided to avoid their consequences. If an observer has trichromatic vision over a portion of his total retinal area, and dichromatic vision over another portion, he may give valid testimony regarding the color perceptions characteristic of the particular form of dichromatic vision possessed by him. Preeminent among such observers are those born with one normal eye and one dichromatic eye. A review of the rather considerable literature on this subject shows that the color perceptions of both protanopic and deuteranopic observers are confined to two hues, yellow and blue, closely like those perceived under usual conditions in the spectrum at 575 and 470 mμ, respectively, by normal observers. By combining this result with standard response functions recently derived (Bureau Research Paper RP1618) for protanopic and deuteranopic vision, it has been possible to give quantitative estimates of the color perceptions typical of these observers for the whole range of colors in the Munsell Book of Color. These estimates take the form of protanopic and deuteranopic Munsell notations, and by using them it is possible not only to arrange the Munsell papers in ways that presumably appear orderly to red-green confusing dichromats, but also to get immediately from the notations an accurate idea of the colors usually perceived in these arrangements by deuteranopes and protanopes, much as the ordinary Munsell notations serve to describe the visual color perceptions of a normal observer.

I. Introduction

The question, "What colors do color-blind observers confuse?" is a very practical one, capable of objective solution by putting each color-blind observer to trial and noting his mistakes. For the two most common forms of partially color-blind observers, deuteranopia and protanopia, each form comprising about 1 percent of the otherwise normal male population, a general answer, approximately valid for all observers properly so classed, has been found and described [51, 81].[1]

The question, "What colors do color-blind observers see?" is a more subtle one, involving a fine point in the theory of knowledge, yet of considerable practical importance, too. Strictly speaking, the subjective life of each observer cannot be known to anyone else, and there is no way of knowing whether the perception of red by one normal observer bears any resemblance to that which another normal observer calls by the same name. In this sense it is also impossible to discover what colors are seen by the partially color-blind. However, from the similarity in responses between normal observers, it is a fairly safe conclusion that their color perceptions are closely similar. In the same inductive sense, it is possible to discover how the color perceptions of the color-blind are related to those of the normal observer. It is one purpose of the present paper to review the evidence by which these are known. A second purpose is to give a comprehensive intertranslation between normal color perceptions of surface colors on the one hand and

[1] Figures in brackets indicate the literature references at the end of this paper.

protanopic and deuteranopic surface-color perceptions on the other.

The outstanding characteristic of protanopic and deuteranopic observers is that they confuse both red and green with gray, and indeed they confuse red with green. For this reason they are rightly called red-green confusers, less aptly red-green blind. Since to the normal eye red is nearly as distinct from green as black is from white, it may be deduced that red-green confusers fail to experience both the normal red and the normal green perception; but the deduction may not be pushed further. From a stimulus normally yielding red, a red-green confuser might perceive red or green or some other of the normal color perceptions, or some perception not normally experienced.

The impossibility of passing from knowledge of what colors are confused to knowledge of those that are seen by color-blind observers was recognized almost as soon as color-blindness was discovered. Thus we find Wilson [97] remarking in 1855, "It must be remembered, however, that there is no common language between the colour-blind and the colour-seeing." Then in 1880–81 Holmgren gave essentially the argument of the preceding two paragraphs in complete and clear detail and published it in four languages [39, 40, 42, 46]. Donders [15] in 1881 stated (p. 84), "If they (the color-blind) name their colors yellow and blue, this by no means proves that they see yellow and blue as we see them, but merely that in our yellow and blue their colors appear most characteristically." A year later v. Kries inserted the argument into his early analysis of visual sensations [60], "For bilateral color-blindness the facts are essentially different. Here is lacking the possibility of comparing directly normal and abnormal sensations with each other. The old statement that we cannot know what the color-blind really sense, self-explanatory as it is, appears, however, still not always to have been fully and completely understood."

These repeated and clear explanations did not, however, prevent Edridge-Green [19] in 1911 from giving a "proof" that red-green confusers see red and violet by means of precisely the same arguments previously used by Pole [82] to "prove" from observations with his own color-blind eyes that they see blue and yellow. These arguments are invalid in either case, as pointed out explicitly by Hartridge [27], but Pole's conjecture, for that is all it was, was corroborated by later valid evidence. After having convinced himself (on insufficient ground) that his sensations were the same as what normal observers call yellow and blue, Pole put forward in 1856 an original, very practical suggestion (Roy. Soc., p. 176; Phil. Mag., p. 285) now in widespread daily use, namely, "It has been thought that the use of these colors (red and green) for railway and ship signals becomes dangerous where color-blind persons have to observe them. This danger may be obviated by very simple means—if the green be made a *blue* green at the same time that the red is a *yellow* red, they become quite as distinct to the color-blind as to the normal eyed." Present color specifications for marine and railway signaling pair a red slightly on the yellow side with a nonyellowish green, and this choice is also prevalent for stop and go signals for highway traffic. This plan has also been extended only recently by the American Standards Association [52] to the marking of industrial hazards.

The practical importance of inquiring into the color perceptions, in addition to the color confusions, of partially color-blind observers lies in the fact that resolution of this question facilitates consideration of precautions against the dangers of color-blindness and also aids in the design of tests for its detection. Thus Pole made his useful suggestion only after he had made a fortunate conjecture as to the connection between his color vision and those of the normal eyed. By this assumption he supplied himself with a terminology that immediately suggested the kind of red and green safe for railway and ship signals. It is the third purpose of this paper to develop a method of expressing the color-perceptions of the average red-green confuser in terms that are immediately comprehensible both to those trained in the interpretation of colorimetric coordinate systems and to the untrained alike. It is expected that this method will assist both normal observers and red-green-confusing observers to understand the relation between their two systems and so aid in avoiding the undesirable consequences of red-green confusion.

II. Review of the Literature

It has been pointed out by Holmgren [42], by v. Kries [62], and doubtless by many others, that

persons born with one normal eye and one color-blind eye give us our most direct evidence of the color perceptions of the color-blind. Less reliable evidence may be obtained from persons who confuse red and green because of diseases of the eyes or optic nerves, and who are therefore familiar with normal colors through past experience before becoming afflicted. And, finally, some information may be obtained from the peripheral parts of the normal retina that respond with confusions similar to those of deuteranopia. Any observer, a portion of whose retinas yields normal color vision while another portion yields either the kind of red-green confusion characteristic of protanopia or that characteristic of deuteranopia, can give valid testimony.

It is now a fairly well accepted view that red-green confusers see neutral colors (black, gray, white, silver, "colorless" and so on) normally, and chromatic colors of two hues, approximately what normal observers call pure yellow and pure blue [14], with little or no admixture of red and green. Evidence obtained from all three types of admissible observers consistently supports this view. We shall, however, review the literature to see whether this rough indication can be made more precise.

1. Peripheral Parts of the Normal Retina

It has been widely stated in textbooks for many years that there is, in the normal eye, a retinal zone of considerable extent (perhaps 20° to 50° from the fovea centralis) within which yellow, blue, black, and white are perceived much as at the fovea, but red-green distinctions are scarcely, if at all, possible. Since the luminosity function of this region in a light-adapted state is substantially the same as normal [30, 61, 68 (p. 46)], the properties of this retinal zone near the periphery approach those of deuteranopia, the distinctions from deuteranopia being reduced visual acuity, reduced ability to distinguish both black from white, and yellow from blue, and presence of a slight, instead of vanishing, ability to distinguish red from green. As a preliminary observation will immediately show, the precise hues of the yellowish and bluish colors seen by means of this retinal zone are hard to determine. A spectrum stimulus yielding a color of orange hue by foveal vision yields a progression of less and less reddish hues as it is moved more toward the periphery. There are determinable for each observer, however, within certain limits the wavelengths of the spectrum stimuli yielding colors of invariable hue regardless of retinal region stimulated. It is obvious that the hues of the bluish and yellowish colors perceived by the nearly deuteranopic peripheral region are to be found among these invariable hues. Table 1 is extracted from a summary by Tschermak [95] and shows results of four investigators. As might be expected from the difficult nature of the observations and the many factors influencing the results [17; 69, p. 273], there is considerable difference between the reports of the various investigators. Goldmann's results refer to a protanomalous observer [24] and on this account have less weight than the others. Some observers can make such observations with good reliability (Hess, 2 to 3 mμ uncertainty), others less certainly (Dreher, 10 mμ uncertainty); and there is furthermore a large individual difference (40-mμ spread among Dreher's three observers). Although Hess' results refer to one observer only (himself), they are probably as good as any, and have, at least, been the most widely quoted [30]. These results indicate the deuteranopic yellow to be a hue corresponding, for normal vision under visual conditions, to about 575 mμ; and deuteranopic blue to be that corresponding to about 470 mμ, with uncertainties of about 10 mμ.

TABLE 1. *Stimuli that yield bluish or yellowish colors of invariable hue, regardless of retinal region affected*

Author	Year	Wavelength of spectrum stimulus yielding invariable hue, regardless of retinal region	
		Yellowish	Bluish
		mμ	mμ
Hess [33]	1889	574.5	471
Baird [4]	1905	570	460
Dreher [17]	1912	568	461
Goldmann [25]	1925	567	466

2. Red-Green Confusion Acquired Through Disease

Toxic agents and disease affecting the conducting (transmissive) elements of the optical apparatus (nerve elements and connections, optic nerve, and tract) cause a progressive lessening of the ability to distinguish red from green. This

defect becomes progressively worse until red-green blindness is reached, which is distinguished from inherited deuteranopia chiefly by its poorer light-dark discrimination. There is also some lessening of the ability to distinguish yellow from blue, which may progress until total color-blindness results [59, p. 141; 68, p. 45]. The luminosity function is essentially the same as for normal vision [57], and white, gray, and black are perceived in a relatively normal way. Köllner [59, p. 148] says, "In the dichromatic state the patient sees in the spectrum only yellow and blue, and the yellow corresponds to the hue which is elicited in the normal eye by light of wavelength 575 mμ, the blue to the hue corresponding to that of wavelength 471 mμ." These facts, like those of peripheral vision by the normal eye, indicate that the deuteranopic observer sees a yellow like that corresponding to about 575 mμ for the normal observer, and a blue corresponding to about 470 mμ.

3. Unilateral Red-Green Blindness

Unilateral inherited defects of vision are probably much more common than would be supposed from accounts of such cases appearing in the literature. An Army physician observed in 1920 [5], "It has been recently discovered that because a man has excellent color vision in one eye he does not necessarily have it in the other." And a recent estimate [66] places the incidence of unilateral defects at about 4 percent of the total color defectives. Since, however, color vision of both eyes is most frequently tested at the same time, it follows that most unilateral defects go unnoticed [58, 66, 88]. Table 2 lists chronologically all cases of unilateral defects in color vision that could be uncovered by a reasonable search of the literature. There are 40 original articles listed involving 37 cases, a case of unilateral protanopia being dealt with twice by Hippel [36, 37] and once by Holmgren [42], a case of unilateral tritanopia being dealt with both by Kirschmann [54] and by Dieter [13], a case of unilateral deuteranomaly both by v. Kries [62] and by Trendelenburg [94] and one article by Bonner [101] mentioning two cases previously unreported.

It should be noted that the skill and resources of the several investigators varied over a wide range, so that both the type of defect for the defective eye and the degree of approach to the norm in cases having one supposedly normal eye are subject to various degrees of doubt. Similarly, in many cases the report of the probable cause of the defect is based on very incomplete data. If there were no evidence of disease or

TABLE 2. *Unilateral defects of color vision*

Author	Date	Probable cause of defect	Type of defect
v. Baumgartner [6].	1858	Blow on eye	Temporary achromatopsia.
Brische [11]	1862	Attack of vertigo	Temporary cyanopsia.
Niemetscheck [77]	1868	Skull-bone degeneration.	Tritanopia and chloropsia.
Woinow [98]	1871	Noticed after head-wound, but perhaps inherited.	Atypical, red phobia.
Becker [7]	1879	Inherited	Acromatopsia.
Hippel [36]	1880	do	Protanopia.
Holmgren [42]	1881	do	Do.
Hippel [37]	1881	do	Do.
Holmgren [44]	1881	do	Tritanopia.
Steffan [90]	1881	Apoplexy	Approach to achromatopsia.
Snell [88]	1881	Skull fracture	Protanopia, deuteranomaly.
Hermann [32]	1882	Unknown	Tritanopia.
Kolbe [56]	1882	Inherited	Red-green weakness.
Shufeldt [86]	1883	do	Red-brown confusion.
Donders [16]	1884	do	Abnormal Rayleigh equation.
Eldridge-Green [18].	1889	Probably retinitis	Tritanopia, yellow-blue weakness.
Hering [31]	1890	Optic-nerve atrophy	Approach to deuteranopia.
Hess [34]	1890	Nerve injury	Do.
Snell [89]	1892	Noticed after blow on head, but perhaps inherited.	Deuteranopia.
Kirschmann [54]	1893	Inherited	Tritanopia.
Hilbert [35]	1894	do	Slight abnormalities.
Beevor [8]	1894	Nerve injury	Achromatopsia.
Piper [80]	1905	do	Achromatopsia, tritanopia.
Samojloff [85]	1906	Inherited	Abnormal Rayleigh equation.
Köllner [57]	1909	Optic-nerve atrophy	Achromatopsia, tritanopia.
Hayes [28]	1911	Inherited	Protanomaly.
Hegner [29]	1915	do	Do.
Lohmann [65]	1917	do	Abnormal contrast effects.
v. Kries [62]	1919	do	Deuteranomaly.
Goldschmidt [26]	1919	Gunshot headwound	Protanomaly.
Bonner [10]	1923	Optic atrophy (tuberculous).	Green weakness.
Jennings [48]	1925	Noticed after blow on head, but perhaps inherited.	Red-green blindness.
Bonner [11]	1926	Unknown	Achromatopsia.
	1926	do	Red-green blindness.
Dieter [13]	1927	Inherited	Tritanopia.
Miles, Beaumont [66].	1931	Unknown	Red-green blindness.
Miles, Craig [67]	1931		Do.
Neipperg [75]	1932	Inherited	Do.
Trendelenberg [94].	1941	do	Deuteranomaly.
Sloan [87]	1947	do	Deuteranopia.

injury, the defect is listed as probably inherited. In one case, however, it is known definitely that the defect was inherited; the subject found by v. Kries to have unilateral deuteranomaly was found later [94] to have transmitted a bilateral deuteroform defect to his daughter. Table 2 is intended to give brief summaries of all cases of unilateral defects of color vision, and the information is as precise as can be given in a few words; but these summaries are, of course, often unsatisfactory substitutes for the original articles that should be consulted if more detailed information is desired.

Since many of these cases are to be neglected as having no bearing on the color perceptions of protanopic and deuteranopic observers, it is convenient to introduce here the definitions of the terms by which the type of defect has been indicated in table 2.

Trichromatism—a type of vision in which the colors seen require in general three independently adjustable primaries (such as red, green, and blue) for their duplication by mixture. Normal vision is one form of trichromatism.

Dichromatism—a type of vision in which the colors seen require in general two independently adjustable primaries (such as red and green, or purple and yellow) for their duplication by mixture.

Monochromatism—a type of vision in which the colors seen require only a single adjustable primary to match them. Any light may serve as the primary.

Protanomaly—a type of trichromatism in which the relative luminosity function is too low at the longwave end to fall within normal limits, and in which an abnormally large proportion of red in a red-green mixture is required to match a given yellow.

Deuteranomaly—a type of trichromatism in which the relative luminosity function falls within normal limits and in which an abnormally large proportion of green is required in a red-green mixture to match a given yellow.

Protanopia—a type of dichromatism in which red and blue-green are confused, but no abnormal proportion of red plus green is required to match a given yellow, and the relative luminosity function is too low at the longwave end to fall within normal limits.

Deuteranopia—a type of dichromatism in which purplish red and green are confused, but no abnormal proportion of red and green is required to match a given yellow, and the relative luminosity function falls within normal limits.

Tritanopia—a type of dichromatism in which reddish blue and greenish yellow are confused.

Achromatopsia—a type of monochromatism in which all colors are perceived as neutral (such as black, gray, and white).

Chloropsia—green vision.

Cyanopsia—blue vision.

Rayleigh [*83*] *equation*—the proportions of red and green required in a mixture to match a given yellow. Usually spectrum red (670 mμ) is mixed with spectrum green (535 mμ) in such proportions as to match spectrum yellow (589 mμ).

It would seem that only cases of protanopia and deuteranopia listed in table 2 need be considered, but it has often been noted [28, 62 (p. 148), 74] that under unfavorable conditions (such as small angular extent of observing field, reduced observing time [29], low field luminance, or dark surrounding field) protanomalous and deuteranomalous observers make the same mistakes as protanopes and deuteranopes, and respond as if they had dichromatic rather than trichromatic visual systems (red-green confusion, presence of a neutral point in the spectrum near 495 mμ, and so on). On this account, many color-perception tests fail to differentiate red-green confusers into groups of dichromats and trichromats. It is possible therefore to obtain information concerning the color perceptions characteristic of dichromatic visual systems from unilateral protanomaly and unilateral deuteranomaly, provided attention is paid to observations obtained by such observers under conditions that reduce these systems to, or nearly to, dichromatism. Table 3 lists all unilateral cases from which information regarding protanopic and deuteranopic color perceptions can be gleaned. It also includes a bilateral case reported by Nagel [72], which has a bearing on deuteranopic color perception. In this case the fovea was dichromatic, the periphery trichromatic, quite beyond the vestigial trace often reported by dichromats. Cases of unilateral achromatopsia and tritanopia listed in table 2 have been omitted, together with those of red-green confusion not giving information regarding color perceptions (Snell,

Kolbe, Shufeldt, Hegner, Lohmann, Jennings, Neippert, Bonner, and Miles and Beaumont). Cases of slight abnormality not approaching dichromatism are also omitted (Donders, Hilbert, Samojloff).

The case of atypical unilateral sense disturbance reported by Woinow [98] has been omitted, because the report is contradictory. The subject was reported to be deuteranopic (green blind) in one eye, and measurements by rotating sector disks indicated confusion of both red and green with gray. There was, however, hysterical fear of red particularly from the eye which, as we have seen, under some conditions could not distinguish red from gray Furthermore, all objects seen by this eye were tinged with red, but spectrum yellow appeared blue. There is no evidence, except this latter rather confusing report, that the color system of the defective eye was dichromatic; it might have been monochromatic. Reports of the subject in other sense fields (taste, temperature, smell, hearing) indicated a profound psychic disturbance.

The case of temporary cyanopsia reported by Brische has also been omitted; the visual system seems to have been monochromatism, black, gray, and white objects, and all parts of the spectrum, appearing blue.

In table 3 the indicated perceptions are specified in many cases simply by color name, and we see, as before, that unilateral defects of vision indicate that the protanopic and deuteranopic perception of white is normal, and those of hue are some kind of a yellow and some kind of a blue. In other cases these indications have been made more exact by direct comparison of the spectrum colors viewed by the defective eye with those of the same spectrum viewed by the normal eye. Orange, for example, is seen as yellow by the dichromatic eye, as is also yellow green; but the part of the spectrum whose hue is the same for both the normal and the defective eye serves as a specification for the particular kind of yellow sensed by the dichromatic eye; that is, we can say from such evidence that the dichromatic yellow is like that perceived at some certain portion of the spectrum by the normal eye. Five of the entries in table 3 are of this nature. Four out of five of these entries refer to subjects who had in the defective eye slight, rather than vanishing, ability to distinguish red from green, but reports of hue difference between the two eyes could still be made and the spectral region yielding the same hue for both eyes determined. In general, it will be noted that for both the deuteranopic and protanopic forms the yellow is closely like that of the spectrum at 575 mμ to the normal eye, and the blue like that of 470 mμ. This agrees with indications for the deuteranopic form obtained from the periphery of the normal retina and from acquired bilateral color-blindness.

The three exceptions to this generalization are, first, the wavelength 589 mμ found by Hippel for his unilaterally color-blind observer; second, the designation, orange-yellow, shown for Goldschmidt's case of unilateral protanomaly; and third, the contradictory report by Sloan's unilateral deuteranope. The first two exceptions suggest that some protanopes, at least, see orange-yellow instead of the slightly greenish yellow of 575 mμ. Hippel, however, depended on the observation of flame spectra under the unfavorable condition of a dark background and did not report tests of any yellowish spectrum color other than 589 mμ (that is, none nearer than this to 575 mμ), so his finding may merely be an imprecise check of 575 mμ. Furthermore, the report of orange-yellow is rendered doubtful by the report by Holmgren of greenish yellow ("greenish yellow, or citron yellow, not golden yellow") for the same case [42] examined by means of dyed wools. In the second exception, it was stated [26] rather inexplicitly that for the defective eye, "the green appeared in the spectrum stretched out into the yellow, and the blue stretched out into the violet, . . ." Neither of these reports can be taken as established exceptions to the otherwise consistent indication that the yellow and blue of red-green confusers are, respectively, closely what the normal eye sees in the spectral regions near 575 and 470 mμ.[2]

Some writers [28] have classified the Hering and Hess cases as probably protanomaly because of

[2] Since the indicated perceptions for both protanopic and deuteranopic vision are not significantly different, no extended discussion of discrepancies in classification of the unilateral defects shown in table 3 is required. For the same reason, it is unimportant for the present purpose to determine whether the defect is inherited or acquired. However, it may be remarked that the classification by Hippel of his patient as what we now call deuteranopic rests on his failure to find the spectrum shortened on the long-wave end relative to that for the normal eye, all of the various spectral emission lines used being either visible to both eyes or invisible to both. The classification of protanopia, however, is firmly grounded not only on Holmgren's finding based upon the Holmgren wool test, which includes a chromaticity method of diagnosing protanopia, but also on Hippel's own report that the brightest part of the spectrum for the defective eye was shifted considerably toward the short-wave end relative to that for the normal eye.

the statement that the long-wave end of the spectrum was shortened. This minor shortening is to be expected because of the partial impairment of the yellow-blue and light-dark senses, as well as the almost complete disappearance of the red-green sense. It is not to be confused [68, (p. 45)] with the much larger departure from normal characteristic of protanopia, designated by Hering as "blue-sighted red-green blindness."

The reclassification of Hayes' subject from protanopia to protanomaly is based upon the fact that the normal setting of a red plus a green by disk mixture to match a yellow plus black plus white was found by the subject's defective eye to be much too green. To satisfy the defective eye, she had to put by far more red in the first mixture. Hayes' conclusions are sound if translated into accepted terminology.

A further word is required regarding the apparently contradictory report by Sloan's unilateral deuteranope [87] that, on the one hand, the hues seen are like Munsell 5Y 5/5 (dominant wavelength 575 mμ) and 3PB 5/5 (dominant wavelength 478 mμ), and that, on the other they are like the spectrum at 584 and 452 mμ. There are several possibilities to be explored, but it will be sufficient for the present to point out that if both eyes of this subject had an abnormally large amount of ocular pigmentation and so were provided with a permanent adaptation to reddish yellow, the discrepancy would be explained. The same explanation would also account for the discrepancy between the wavelength of neutral point estimated from the Munsell 5/5 locus (498 mμ, which is typical of deuteranopia [50, 51]) and that estimated directly from the spectrum (503 mμ, corresponding to reddish yellow adaptation). A more complete study of this observer might be worth while.

III. Agreement with Theories of Color Vision

The evidence just reviewed that red-green confusers see yellow and blue does not, of course, prove that all red-green confusers have those color perceptions, though the absence of reliable conflicting evidence renders such a conclusion highly probable. Thus, Parsons [79, p. 191] remarked in 1924, "Most observers think that the two sensations experienced (by protanopes and deuteranopes) correspond most closely to normal yellow and blue. Uncomplicated cases of unilateral congenital colour blindness would afford valuable evidence . . .". Similarly, in 1927, Dieter [13, p. 79] said, "Only if still more cases of the same kind are completely analysed will there be sufficient ground for the alluring possibility of theoretical appraisal." Unilateral color-blindness, however, has already had an important influence on color theory.

During the period (1880–1920) when the experimental facts of protanopic and deuteranopic color perceptions were being established, the controversy between the three-components (Young-Helmholtz) theory of color vision and opponent-colors (Hering) theory reached its height [64].

According to the three-components theory, there are in the normal retina three independent photosensitive mechanisms, one sensitive preponderantly to the long-wave portion of the spectrum and yielding a red response, another sensitive preponderantly to the middle portion of the spectrum and yielding a green response, and the third sensitive preponderantly to the short-wave portion of the spectrum and yielding a blue or violet response.

According to the opponent-colors theory, there are in the normal visual mechanism three pairs of opposing processes, a black-white pair, which cancels to leave gray, and two chromatic pairs, blue-yellow, and red-green, which cancel to gray when both members of the pair are excited equally.

Red-green blindness according to the three-components theory comes from failure of either the red-component (protanopia) or the green-component (deuteranopia), leading to the indication that protanopes must see only mixtures of green and violet, and deuteranopes, only mixtures of red and violet. But, by the opponent-colors theory, only one type of red-green blindness is to be expected, that arising from elimination of the red-green process, leaving the perceptions white and black, blue and yellow.

The case of unilateral protanopia (Hippel, Holmgren, table 3) was a blow to the original form of three-components theory. It showed that one red-green blind eye, at least, saw yellow and blue, not green and violet. The three-components theory can be thrown into a form accounting both conveniently and precisely for the red-green confusions of protanopes and deuteranopes [51], but this single case of unilateral color-blindness showed that it is not a reliable guide to what they

803370—48——2

TABLE 3. *Cases of unilateral defect of vision giving information regarding protanopic and deuteranopic color perceptions*

Author	Date	Classification of the defect		Indicated perceptions	
		Author's own	Present		
Hippel [36]	1880	Deuteranopia	Protanopia	Yellow	Blue.
Holmgren [42]	1881	Protanopia	do	Greenish yellow	Violet blue.
Hippel [37]	1881	Deuteranopia	do	Like 589 μ	Blue.
Hering [31]	1890	Approach to deuteranopia	Approach to deuteranopia	Yellow	Do.
Hess [34]	1890	do	do	Like 575 μ	Like 471 mμ.
Nagel [72]	1905	Deuteranopia	Deuteranopia	Yellow	Blue.
Hayes [28]	1911	Protanopia	Protanomaly	do	Do.
v. Kries [62]	1919	Deuteranomaly	Deuteranomaly	Like 573 μ	Like 464 to 480 mμ.
Goldschmidt [26]	1919	Protanomaly	Protanomaly	Orange, yellow	Blue.
Sloan [87]	1947	Deuteranopia	Deuteranopia	Like 5 Y 5/5, also 584 mμ	Like 3PB, 5/5, also 452 mμ.

see. The opponent-colors theory, on the other hand, received dramatic support from the color perceptions reported for this case. This latter theory, however, does not account for two forms of red-green blindness, but only one, deuteranopia.

It may be said, therefore, that both of these simple visual theories received fatal blows from discovery of the facts of protanopia and deuteranopia. Some advocates of the three-components theory refused to be impressed by the Hippel-Holmgren case of unilateral protanopia. Holmgren, himself, continued to use the terms, "red blind", "green blind" and "violet blind", and offered a prize of 400 crowns to anyone who would bring to his attention a case of unilateral "green blindness" [45]. Some three-component advocates took refuge in Fick's [21, 22] suggestion that red-green blindness results, not from the complete failure of one of the three components, the red or the green, but from the receptors for red and green having identical photo-sensitive substances, either that normally used for red or that normally used for green. Other advocates of the three-components theory (König, v. Kries) eventually took up the very similar theoretical position [54a, 60 (p. 169)] originally proposed by Donders [15] that the three-components theory holds for processes in one stage or zone of the visual mechanism (perhaps the photosensitive substances), whereas the opponent-colors theory holds for processes in a later stage or zone (perhaps the optic nerve). This view is known as the zone or stage theory of vision. Furthermore, a very able advocate of the opponent-colors theory, G. E. Müller, adopted a theoretical view which, although divergent in detail and more elaborated, was essentially in agreement with the zone theories favored by Donders, König, and v. Kries. All of these theories allow for protanopic and deuteranopic perception of yellow and blue, though that of Müller does not require it for protanopes. Müller remarks (p. 49), "If the color-blind is a deuteranope, his chromatic color sensations must therefore (by this theory) be pure yellow and pure blue . . . . It is otherwise with protanopes. If in an individual outer red-green sensitivity is absent, it makes no difference in his behavior, either in practical living or in any investigation, whether the remaining greenish-yellow and reddish-blue processes excite only yellow and blue in the optic nerve, or whether, . . ., they excite greenish-yellow or reddish-blue sensations, or whether, . . . they excite only green and red, or . . . even only green and blue, or . . . yellow and red. An individual lacking outer red-green sensitivity will give exactly the same color equations, exactly the same spectral positions of brightness maximum and neutral point regardless of whether his greenish yellow and reddish blue processes evoke nerve excitations corresponding to the like-named excitations (yellow and blue) or unlike-named excitations (green and red), or by simultaneous action of both sorts, excitations of exactly the same kind as the processes themselves. We would therefore not be particularly astonished if it were established definitely in a unilateral case of protanopia that the yellow sensation experienced actually was somewhat greenish and that the blue sensation experienced actually was somewhat reddish, and we would not believe that the ground was disappearing under our feet if sometime there should occur a (quite improbable) case establishing

the two chromatic color sensations of a protanopic eye as the pure-green sensation and the pure-red sensation."

Since all theories of vision with any pretense of being complete provide for the perception of yellow and blue by red-green confusers, and since a reasonable search of the literature has failed to uncover any reliable evidence against this indication, it is proposed to build a method of designating protanopic and deuteranopic perceptions of surface colors on the finding that such observers see a yellow and a blue like those seen by the normal observer in the spectrum near 575 and 470 $m\mu$, respectively. The consequences of this choice of hues are bound to appear correct to binocular red-green confusers. These consequences can be contradicted only by observers having unilateral defects; and the probability of such contradiction arising may be estimated from the fact that the eight cases recorded so far (see table 3) fail to contradict it.

IV. Derivation of Deuteranopic and Protanopic Munsell Notations

Object-color perceptions by normal observers are most commonly described in terms of the attributes, hue, lightness, and saturation [78] defined [2] as follows:

"*Hue* is the attribute which determines whether the color perception is red, yellow, green, blue, purple, or the like.

"*Lightness* is the attribute which permits an object-color perception to be classified as equivalent to some member of the series of grays ranging between black and white.

"*Saturation* is the attribute of an object-color perception which determines the degree of its difference from the gray of the same lightness."

The Munsell color system is based upon this method of description. Munsell hue, value, and chroma are intended to correspond to hue, lightness, and saturation, respectively, and the samples in the Munsell Book of Color [70] when viewed in daylight by a normal observer under usual viewing conditions (daylight adapted eye, light to medium-gray surrounding field) yield color perceptions such that Munsell hue correlates closely with the perceived hue, Munsell value with the perceived lightness, and Munsell chroma with the perceived saturation. A method has been developed [49] by means of which readily understood color names may be found for any color from its Munsell notation.

When the samples of the Munsell Book of Color are viewed by a protanopic or a deuteranopic observer, however, the color perceptions obtained are not even approximately indicated by the Munsell notation. It is proposed to develop a method of deriving protanopic and deuteranopic Munsell notations, analogous to the present normal Munsell notations, that will correlate with the color-perceptions that red-green-blind observers obtain from objects viewed in daylight uuder usual conditions. It has been shown [51] that the color confusions of red-green-blind observers can be found from three numbers (K, W_p, W_d) related to the tristimulus values (X, Y, Z) of the ICI standard observer by the transformation equations:

$$\left.\begin{aligned} K &= Z, \\ W_p &= -0.460\ X + 1.359\ Y + 0.101\ Z, \\ W_d &= Y. \end{aligned}\right\} \qquad (1)$$

Any two colors having identical values of K and W_p are identical to the average protanope; those having identical values of K and W_d are identical to the average deuteranope. Figure 1 shows in arbitrary units the values of K, W_p, and W_d for all parts of a spectrum of unit irradiance per unit wavelength.

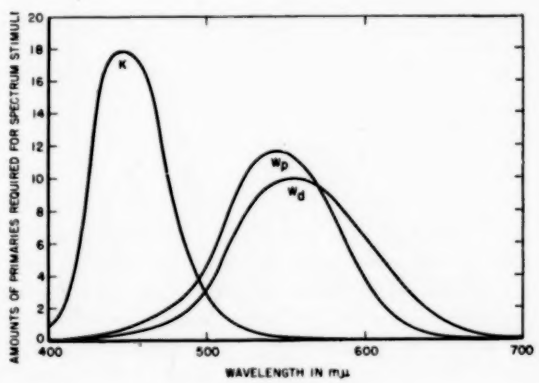

FIGURE 1

One of each of the two pairs of numbers (W_d, W_p), used in judging equivalence of colors for deuteranopic and protanopic observers, refers to the luminous aspect of the color (luminance for a self-luminous area, luminous directional reflect-

ance for a surface), the other number, K, of each pair taken relative to the first refers to the chromatic aspect. For the ICI observer, luminous directional reflectance is customarily expressed relative to that (Y_0) of magnesium oxide. By analogy we take $W_d/(W_d)_0 = Y/Y_0$ for deuteranopic luminous directional reflectance, and

$$\frac{W_p}{(W_p)_0} = \frac{-0.460X + 1.359Y + 0.101Z}{-0.460X_0 + 1.359Y_0 + 0.101Z_0},$$

for protanopic luminous directional reflectance. But since for magnesium oxide it is customary to take $X_0 = 0.9804$, $Y_0 = 1.0000$, and $Z_0 = 1.1512$, protanopic luminous directional reflectance may be written simply as $0.9733W_p$.

It is customary to specify the chromatic aspect of a color for the ICI standard observer by means of trichromatic coordinates, or chromaticity coordinates x, y, and z. By analogy with this practice, the chromaticity coordinates for deuteranopic and protanopic observers are the dichromatic coordinates (w_d, k_d; w_p, k_p) defined as follows:

$$\left.\begin{aligned} w_d &\equiv W_d/(W_d+K) = \\ &\quad Y/(Y+Z) = y/(y+z) = y/(1-x), \\ k_d &\equiv K/(W_d+K) = Z/(Y+Z) = \\ &\quad z/(y+z) = (1-x-y)/(1-x). \end{aligned}\right\} \quad (2d)$$

$$\left.\begin{aligned} w_p &\equiv \frac{W_p}{W_p+K} = \frac{-0.460X + 1.359Y + 0.101Z}{-0.460X + 1.359Y + 1.101Z} \\ &= \frac{-0.561x + 1.258y + 0.101}{-1.561x + 0.258y + 1.101}, \\ k_p &\equiv \frac{K}{W_p+K} = \frac{Z}{-0.460X + 1.359Y + 1.101Z} \\ &= \frac{1.000 - x - y}{-1.561x + 0.258y + 1.101}. \end{aligned}\right\} \quad (2p)$$

From eq 2d and 2p it will be noted that w_p and k_p sum to unity; likewise, w_d and k_d. Hence only one of the dichromatic chromaticity coordinates need be used. We will use w_d and w_p, which may be taken as measures of the deuteranopic and protanopic "warm" quality, respectively. According to the data and views already summarized in sections II and III, it is legitimate to take them more precisely as indications of "yellowness."

Since for the approximately 400 samples of the Munsell Book of Color, the tristimulus values, X, Y, Z, have already been evaluated from spectrophotometric measurements [23, 53], it is a simple matter to compute $W_d/(W_d)_0$ and w_d from eq 1 and 2d, and so arrive at a specification of deuteranopic luminous directional reflectance and chromaticity. The results are shown in table 4. Similarly there have been computed for these 400 samples values of $W_p/(W_p)_0$ and w_p, which serve as specifications of protanopic luminous directional reflectance and chromaticity, respectively. These results are shown in table 5. In both tables 4 and 5, the samples have been arranged in a sequence, which would appear orderly to the average deuteranope (table 4) or protanope (table 5). The samples were first arranged according to reflectance, and, as expected, for deuteranopic vision were found to form seven groups of nearly constant reflectance (one for each of the Munsell values 2 to 8) with definite reflectance gaps separating them. The samples of each group are arranged according to yellowness, approximately as indicated by the chromaticity coordinate, w_d. Also, as expected, no such grouping was found after arranging the samples according to protanopic reflectance. However, the samples were arranged arbitrarily into 14 groups (one for each of the Munsell values 2.0, 2.5, . . . 8.5) so that the protanopic reflectance of each sample in one group is both lower than all of those in the group above and higher than all of those in the group below. Within each of these 14 groups the samples were arranged according to yellowness, approximately as indicated by the chromaticity coordinate w_p.

From the first three columns of tables 4 and 5, it may be seen that an arrangement that seems orderly to a deuteranope or protanope may contain outstanding irregularities to a normal observer. For example, the first four entries in table 4 are Y 8/12, Y 8/10, 10Y 8/8, Y 8/8. The second column indicates that these samples all have reflectances close to 0.58; that is, the colors of these surfaces appear to the average deuteranope as well as to the average normal observer to be about equally light. The third column indicates that the first sample is the yellowest and fourth the least yellow. With the exception of the third sample (10Y 8/8), this classification accords with that of the normal observer, which is indicated closely by the Munsell notation (Hue Value/Chroma) Y 8/12, Y 8/10, Y 8/8. The third sample, however, is a more greenish yellow than the others and for the normal observer does not

fit into the series. In this instance table 4 has served to indicate with some precision the kind of greenish yellow that the average deuteranope may be expected to confuse with a certain group of yellows. It indicates in general exactly the red-green confusions characteristic of deuteranopia. Table 5 indicates in a similar way the red-green confusions characteristic of protanopia.

TABLE 4. *Deuteranopic arrangement*

Munsell book notation	Deuteranopic reflectance, $W_d = Y$	Deuteranopic chromaticity coordinate, s_d	Munsell renotations	
			Deuteranopic	Normal
5Y 8/12	0.5706	0.8911	5Y 7.9/12.2	5.5Y 7.9/12.3
5Y 8/10	.5784	.8578	5Y 7.9/11.0	5.5Y 7.9/11.1
10Y 8/ 8	.6035	.7918	5Y 8.1/ 9.2	0.5GY 8.1/ 9.1
5Y 8/ 8	.5794	.7660	5Y 7.9/ 8.2	5.5Y 7.9/ 8.2
5Y 8/ 8	.5732	.7606	5Y 7.9/ 8.1	5.5Y 7.9/ 8.3
5GY 8/ 8	.6022	.7464	5Y 8.1/ 7.9	4.5GY 8.1/ 8.7
10YR 8/ 8	.6049	.7064	5Y 8.1/ 6.9	0.5Y 8.1/ 7.6
5Y 8/ 6	.5784	.6981	5Y 7.9/ 5.7	4.5Y 7.9/ 5.8
10Y 8/ 6	.5906	.6664	5Y 8.0/ 5.7	0.5GY 8.0/ 5.7
5GY 8/ 6	.5929	.6605	5Y 8.0/ 5.5	5.5GY 8.0/ 6.2
10YR 8/ 6	.6134	.6263	5Y 8.1/ 4.7	9.0YR 8.1/ 5.5
5Y 8/ 4	.5651	.5851	5Y 7.8/ 3.4	4.0Y 7.8/ 3.5
10Y 8/ 4	.5997	.5827	5Y 8.0/ 3.4	1.0GY 8.0/ 3.4
10GY 8/ 6	.5793	.5720	5Y 7.9/ 3.1	9.5GY 7.9/ 5.1
5GY 8/ 4	.6041	.5719	5Y 8.1/ 3.2	6.0GY 8.1/ 3.6
10YR 8/ 4	.5972	.5579	5Y 8.0/ 2.8	9.0YR 8.0/ 3.4
10GY 8/ 4	.6181	.5406	5Y 8.2/ 2.3	0.5G 8.2/ 4.0
5YR 8/ 4	.5970	.5311	5Y 8.0/ 2.0	4.0YR 8.0/ 3.5
10R 8/ 4	.6115	.5156	5Y 8.1/ 1.6	10.0R 8.1/ 3.7
5Y 8/ 2	.5570	.5141	5Y 7.8/ 1.5	3.5Y 7.8/ 1.6
5GY 8/ 2	.5851	.5107	5Y 8.0/ 1.5	6.0GY 8.0/ 1.6
5G 8/ 6	.5595	.4904	5Y 7.8/ 1.1	6.5G 7.8/ 4.7
5YR 8/ 2	.5917	.4949	5Y 8.0/ 1.0	4.0YR 8.0/ 2.0
5G 8/ 4	.5881	.4809	5Y 8.0/ 0.9	5.5G 8.0/ 3.3
5G 8/ 2	.5694	.4847	5Y 7.9/ 0.8	4.5G 7.9/ 2.1
5R 8/ 4	.5862	.4834	5Y 8.0/ 0.7	3.5R 8.0/ 3.6
10G 8/ 2	.5965	.4806	5Y 8.0/ 0.6	5.0G 8.0/ 2.0
N 8/	.5751	.4700	5Y 7.9/ 0.4	2.5GY 7.9/ 0.3
5R 8/ 2	.6021	.4699	5Y 8.1/ 0.4	2.0R 8.1/ 2.2
10RP 8/ 6	.6251	.4693	5Y 8.2/ 0.4	8.5RP 8.2/ 3.6
10RP 8/ 4	.6107	.4678	5Y 8.1/ 0.3	9.5RP 8.1/ 2.7
5BG 8/ 2	.6082	.4656	5Y 8.1/ 0.3	1.0BG 8.1/ 2.0
5RP 8/ 2	.6435	.4633	5Y 8.3/ 0.2	8.0RP 8.3/ 1.9
5RP 8/ 6	.6038	.4611	5Y 8.1/ 0.1	6.5RP 8.1/ 3.4
5RP 8/ 4	.6050	.4588	5Y 8.1/ 0.1	5.5RP 8.1/ 2.8
10BG 8/ 2	.6258	.4557	5PB 8.2/ 0.4	5.0BG 8.2/ 1.9
5B 8/ 2	.6179	.4361	5PB 8.2/ 1.7	4.0B 8.2/ 2.2
5P 8/ 2	.5897	.4330	5PB 8.0/ 1.8	5.0P 8.0/ 2.5
10P 8/ 4	.6182	.4289	5PB 8.2/ 2.2	7.5P 8.2/ 3.5
5B 8/ 4	.6025	.4272	5PB 8.1/ 2.3	4.0B 8.1/ 2.9
10B 8/ 2	.6514	.4170	5PB 8.3/ 3.1	1.0PB 8.3/ 3.0
5PB 8/ 2	.6380	.4139	5PB 8.3/ 3.2	5.0PB 8.3/ 3.2
10PB 8/ 2	.6499	.4099	5PB 8.3/ 3.4	7.5PB 8.3/ 3.4
P 8/ 4	.5940	.4004	5PB 8.0/ 3.9	4.5P 8.0/ 4.8

TABLE 4. *Deuteranopic arrangement*—Continued

Munsell book notation	Deuteranopic reflectance, $W_d = Y$	Deuteranopic chromaticity coordinate, s_d	Munsell renotations	
			Deuteranopic	Normal
Y 7/10	0.4189	0.8502	5Y 6.9/ 9.7	5.0Y 6.9/ 9.7
Y 7/ 8	.4220	.8430	5Y 6.9/ 9.6	6.0Y 6.9/ 9.5
10YR 7/10	.4179	.8405	5Y 6.9/ 9.4	1.0Y 6.9/10.5
10Y 7/ 8	.4440	.8358	5Y 7.1/ 9.5	10.0Y 7.1/ 9.3
GY 7/10	.4263	.8160	5Y 7.0/ 9.0	4.0GY 7.0/ 9.5
YR 7/10	.4178	.7614	5Y 6.9/ 7.4	5.5YR 6.9/10.1
10YR 7/ 8	.4397	.7571	5Y 7.1/ 7.4	0.5Y 7.1/ 8.3
GY 7/ 8	.4512	.7437	5Y 7.1/ 7.1	5.0GY 7.1/ 8.0
10Y 7/ 6	.4334	.7406	5Y 7.0/ 7.0	0.5GY 7.0/ 6.9
Y 7/ 6	.4158	.7286	5Y 6.9/ 6.4	4.5Y 6.9/ 6.6
GY 7/ 6	.4509	.6867	5Y 7.1/ 5.7	5.0GY 7.1/ 6.4
YR 7/ 8	.4356	.6851	5Y 7.0/ 5.6	4.5YR 7.0/ 8.2
10YR 7/ 6	.4347	.6818	5Y 7.0/ 5.5	10.0YR 7.0/ 6.3
10GY 7/ 8	.4399	.6509	5Y 7.1/ 4.8	10.0GY 7.1/ 8.3
YR 7/ 6	.4262	.6143	5Y 7.0/ 3.9	3.5YR 7.0/ 6.0
YR 7/ 6	.4180	.6134	5Y 6.9/ 3.8	3.5YR 6.9/ 5.9
Y 7/ 4	.4282	.6084	5Y 7.0/ 3.7	4.0Y 7.0/ 3.8
10R 7/ 8	.4290	.6071	5Y 7.0/ 3.7	10.0R 7.0/ 7.5
10Y 7/ 4	.4439	.6053	5Y 7.1/ 3.6	1.0GY 7.1/ 3.6
10GY 7/ 6	.4507	.6046	5Y 7.1/ 3.6	10.0GY 7.1/ 6.5
GY 7/ 4	.4369	.5910	5Y 7.0/ 3.3	5.5GY 7.0/ 3.8
10YR 7/ 4	.4602	.5848	5Y 7.2/ 2.5	9.0YR 7.2/ 3.8
YR 7/ 4	.4376	.5567	5Y 7.0/ 2.5	3.0YR 7.0/ 4.1
10R 7/ 6	.4550	.5559	5Y 7.2/ 2.5	9.0R 7.2/ 5.7
10GY 7/ 4	.4571	.5486	5Y 7.2/ 2.3	10.0GY 7.2/ 4.1
10R 7/ 4	.4537	.5316	5Y 7.2/ 1.8	8.5R 7.2/ 4.7
Y 7/ 2	.4454	5199	5Y 7.1/ 1.6	4.0Y 7.1/ 1.6
R 7/ 8	.4244	.5188	5Y 7.0/ 1.7	3.5R 7.0/ 7.0
GY 7/ 2	.4261	.5177	5Y 7.0/ 1.7	5.5GY 7.0/ 1.8
R 7/ 6	.4452	.5099	5Y 7.1/ 1.3	3.5R 7.1/ 5.7
YR 7/ 2	.4375	.5058	5Y 7.0/ 1.2	3.0YR 7.0/ 2.1
G 7/ 6	.4381	.5030	5Y 7.0/ 1.1	7.0G 7.0/ 6.1
R 7/ 4	.4402	.4973	5Y 7.1/ 1.0	3.0R 7.1/ 5.2
G 7/ 4	.4340	.4948	5Y 7.0/ 0.9	6.5G 7.0/ 4.3
10RP 7/ 8	.4412	.4801	5Y 7.1/ 0.6	9.0RP 7.1/ 5.8
G 7/ 2	.4231	.4777	5Y 7.0/ 0.5	6.5G 7.0/ 2.1
10RP 7/ 6	.4551	.4773	5Y 7.2/ 0.5	9.5RP 7.2/ 4.7
5R 7/ 2	.4521	.4766	5Y 7.2/ 0.5	2.5R 7.2/ 2.6
10G 7/ 4	.4672	.4734	5Y 7.2/ 0.4	0.5BG 7.2/ 3.9
10RP 7/ 4	.4397	.4732	5Y 7.1/ 0.4	9.5RP 7.1/ 3.5
RP 7/ 2	.4727	.4601	5Y 7.3/ 0.1	6.5RP 7.3/ 2.3
RP 7/ 4	.4885	.4590	N 7.4/	6.0RP 7.4/ 3.3
BG 7/ 2	.4729	.4589	N 7.3/	3.5BG 7.3/ 2.1
N 7/	.4433	.4562	5PB 7.1/ 0.2	7.5PB 7.1/ 0.1
RP 7/ 6	.4955	.4533	5PB 7.4/ 0.3	5.0RP 7.4/ 4.4
BG 7/ 4	.4634	.4522	5PB 7.2/ 0.3	4.5BG 7.2/ 3.4
RP 7/ 8	.4845	.4494	5PB 7.4/ 0.4	4.5RP 7.4/ 4.9
B 7/ 2	.4718	.4348	5PB 7.3/ 1.5	3.5B 7.3/ 2.2
10P 7/ 4	.4657	.4285	5PB 7.2/ 1.9	10.0P 7.2/ 4.0
10BG 7/ 4	.4555	.4244	5PB 7.2/ 2.2	0.5B 7.2/ 3.6
10P 7/ 6	.4675	.4228	5PB 7.2/ 2.3	9.5P 7.2/ 4.6
P 7/ 2	.4108	.4206	5PB 6.9/ 2.6	4.5P 6.9/ 2.7
10P 7/ 8	.4735	.4125	5PB 7.3/ 2.9	9.5P 7.3/ 6.0
PB 7/ 2	.4907	.4125	5PB 7.4/ 3.0	3.5PB 7.4/ 3.0
B 7/ 4	.4575	.4092	5PB 7.2/ 3.0	5.0B 7.2/ 3.7
10PB 7/ 4	.4498	.3982	5PB 7.1/ 3.7	10.0PB 7.1/ 4.0

TABLE 4. *Deuteranopic arrangement*—Continued

Munsell book notation	Deuteranopic reflectance, $W_d = Y$	Deuteranopic chromaticity coordinate, u'_d	Munsell renotations	
			Deuteranopic	Normal
P 7/ 4	0.4457	0.3961	5PB 7.1/ 3.8	5.0P 7.1/ 4.8
B 7/ 6	.4436	.3958	5PB 7.1/ 3.8	5.0B 7.1/ 4.7
10B 7/ 4	.4526	.3954	5PB 7.2/ 3.8	9.0B 7.2/ 4.0
PB 7/ 4	.4743	.3885	5PB 7.3/ 4.4	4.0PB 7.3/ 4.5
P 7/ 6	.4381	.3765	5PB 7.0/ 4.9	5.5P 7.0/ 6.4
10PB 7/ 6	.4365	.3737	5PB 7.0/ 5.0	10.0PB 7.0/ 5.3
10B 7/ 6	.4576	.3709	5PB 7.2/ 5.2	9.5B 7.2/ 5.7
PB 7/ 6	.4556	.3687	5PB 7.2/ 5.4	4.0PB 7.2/ 5.6
10YR 6/10	.3595	.8349	5Y 6.5/ 8.8	10.0YR 6.5/ 9.8
5YR 6/12	.3241	.8401	5Y 6.2/ 8.6	6.0YR 6.2/11.5
Y 6/ 8	.3242	.8313	5Y 6.1/ 8.4	5.5Y 6.2/ 8.3
Y 6/ 8	.3145	.8289	5Y 6.1/ 8.2	5.5Y 6.1/ 8.1
10Y 6/ 6	.3278	.7980	5Y 6.2/ 7.7	9.5Y 6.2/ 7.4
YR 6/10	.3350	.7855	5Y 6.3/ 7.4	6.0YR 6.3/ 9.8
Y 6/ 6	.3179	.7817	5Y 6.2/ 7.2	5.0Y 6.2/ 7.2
10YR 6/ 8	.3457	.7653	5Y 6.4/ 7.0	9.5YR 6.4/ 8.0
GY 6/ 8	.3238	.7457	5Y 6.2/ 6.5	4.0GY 6.2/ 7.2
GY 6/ 6	.3200	.7246	5Y 6.2/ 5.9	5.0GY 6.2/ 6.7
YR 6/ 8	.3274	.7192	5Y 6.2/ 5.9	5.0YR 6.2/ 8.3
10YR 6/ 6	.3392	.7150	5Y 6.3/ 5.8	9.5YR 6.3/ 6.7
10R 6/10	.3243	.7068	5Y 6.2/ 5.6	0.5YR 6.2/10.1
10GY 6/10	.3032	.7025	5Y 6.0/ 5.4	9.0GY 6.0/ 8.7
10GY 6/ 8	.3224	.6692	5Y 6.2/ 4.8	9.0GY 6.2/ 7.7
10R 6/ 8	.3345	.6466	5Y 6.3/ 4.3	0.5YR 6.3/ 8.2
10Y 6/ 4	.3291	.6411	5Y 6.2/ 4.2	10.0Y 6.2/ 4.1
YR 6/ 6	.3221	.6410	5Y 6.2/ 4.2	4.5YR 6.2/ 6.0
Y 6/ 4	.3100	.6385	5Y 6.1/ 4.1	4.5Y 6.1/ 4.0
10GY 6/ 6	.3168	.6299	5Y 6.1/ 3.9	10.0GY 6.1/ 6.7
10YR 6/ 4	.3140	.6173	5Y 6.1/ 3.6	0.5Y 6.1/ 4.1
GY 6/ 4	.3217	.6151	5Y 6.2/ 3.6	5.0GY 6.2/ 4.0
10R 6/ 6	.3384	.5995	5Y 6.3/ 3.3	0.5YR 6.3/ 6.5
YR 6/ 4	.3113	.5751	5Y 6.2/ 2.6	4.0YR 6.1/ 4.0
R 6/10	.3236	.5628	5Y 6.2/ 2.4	4.0R 6.2/ 9.7
10GY 6/4	.3101	.5598	5Y 6.1/ 2.3	0.5G 6.1/ 4.4
R 6/ 8	.3236	.5436	5Y 6.2/ 1.9	4.0R 6.2/ 8.1
10R 6/ 4	.3262	.5432	5Y 6.2/ 1.9	9.0R 6.2/ 4.2
Y 6/ 2	.3211	.5317	5Y 6.2/ 1.7	4.0Y 6.2/ 1.7
GY 6/ 2	.3245	.5239	5Y 6.2/ 1.7	5.0GY 6.2/ 1.7
G 6/ 6	.3040	.5237	5Y 6.0/ 1.5	6.0G 6.0/ 7.4
R 6/ 6	.3308	.5200	5Y 6.2/ 1.4	3.5R 6.2/ 6.3
YR 6/ 2	.3124	.5155	5Y 6.1/ 1.3	4.5YR 6.1/ 2.0
R 6/ 4	.3313	.5065	5Y 6.3/ 1.1	4.5R 6.3/ 4.5
G 6/ 4	.3151	.5018	5Y 6.1/ 1.0	6.0G 6.1/ 4.6
10RP 6/10	.3210	.4964	5Y 6.2/ 0.9	9.5RP 6.2/ 8.8
10RP 6/ 8	.3248	.4875	5Y 6.2/ 0.7	9.0RP 6.2/ 7.0
10G 6/ 2	.3032	.4836	5Y 6.0/ 0.6	6.0G 6.0/ 2.4
R 6/ 2	.3205	.4806	5Y 6.2/ 0.6	4.0R 6.2/ 2.3
10RP 6/ 6	.3240	.4792	5Y 6.2/ 0.6	9.0RP 6.2/ 5.5
10G 6/ 6	.3538	.4756	5Y 6.4/ 0.5	1.0BG 6.4/ 6.0
10RP 6/ 4	.3239	.4700	5Y 6.2/ 0.5	8.5RP 6.2/ 4.0
G 6/ 4	.3458	.4677	5Y 6.4/ 0.3	2.0BG 6.4/ 4.5
N 6/	.3032	.4586	N 6.0/	N 6.0/
5RP 6/ 2	.3169	.4548	5PB 6.1/ 0.2	4.0RP 6.1/ 2.2
5BG 6/ 2	.3429	.4524	5PB 6.4/ 0.2	5.0BG 6.4/ 2.4
5RP 6/ 4	.3454	.4504	5PB 6.4/ 0.3	4.5RP 6.4/ 4.2
5RP 6/ 6	.3345	.4503	5PB 6.3/ 0.3	4.5RP 6.3/ 5.6
5RP 6/ 8	.3349	.4438	5PB 6.3/ 0.7	5.0RP 6.3/ 7.3

TABLE 4. *Deuteranopic arrangement*—Continued

Munsell book notation	Deuteranopic reflectance, $W_d = Y$	Deuteranopic chromaticity coordinate, u'_d	Munsell renotations	
			Deuteranopic	Normal
BG 6/ 4	0.3425	0.4431	5PB 6.4/ 0.8	5.5BG 6.4/ 4.1
BG 6/ 6	.3473	.4379	5PB 6.4/ 1.1	5.5BG 6.4/ 5.2
RP 6/10	.3389	.4358	5PB 6.3/ 1.1	4.5RP 6.3/ 8.5
10P 6/ 4	.3238	.4176	5PB 6.2/ 2.2	10.0P 6.2/ 4.6
10BG 6/ 4	.3316	.4163	5PB 6.3/ 2.3	10.0BG 6.3/ 4.1
P 6/ 2	.3238	.4126	5PB 6.2/ 2.5	4.5P 6.2/ 3.0
B 6/ 2	.3234	.4109	5PB 6.2/ 2.6	7.5B 6.2/ 3.0
PB 6/ 2	.3432	.4007	5PB 6.4/ 3.1	5.0PB 6.4/ 3.2
10P 6/ 6	.3307	.4005	5PB 6.2/ 3.1	9.5P 6.2/ 6.2
10BG 6/ 6	.3375	.3995	5PB 6.3/ 3.2	10.0BG 6.3/ 5.8
B 6/ 4	.3250	.3858	5PB 6.2/ 3.9	6.5B 6.2/ 4.5
P 6/ 4	.3301	.3840	5PB 6.2/ 4.0	4.0P 6.2/ 4.9
10P 6/ 8	.3245	.3820	5PB 6.2/ 4.1	9.0P 6.2/ 8.0
10B 6/ 4	.3415	.3777	5PB 6.3/ 4.5	10.0B 6.3/ 4.6
PB 6/ 4	.3589	.3753	5PB 6.5/ 4.6	5.0PB 6.5/ 4.7
10PB 6/ 4	.3394	.3729	5PB 6.3/ 4.6	0.5P 6.3/ 4.8
B 6/ 6	.3128	.3586	5PB 6.1/ 5.3	5.5B 6.1/ 6.4
10B 6/ 6	.3320	.3557	5PB 6.3/ 5.4	9.0B 6.3/ 6.3
P6/ 6	.3179	.3545	5PB 6.2/ 5.4	4.5P 6.2/ 7.1
10PB 6/ 6	.3161	.3455	5PB 6.1/ 5.9	10.0PB 6.1/ 6.3
PB 6/ 6	.3404	.3447	5PB 6.3/ 6.1	5.0PB 6.3/ 6.2
P 6/ 8	.3157	.3316	5PB 6.1/ 6.7	5.0P 6.1/ 9.1
PB 6/ 8	.3329	.3260	5PB 6.3/ 7.4	5.0PB 6.3/ 7.4
10PB 6/ 8	.3200	.3210	5PY 6.2/ 7.4	0.5P 6.2/ 8.0
5YR 5/10	.2056	.8101	5Y 5.1/ 6.9	5.5YR 5.1/ 9.0
10YR 5/ 8	.2099	.8054	5Y 5.1/ 6.8	0.5Y 5.1/ 7.6
Y 5/ 6	.1984	.7817	5Y 5.0/ 6.1	6.0Y 5.0/ 6.0
GY 5/ 8	.2100	.7743	5Y 5.1/ 6.1	5.0GY 5.1/ 7.1
YR 5/ 8	.2081	.7537	5Y 5.1/ 5.7	5.5YR 5.1/ 7.7
10Y 5/ 6	.2250	.7535	5Y 5.3/ 5.8	10.0Y 5.3/ 5.8
10R 5/10	.1977	.7446	5Y 5.0/ 5.7	10.0R 5.0/ 9.9
10YR 5/ 6	.2121	.7132	5Y 5.2/ 5.0	10.0YR 5.2/ 5.7
10R 5/ 8	.2175	.6976	5Y 5.2/ 4.7	0.5YR 5.2/ 8.7
GY 5/ 6	.2066	.6931	5Y 5.1/ 4.6	5.0GY 5.1/ 5.4
10GY 5/ 8	.1910	.6963	5Y 4.9/ 4.4	9.5GY 4.9/ 7.8
YR 5/ 6	.1981	.6895	5Y, 5.0/ 4.4	5.0YR 5.0/ 6.2
10Y 5/ 4	.2224	.6776	5Y 5.3/ 4.4	0.5GY 5.3/ 4.4
Y 5/ 4	.1987	.6657	5Y 5.0/ 4.0	5.0Y 5.0/ 3.9
10GY 5/ 6	.2141	.6645	5Y 5.2/ 4.0	9.5GY 5.2/ 7.1
R 5/12	.1938	.6608	5Y 5.0/ 3.8	5.5R 5.0/12.8
10YR 5/ 4	.2048	.6554	5Y 5.1/ 3.8	10.0YR 5.1/ 4.4
10R 5/ 6	.2073	.6472	5Y 5.1/ 3.6	10.0R 5.1/ 7.1
GY 5/ 4	.2070	.6338	5Y 5.1/ 3.4	5.0GY 5.1/ 4.1
R 5/10	.2128	.6224	5Y 5.2/ 3.3	5.0R 5.2/10.9
YR 5/ 4	.1905	.6173	5Y 4.9/ 3.1	4.5YR 4.9/ 4.6
R 5/ 8	.1963	.5988	5Y 5.0/ 2.7	4.5R 5.0/10.0
10R 5/ 4	.2028	.5774	5Y 5.1/ 2.3	9.5R 5.1/ 4.9
10GY 5/ 4	.2025	.5766	5Y 5.0/ 2.3	10.0GY 5.0/ 4.3
R 5/ 6	.1998	.5594	5Y 5.0/ 2.0	4.0R 5.0/ 8.0
G 5/ 8	.1875	.5521	5Y 4.9/ 1.8	5.0G 4.9/ 8.2
Y 5/ 2	.2117	.5412	5Y 5.2/ 1.7	4.5Y 5.2/ 1.7
GY 5/ 2	.2097	.5376	5Y 5.1/ 1.6	5.0GY 5.1/ 2.0
G 5/ 6	.1869	.5348	5Y 4.9/ 1.5	5.0G 4.9/ 6.6
R 5/ 4	.1915	.5275	5Y 4.9/ 1.4	4.0R 4.9/ 5.3
YR 5/ 2	.1927	.5234	5Y 4.9/ 1.3	4.0YR 4.9/ 2.1
G 5/ 4	.1856	.5195	5Y 4.9/ 1.2	5.0G 4.9/ 4.8

TABLE 4. *Deuteranopic arrangement*—Continued

Munsell book notation	Deuteranopic reflectance, $W_d = Y$	Deuteranopic chromaticity coordinate, w_d	Munsell renotations	
			Deuteranopic	Normal
10RP 5/10	0.2180	0.5156	5Y 5.2/ 1.2	10.0RP 5.2/10.3
10RP 5/ 8	.2111	.5086	5Y 5.2/ 1.0	10.0RP 5.2/ 8.6
10RP 5/ 6	.2191	.4932	5Y 5.2/ 0.7	10.0RP 5.2/ 6.6
R 5/ 2	.1954	.4891	5Y 5.0/ 0.6	4.0R 5.0/ 2.8
G 5/ 2	.1888	.4835	5Y 4.9/ 0.5	6.5G 4.9/ 2.4
10RP 5/ 4	.2260	.4814	5Y 5.3/ 0.5	10.0RP 5.3/ 4.2
10G 5/ 6	.2013	.4767	5Y 5.0/ 0.4	1.0BG 5.0/ 7.0
10G 5/ 4	.2047	.4707	5Y 5.1/ 0.2	0.5BG 5.1/ 4.6
RP 5/ 2	.2138	.4552	5PB 5.2/ 0.1	5.0RP 5.2/ 2.3
N 5/	.1906	.4540	5PB 4.9/ 0.2	5.0PB 4.9/ 0.1
BG 5/ 2	.2077	.4501	5PB 5.1/ 0.3	4.5BG 5.1/ 2.5
RP 5/ 4	.2110	.4458	5PB 5.2/ 0.4	5.0RP 5.2/ 4.3
RP 5/ 6	.2099	.4410	5PB 5.1/ 0.7	4.5RP 5.1/ 6.2
5RP 5/10	.2301	.4395	5PB 5.3/ 0.8	5.5RP 5.3/ 9.7
RP 5/ 8	.2206	.4356	5PB 5.2/ 1.0	4.5RP 5.2/ 8.0
BG 5/ 4	.2112	.4323	5PB 5.2/ 1.1	5.5BG 5.2/ 4.4
BG 5/ 6	.2097	.4250	5PB 5.1/ 1.4	5.0BG 5.1/ 6.4
P 5/ 2	.1959	.4101	5PB 5.0/ 2.0	5.0P 5.0/ 2.5
10P 5/ 4	.2143	.4089	5PB 5.2/ 2.2	1.0RP 5.2/ 4.9
B 5/ 2	.1917	.4037	5PB 4.9/ 2.2	6.5B 4.9/ 2.6
10BG 5/ 4	.2062	.3998	5PB 5.1/ 2.5	0.5B 5.1/ 4.4
10P 5/ 6	.2129	.3922	5PB 5.2/ 2.9	1.0RP 5.2/ 6.7
PB 5/ 2	.2087	.3891	5PB 5.1/ 3.0	5.0PB 5.1/ 3.1
10P 5/ 8	.2174	.3737	5PB 5.2/ 3.8	1.0RP 5.2/ 8.6
P 5/ 4	.1934	.3697	5PB 5.0/ 3.8	4.5P 5.0/ 4.7
10BG 5/ 6	.2160	.3687	5PB 5.2/ 4.0	1.0B 5.2/ 6.5
B 5/ 4	.1959	.3618	5PB 5.0/ 4.2	5.5B 5.0/ 5.1
10B 5/ 4	.2134	.3616	5PB 5.2/ 4.3	10.0B 5.2/ 4.6
PB 5/ 4	.2170	.3599	5PB 5.2/ 4.5	4.5PB 5.2/ 4.4
10P 5/10	.2226	.3576	5PB 5.3/ 4.6	0.5RP 5.3/10.4
10PB 5/ 4	.2180	.3528	5PB 5.2/ 4.7	10.0PB 5.2/ 5.0
P 5/ 6	.1965	.3424	5PB 5.0/ 5.1	5.0P 5.0/ 6.8
B 5/ 6	.1940	.3333	5PB 5.0/ 5.5	5.0B 5.0/ 6.8
10B 5/ 6	.2132	.3292	5PB 5.2/ 5.8	9.5B 5.2/ 6.3
PB 5/ 6	.2241	.3299	5PB 5.3/ 6.1	4.0PB 5.3/ 6.2
10PB 5/ 6	.2149	.3223	5PB 5.2/ 6.3	10.0PB 5.2/ 6.8
P 5/ 8	.2107	.3154	5PB 5.1/ 6.6	5.0P 5.1/ 8.9
PB 5/ 8	.2345	.3036	5PB 5.4/ 7.5	4.0PB 5.4/ 7.9
10PB 5/ 8	.2126	.2938	5PB 5.2/ 7.8	10.0PB 5.2/ 8.4
P 5/10	.2039	.2893	5PB 5.1/ 8.1	5.0P 5.1/10.9
PB 5/10	.2263	.2871	5PB 5.3/ 8.4	3.5PB 5.3/ 8.6
10PB 5/10	.2014	.2757	5PB 5.0/ 8.8	10.0PB 5.0/ 9.6
5YR 4/ 8	.1354	.7407	5Y 4.2/ 5.8	6.0YR 4.2/ 6.3
10R 4/10	.1493	.7234	5Y 4.4/ 4.6	9.5R 4.4/ 9.0
10R 4/ 8	.1428	.7112	5Y 4.3/ 4.3	10.0R 4.3/ 8.4
10YR 4/ 4	.1318	.7063	5Y 4.2/ 4.2	10.0YR 4.2/ 4.6
R 4/14	.1334	.7081	5Y 4.2/ 4.2	5.5R 4.2/13.2
R 4/14	.1335	.7034	5Y 4.2/ 4.2	5.5R 4.2/13.2
YR 4/ 6	.1445	.7032	5Y 4.4/ 4.2	5.0YR 4.4/ 5.8
Y 4/ 4	.1243	.6871	5Y 4.1/ 3.7	5.0Y 4.1/ 3.6
R 4/12	.1360	.6831	5Y 4.2/ 3.8	5.0R 4.2/12.6
10Y 4/ 4	.1385	.6733	5Y 4.3/ 3.7	10.0Y 4.3/ 3.7
10R 4/ 6	.1424	.6726	5Y 4.3/ 3.7	10.0R 4.3/ 7.3
GY 4/ 6	.1249	.6661	5Y 4.1/ 3.4	5.0GY 4.1/ 4.0
YR 4/ 4	.1416	.6556	5Y 4.3/ 3.4	5.0YR 4.3/ 4.6
R 4/10	.1303	.6307	5Y 4.2/ 3.0	4.5R 4.2/10.8

TABLE 4. *Deuteranopic arrangement*—Continued

Munsell book notation	Deuteranopic reflectance, $W_d = Y$	Deuteranopic chromaticity coordinate, w_d	Munsell renotations	
			Deuteranopic	Normal
10GY 4/ 6	0.1355	0.6279	5Y 4.2/ 2.9	10.0GY 4.2/ 5.4
GY 4/ 4	.1313	.6173	5Y 4.2/ 2.7	5.0GY 4.2/ 3.2
R 4/ 8	.1306	.6111	5Y 4.2/ 2.6	4.5R 4.2/ 9.4
10R 4/ 4	.1348	.6007	5Y 4.2/ 2.5	0.5YR 4.2/ 4.7
10GY 4/ 4	.1337	.5716	5Y 4.2/ 2.0	1.0G 4.2/ 4.1
R 4/ 6	.1247	.5663	5Y 4.1/ 1.9	4.5R 4.1/ 6.8
Y 4/ 2	.1419	.5534	5Y 4.3/ 1.7	5.5Y 4.3/ 1.7
YR 4/ 2	.1268	.5484	5Y 4.1/ 1.5	4.0YR 4.1/ 2.3
GY 4/ 2	.1357	.5357	5Y 4.2/ 1.4	5.5GY 4.2/ 1.7
R 4/ 4	.1236	.5257	5Y 4.1/ 1.2	3.5R 4.1/ 4.7
G 4/ 4	.1291	.5218	5Y 4.1/ 1.1	5.0G 4.1/ 4.9
10RP 4/10	.1358	.5024	5Y 4.2/ 0.8	9.5RP 4.2/ 9.5
R 4/ 2	.1280	.4963	5Y 4.1/ 0.7	4.0R 4.1/ 2.6
10RP 4/ 6	.1262	.4903	5Y 4.1/ 0.6	9.5RP 4.1/ 6.4
G 4/ 2	.1282	.4884	5Y 4.1/ 0.6	6.0G 4.1/ 2.4
10RP 4/ 8	.1332	.4876	5Y 4.2/ 0.5	9.0RP 4.2/ 8.2
10RP 4/ 4	.1277	.4754	5Y 4.1/ 0.3	9.0RP 4.1/ 4.1
10G 4/ 4	.1283	.4731	5Y 4.1/ 0.3	0.5BG 4.1/ 4.5
N 4/	.1209	.4526	5PB 4.0/ 0.1	5.0PB 4.0/ 0.1
RP 4/ 2	.1445	.4474	5PB 4.4/ 0.3	4.0RP 4.4/ 2.1
BG 4/ 2	.1382	.4424	5PB 4.3/ 0.4	5.5BG 4.3/ 2.5
RP 4/ 4	.1418	.4332	5PB 4.3/ 0.8	4.0RP 4.3/ 4.4
BG 4/ 4	.1413	.4296	5PB 4.3/ 0.9	5.5BG 4.3/ 4.0
RP 4/ 6	.1406	.4230	5PB 4.3/ 1.1	4.5RP 4.3/ 6.4
RP 4/ 8	.1341	.4172	5PB 4.2/ 1.3	4.5RP 4.2/ 7.9
RP 4/10	.1359	.4127	5PB 4.2/ 1.5	4.5RP 4.2/ 9.4
BG 4/ 6	.1354	.4114	5PB 4.2/ 1.5	5.5BG 4.2/ 6.0
5RP 4/12	.1396	.4076	5PB 4.3/ 1.7	5.0RP 4.3/10.7
5P 4/ 2	.1248	.4028	5PB 4.1/ 1.8	5.0P 4.1/ 2.2
5B 4/ 2	.1374	.4005	5PB 4.3/ 1.9	5.0B 4.3/ 2.7
10BG 4/ 4	.1290	.4002	5PB 4.1/ 1.9	9.5BG 4.1/ 4.0
10P 4/ 4	.1428	.3969	5PB 4.3/ 2.1	0.5RP 4.3/ 4.5
PB 4/ 2	.1313	.3888	5PB 4.2/ 2.4	5.0PB 4.2/ 2.5
10BG 4/ 6	.1349	.3721	5PB 4.2/ 3.0	10.0BG 4.2/ 5.7
10P 4/ 6	.1407	.3718	5PB 4.3/ 3.1	0.5RP 4.3/ 6.6
P 4/ 4	.1289	.3653	5PB 4.1/ 3.2	5.0P 4.1/ 4.2
B 4/ 4	.1447	.3557	5PB 4.4/ 3.7	6 0B 4.4/ 4.6
10B 4/ 4	.1299	.3527	5PB 4.2/ 3.7	0.5PB 4.2/ 4.1
10P 4/ 8	.1406	.3519	5PB 4.3/ 3.9	0.5RP 4.3/ 8.5
PB 4/ 4	.1355	.3441	5PB 4.2/ 4.2	5.0PB 4.2/ 4.3
10PB 4/ 4	.1288	.3377	5PB 4.1/ 4.4	10.0PB 4.1/ 4.6
P 4/ 6	.1240	.3313	5PB 4.1/ 4.6	5.0P 4.1/ 6.1
10P 4/10	.1331	.3291	5PB 4.2/ 4.8	0.5RP 4.2/10.4
B 4/ 6	.1287	.3144	5PB 4.1/ 5.4	5.5B 4.1/ 6.4
PB 4/ 6	.1364	.3071	5PB 4.2/ 5.9	4.5PB 4.2/ 6.0
P 4/ 8	.1278	.3020	5PB 4.1/ 5.9	5.0P 4.1/ 8.2
10B 4/ 6	.1316	.3014	5PB 4.2/ 6.0	0.5PB 4.2/ 6.3
B 4/ 8	.1172	.2991	5PB 4.0/ 5.9	6.5B 4.0/ 6.9
10PB 4/ 6	.1321	.2985	5PB 4.2/ 6.2	10.0PB 4.2/ 6.6
10B 4, 8	.1292	.2831	5PB 4.1/ 7.0	10.0B 4.1/ 7.3
P 4/10	.1292	.2828	5PB 4.1/ 6.9	5.0P 4.1/10.1
PB 4/ 8	.1387	.2783	5PB 4.3/ 7.3	4.5PB 4.3/ 7.4
10PB 4/ 8	.1291	.2685	5PB 4.1/ 7.6	10.0PB 4.1/ 8.5
P 4/12	.1252	.2504	5PB 4.1/ 8.6	5.5P 4.1/12.6
10PB 4/10	.1224	.2492	5PB 4.0/ 8.6	10.0PB 4.0/ 9.7
PB 4/10	.1446	.2560	5PB 4.4/ 8.9	4.0PB 4.4/ 8.9

TABLE 4. *Deuteranopic arrangement*—Continued

Munsell book notation	Deuteranopic reflectance, $W_d = Y$	Deuteranopic chromaticity coordinate, w_d	Munsell renotations	
			Deuteranopic	Normal
5YR 3/ 4	0.0783	0.6552	5Y 3.3/ 3.0	5.0YR 3.3/ 4.1
10R 3/ 6	.0786	.6380	5Y 3.3/ 2.8	10.0R 3.3/ 5.4
R 3/10	.0744	.6332	5Y 3.2/ 2.7	5.0R 3.2/ 8.3
10YR 3/ 2	.0696	.6231	5Y 3.1/ 2.5	10.0YR 3.1/ 2.7
10GY 3/ 4	.0756	.6102	5Y 3.2/ 2.3	10.0GY 3.2/ 4.5
R 3/ 8	.0743	.6055	5Y 3.2/ 2.2	5.0R 3.2/ 7.4
10R 3/ 4	.0741	.5961	5Y 3.2/ 2.1	10.0R 3.2/ 4.1
GY 3/ 4	.0739	.5960	5Y 3.2/ 2.1	5.0GY 3.2/ 2.6
10Y 3/ 2	.0788	.5685	5Y 3.3/ 1.7	0.5GY 3.3/ 1.8
R 3/ 6	.0829	.5647	5Y 3.4/ 1.7	4.5R 3.4/ 6.2
YR 3/ 2	.0698	.5602	5Y 3.1/ 1.6	5.0YR 3.1/ 2.0
YR 3/ 2	.0701	.5577	5Y 3.1/ 1.5	5.0YR 3.1/ 2.1
GY 3/ 2	.0748	.5533	5Y 3.2/ 1.4	4.5GY 3.2/ 1.9
R 3/ 4	.0734	.5306	5Y 3.2/ 1.4	5.0R 3.2/ 4.6
G 3/ 4	.0803	.5407	5Y 3.3/ 1.3	4.0G 3.3/ 4.8
Y 3/ 2	.0689	.5362	5Y 3.1/ 1.2	6.0Y 3.1/ 1.1
G 3/ 2	.0703	.4989	5Y 3.1/ 0.6	5.0G 3.1/ 2.7
R 3/ 2	.0716	.4979	5Y 3.1/ 0.6	3.5R 3.1/ 2.1
10RP 3/ 8	.0698	.4847	5Y 3.1/ 0.5	9.0RP 3.1/ 7.0
10RP 3/ 6	.0712	.4821	5Y 3.1/ 0.4	9.0RP 3.1/ 5.6
10G 3/ 4	.0754	.4736	5Y 3.2/ 0.3	10.0G 3.2/ 4.7
10RP 3/ 4	.0678	.4703	5Y 3.0/ 0.3	9.0RP 3.0/ 3.4
10RP 3/10	.0735	.4640	5Y 3.2/ 0.1	8.5RP 3.2/ 8.5
N 3/	.0651	.4511	5PB 3.0/ 0.1	2.5P 3.0/ 0.2
RP 3/ 2	.0654	.4404	5PB 3.0/ 0.3	4.5RP 3.0/ 1.9
BG 3/ 2	.0727	.4327	5PB 3.2/ 0.6	5.0BG 3.2/ 2.8
RP 3/ 4	.0675	.4299	5PB 3.0/ 0.6	5.0RP 3.0/ 3.7
RP 3/ 6	.0664	.4229	5PB 3.0/ 0.8	5.0RP 3.0/ 5.2
BG 3/ 4	.0716	.4180	5PB 3.1/ 0.9	5.0BG 3.1/ 4.1
RP 3/ 8	.0706	.4060	5PB 3.1/ 1.2	5.0RP 3.1/ 6.8
RP 3/10	.0743	.3975	5PB 3.2/ 1.5	5.0RP 3.2/ 8.4
BG 3/ 6	.0767	.3970	5PB 3.2/ 1.5	6.0BG 3.2/ 5.3
P 3/ 2	.0736	.3870	5PB 3.2/ 1.8	5.0P 3.2/ 2.2
B 3/ 2	.0715	.3854	5PB 3.1/ 1.8	5.5B 3.1/ 2.3
10BG 3/ 4	.0778	.3788	5PB 3.3/ 2.0	9.5BG 3.3/ 4.3
PB 3/ 2	.0689	.3710	5PB 3.1/ 2.2	5.0PB 3.1/ 2.1
10P 3/ 4	.0731	.3699	5PB 3.2/ 2.3	10.0P 3.2/ 4.5
10BG 3/ 6	.0727	.3475	5PB 3.2/ 2.9	9.5BG 3.2/ 5.8
B 3/ 4	.0700	.3393	5PB 3.1/ 3.1	4.5B 3.1/ 4.2
10P 3/ 6	.0722	.3327	5PB 3.2/ 3.4	9.0P 3.2/ 6.3
P 3/ 4	.0705	.3278	5PB 3.1/ 3.5	5.0P 3.1/ 4.5
10B 3/ 4	.0708	.3236	5PB 3.1/ 3.6	9.5B 3.1/ 3.9
5PB 3/ 4	.0699	.3179	5PB 3.1/ 3.8	5.0PB 3.1/ 3.9
10P 3/ 8	.0709	.3097	5PB 3.1/ 4.1	10.0P 3.1/ 8.3
B 3/ 6	.0802	.3047	5PB 3.3/ 4.5	5.0B 3.3/ 5.9
10PB 3/ 4	.0713	.3026	5PB 3.1/ 4.5	10.0PB 3.1/ 4.7
P 3/ 6	.0744	.2950	5PB 3.2/ 4.8	4.5P 3.2/ 6.4
10P 3/10	.0648	.2767	5PB 3.0/ 5.2	9.0P 3.0/ 9.8
10B 3/ 6	.0765	.2840	5PB 3.2/ 5.3	9.5B 3.2/ 5.6
PB 3/ 6	.0749	.2803	5PB 3.2/ 5.5	5.0PB 3.2/ 5.6
10PB 3/ 6	.0711	.2750	5PB 3.1/ 5.5	10.0PB 3.1/ 6.1
P 3/ 8	.0759	.2681	5PB 3.2/ 6.0	5.0P 3.2/ 8.4
10B 3/ 8	.0812	.2542	5PB 3.3/ 6.9	9.0B 3.3/ 7.1
10PB 3/ 8	.0724	.2525	5PB 3.2/ 6.8	10.0PB 3.2/ 7.4
PB 3/ 8	.0768	.2498	5PB 3.2/ 7.0	4.5PB 3.2/ 7.0
P 3/10	.0769	.2342	5PB 3.2/ 7.8	5.0P 3.3/11.2

TABLE 4. *Deuteranopic arrangement*—Continued

Munsell book notation	Deuteranopic reflectance, $W_d = Y$	Deuteranopic chromaticity coordinate, w_d	Munsell renotations	
			Deuteranopic	Normal
PB 3/10	0.0844	0.2323	5PB 3.4/ 8.4	4.5PB 3.4/ 8.5
PB 3/12	.0802	.2119	5PB 3.3/ 9.4	4.0PB 3.3/ 9.4
10PB 3/10	.0693	.1960	5PB 3.1/ 9.7	10.0PB 3.1/10.0
5GY 2/ 2	.0461	.5595	5Y 2.5/ 1.6	5.5GY 2.5/ 2.2
10Y 2/ 2	.0484	.5589	5Y 2.6/ 1.4	10.0Y 2.6/ 1.6
Y 2/ 2	.0472	.5579	5Y 2.5/ 1.4	5.0Y 2.5/ 1.4
10YR 2/ 2	.0505	.5519	5Y 2.6/ 1.3	7.5YR 2.6/ 1.6
YR 2/ 2	.0439	.5420	5Y 2.4/ 1.2	4.5YR 2.4/ 1.8
10GY 2/ 2	.0440	.5399	5Y 2.4/ 1.1	9.5GY 2.4/ 2.5
10R 2/ 2	.0458	.5344	5Y 2.5/ 1.0	8.5R 2.5/ 2.6
R 2/ 4	.0384	.5168	5Y 2.3/ 0.8	4.0R 2.3/ 3.8
R 2/ 6	.0461	.5151	5Y 2.5/ 0.8	3.0R 2.5/ 4.8
R 2/ 2	.0400	.4878	5Y 2.3/ 0.5	3.5R 2.3/ 2.2
G 2/ 2	.0373	.4850	5Y 2.2/ 0.4	7.0G 2.2/ 2.4
10G 2/ 2	.0407	.4678	5Y 2.3/ 0.2	10.0G 2.3/ 3.1
N 2/	.0300	.4505	5PB 2.0/ 0.1	5.0P 2.0/ 0.2
10RP 2/ 4	.0395	.4458	5PB 2.3/ 0.1	8.0RP 2.3/ 3.7
RP 2/ 2	.0386	.4362	5PB 2.3/ 0.3	6.0RP 2.3/ 2.3
BG 2/ 2	.0379	.4351	5PB 2.2/ 0.3	4.5BG 2.2/ 2.1
10RP 2/ 6	.0416	.4333	5PB 2.4/ 0.4	8.0RP 2.4/ 5.0
BG 2/ 4	.0395	.4180	5PB 2.3/ 0.7	5.0BG 2.3/ 3.7
10BG 2/ 2	.0455	.4070	5PB 2.5/ 1.0	7.0BG 2.5/ 3.1
RP 2/ 4	.0411	.4045	5PB 2.4/ 1.0	5.0RP 2.4/ 4.6
B 2/ 2	.0381	.3952	5PB 2.2/ 1.3	2.0B 2.2/ 2.2
RP 2/ 6	.0440	.3790	5PB 2.4/ 1.7	4.0RP 2.4/ 5.9
P 2/ 2	.0351	.3506	5PB 2.1/ 2.2	5.5P 2.1/ 2.9
PB 2/ 2	.0353	.3388	5PB 2.2/ 2.5	4.5PB 2.2/ 2.8
10B 2/ 2	.0390	.3353	5PB 2.3/ 2.7	8.5B 2.2/ 3.1
10P 2/ 4	.0370	.3220	5PB 2.2/ 3.0	9.0P 2.2/ 5.3
P 2/ 4	.0358	.3102	5PB 2.2/ 3.3	5.0P 2.2/ 4.9
10P 2/ 6	.0377	.2957	5PB 2.2/ 3.7	9.0P 2.2/ 6.8
10PB 2/ 4	.0380	.2770	5PB 2.2/ 4.6	10.0PB 2.2/ 4.8
PB 2/ 4	.0385	.2715	5PB 2.3/ 4.7	4.0PB 2.3/ 4.8
10PB 2/ 6	.0358	.2660	5PB 2.2/ 4.6	10.0PB 2.2/ 5.5
P 2/ 6	.0346	.2659	5PB 2.1/ 4.6	5.0P 2.1/ 6.8
PB 2/ 6	.0405	.2446	5PB 2.3/ 5.8	4.0PB 2.3/ 5.9

TABLE 5. *Protanopic arrangement*

Munsell book notation	Protanopic reflectance, 0.9733 W_p	Protanopic chromaticity coordinate, w_p	Munsell renotations	
			Protanopic	Normal
N 9	0.7244	0.4708	5Y 8.7/ 0.2	7.5Y 8.7/ 0.1
10BG 8/ 2	.6464	.4705	5Y 8.3/ 0.2	5.0BG 8.2/ 1.9
5B 8/ 2	.6391	.4511	5PB 8.3/ 1.3	4.0B 8.2/ 2.2
10B 8/ 2	.6732	.4317	5PB 8.4/ 2.8	1.0PB 8.3/ 3.0
5PB 8/ 2	.6543	.4267	5PB 8.3/ 3.2	5.0PB 8.3/ 3.2
10PB 8/ 2	.6608	.4205	5PB 8.4/ 3.5	7.5PB 8.3/ 3.4
10Y 8/ 8	.5773	.7889	5Y 7.9/ 9.3	0.5GY 8.1/ 9.1
5GY 8/ 8	.5991	.7505	5Y 8.0/ 8.3	4.5GY 8.1/ 8.7
5GY 8/ 6	.5914	.6659	5Y 8.0/ 5.9	5.5GY 8.0/ 6.2
10Y 8/ 6	.5817	.6657	5Y 8.0/ 5.8	0.5GY 8.0/ 5.7
5Y 8/ 6	.5451	.6609	5Y 7.7/ 5.7	4.5Y 7.9/ 5.8

TABLE 5. *Protanopic arrangement*—Continued

Munsell book notation	Protanopic reflectance, 0.9733 W_p	Protanopic chromaticity coordinate, w_p	Munsell renotations	
			Protanopic	Normal
10YR 8/ 6	0. 5632	0. 6134	5Y 7. 8/ 4. 3	9. 0YR 8. 1/ 5. 5
10GY 8/ 6	. 5987	. 5866	5Y 8. 0/ 3. 6	9. 5GY 7. 9/ 5. 1
10Y 8/ 4	. 5873	. 5842	5Y 8. 0/ 3. 5	1. 0GY 8. 0/ 3. 4
5GY 8/ 4	. 6044	. 5786	5Y 8. 1/ 3. 4	6. 0GY 8. 1/ 3. 6
10GY 8/ 4	. 6362	. 5545	5Y 8. 2/ 2. 7	0. 5G 8. 2/ 4. 0
10YR 8/ 4	. 5656	. 5512	5Y 7. 9/ 2. 5	9. 0YR 8. 0/ 3. 4
5YR 8/ 4	. 5614	. 5225	5Y 7. 8/ 1. 6	4. 0YR 8. 0/ 3. 5
5G 8/ 6	. 5954	. 5187	5Y 8. 0/ 1. 5	6. 5G 7. 8/ 4. 7
5GY 8/ 2	. 5851	. 5174	5Y 8. 0/ 1. 5	6. 0GY 8. 0/ 1. 6
5G 8/ 4	. 6141	. 5075	5Y 8. 1/ 1. 3	5. 5G 8. 0/ 3. 3
10R 8/ 4	. 5725	. 5059	5Y 7. 9/ 1. 2	10. 0R 8. 1/ 3. 7
5G 8/ 2	. 5854	. 4984	5Y 8. 0/ 0. 9	4. 5G 7. 9/ 2. 1
10G 8/ 2	. 6133	. 4943	5Y 8. 1/ 0. 8	5. 0G 8. 0/ 2. 0
5YR 8/ 2	. 5731	. 4937	5Y 7. 9/ 0. 8	4. 0YR 8. 0/ 2. 0
5BG 8/ 2	. 6281	. 4803	5Y 8. 2/ 0. 5	1. 0BG 8. 1/ 2. 0
5R 8/ 4	. 5565	. 4772	5Y 7. 8/ 0. 4	3. 5R 8. 0/ 3. 6
N 8/	. 5741	. 4764	5Y 7. 9/ 0. 3	2. 5GY 7. 9/ 0. 3
5R 8/ 2	. 5857	. 4698	5Y 8. 0/ 0. 2	2. 0R 8. 1/ 2. 2
5RP 8/ 2	. 6317	. 4654	N 8. 2/	8. 0RP 8. 3/ 1. 9
10RP 8/ 4	. 5905	. 4662	N 8. 0/	9. 5RP 8. 1/ 2. 7
10RP 8/ 6	. 5958	. 4641	5PB 8. 0/ 0. 1	8. 5RP 8. 2/ 3. 6
5RP 8/ 6	. 5839	. 4586	5PB 8. 0/ 0. 6	6. 5RP 8. 1/ 3. 4
5RP 8/ 4	. 5874	. 4582	5PB 8. 0/ 0. 7	5. 5RP 8. 1/ 2. 8
5B 8/ 4	. 6310	. 4452	5PB 8. 2/ 1. 8	4. 0B 8. 1/ 2. 9
5P 8/ 2	. 5877	. 4388	5PB 8. 0/ 2. 2	5. 0P 8. 0/ 2. 5
10P 8/ 4	. 6081	. 4316	5PB 8. 1/ 2. 8	7. 5P 8. 2/ 3. 5
5P 8/ 4	. 5903	. 4054	5PB 8. 0/ 4. 5	4. 5P 8. 0/ 4. 8
5Y 8/12	. 5208	. 8848	5Y 7. 6/11. 8	5. 5Y 7. 9/12. 3
Y 8/10	. 5292	. 8501	5Y 7. 6/10. 8	5. 5Y 7. 9/11. 1
Y 8/ 8	. 5393	. 7579	5Y 7. 7/ 8. 3	5. 5Y 7. 9/ 8. 3
Y 8/ 8	. 5339	. 7525	5Y 7. 7/ 8. 2	5. 5Y 7. 9/ 8. 2
10GY 7/ 6	. 4726	. 6222	5Y 7. 3/ 4. 3	10. 0GY 7. 1/ 6. 5
Y 8/ 4	. 5426	. 5818	5Y 7. 7/ 3. 4	4. 0Y 7. 8/ 3. 5
10GY 7/ 4	. 4718	. 5631	5Y 7. 3/ 2. 7	10. 0Y 7. 2/ 4. 1
G 7/ 6	. 4749	. 5299	5Y 7. 3/ 1. 8	7. 0G 7. 0/ 6. 1
Y 8/ 2	. 5455	. 5156	5Y 7. 7/ 1. 5	3. 5Y 7. 8/ 1. 6
10G 7/ 4	. 4960	. 4951	5Y 7. 4/ 0. 8	0. 5BG 7. 2/ 3. 9
BG 7/ 2	. 4913	. 4752	5Y 7. 4/ 0. 3	3. 5BG 7. 3/ 2. 1
BG 7/ 4	. 4908	. 4733	5Y 7. 4/ 0. 2	4. 5BG 7. 2/ 3. 4
RP 7/ 4	. 4693	. 4558	5PB 7. 3/ 0. 8	6. 0RP 7. 4/ 3. 3
B 7/ 2	. 4895	. 4505	5PB 7. 4/ 1. 2	3. 5B 7. 3/ 2. 2
10BG 7/ 4	. 4863	. 4471	5PB 7. 4/ 1. 4	0. 5B 7. 2/ 3. 6
RP 7/ 6	. 4687	. 4463	5PB 7. 3/ 1. 6	5. 0RP 7. 4/ 4. 4
B 7/ 4	. 4875	. 4313	5PB 7. 4/ 2. 5	5. 0B 7. 2/ 3. 7
PB 7/ 2	. 5049	. 4260	5PB 7. 5/ 2. 9	3. 5PB 7. 4/ 3. 0
B 7/ 6	. 4798	. 4213	5PB 7. 3/ 3. 1	5. 0B 7. 1/ 4. 7
10B 7/ 4	. 4794	. 4158	5PB 7. 3/ 3. 5	9. 0B 7. 2/ 4. 0
PB 7/ 4	. 4942	. 4048	5PB 7. 4/ 4. 3	4. 0PB 7. 3/ 4. 5
10B 7/ 6	. 4959	. 3963	5PB 7. 5/ 4. 9	9. 5B 7. 2/ 5. 7
PB 7/ 6	. 4817	. 3878	5PB 7. 3/ 5. 4	4. 0PB 7. 2/ 5. 6
10Y 7/ 8	. 4214	. 8324	5Y 6. 9/ 9. 5	10. 0Y 7. 1/ 9. 3
GY 7/10	. 4235	. 8191	5Y 7. 0/ 9. 2	4. 0GY 7. 0/ 9. 5
GY 7/ 8	. 4506	. 7486	5Y 7. 1/ 7. 5	5. 0GY 7. 1/ 8. 0
10Y 7/ 6	. 4176	. 7387	5Y 6. 9/ 7. 0	0. 5GY 7. 0/ 6. 9
GY 7/ 6	. 4502	. 6922	5Y 7. 1/ 6. 1	5. 0GY 7. 1/ 6. 4
10GY 7/ 8	. 4655	. 6697	5Y 7. 2/ 5. 5	10. 0GY 7. 1/ 8. 3
10Y 7/ 4	. 4340	. 6064	5Y 7. 0/ 3. 8	1. 0GY 7. 1/ 3. 6

TABLE 5. *Protanopic arrangement*—Continued

Munsell book notation	Protanopic reflectance, 0.9733 W_p	Protanopic chromaticity coordinate, w_p	Munsell renotations	
			Protanopic	Normal
GY 7/ 4	0. 4364	0. 5973	5Y 7. 0/ 3. 6	5. 5GY 7. 0/ 3. 8
Y 7/ 4	. 4079	. 6033	5Y 6. 8/ 3. 5	4. 0Y 7. 0/ 3. 8
10YR 7/ 4	. 4296	. 5746	5Y 7. 0/ 2. 9	9. 0YR 7. 2/ 3. 8
YR 7/ 4	. 4016	. 5422	5Y 6. 8/ 2. 0	3. 0YR 7. 0/ 4. 1
10R 7/ 6	. 4036	. 5329	5Y 6. 8/ 1. 8	9. 0R 7. 2/ 5. 7
GY 7/ 2	. 4261	. 5244	5Y 7. 0/ 1. 6	5. 5GY 7. 0/ 1. 8
Y 7/ 2	. 4359	. 5213	5Y 7. 0/ 1. 6	4. 0Y 7. 1/ 1. 6
G 7/ 4	. 4613	. 5168	5Y 7. 2/ 1. 4	6. 5G 7. 0/ 4. 3
10R 7/ 4	. 4122	. 5145	5Y 6. 9/ 1. 3	8. 5R 7. 2/ 4. 7
5YR 7/ 2	. 4183	. 5013	5Y 6. 9/ 1. 0	3. 0YR 7. 0/ 2. 1
G 7/ 2	. 4371	. 4926	5Y 7. 0/ 0. 7	6. 5G 7. 0/ 2. 1
R 7/ 6	. 3999	. 4899	5Y 6. 8/ 0. 6	3. 5R 7. 1/ 5. 7
R 7/ 4	. 4012	. 4809	5Y 6. 8/ 0. 4	3. 0R 7. 1/ 5. 2
R 7/ 2	. 4336	. 4729	5Y 7. 0/ 0. 2	2. 5R 7. 2/ 2. 6
10RP 7/ 4	. 4154	. 4657	N 6. 9/	9. 5RP 7. 1/ 3. 5
10RP 7/ 6	. 4213	. 4649	N 6. 9/	9. 5RP 7. 2/ 4. 7
N 7/	. 4441	. 4633	5PB 7. 1/ 0. 1	7. 5PB 7. 1/ 0. 1
10RP 7/ 8	. 3999	. 4625	5PB 6. 8/ 0. 2	9. 0RP 7. 1/ 5. 8
RP 7/ 2	. 4599	. 4600	5PB 7. 2/ 0. 4	6. 5RP 7. 3/ 2. 3
RP 7/ 8	. 4540	. 4400	5PB 7. 2/ 1. 9	4. 5RP 7. 4/ 4. 9
10P 7/ 4	. 4510	. 4273	5PB 7. 1/ 2. 7	10. 0P 7. 2/ 4. 0
P 7/ 2	. 4085	. 4259	5PB 6. 8/ 2. 7	4. 5P 6. 9/ 2. 7
10P 7/ 6	. 4505	. 4204	5PB 7. 1/ 3. 1	9. 5P 7. 2/ 4. 6
10PB 7/ 4	. 4544	. 4072	5PB 7. 2/ 4. 0	10. 0PB 7. 1/ 4. 0
10P 7/ 8	. 4489	. 4061	5PB 7. 1/ 4. 2	9. 5P 7. 3/ 6. 0
P 7/ 4	. 4419	. 4005	5PB 7. 1/ 4. 4	5. 0P 7. 1/ 4. 8
10PB 7/ 6	. 4435	. 3838	5PB 7. 1/ 5. 6	10. 0PB 7. 0/ 5. 3
P 7/ 6	. 4283	. 3775	5PB 7. 0/ 5. 8	5. 5P 7. 0/ 6. 4
Y 7/10	. 3814	. 8415	5Y 6. 6/ 9. 5	5. 0Y 6. 9/ 9. 7
Y 7/ 8	. 3879	. 8353	5Y 6. 7/ 9. 4	6. 0Y 6. 9/ 9. 5
10YR 7/10	. 3602	. 8235	5Y 6. 5/ 8. 7	1. 0Y 6. 9/10. 5
10YR 7/ 8	. 3885	. 7388	5Y 6. 7/ 6. 9	0. 5Y 7. 1/ 8. 3
YR 7/10	. 3443	. 7299	5Y 6. 4/ 6. 4	5. 5YR 6. 9/10. 1
Y 7/ 6	. 3854	. 7188	5Y 6. 7/ 6. 4	4. 5Y 6. 9/ 6. 6
10GY 6/ 8	. 3403	. 6868	5Y 6. 3/ 5. 3	9. 0GY 6. 2/ 7. 7
10YR 7/ 6	. 3919	. 6650	5Y 6. 7/ 5. 2	10. 0YR 7. 0/ 6. 3
YR 7/ 8	. 3696	. 6548	5Y 6. 6/ 4. 7	4. 5YR 7. 0/ 8. 2
10GY 6/ 6	. 3343	. 6486	5Y 6. 3/ 4. 5	10. 0GY 6. 1/ 6. 7
YR 7/ 6	. 3757	. 5906	5Y 6. 6/ 3. 2	3. 5YR 7. 0/ 6. 0
YR 7/ 6	. 3682	. 5894	5Y 6. 5/ 3. 2	3. 5YR 6. 9/ 5. 9
10R 7/ 8	. 3635	. 5736	5Y 6. 5/ 2. 8	10. 0R 7. 0/ 7. 5
G 6/ 6	. 3378	. 5566	5Y 6. 3/ 2. 3	6. 0G 6. 0/ 7. 4
G 6/ 4	. 3377	. 5239	5Y 6. 3/ 1. 5	6. 0G 6. 1/ 4. 6
10G 6/ 6	. 3889	. 5060	5Y 6. 7/ 1. 1	1. 0BG 6. 4/ 6. 0
10G 6/ 4	. 3743	. 4943	5Y 6. 6/ 0. 7	2. 0BG 6. 4/ 4. 5
R 7/ 8	. 3698	. 4911	5Y 6. 6/ 0. 7	3. 5R 7. 0/ 7. 0
BG 6/ 2	. 3593	. 4708	5Y 6. 5/ 0. 2	5. 0BG 6. 4/ 2. 4
BG 6/ 4	. 3700	. 4690	5Y 6. 6/ 0. 1	5. 5BG 6. 4/ 4. 1
5BG 6/ 6	. 3810	. 4676	5Y 6. 6/ 0. 1	5. 5BG 6. 4/ 5. 2
10BG 6/ 4	. 3593	. 4426	5PB 6. 5/ 1. 5	10. 0BG 6. 3/ 4. 1
10BG 6/ 6	. 3776	. 4334	5PB 6. 6/ 2. 1	10. 0BG 6. 3/ 5. 8
B 6/ 2	. 3400	. 4296	5PB 6. 3/ 2. 2	7. 5B 6. 2/ 3. 0
PB 6/ 2	. 3530	. 4141	5PB 6. 4/ 3. 2	5. 0PB 6. 4/ 3. 2
B 6/ 4	. 3527	. 4119	5PB 6. 4/ 3. 4	6. 5B 6. 2/ 4. 5
10B 6/ 4	. 3665	. 4010	5BP 6. 5/ 4. 0	10. 0B 6. 3/ 4. 6
B 6/ 6	. 3527	. 3931	5PB 6. 4/ 4. 5	5. 5B 6. 1/ 6. 4
PB 6/ 4	. 3759	. 3927	5PB 6. 6/ 4. 7	5. 0PB 6. 5/ 4. 7
10B 6/ 6	. 3654	. 3843	5PB 6. 5/ 5. 1	9. 0B 6. 3/ 6. 3

TABLE 5. *Protanopic arrangement*—Continued

Munsell book notation	Protanopic reflectance, 0.9733 W_p	Protanopic chromaticity coordinate, u_p	Munsell renotations	
			Protanopic	Normal
10PB 6/ 4	0.3436	0.3821	5PB 6.4/ 5.2	0.5P 6.3/ 4.8
PB 6/ 6	.3634	.3659	5PB 6.5/ 6.3	5.0PB 6.3/ 6.2
PB 6/ 8	.3575	.3624	5PB 6.5/ 6.4	5.0PB 6.3/ 7.4
10YR 6/10	.3090	.8170	5Y 6.1/ 8.2	10.0YR 6.5/ 9.8
Y 6/ 8	.2967	.8224	5Y 6.0/ 8.1	5.5Y 6.2/ 8.3
Y 6/ 6	.2876	.8199	5Y 5.9/ 8.0	5.5Y 6.1/ 8.1
10Y 6/ 6	.3115	.7940	5Y 6.1/ 7.7	9.5Y 6.2/ 7.4
Y 6/ 6	.2924	.7718	5Y 5.9/ 7.0	5.0Y 6.2/ 7.2
YR 6/10	.2735	.7544	5Y 5.8/ 6.5	6.0YR 6.3/ 9.8
GY 6/ 8	.3222	.7499	5Y 6.2/ 6.7	4.0GY 6.2/ 7.2
10YR 6/ 8	.3013	.7449	5Y 6.0/ 6.5	9.5YR 6.4/ 8.0
GY 6/ 6	.3198	.7299	5Y 6.2/ 6.2	5.0GY 6.2/ 6.7
10GY 6/10	.3224	.7206	5Y 6.2/ 6.1	9.0GY 6.0/ 8.7
10YR 6/ 6	.3003	.6953	5Y 6.0/ 5.4	9.5YR 6.3/ 6.7
YR 6/ 8	.2731	.6871	5Y 5.8/ 5.0	5.0YR 6.2/ 8.3
10Y 6/ 4	.3188	.6400	5Y 6.2/ 4.2	10.0Y 6.2/ 4.1
Y 6/ 4	.2930	.6317	5Y 5.9/ 3.9	4.5Y 6.1/ 4.0
GY 6/ 4	.3212	.6211	5Y 6.2/ 3.8	5.0GY 6.2/ 4.0
YR 6/ 6	.2808	.6153	5Y 5.8/ 3.5	4.5YR 6.2/ 6.0
10R 6/ 8	.2737	.6060	5Y 5.8/ 3.3	0.5YR 6.3/ 8.2
10YR 6/ 4	.2916	.6055	5Y 5.9/ 3.3	0.5Y 6.1/ 4.1
10GY 6/ 4	.3239	.5772	5Y 6.2/ 2.8	0.5G 6.1/ 4.4
10R 6/ 6	.2808	.5683	5Y 5.9/ 2.4	0.5YR 6.3/ 6.5
YR 6/ 4	.2826	.5580	5Y 5.8/ 2.2	4.0YR 6.1/ 4.0
Y 6/ 2	.3127	.5319	5Y 6.1/ 1.7	4.0Y 6.2/ 1.7
GY 6/ 2	.3243	.5305	5Y 6.2/ 1.7	5.0GY 6.2/ 1.7
10R 6/ 4	.2944	.5244	5Y 5.9/ 1.4	9.0R 6.2/ 4.2
5YR 6/ 2	.2977	.5103	5Y 6.0/ 1.1	4.5YR 6.1/ 2.0
5G 6/ 2	.3158	.5006	5Y 6.1/ 0.9	6.0G 6.0/ 2.4
R 6/ 6	.2879	.4921	5Y 5.9/ 0.6	3.5R 6.2/ 6.3
R 6/ 4	.3004	.4888	5Y 6.0/ 0.6	4.5R 6.3/ 4.5
R 6/ 2	.3060	.4758	5Y 6.0/ 0.2	4.0R 6.2/ 2.3
N 6/	.3032	.4653	N 6.0/	N 6.0/
10RP 6/ 6	.2915	.4506	5PB 5.9/ 0.4	9.0RP 6.2/ 5.5
10RP 6/ 4	.3019	.4503	5PB 6.0/ 0.3	8.5RP 6.2/ 4.0
10RP 6/ 8	.2811	.4583	5PB 5.8/ 0.4	9.0RP 6.2/ 7.0
RP 6/ 2	.3072	.4538	5PB 6.1/ 0.8	4.0RP 6.1/ 2.2
RP 6/ 4	.3260	.4428	5PB 6.2/ 1.4	4.5RP 6.4/ 4.2
RP 6/ 6	.3057	.4347	5PB 6.0/ 1.8	4.5RP 6.3/ 5.6
RP 6/ 8	.2968	.4208	5PB 6.0/ 2.6	5.0RP 6.3/ 7.3
P 6/ 2	.3218	.4176	5PB 6.2/ 2.9	4.5P 6.2/ 3.0
10P 6/ 4	.3098	.4135	5PB 6.1/ 3.1	10.0P 6.2/ 4.6
RP 6/10	.2951	.4086	5PB 6.0/ 3.3	4.5RP 6.3/ 8.5
10P 6/ 6	.3121	.3931	5PB 6.1/ 4.4	9.5P 6.2/ 6.2
P 6/ 4	.3270	.3882	5PB 6.2/ 4.7	4.0P 6.2/ 4.9
10P 6/ 8	.3013	.3710	5PB 6.0/ 5.6	9.0P 6.2/ 8.0
P 6/ 6	.3126	.3569	5PB 6.1/ 6.7	4.5P 6.2/ 7.1
10PB 6/ 6	.3227	.3564	5PB 6.2/ 6.7	10.0PB 6.1/ 6.3
P 6/ 8	.3080	.3322	5PB 6.1/ 8.4	5.0P 6.1/ 9.1
10PB 6/ 8	.3277	.3322	5PB 6.2/ 8.4	0.5P 6.2/ 8.0
YR 6/12	.2572	.8107	5Y 5.6/ 7.5	6.0YR 6.2/11.5
10GY 5/ 6	.2272	.6835	5Y 5.3/ 4.6	9.5GY 5.2/ 7.1
10R 6/10	.2909	.6572	5Y 5.6/ 4.2	0.5YR 6.2/10.1
10G 5/ 6	.2292	.5159	5Y 5.3/ 1.2	1.0BG 5.0/ 7.0
R 6/10	.2571	.5124	5Y 5.6/ 1.1	4.0R 6.2/ 9.7
R 6/ 8	.2992	.5045	5Y 5.7/ 0.9	4.0R 6.2/ 8.1

TABLE 5. *Protanopic arrangement*—Continued

Munsell book notation	Protanopic reflectance, 0.9733 W_p	Protanopic chromaticity coordinate, u_p	Munsell renotations	
			Protanopic	Normal
10G 5/ 4	0.2235	0.4093	5Y 5.3/ 0.8	0.5BG 5.1/ 4.6
BG 5/ 6	.2393	.4643	5PB 5.4/ 0.1	5.0BG 5.1/ 6.4
BG 5/ 4	.2320	.4623	5PB 5.4/ 0.2	5.5BG 5.2/ 4.4
10RP 6/10	.2666	.4563	5PB 5.7/ 0.6	9.5RP 6.2/ 8.8
10BG 5/ 4	.2276	.4303	5PB 5.3/ 1.8	0.5B 5.1/ 4.4
10BG 5/ 6	.2493	.4091	5PB 5.5/ 2.9	1.0B 5.2/ 6.3
10B 5/ 4	.2315	.3869	5PB 5.4/ 4.2	10.0B 5.2/ 4.6
PB 5/ 4	.2294	.3792	5PB 5.3/ 4.5	4.5PB 5.2/ 4.4
B 5/ 6	.2252	.3735	5PB 5.3/ 4.8	5.0B 5.0/ 6.8
10PB 5/ 4	.2219	.3631	5PB 5.3/ 5.3	10.0PB 5.2/ 5.0
10B 5/ 6	.2393	.3615	5PB 5.4/ 5.5	9.5B 5.2/ 6.3
5PB 5/ 6	.2426	.3539	5PB 5.5/ 6.0	4.0PB 5.3/ 6.2
PB 5/ 8	.2606	.3323	5PB 5.6/ 7.6	4.0PB 5.4/ 7.9
PB 5/10	.2567	.3194	5PB 5.6/ 8.5	3.5PB 5.3/ 8.6
GY 5/ 8	.2112	.7800	5Y 5.2/ 6.4	5.0GY 5.1/ 7.1
10YR 5/ 8	.1811	.7859	5Y 4.8/ 6.2	0.5Y 5.1/ 7.6
Y 5/ 6	.1831	.7725	5Y 4.8/ 5.9	6.0Y 5.0/ 6.9
10Y 5/ 6	.2155	.7505	5Y 5.2/ 5.9	10.0Y 5.3/ 5.8
10GY 5/ 8	.2044	.7160	5Y 5.1/ 5.2	9.5GY 4.9/ 7.8
GY 5/ 6	.2076	.6998	5Y 5.1/ 4.8	5.0GY 5.1/ 5.4
10YR 5/ 6	.1873	.6928	5Y 4.9/ 4.5	10.0YR 5.2/ 5.7
10Y 5/ 4	.2154	.6766	5Y 5.2/ 4.4	0.5GY 5.3/ 4.9
Y 5/ 4	.1871	.6582	5Y 4.9/ 3.9	5.0Y 5.0/ 3.9
GY 5/ 4	.2069	.6400	5Y 5.1/ 3.7	5.0GY 5.1/ 4.1
10YR 5/ 4	.1854	.6388	5Y 4.9/ 3.5	10.0YR 5.1/ 4.4
10GY 5/ 4	.2111	.5933	5Y 5.2/ 2.8	10.0GY 5.0/ 4.2
G 5/ 8	.2122	.5890	5Y 5.2/ 2.7	5.0G 4.9/ 8.2
G 5/ 6	.2075	.5673	5Y 5.1/ 2.3	5.0G 4.9/ 6.6
G 5/ 4	.2008	.5458	5Y 5.0/ 1.8	5.0G 4.9/ 4.8
GY 5/ 2	.2097	.5443	5Y 5.1/ 1.8	5.0GY 5.1/ 2.0
Y 5/ 2	.2056	.5406	5Y 5.1/ 1.7	4.5Y 5.2/ 1.7
YR 5/ 2	.1813	.5149	5Y 4.8/ 1.0	4.0YR 4.9/ 2.1
G 5/ 2	1971	.5010	5Y 5.0/ 0.8	6.5G 4.9/ 2.4
R 5/ 2	1819	.4780	5Y 4.8/ 0.3	4.0R 5.0/ 2.8
BG 5/ 2	2200	.4710	5Y 5.2/ 0.1	4.5BG 5.1/ 2.7
10RP 5/ 4	.2050	.4638	5PB 5.1/ 0.1	10.1RP 5.3/ 4.2
N 5/	.1908	.4610	5PB 4.9/ 0.2	5.0PB 4.9/ 0.1
10RP 5/ 6	.1857	.4588	5PB 4.9/ 0.3	10.0RP 5.2/ 5.6
RP 5/ 2	.2048	.4512	5PB 5.1/ 0.7	5.0RP 5.2/ 2.3
RP 5/ 4	.1943	.4321	5PB 5.0/ 1.5	5.0RP 5.2/ 4.3
B 5/ 2	.2031	.4244	5PB 5.1/ 2.0	6.5B 4.9/ 2.6
RP 5/ 6	.1843	.4158	5PB 4.8/ 2.2	4.5RP 5.1/ 6.2
P 5/ 2	.1941	.4144	5PB 5.0/ 2.4	5.0P 5.0/ 2.5
RP 5/ 8	.1863	.4011	5PB 4.9/ 2.9	4.5RP 5.2/ 8.0
PB 5/ 2	.2164	.4042	5PB 5.2/3.0	5.0PB 5.1/ 3.1
10P 5/ 4	.2005	.3994	5PB 5.0/3.2	1.0RP 5.2/ 4.9
RP 5/10	.1862	.3947	5PB 4.9/ 3.3	5.5RP 5.3/ 9.7
B 5/ 4	.2187	.3941	5PB 5.2/ 3.3	5.5B 5.0/ 5.1
10P 5/ 6	.1937	.3763	5PB 5.0/ 4.4	1.0RP 5.2/ 6.7
5P 5/ 4	.1903	.3722	5PB 4.9/ 4.5	4.5P 5.0/ 4.7
10P 5/ 8	.1933	.3528	5PB 5.0/ 5.6	1.0RP 5.2/ 8.6
P 5/ 6	.1910	.3420	5PB 4.9/ 6.2	5.0P 5.0/ 6.8
10P 5/10	.1922	.3306	5PB 4.9/ 7.0	0.5RP 5.3/10.4
10PB 5/ 6	.2213	.3348	5PB 5.3/ 7.2	10.0PB 5.2/ 6.8
P 5/ 8	.2035	.3137	5PB 5.1/ 8.5	5.0P 5.1/ 8.9
10PB 5/ 8	.2206	.3073	5PB 5.2/ 9.1	10.0PB 5.2/ 8.4
10PB 5/10	.2104	.2901	5PB 5.1/10.3	10.0PB 5.0/ 9.6

TABLE 5. *Protanopic arrangement*—Continued

Munsell book notation	Protanopic reflectance, 0.9733 W_p	Protanopic chromaticity coordinate, u_p	Munsell renotations	
			Protanopic	Normal
P 5/10	0.1950	0.2858	5PB 5.0/10.4	5.0P 5.1/10.9
YR 5/10	.1634	.7770	5Y 4.6/ 5.8	5.5YR 5.1/ 9.0
YR 5/ 8	.1698	.7196	5Y 4.7/ 4.9	5.5YR 5.1/ 7.7
10R 5/10	.1445	.6865	5Y 4.4/ 4.1	10.0R 5.0/ 9.9
YR 5/ 6	.1668	.6577	5Y 4.6/ 3.7	5.0YR 5.0/ 6.2
10GY 4/ 6	.1443	.6487	5Y 4.4/ 3.4	10.0GY 4.2/ 5.4
10R 5/ 8	.1678	.6464	5Y 4.7/ 3.5	0.5YR 5.2/ 8.7
10R 5/ 6	.1665	.6023	5Y 4.6/ 2.7	10.0R 5.1/ 7.1
YR 5/ 4	.1671	.5025	5Y 4.6/ 2.6	4.5YR 4.9/ 4.6
10GY 4/ 4	.1412	.5915	5Y 4.3/ 2.4	1.0G 4.2/ 4.1
Y 4/ 2	.1376	.5526	5Y 4.3/ 1.7	5.5Y 4.3/ 1.7
G 4/ 4	.1414	.5512	5Y 4.3/ 1.7	5.0G 4.1/ 4.9
10R 5/ 4	.1749	.5477	5Y 4.7/ 1.7	9.5R 5.1/ 4.9
R 5/10	.1497	.5437	5Y 4.4/ 1.5	5.0R 5.2/10.9
R 5/ 8	.1427	.5271	5Y 4.3/ 1.2	4.5R 5.0/10.0
R 5/ 6	.1572	.5064	5Y 4.5/ 0.9	4.0R 5.0/ 8.0
10G 4/ 4	.1421	.5054	5Y 4.3/ 0.8	0.5BG 4.1/ 4.5
R 5/ 4	.1636	.4950	5Y 4.6/ 0.6	4.0R 4.9/ 5.3
BG 4/ 2	.1475	.4652	N 4.4/	5.5BG 4.3/ 2.5
BG 4/ 4	.1561	.4609	5PB 4.5/ 0.1	5.5BG 4.3/ 4.0
10RP 5/ 8	.1665	.4561	5PB 4.6/ 0.4	10.0RP 5.2/ 8.6
BG 4/ 6	.1563	.4533	5PB 4.5/ 0.5	5.5BG 4.2/ 6.0
10RP 5/10	.1648	.4526	5PB 4.6/ 0.5	10.0RP 5.2/10.3
RP 4/ 2	.1379	.4425	5PB 4.3/ 0.8	4.0RP 4.4/ 2.1
10BG 4/ 4	.1437	.4330	5PB 4.3/ 1.2	9.5BG 4.1/ 4.0
B 4/ 2	.1468	.4230	5PB 4.4/ 1.6	5.0B 4.3/ 2.7
10BG 4/ 6	.1564	.4139	5PB 4.5/ 2.0	10.0BG 4.2/ 5.7
B 4/ 4	.1619	.3882	5PB 4.6/ 3.2	6.0B 4.4/ 4.6
10B 4/ 4	.1416	.3790	5PB 4.3/ 3.5	0.5PB 4.2/ 4.1
PB 4/ 4	.1444	.3649	5PB 4.4/ 4.3	5.0PB 4.2/ 4.3
B 4/ 6	.1511	.3561	5PB 4.4/ 4.9	5.5B 4.1/ 6.4
5B 4/ 8	.1398	.3433	5PB 4.3/ 5.3	6.5B 4.0/ 6.9
10B 4/ 6	.1505	.3363	5PB 4.4/ 5.9	0.5PB 4.2/ 6.3
PB 4/ 6	.1502	.3339	5PB 4.4/ 5.9	4.5PB 4.2/ 6.0
10B 4/ 8	.1524	.3238	5PB 4.5/ 6.7	10.0B 4.1/ 7.3
PB 4/ 8	.1569	.3095	5PB 4.5/ 7.6	4.5PB 4.3/ 7.4
PB 4/10	.1681	.2913	5PB 4.7/ 9.3	4.0PB 4.4/ 8.9
YR 4/ 8	.1114	.7072	5Y 3.9/ 4.1	6.0YR 4.2/ 6.3
10YR 4/ 4	.1165	.6860	5Y 3.9/ 3.8	10.0YR 4.2/ 4.6
10Y 4/ 4	.1340	.6720	5Y 4.2/ 3.8	10.0Y 4.3/ 3.7
Y 4/ 4	.1162	.6784	5Y 3.9/ 3.7	5.0Y 4.1/ 3.6
GY 4/ 6	.1251	.6724	5Y 4.1/ 3.7	5.0GY 4.1/ 4.0
YR 4/ 6	.1203	.6696	5Y 4.0/ 3.6	5.0YR 4.4/ 5.8
10R 4/10	.1078	.6599	5Y 3.8/ 3.4	9.5R 4.4/ 9.0
10R 4/ 8	.1055	.6514	5Y 3.8/ 3.2	10.0R 4.3/ 8.4
YR 4/ 4	.1215	.6265	5Y 4.0/ 2.9	5.0YR 4.3/ 4.6
GY 4/ 4	.1316	.6242	5Y 4.2/ 2.9	5.0GY 4.2/ 3.2
10R 4/ 6	.1102	.6203	5Y 3.9/ 2.7	10.0R 4.3/ 7.3
10R 4/ 4	.1138	.5661	5Y 3.9/ 1.8	0.5YR 4.2/ 4.7
R 5/12	.1252	.5638	5Y 4.1/ 1.8	5.5R 5.0/12.8
GY 4/ 2	.1360	.5429	5Y 4.2/ 1.5	5.5GY 4.2/ 1.7
YR 4/ 2	.1166	.5343	5Y 3.9/ 1.2	4.0YR 4.1/ 2.3
G 4/ 2	.1347	.5075	5Y 4.2/ 0.8	6.0G 4.1/ 2.4
R 4/ 4	.1046	.4909	5Y 3.8/ 0.5	3.5R 4.1/ 4.7
R 4/ 2	.1180	.4827	5Y 4.0/ 0.3	4.0R 4.1/ 2.6
N 4/	.1211	.4597	5PB 4.0/ 0.1	5.0PB 4.0/ 0.1
10RP 4/ 4	.1128	.4513	5PB 3.9/ 0.4	9.0RP 4.1/ 4.1

TABLE 5. *Protanopic arrangement*—Continued

Munsell book notation	Protanopic reflectance, 0.9733 W_p	Protanopic chromaticity coordinate, u_p	Munsell renotations	
			Protanopic	Normal
RP 4/ 4	0.1282	0.4152	5PB 4.1/ 1.8	4.0RP 4.3/ 4.4
P 4/ 2	.1234	.4067	5PB 4.1/ 2.2	5.0P 4.1/ 2.2
PB 4/ 2	.1359	.4035	5PB 4.2/ 2.4	5.0PB 4.2/ 2.5
RP 4/ 6	.1206	.3925	5PB 4.0/ 2.7	4.5RP 4.3/ 6.4
10P 4/ 4	.1329	.3861	5PB 4.2/ 3.1	0.5RP 4.3/ 4.5
RP 4/ 8	.1068	.3759	5PB 3.8/ 3.1	4.5RP 4.2/ 7.9
RP 4/10	.1060	.3602	5PB 3.8/ 3.8	4.5RP 4.2/ 9.4
P 4/ 4	.1256	.3654	5PB 4.1/ 4.0	5.0P 4.1/ 4.2
RP 4/12	.1047	.3465	5PB 3.8/ 4.5	5.0RP 4.3/10.7
10P 4/ 6	.1262	.3530	5PB 4.1/ 4.6	0.5RP 4.3/ 6.6
10PB 4/ 4	.1314	.3483	5PB 4.2/ 5.0	10.0PB 4.1/ 4.6
P 4/ 6	.1198	.3297	5BP 4.0/ 5.8	5.0P 4.1/ 6.1
10P 4/ 8	.1226	.3274	5PB 4.0/ 5.9	0.5RP 4.3/ 8.5
10PB 4/ 6	.1365	.3111	5PB 4.2/ 7.1	10.0PB 4.2/ 6.6
P 4/ 8	.1219	.2977	5PB 4.0 /7.8	5.0P 4.1/ 8.2
10P 4/10	.1112	.2964	5PB 3.9/ 7.5	0.5RP 4.2/10.4
10PB 4/ 8	.1347	.2824	5PB 4.2/ 9.2	10.0PB 4.1/ 8.5
5P 4/10	.1212	.2754	5PB 4.0/ 9.3	5.0P 4.1/10.1
10PB 4/10	.1283	.2633	5PB 4.1/10.2	10.0PB 4.0/ 9.7
P 4/12	.1145	.2388	5PB 3.9/12.1	5.5P 4.1/12.6
10GY 3/ 4	.0804	.6310	5Y 3.3/ 2.8	10.0GY 3.2/ 4.5
G 3/ 4	.0885	.5713	5Y 3.3/ 1.8	4.0G 3.3/ 4.8
10Y 3/ 2	.0775	.5710	5Y 3.3/ 1.8	0.5GY 3.3/ 1.8
R 4/12	.0812	.5693	5Y 3.3/ 1.8	5.0R 4.2/12.6
R 4/10	.0851	.5339	5Y 3.4/ 1.2	4.5R 4.2/10.8
R 4/ 8	.0912	.5300	5Y 3.5/ 1.1	4.5R 4.2/ 9.4
R 4/ 6	.0967	.5160	5Y 3.6/ 0.8	4.5R 4.1/ 6.8
10G 3/ 4	.0849	.5099	5Y 3.4/ 0.8	10.0G 3.2/ 4.7
5BG 3/ 2	.0791	.4604	5PB 3.3/ 0.1	5.0BG 3.2/ 2.8
BG 3/ 4	.0809	.4546	5PB 3.3/ 0.3	5.0BG 3.1/ 4.1
10RP 4/ 6	.1019	.4438	5PB 3.7/ 0.6	9.5RP 4.1/ 6.4
BG 3/ 6	.0893	.4407	5PB 3.5/ 0.7	6.0BG 3.2/ 5.3
10RP 4/ 8	.1027	.4297	5PB 3.7/ 1.1	9.0RP 4.2/ 8.2
10RP 4/10	.0980	.4281	5PB 3.6/ 1.1	9.5RP 4.2/ 9.5
10BG 3/ 4	.0888	.4168	5PB 3.5/ 1.4	9.5BG 3.3/ 4.3
B 3/ 2	.0774	.4109	5PB 3.3/ 1.5	5.5B 3.1/ 2.3
10BG 3/ 6	.0870	.3958	5PB 3.4/ 2.1	9.5BG 3.2/ 5.8
B 3/ 4	.0803	.3771	5PB 3.3/ 2.6	4.5B 3.1/ 4.2
10B 3/ 4	.0794	.3554	5PB 3.3/ 3.4	9.5B 3.1/ 3.9
B 3/ 6	.0961	.3504	5PB 3.6/ 3.9	5.0B 3.3/ 5.9
10B 3/ 6	.0909	.3241	5PB 3.5/ 5.2	9.5B 3.2/ 5.6
PB 3/ 6	.0829	.3095	5PB 3.4/ 5.8	5.0PB 3.2/ 5.6
10B 3/ 8	.0997	.3006	5PB 3.7/ 6.7	9.0B 3.3/ 7.1
PB 3/ 8	.0892	.2843	5PB 3.5/ 7.3	4.5PB 3.2/ 7.0
PB 3/10	.1002	.2694	5PB 3.7/ 9.0	4.5PB 3.4/ 8.5
PB 3/12	.0982	.2528	5PB 3.6/ 9.5	4.0PB 3.3/ 9.4
YR 3/ 4	.0665	.6237	5Y 3.0/ 2.6	5.0YR 3.3/ 4.1
10YR 3/ 2	.0636	.6080	5Y 3.0/ 2.3	10.0YR 3.1/ 2.7
GY 3/ 4	.0741	.6030	5Y 3.2/ 2.3	5.0GY 3.2/ 2.6
R 4/14	.0762	.5874	5Y 3.2/ 2.1	5.5R 4.2/13.2
R 4/14	.0763	.5820	5Y 3.2/ 2.1	5.5R 4.2/13.2
10R 3/ 6	.0614	.5859	5Y 2.9/ 2.0	10.0R 3.3/ 5.4
5GY 3/ 2	.0747	.5598	5Y 3.2/ 1.6	4.5GY 3.2/ 1.9
10R 3/ 4	.0611	.5558	5Y 2.9/ 1.4	10.0R 3.2/ 4.1
YR 3/ 2	.0636	.5437	5Y 3.0/ 1.3	5.0YR 3.1/ 2.1
YR 3/ 2	.0641	.5424	5Y 3.0/ 1.3	5.0YR 3.1/ 2.0
Y 3/ 2	.0671	.5362	5Y 3.0/ 1.2	6.0Y 3.1/ 1.1
G 3/ 2	.0747	.5207	5Y 3.2/ 1.0	5.0G 3.1/ 2.7
R 3/ 4	.0593	.5041	5Y 2.9/ 0.6	5.0R 3.2/ 4.6
R 3/ 6	.0630	.5031	5Y 2.9/ 0.6	4.5R 3.4/ 6.2
R 3/ 2	.0649	.4802	5Y 3.0/ 0.2	3.5R 3.1/ 2.1
N 3/	.0651	.4579	5PB 3.0/ 0.2	2.5P 3.0/ 0.2

TABLE 5. *Protanopic arrangement*—Continued

Munsell book notation	Protanopic reflectance, 0.9733 W_p	Protanopic chromaticity coordinate, w_p	Munsell renotations	
			Protanopic	Normal
10RP 3/ 4	0.0569	0.4412	5PB 2.8/ 0.5	9.0RP 3.0/ 3.4
RP 3/ 2	.0611	.4304	5PB 2.9/ 0.8	4.5RP 3.0/ 1.9
10RP 3/ 6	.0562	.4300	5PB 2.8/ 0.8	9.0RP 3.1/ 5.6
RP 3/ 4	.0590	.4037	5PB 2.8/ 1.4	5.0RP 3.0/ 3.7
P 3/ 2	.0722	.3889	5PB 3.1/ 2.1	5.0P 3.2/ 2.2
PB 3/ 2	.0719	.3875	5PB 3.1/ 2.1	5.0PB 3.1/ 2.1
RP 3/ 8	.0551	.3540	5PB 2.7/ 3.0	5.0RP 3.1/ 6.8
10P 3/ 4	.0665	.3543	5PB 3.0/ 3.2	10.0P 3.2/ 4.5
RP 3/10	.0553	.3353	5PB 2.8/ 3.7	5.0RP 3.2/ 8.4
PB 3/ 4	.0757	.3415	5PB 3.2/ 3.9	5.0PB 3.1/ 3.9
P 3/ 4	.0679	.3256	5PB 3.1/ 4.2	5.0P 3.1/ 4.5
10P 3/ 6	.0645	.3141	5PB 3.0/ 4.9	9.0P 3.2/ 6.3
10PB 3/ 4	.0728	.3128	5PB 3.2/ 5.3	10.0PB 3.1/ 4.7
P 3/ 6	.0711	.2914	5PB 3.1/ 6.2	4.5P 3.2/ 6.4
10PB 3/ 6	.0730	.2858	5PB 3.2/ 6.7	10.0PB 3.1/ 6.1
10P 3/ 8	.0589	.2794	5PB 2.8/ 6.5	10.0P 3.1/ 8.3
P 3/ 8	.0712	.2611	5PB 3.1/ 8.1	5.0P 3.2/ 8.4
10PB 3/ 8	.0749	.2643	5PB 3.2/ 8.2	10.0PB 3.2/ 7.4
P 3/10	.0700	.2224	5PB 3.1/11.0	5.0P 3.3/11.2
10PB 3/10	.0735	.2098	5PB 3.2/11.8	10.0PB 3.1/10.6
GY 2/ 2	.0465	.5684	5Y 2.5/ 1.6	5.5GY 2.5/ 2.2
10Y 2/ 2	.0475	.5609	5Y 2.5/ 1.5	10.0Y 2.6/ 1.6
Y 2/ 2	.0455	.5553	5Y 2.5/ 1.4	5.0Y 2.5/ 1.4
10GY 2/ 2	.0456	.5552	5Y 2.5/ 1.4	9.5GY 2.4/ 2.5
10YR 2/ 2	.0472	.5419	5Y 2.5/ 1.2	7.5YR 2.6/ 1.6
R 3/10	.0487	.5371	5Y 2.6/ 1.1	5.0R 3.2/ 8.3
YR 2/ 2	.0403	.5274	5Y 2.3/ 0.9	4.5YR 2.4/ 1.8
R 3/ 8	.0519	.5241	5Y 2.7/ 0.9	5.0R 3.2/ 7.4
G 2/ 2	.0398	.5081	5Y 2.3/ 0.6	7.0G 2.2/ 2.4
10R 2/ 2	.0397	.5056	5Y 2.3/ 0.6	8.5R 2.5/ 2.6
10G 2/ 2	.0445	.4967	5Y 2.5/ 0.4	10.0G 2.3/ 3.1
5BG 2/ 2	.0412	.4623	5PB 2.3/ 0.1	4.5BG 2.2/ 2.5
BG 2/ 4	.0446	.4544	5PB 2.5/ 0.2	5.0BG 2.3/ 3.7
10BG 2/ 2	.0507	.4400	5PB 2.6/ 0.5	7.0BG 2.5/ 3.1
B 2/ 2	.0414	.4216	5PB 2.4/ 0.9	2.0B 2.2/ 2.2
10RP 3/ 8	.0516	.4167	5PB 2.7/ 1.0	9.0RP 3.1/ 7.0
RP 3/ 6	.0549	.3837	5PB 2.7/ 2.0	5.0RP 3.0/ 5.2
10RP 3/10	.0508	.3807	5PB 2.6/ 2.0	8.5RP 3.2/ 8.5
10B 2/ 2	.0435	.3664	5PB 2.4/ 2.4	8.5B 2.2/ 3.1
PB 2/ 4	.0437	.3030	5PB 2.4/ 4.7	4.0PB 2.3/ 4.8
10PB 2/ 4	.0391	.2884	5PB 2.3/ 5.1	10.0PB 2.2/ 4.8
PB 2/ 6	.0474	.2802	5PB 2.5/ 5.8	4.0PB 2.3/ 5.9
10P 3/10	.0531	.2438	5PB 2.7/ 8.3	9.0P 3.0/ 9.8
R 2/ 4	.0311	.4713	5Y 2.0/ 0.1	4.0R 2.3/ 3.8
R 2/ 2	.0357	.4663	5Y 2.2/0.05	3.5R 2.3/ 2.2
R 2/ 6	.0359	.4595	5PB 2.0/ 0.1	3.0R 2.5/ 4.8
N 2/	.0309	.4570	5PB 2.0/ 0.1	5.0P 2.0/ 0.2
RP 2/ 2	.0352	.4204	5PB 2.1/ 0.9	6.0RP 2.3/ 2.3
10RP 2/ 4	.0336	.4127	5PB 2.1/ 1.1	8.0RP 2.3/ 3.7
10RP 2/ 6	.0323	.3790	5PB 2.0/ 1.9	8.0RP 2.4/ 5.6
RP 2/ 4	.0345	.3691	5PB 2.1/ 2.2	5.0RP 2.4/ 4.6
PB 2/ 2	.0378	.3603	5PB 2.2/ 2.5	4.5PB 2.2/ 2.6
P 2/ 2	.0340	.3493	5PB 2.1/ 2.8	5.5P 2.1/ 2.9
RP 2/ 6	.0359	.3385	5PB 2.2/ 3.1	4.0RP 2.4/ 5.9
P 2/ 4	.0344	.3072	5PB 2.1/ 4.2	5.0P 2.2/ 4.6
10P 2/ 4	.0333	.3051	5PB 2.1/ 4.3	9.0P 2.2/ 5.3
10PB 2/ 6	.0368	.2767	5PB 2.2/ 5.6	10.0PB 2.2/ 5.5
10P 2/ 6	.0327	.2723	5PB 2.1/ 5.6	9.0P 2.2/ 6.8
P 2/ 6	.0323	.2580	5PB 2.0/ 6.2	5.0P 2.1/ 6.8

Thus far no precise indication has been given of the color perceptions of deuteranopes and protanopes corresponding to the 400 samples in the Munsell Book of Color; we have only grouped together those samples that differ least and that are therefore most likely to be confused. We know, however, that deuteranopes and protanopes in all probability perceive black, gray, and white normally; furthermore, we know (see table 3) that their yellow corresponds closely to what the normal observer sees in the spectrum at 575mμ, and their blue corresponds closely to 470mμ. These facts may be conveniently expressed in the Munsell color system by giving for each set of values of W/W_0 and w the Munsell equivalent of the purple-blue (PB) or yellow (Y) hue; see master hue chart, figure 13 of the OSA Subcommittee on the Spacing of the Munsell Colors [76]. These Munsell hues correspond closely to those of the spectrum at 470 and 575mμ, respectively, and since the exact hues corresponding to these portions of the spectrum depend somewhat on the observing conditions [14, 17, 96] more precise fitting (as by $6PB$ and $7Y$) is probably not warranted.

The deuteranopic and protanopic Munsell renotations based in this way resulted from the following steps: (a) from table 1 of the OSA Subcommittee Report [76] (pp. 399 and 402) were read the chromaticity coordinates (x, y) for enough colors of the hues 5Y and 5PB to cover the range of the Munsell papers; (b) from these chromaticity coordinates were computed the dichromatic coordinates w_d and w_p, according to eq 2d and 2p and these coordinates were tabulated in table 6; (c) from the data of table 6 families of curves were plotted on each of two graphs, one with w_d as the abscissa, the other with w_p as the abscissa, the ordinate being Munsell chroma and each curve showed the variation of Munsell chroma for hue 5Y or 5PB with dichromatic coordinate (w_d or w_p) for some one Munsell value; (d) from the reflectance relative to magnesium oxide, W/W_0, (second col of tables 4 and 5), the Munsell value was read from table 2 of the subcommittee report [76]; and (e) by interpolation among the curves of the corresponding family according to this Munsell value, the Munsell hue (whether 5Y or 5PB) was determined, and the Munsell chroma corresponding to the dichromatic coordinate, w_d or w_p, was read with an uncertainty of about 0.1 chroma step. The Munsell di-

chromatic renotations (Hue Value/Chroma) so found are given in the fourth column of tables 4 and 5. The fifth column is the normal Munsell renotation copied from table 3 of the subcommittee report [76].

Comparison of these two columns (dichromatic Munsell renotation with normal Munsell renotation) indicates in a precise and detailed way the difference between the surface-color perceptions of the normal observer and those of the average deuteranope and average protanope, respectively.

TABLE 6. *Deuteranopic and protanopic chromaticity coordinates for Munsell renotations of hues 5Y and 5PB*

Munsell renotation	Chromaticity coordinates		Munsell renotation	Chromaticity coordinates	
	u'_d	u'_p		u'_d	u'_p
5Y 9/12	0.8510	0.8433	5PB 8/ 6	0.3615	0.3810
5Y 9/10	.7911	.7827	5PB 8/ 4	.3973	.4119
5Y 9/ 8	.7296	.7218	5PB 8/ 2	.4325	.4425
5Y 9/ 6	.6628	.6569			
5Y 9/ 4	.5955	.5929	5PB 7/10	.2927	.3214
5Y 9/ 2	.5291	.5305	5PB 7/ 8	.3246	.3489
			5PB 7/ 6	.3570	.3768
5Y 8/12	.8805	.8731	5PB 7/ 4	.3913	.4065
5Y 8/10	.8181	.8093	5PB 7/ 2	.4272	.4377
5Y 8/ 8	.7494	.7408			
5Y 8/ 6	.6764	.6696	5PB 6/12	.2507	.2856
5Y 8/ 4	.6025	.5993	5PB 6/10	.2804	.3107
5Y 8/ 2	.5325	.5335	5PB 6/ 8	.3096	.3354
			5PB 6/ 6	.3426	.3638
5Y 7/12	.9125	.9061	5PB 6/ 4	.3823	.3984
5Y 7/10	.8552	.8466	5PB 6/ 2	.4208	.4319
5Y 7/ 8	.7788	.7693			
5Y 7/ 6	.7007	.6927	5PB 5/12	.2299	.2675
5Y 7/ 4	.6184	.6139	5PB 5/10	.2577	.2909
5Y 7/ 2	.5379	.5383	5PB 5/ 8	.2891	.3176
			5PB 5/ 6	.3242	.3476
5Y 6/12	.9425	.9377	5PB 5/ 4	.3662	.3838
5Y 6/10	.8935	.8859	5PB 5/ 2	.4106	.4226
5Y 6/ 8	.8231	.8134			
5Y 6/ 6	.7346	.7251	5PB 4/12	.2017	.2426
5Y 6/ 4	.6373	.6314	5PB 4/10	.2282	.2653
5Y 6/ 2	.5471	.5468	5PB 4/ 8	.2596	.2919
			5PB 4/ 6	.2997	.3261
5Y 5/12	.9903	.9894	5PB 4/ 4	.3442	.3642
5Y 5/10	.9336	.9279	5PB 4/ 2	.3956	.4091
5Y 5/ 8	.8655	.8562			
5Y 5/ 6	.7783	.7677	5PB 3/12	.1606	.2065
5Y 5/ 4	.6667	.6588	5PB 3/10	.1886	.2305
5Y 5/ 2	.5569	.5556	5PB 3/ 8	.2223	.2594
			5PB 3/ 6	.2605	.2919
5Y 4/ 8	.9153	.9081	5PB 3/ 4	.3104	.3346
5Y 4/ 6	.8200	.8092	5PB 3/ 2	.3729	.3890
5Y 4/ 4	.7061	.6962			
5Y 4/ 2	.5774	.5741	5PB 2/12	.1213	.1709
			5PB 2/10	.1439	.1925
5Y 3/ 6	.8839	.8745	5PB 2/ 8	.1703	.2215
5Y 3/ 4	.7373	.7261	5PB 2/ 6	.2247	.2604
5Y 3/ 2	.5899	.5854	5PB 2/ 4	.2833	.3107
			5PB 2/ 2	.3564	.3740
5Y 2/ 4	.8380	.8266			
5Y 2/ 2	.6149	.6182	5PB 1/10	.0998	.1506
			5PB 1/ 8	.1314	.1785
5Y 1/ 2	.7392	.7267	5PB 1/ 6	.1739	.2157
			5PB 1/ 4	.2337	.2671
N 1/ to 9/	.4585	.4652	5PB 1/ 2	.3127	.3355
5PB 9/ 2	.4362	.4457			

It will be noted, of course, first that the normal observer perceives a multiplicity of hues (red, yellow-red, yellow, green-yellow, green, and so on), while the deuteranope and protanope perceive but two—Munsell yellow and Munsell purple-blue. Second, it will be noted from table 4 that the Munsell value of each sample for the deuteranope is the same as that for the normal observer, but from table 5 the protanopic and normal Munsell value differs except for hues near to yellow-green (3GY) and bluish purple (2P). The reddish colors have lower protanopic values, and the greenish have higher; the amount of the difference from the normal values varying from one value step for R 4/14 to zero for nearly neutral colors.

Table 5 also serves to indicate the degree to which protanopic vision leads to confusions between colors easily distinguishable by a normal observer. For samples of small size, such as those that yield ideal protanopic vision, a difference of 0.1-value step or 0.2-chroma step is so small as to be easily confusible with zero difference. From table 5 it may be seen therefore, that Munsell samples GY 8/6 and 10Y 8/6 would be confusible to a typical dichromat if viewed in small size, though to the normal observer, of course, these two samples are distinctly different. By proceeding along the fourth column of table 5 and noting the samples whose protanopic renotations differ by 0.1 or less in value and at the same time by 0.2 or less in chroma, we may make an estimate of the frequency with which a protanope will be troubled to distinguish colors that to the normal observer are separated by at least 10 just noticeable steps. It is found that there are 97 such pairs among the 410 different colors listed; that is, in a group of colors chosen in such a way as to be unrelated to the characteristic protanopic confusions, still about one-fourth of the colors are by chance confusible with another of the group.[3] This result may explain, on the one hand, why dichromatic observers often reach maturity without having become convinced that there is anything abnormal about them other than unusual unfamiliarity with the meaning of color terms, since in about three-fourths of the pairs that they are called upon to

[3] A similar count of pairs confusible by the deuteranope can be made from the fourth column of table 4, and about 200 will be found, roughly twice as many, as from table 5. This is ascribable to the fact that the samples are not unrelated to deuteranopic confusions, being divisible into seven groups, each composed of samples differing but slightly in deuteranopic Munsell value.

compare, they see a difference but describe it in terms not used by the normal observer. On the other hand, since one-fourth of the differences that the normal observer sees plainly are so slight to the red-green confusing dichromat that he must look long and closely to decide about them, and occasionally fails completely, it is easy to understand that a characteristic by which the dichromat is marked is his tendency to hesitate before making a decision, to wait for someone else to speak up, and then to agree with him.

It is suggested that persons who have been found to have either protanopic or deuteranopic vision by the usual tests might find it interesting and possibly instructive to lay out the Munsell papers in the order given in table 4 or table 5, as the case may be, and see to what degree the Munsell dichromatic notation accords with their own perceptions. To the extent that the accord is good, the person will discover how well his type of vision is known; and he may be encouraged to study the basis of the Munsell dichromatic notation, and so gain an additional insight into the relation of his own vision to that possessed by the majority. If the Munsell dichromatic notation fails to accord with his perceptions in ways not to be corrected by viewing the papers through bluish or brownish goggles, it is likely that the observer will find that he has been mistyped by careless administration or interpretation of a routine test, and a retest would be in order. Should the observer find that he is indeed a red-green confusing dichromat, he would have a chance to contribute to the knowledge of color perceptions by studying and reporting the nature and degree of any contradictions.

V. Analysis of Color-Blindness Tests in Terms of Dichromatic Munsell Notations

To show how tables 4 and 5 make available the color perceptions of deuteranopes and protanopes, respectively, it will be sufficient to analyse a few of the color-blindness tests based upon light-reflecting objects whose colors are fairly well established.

1. Holmgren Wool Test

Probably the oldest color-blindness test still in fairly common use is the famous wool test developed by Holmgren [38]. In this test a considerable number (50 to 200) of small skeins of differently colored yarns are placed in a pile on a flat surface sufficiently spacious and illuminated with full daylight. The skein having the trial color is taken from the pile by the examiner and placed to the side far enough from the others not to be confused with them during the test. The examiner requests the subject to pick out the other skeins that come closest to the test skein in color and to place them beside it. Three tests are recommended by Holmgren, one with a green trial skein, one with a purple or rose colored skein, and a third with a red skein. The color chart (p. 120) "serves to guide the examiner in the choice of colors for the test skeins and in appreciating the mistakes of the deficients. We have tried to render there the colors mentioned in this chapter. We divide them into two classes:

"1. The test colors, that is to say, those which the examiner offers to the subject, and

"2. The confusion colors, that is to say, those which the deficient picks from the pile because he confuses them with that of the specimen."

Table 7 gives the Munsell book notations found in April 1942 for the colors of the chart that forms the frontispiece of a book [38] sent by Holmgren personally to the Smithsonian Institution from which it was turned over on October 10, 1884, to the Library of Congress as volume 150530. Some of the colors were found to be obviously faded; for example color I, supposed to be a green (neither yellow green nor blue green), was found to be a weak greenish yellow, and color IIa, supposed to be a purple, was found to be a light brown. However, the colors relating to the third test seem not to have faded seriously and will serve as an example of how to analyse a color-blindness test by means of dichromatic Munsell notations.

Of the third test Holmgren says, "The red skein is presented to the subject. It should have a vivid red color like the red flag serving as a signal for the railroads. This color corresponds to IIb of the chart, which ought perhaps to incline a little more definitely toward yellowish red. The test, which is to be made only with subjects that are completely defective, ought to be continued until the subject has placed with the test skein all of the skeins having that hue, or until he has selected one or more of the confusion colors (10 to 13). The red-blind (protanope, by present-day terminology) chooses in addition to red some

shades of green and brown (10 and 11) that for the normal sense appear darker than the red. But the green-blind (deuteranope) chooses contrasting hues which appear lighter than the red."

The analysis of this test consists in finding the dichromatic Munsell notations of the confusion colors (10 to 13) and comparing them to the dichromatic Munsell notation of the trial color (IIb). From tables 4 and 5, the dichromatic Munsell notations of these five colors have been obtained by reading the notations for neighboring colors and interpolating among them. For example, color IIb was found to have a Munsell book notation of 5.5R 4.8/10. The two closest colors in table 5 are R 5/10 and 10R 5/10, from which we read protanopic equivalents of Y 4.4/1.5 and Y 4.4/4.1, from which in turn by interpolation we would get a protanopic equivalent of Y 4.4/1.8 for 5.5R 5.0/10, and Y 4.2/1.8 for the required book notation 5.5R 4.8/10. This equivalent is given in table 7, together with deuteranopic and protanopic equivalents similarly found for colors IIb, 10, 11, 12, and 13.

TABLE 7. *Munsell book notations of the color chart published by Holmgren to indicate how to administer and interpret his wool test; also dichromatic Munsell renotations of five of the colors*

Holmgren's—		Munsell book notation	Dichromatic Munsell renotation	
Description	Number		Protanopic	Deuteranopic
Green	I	9Y 7/4		
Colors confused with green	1	6Y 6 /2		
	2	1Y 6 /2.5		
	3	4Y 8 /5		
	4	7YR 8 /5		
	5	7YR 7 /3		
Purple	IIa	6YR 6.5/3		
Protanopic confusions with purple.	6	5PB 3.0/8		
	7	5P 4.0/6.5		
Deuteranopic confusions with purple.	8	5Y 5.5/1		
	9	7G 4.8/3		
Red	IIb	5.5R 4.8/10	Y 4.2/1.8	Y 4.9/3.5
Protanopic confusions with red.	10	7GY 3.5/2	Y 3.8/1.5	Y 3.7/1.3
	11	10YR 3.6/2	Y 3.6/2.1	Y 3.7/2.3
Deuteranopic confusions with red.	12	5GY 6.0/6	Y 6.2/6.2	Y 6.2/5.9
	13	5YR 4.0/6	Y 4.0/3.6	Y 4.4/4.2

It is evident from an examination of table 7 why the protanope would be expected to confuse colors 10 and 11 with the red color IIb. The protanopic renotations of these colors differ from that of the red by 0.6 of a value step or less and by only 0.3-chroma step. Similarly, color 13 would be expected to be moderately confusible by deuteranopes with the red color IIb, because the deuteranopic Munsell renotations of these two colors differ by only 0.5 of a value step and 0.7-chroma step; but color 12 should be distinct from the red color IIb to deuteranopes because it is lighter by 1.3 value steps and higher in chroma by 2.4 steps (compare Y 6.2/5.9 with Y 4.9/3.5). This analysis shows that the colors in Holmgren's book conform to his statements regarding the test with the red skein except for color 12, which was probably not correctly rendered originally by the lithographer. The other discrepancies are too small to be significant in view of Holmgren's statement: "The resemblance need not be perfect in all respects; there are no two skeins that are exactly alike. The question is particularly on resemblance in *hue*, and on this account the subject ought to look for those that are similar and belong to the same hue, that which is paler or deeper but of the same color, and so on. . . . Not too much attention should be paid to lightness nor to slight shades of off-gray color."

Similar analyses of tests by means of green and purple skeins give similar corroboration of Holmgren's interpretation of his tests, but these analyses have to be carried out with reference to the actual colors of the green and purple skeins used instead of the faded colors I and IIa of the color chart.

2. Stilling Pseudo-Isochromatic Plates

The plates developed by Stilling in 1878 [91] are still used [71, 93], and copies and developments of them are widely distributed in this country [1, 41]. The subject is shown a series of printed pages in succession, each page covered with a pattern of irregularly shaped spots. The spots are so colored and so arranged that numbers can be read on the plates by many observers of normal vision, but to observers having various types of abnormal vision certain of the plates seem to have uniform colors or a uniform mixture of colors, so that no number can be read. Because of this, they are called pseudo-isochromatic plates.

The analysis of a psuedo-isochromatic plate designed to detect protanopia or deuteranopia can be carried out by obtaining the Munsell book notations of typical background spots and typical spots making up the number, reading their pro-

tanopic and deuteranopic Munsell notations by interpolation in tables 4 and 5, and comparing them. These charts were designed, however, to accord with a view of the color perceptions of dichromatic observers developed by Stilling and described by him in detail by means of a color chart printed in 1909 [92]. It will suffice for illustration of the method to confine our analysis to these printing-ink reproductions of the colors.

Table 8 gives the Munsell book notations of most of the colors found in 1944 on the color chart in the Library of Congress copy of Stilling's paper, Über Entsteheng und Wesen der Anomalien des Farbensinnes [92]. The colors dealing with Stilling's view of the color perceptions of tritanopes have been omitted. Table 8 also shows the protanopic and deuteranopic Munsell renotations corresponding to these book notations read by interpolation from tables 4 and 5.

From the Munsell book notations of the brown, light brown, and gray colors representing Stilling's view of what the red-green confuser's color perceptions are, it may be seen that his idea of the hue of these perceptions is close to that taken in the present paper; in no case does his estimate depart from the present one (5Y) by as much as five Munsell hue steps. The value and chroma estimates are also fairly close, particularly those for the color-blind equivalent of blue green; compare Y 6.9/4.3 with Y 5.8/3.6 and Y 6.7/3.6 with Y 6.0/3.8. The light brown chosen is only slightly darker (0.9 of a value step) than that which would represent an average confusion color for protanope and deuteranope. The yellowish gray shown as an estimate of the color-blind perception of violet is very close to the present estimate of the deuteranopic perception of the violet shown (compare Y 5.7/0.6 with Y 6.2/0.9); but since the name given to this sample was gray, the agreement may signify only that there has been a yellowing of the printing-ink representation of gray since its preparation in 1909. Actually the average of the protanopic (PB 5.4/0.4) and deuteranopic (Y 5.7/0.6) Munsell renotations for the violet shown on the chart is very close to a neutral gray.

The protanopic and deuteranopic confusion colors for red (7R 4.5/8), also shown in table 8 are not in very striking agreement; in each case the green is too light and of too high a chroma to be confused by an average protanope or deuteranope. Since the difference between the two colors corresponds well with the difference between the present estimate of the protanope and deuteranope color perceptions, it is reasonable to suppose that the greenish printing-ink specimens, like the gray, have yellowed with age by one chroma step since 1909. Note that the protanopic equivalent of the red is lower in chroma by $3.4-2.0=1.4$ chroma steps than the deuteranopic equivalent. The green chosen by Stilling as a protanope confusion for red also gives a dichromatic equivalent of lower chroma ($6.0-3.5=2.5$, $5.8-3.2=2.6$) than that chosen as the deuteranope confusion for the same red. The two printing-ink specimens thus give the correct idea of the difference between the greens that are confused with red by red-green confusers, but the amount of chroma difference is exaggerated. Similarly, the correct idea of the lightness difference is given ($4.6-4.0=0.6$), but the amount is in this case too small ($5.6-5.4=0.2$, $5.7-5.4=0.3$). Stilling was perfectly well aware of the direction of this difference, because he refers to the protanope confusion green as a "somewhat darker green"; whether he had very precise quantitative information cannot be told from this illustrative example because of the uncertainties

TABLE 8. *Munsell book notations of the color chart published by Stilling [92] to indicate his view of the color perceptions and confusions of red-green confusers; also protanopic and deuteranopic Munsell renotations of them*

Stilling's description	Munsell book notation	Dichromatic Munsell renotations	
		Protanopic	Deuteranopic
Red	7.4R 4.8/9	Y 4.2/2.6	Y 4.9/1
Brown seen by color-blind instead.	0.2Y 5.9/6	Y 5.9/5.4	Y 6.2/5
Pink	7.4R 6.2/8	Y 5.9/2.1	Y 6.4/1
Light brown seen instead	2.5Y 5.9/4	Y 5.8/3.6	Y 6.0/3
Violet	9RP 5.5/6	PB 5.4/0.4	Y 5.7/0
Gray seen by color-blind instead.	7.5Y 6.0/1	Y 6.2/0.9	Y 6.2/0
Blue-green	2G 6.6/8	Y 6.9/4.3	Y 6.7/3
Light brown seen instead	2.5Y 5.9/4	Y 5.8/3.6	Y 6.0/3
Yellow-green	8GY 7.3/4.6	Y 7.5/3.7	Y 7.4/2
Brown seen by color-blind instead.	0.2Y 5.9/6	Y 5.9/5.4	Y 6.2/5
Red	7R 4.5/8	Y 4.0/2.0	Y 4.6/1
Yellow-green confused with red by deuteranope.	3GY 5.5/6.0	Y 5.6/6.0	Y 5.7/3
Green confused with red by protanope.	6GY 5.3/4	Y 5.4/3.5	Y 5.4/2

ntroduced by possible failure of the lithographic process to render the colors correctly, and because f possible changes of the colors with time.

3. Farnsworth Dichotomous Test (B–20)

The serial order test devised by Farnsworth [20] t the beginning of the war for screening observers nto two groups is particularly easy to analyse in erms of dichromatic Munsell notations, because t is based upon Munsell papers whose color char- teristics are known through spectrophotome- ry [23, 53]. Table 9 shows the protanopic renota- ions of these papers arranged in the order given y Farnsworth for a typical protanope; and it also hows the deuteranopic renotations of the papers rranged in the order given by Farnsworth for a ypical deuteranope. The values of W_p, w_p, W_d, nd w_d are taken from a previous publication [51].

It will be noted that the arrangement of these apers made by the observer chosen by Farns- orth as a typical protanope is closely, but not erfectly, given by the protanopic Munsell reno- ation ranging from a yellow of chroma 2.2 through near neutral (Y 5.2/0.1) to a purple blue of hroma 3.3. A similar correspondence may also e noted between the Farnsworth deuteranopic rrangement and deuteranopic Munsell renota- ion. Possible causes for the failure of the cor- relation to be perfect are the same as those previously discussed with reference to the chro- maticity coordinates, w_p and w_d [51]. The chief cause of the discrepancies seems to be a slight but consistent difference between the hypothetical average observers defined by eq 1, on the one hand, and the actual observers chosen by Farns- worth as typical on the other. The discrepancies may thus be taken as indicating about the degree of agreement to be expected between an average red-green confuser and some one observer of the same type chosen at random.

VI. Summary

A review of the literature on color perceptions mediated by dichromatic, red-green-confusing, visual mechanisms for an observer capable of relating them to normal color perceptions has been carried out, and it shows that both types of such mechanisms (protanopia and deuteranopia) yield color perceptions of two hues, and two hues only, yellow and blue. A review of the chief theories of vision shows that they also all provide for this kind of color perception. A method of deriving protanopic and deuteranopic Munsell notations of colors from their specification in the standard ICI colorimetric coordinate system has

TABLE 9. *Protanopic and deuteranopic Munsell renotations of the chips of the Farnsworth dichotomous test [20] arranged in the order found by Farnsworth for a typical protanope and a typical deuteranope, respectively*

Protanopic arrangement	Normal serial number	0.9733 W_p	w_p	Protanopic Munsell renotation	Deuteranopic arrangement	Normal serial number	W_d	w_d	Deuteranopic Munsell renotation
1	8	0.2253	0.5628	Y 5.3/2.2	1	10	0.2143	0.5463	Y 5.2/1.8
2	10	.2038	.5405	Y 5.1/1.7	2	9	.2117	.5412	Y 5.2/1.7
3	7	.2096	.5442	Y 5.1/1.8	3	8	.2292	.5604	Y 5.3/2.1
4	6	.2061	.5307	Y 5.1/1.5	4	7	.2097	.5376	Y 5.1/1.6
5	9	.2056	.5406	Y 5.1/1.7	5	11	.1927	.5234	Y 4.9/1.3
6	11	.1813	.5149	Y 4.8/1.0	6	12	.2185	.5153	Y 5.2/1.2
7	5	.1972	.5011	Y 5.0/0.8	7	6	.2017	.5185	Y 5.0/1.2
8	12	.2034	.5042	Y 5.1/0.9	8	13	.1954	.4891	Y 5.0/0.6
9	13	.1818	.4779	Y 4.8/0.3	9	14	.2229	.4761	Y 5.3/0.4
10	4	.2199	.4709	Y 5.2/0.1	10	5	.1888	.4835	Y 4.9/0.5
11	3	.2162	.4432	PB 5.2/1.0	11	15	.2138	.4552	PB 5.2/0.1
12	15	.2048	.4512	PB 5.1/0.7	12	16	.2092	.4320	PB 5.1/1.1
13	14	.2103	.4684	Y 5.1/0.1	13	4	.2077	.4501	PB 5.1/0.3
14	2	.2030	.4242	PB 5.1/2.0	14	17	.1959	.4101	PB 5.0/2.0
15	16	.2027	.4309	PB 5.1/1.6	15	3	.2043	.4227	PB 5.1/1.6
16	17	.1942	.4145	PB 5.0/2.4	16	2	.1917	.4037	PB 4.9/2.2
17	1	.2321	.4201	PB 5.4/2.3	17	18	.2118	.3908	PB 5.2/3.0
18	19	.2071	.4121	PB 5.1/2.5	18	20	.2087	.3891	PB 5.1/3.0
19	20	.2164	.4042	PB 5.2/3.0	19	19	.2035	.4013	PB 5.1/2.5
20	18	.2140	.3908	PB 5.2/3.3	20	1	.2229	.4037	PB 5.3/2.5

been worked out on the basis of this kind of color perception. It is concluded that these notations of colors conform to the usual perceptions of them by protanopic and deuteranopic observers in the sense that the chance of any protanope or deuteranope of average ocular pigmentation having valid ground for objecting to them is remote. These protanopic and deuteranopic Munsell notations therefore serve to relate in a complete and detailed way the color perceptions of red-green-confusing dichromats with those of normal vision. It is expected that this detailed information will assist in the design of color-blindness tests, and will help color-blind persons to understand the relation of their own visual systems to the normal system and so give them a better chance to avoid the embarrassments and dangers of living in a tridimensional color world with a two-dimensional color detector.

VII. References

[1] American Optical Co., Pseudo-isochromatic plates for testing color perception (1940).

[2] Tentative definitions of terms relating to paint, varnish, lacquer and related products (ASTM Designation: D 16–42 T).

[3] Standard method of test for spectral characteristics and color of objects and materials (ASTM Designation: D 307–44).

[4] J. W. Baird, Color sensitivity of the peripheral retina (Carnegie Institution, Washington, D. C., 1905).

[5] L. H. Bauer and W. MacLake, Military Surgeon **46,** 40 (Jan. 1920).

[6] A. Von Baumgartner, Wien Ber. **29,** 257 (1858).

[7] O. Becker, Arch. Ophthalmol. [2], **25,** 205 (1879); Centr. prakt. Augenheilk. **4,** 48 (1879).

[8] Beevor, Trans. Ophthalmol. Soc. U. K. **14,** 249 (1894).

[9] W. F. Bonner, J. Am. Med. Assn. **81,** 1837 (1923).

[10] W. F. Bonner, Am. J. Ophthalmol. **9,** 604 (1926).

[11] J. Brische, Ann. Soc. med. Chir. de Liege **1,** 87 (1862).

[12] Committee on colorimetry, Optical Society of America, The Concept of Color, J. Opt. Soc. Am. **33,** 552 (1943).

[13] W. Dieter, Z. Sinnesphysiol. **58,** 73 (1927).

[14] F. L. Dimmick and M. R. Hubbard, Am. J. Physchol. **52,** 242 (1939).

[15] F. C. Donders, Arch. Ophthalmol. **27,** (I) 155 (1881); Abstract in Centr. Augenheilk. **5,** 403 (1881).

[16] F. C. Donders, Farbengleichungen, duBois-Reymonds Arch. Anat. Physiol. p. 518 (1884).

[17] E. Dreher, Z. Sinnesphysiol. **46,** 1 (1912).

[18] F. W. Edridge-Green, Note on a case of asymmetrical colour-blindness, p. 53 (Med. Press, London, 1889); Colour-blindness and colour-perception, 2d ed., p. 197 (1909).

[19] F. W. Edridge-Green, The Hunterian lectures on colour-vision and colour-blindness (Kegan Paul Co., 1911).

[20] D. Farnsworth, J. Opt. Soc. Am. **33,** 568 (1943).

[21] A. Fick, Zur Theorie der Farbenblindheit, Verhandl. Physik.-Med. zu Wurzburg, N. F. V., p. 129 (1873).

[22] A. Fick, Die Lehre von der Lichtempfindung, in Hermann's Handb. Physiol. III, 139, 207 (Leipzig 1879).

[23] J. J. Glenn, and J. T. Killian, J. Opt. Soc. Am. **30,** 609 (1940).

[24] H. Goldmann, Arch. ges Physiol. (Pfluger's) **194,** 30 (1922).

[25] H. Goldmann, Arch. ges. Physiol. (Pfluger's), **210,** 7 (1925).

[26] R. H. Goldschmidt, Z. Sinnesphysiol. **50,** 192 (1919).

[27] H. Hartridge, Brit. J. Ophthalmol. **4,** 318 (1920).

[28] S. P. Hayes, Am. J. Psychol. **22,** 369 (1911).

[29] C. A. Hegner, Z. Sinnesphysiol. **49,** 18 (1916); Klin. Monatsbl. Augenheilk. **54,** 81 (1915).

[30] H. vonHelmholtz, Physiological optics *II*, 415, translated by J. P. C. Southall (Optical Society of America, Banta, Wisconsin, 1924).

[31] E. Hering, Arch. Ophthalmol. **36,** (III) (1890).

[32] G. Hermann, Ein Beitrag zur Casuistik der Farbenblindheit, Inaug. Diss. (Dorpat, 1882).

[33] C. Hess, Arch. Ophthalmol. **35,** [4], 1 (1889).

[34] C. Hess, Arch. Ophthalmol. **36,** (III) 24 (1890).

[35] R. Hilbert, Arch. ges. Physiol. (Pflüger's) **57,** 6 (1894).

[36] A. von Hippel, Arch. Ophthalmol. [2] **26,** 176 (1880).

[37] A. von Hippel, Arch. Ophthalmol. **27,** III, 47 (1881); Abstract in Centr. prakt. Augenheilk. **5,** 516 (1881).

[38] F. Holmgren, De la Cécité des Couleurs, dans ses Rapports avec les Chemin-de-fer et la Marine. Authorized translation (Stockholm, 1877).

[39] F. Holmgren, Upsala Läkarfören Förh. **16,** 69 (1880).

[40] F. Holmgren, Centr. med. Wiss. Berlin **18,** 913 (1880).

[41] F. Holmgren, Upsala Läkarfören. Förh. **16,** 147 (1881); brief abstract in Centr. prakt. Augenheilk. **5,** 476 (1881).[4]

[42] F. Holmgren, Proc. Roy. Soc. (Liondon) **31,** 302 (1881).

[43] F. Holmgren, Upsala Läkarfören. Förh. **16,** 308 (1881); brief abstract in Centr. prakt. Augenheilk. **5,** 475 (1881).

[44] F. Holmgren, Upsala Läkarfören. Förh. **16,** 363 (1881); brief abstract in Centr. prakt. Augenheilk. **5,** 476 (1881).

[45] F. Holmgren, Upsala Läkarfören. Förh. **16,** 222 (1881); brief abstract in Centr. prakt. Augenheilk. **5,** 476 (1881).

[46] F. Holmgren, Upsala Läkarfören. Förh. **16,** Beil. zu Heft 2/3, p. 1 (1881); brief abstract in Centr. prakt. Augenheilk. **5,** 476 (1881).

[47] S. Ishihara, Tests for colour-blindness (Handaya, Tokyo, Hongo Harukicho, 1917).

[48] J. E. Jennings, Am. J. Ophthalmol. **8,** 384 (1925).

[49] D. B. Judd and K. L. Kelly, J. Research NBS **23,** 355 (1939) RP1239.

[50] D. B. Judd, J. Opt. Soc. Am. **33,** 294 (1943).

[51] D. B. Judd, J. Research NBS **33,** 407 (1944) RP1618; J. Opt. Soc. Am. **35,** 199. (1945).
[52] H. J. Keegan, J. Opt. Soc. Am. **36,** 367 (1946); Ind. Standardization **18,** 92 (Apr. 1947).
[53] K. L. Kelly, K. S. Gibson, and D. Nickerson, J. Research NBS **31,** 55 (1943) RP1549; J. Opt. Soc. Am. **33,** 355 (1943).
[54] A. Kirschmann, Wundt's Philos. Studien **8,** 173, 407 (1892–93).
[55] M. Knies, Arch. Augenheilk. **17,** 379 (1887); **18,** 50 (1887); (Color sensations of the tritanopic observer) **19,** 253 (1888).
[56] B. Kolbe, Centr. prakt. Augenheilk. **6,** 291–295 (1882).
[57] H. Köllner, Z. Augenheilk. **21,** 193, 309 (1909).
[58] H. Kollner, Ueber das Grenzgebiet zwischen normalem Farbensinn und Farbenschwäche, 37th Versammlung J. ophthalmol. ges. zu Heidelberg. p. 245 (1911).
[59] H. Köllner, Die Storeungen des Farbensinnes. (Karger, Berlin, 1912).
[59a] A. König, Ueber "Blaublindheit", Sitz. Akad. Wiss. Berlin, p. 718 (July 8, 1897); Ges. Abhandl., p. 396 (Barth, Leipzig, 1903).
[60] J. von Kries, Die Gesichtsempfindungen und ihre Analyses, duBois-Reymond's Arch. Physiol. Supplement-Band (1882); Die angeborene Farbenblindheit, pp. 134–153, Die erworbene Farbenblindheit, p. 153–157, Die hysterischen und hypnotischen Farbensinn-störungen, pp. 157–158.
[61] J. von Kries, Die Gesichtsempfindungen. Nagel's Handbuch der Physiologie des Menschen. **3,** 259 (Braun-schweig, 1905).
[62] J. von Kries, Z. Sinnesphysiol. **50,** 137 (1919).
[63] J. von Kries, Note on normal and anomalous colour systems, English Ed. Helmholtz's Treatise on Physiological Optics, **2,** 402 (The Optical Society of America, 1924).
[64] C. Ladd-Franklin, Colour-blindness and William Pole, Science **5,** 310 (1897).
[65] W. Lohmann, Arch. Augenheilk. **82,** 104 (1917).
[66] W. R. Miles and H. Beaumont, Am. J. Ophthalmol. [3], **14,** 636 (1931).
[67] W. R. Miles, and H. Craig, Jr., The Personnel J. **9,** 437 (1931).
[68] G. E. Müller, Darstellung und Erklärung der verschiedenen Typen der Farbenblindheit nebst Erörterung der Funktion des Stäbchenapparates sowie des Farbensinns der Bienen und der Fische. (Vandenhoeck-Ruprecht, Göttingen, 1924.)
[69] G. E. Müller, Z. Psychol. Ergänzungsb. **17,** 18 (1930).
[70] Munsell Book of Color (Library and Pocket ed.), (Munsell Color Co., Baltimore, Md., 1929, 40-hue-chart edition, 1942).
[71] E. Murray, J. Opt. Soc. Am. **33,** 329 (1943).
[72] W. A. Nagel, Z. Psychol. **39,** 93 (1905).
[73] W. A. Nagel, Arch. Anat. Physiol. p. 543 (1907).
[74] W. A. Nagel, Z. Psychol. **44,** 5 (1910).
[75] E. von Neipperg, Münch. med. Wschr. **79,** 1395 (1932).
[76] S. M. Newhall, D. Nickerson, D. B. Judd, J. Opt. Soc. Am. **33,** 385 (1943).
[77] Niemetscheck. Ueber Farbenblindheit und Farbensehen, Prag. Vierteljahrsschr. **25,** (IV) 224 (1868).
[78] Optical Society of American Committee on Colorimetry, The Concept of Color, J. Opt. Soc. Am. **33,** 552 (1943).
[79] J. H. Parsons, An introduction to the study of colour vision, part II. The chief facts of colour blindness, 2d. ed. (University Press, Cambridge, 1924).
[80] H. Piper, Z. Physiol. Sinnesorgane **38,** 153 (1905).
[81] F. H. G. Pitt, Characteristics of dichromatic vision, Medical Research Council, Report of the Committee on the Physiology of Vision, XIV; Special Report Series, No. 200 (London, 1935).
[82] W. O. Pole, Proc. Roy. Soc. **8,** 172 (1856); Phil. Mag. [4], **13,** 282 (1857).
[83] Rayleigh, Nature **25,** 64 (1882).
[84] Reichert, Ueber einseitige Farbensinnanomalein, Inaug. Diss. (Freiburg, 1915).
[85] Samojloff, Z. Sinnesphysiol. **41,** 367 (1906).
[86] R. W. Shufeldt, Medical Record **23,** 319 (Mar. 24, 1883).
[87] Louise L. Sloan and Lorraine Wollach, J. Opt. Soc. Am. **37,** 527 (1947).
[88] S. Snell, Peculiar case of colour-blindness, Lancet, p. 727 (Apr. 30, 1881).
[89] S. Snell, Brit. Med. J. No. 1622, p. 222 (1892).
[90] P. Steffan, Arch. ophthalmol. (Graefe's) **27,** II, (1881); abstract in Centr. prakt. Augenheilk. **5,** 409 (1881).
[91] J. Stilling, Tafeln zur Bestimmung der Röth-Grünblindheit, (Leipzig, 1878).
[92] J. Stilling, Z. Sinnesphysiol. **44,** 371 (1909–10).
[93] J. Stilling, Stillings pseudoisochromatische Tafeln zur Prüfung des Farbensinnes, 19th ed. by E. Hertel (Leipzig, Thieme, 1936).
[94] W. Trendelenburg, Klin. Monatsbl. Augenheilk. **107,** 280 (1941).
[95] A. Tschermak, Licht- und Farbensinn, Bethe's Handbuch der Normalen und pathologischen Physiologie, 12/1. Receptionsorgane **2,** 345 (Springer, Berlin, 1929).
[96] H. Voeste, Z. Psychol. **18,** 257 (1898).
[97] G. Wilson, Researches on colour-blindness, p. 11 (Sutherland and Knox, Edinburg, 1852).
[98] M. Woienow, Arch. Ophthalmol. **17,** II, 241 (1871); Klin. Monatsbl. Augenheilk. **9,** 377 (1871).

WASHINGTON, MAY 21, 1948.

U. S. Department of Commerce
National Bureau of Standards

Research Paper RP1923
Volume 41, October 1948

Part of the Journal of Research of the National Bureau of Standards

Electrode Function (pH Response) of the Soda-Silica Glasses

By Gerald F. Rynders, Oscar H. Grauer, and Donald Hubbard

A series of Na_2O-SiO_2 glasses was studied for durability, hygroscopicity, glass electrode function, and apparent response to [Na^+]. These glasses show three distinct regions of durability characteristics at pH 4.6: Below 81 percent of SiO_2, where the glass is carried into solution; between 81 and 89.5 percent of SiO_2, where differential solution of the constituents of the glass leaves a swollen silica-rich layer; and a region in which greatly reduced attack was indicated. Glass electrodes of low silica content having poor chemical durability and high hygroscopicity exhibited large voltage departures approaching the values of a "punctured" mercury-filled electrode and a calomel half cell. The apparent response to [Na^+] ranged from 9 to 339 millivolts per pNa for the glasses of 82.6 and 56.6 percent of SiO_2, respectively.

I. Introduction

For a glass to function satisfactorily as a glass electrode, it must have uniform durability over an extended pH range as well as adequate hygroscopicity. It has been shown that where the glass is attacked excessively [1, 2, 3],[1] or where the glass has inadequate hygroscopicity [4, 5], departures from the Nernst equation occur. These departures at times have been attributed to specific equilibrative responses to ions other than hydrogen [6]. To obtain more extensive data on these subjects, a series of glasses of the soda-silica system was studied in continuation of the work done on the potash-silica glasses [5]. The portion of the latter system investigated was found to have some very hygroscopic glasses, but because of their limited durability, these glasses were unsuitable for use as glass electrodes. Accordingly, in the present investigation both durability and hygroscopicity were studied in an attempt to determine which glasses of the soda-silica system would make satisfactory electrodes.

II. Experimental Procedure

Ten glasses of the soda-silica system were prepared in a platinum crucible from raw materials of the high quality used in the production of optical glass. The batches were prepared to provide a series varying in steps of about 4 percent in the range from 55 to 91 percent of silica. Glasses of higher silica content were not obtained, because the field of practical glassmaking is limited by the tendency of glasses to devitrify, their high liquidus temperatures, or their high viscosity. To insure homogeneity, the glasses were stirred with a platinum stirrer. Since volatilization of soda occurs during melting, the compositions of these glasses were determined from index of refraction measurements [7, 8].

Hygroscopicity measurements were made on samples of glass that passed through a standard 150-mesh sieve. These weighed samples (approximately 1.5 g) were subjected to the high (approximately 98%) humidity maintained by a saturated solution of $CaSO_4 \cdot 2H_2O$ at 25° C, in accordance with a previously described method [4, 5]. The values are reported in milligrams of water sorbed per cubic centimeter of glass exposed, to compensate for differences in density of the glasses.

Durability measurements were made on the glass by partially immersing polished optical flats in Britton-Robinson Universal buffer mixture (pH 1.9 to 11.9) [9] at 80°±0.2° C for 6 hr and measuring the change in thickness of the exposed

[1] Figures in brackets indicate the literature references at the end of this paper.

portion of the sample by an interferometer method [1, 3]. These values are reported as fringes of attack or swelling, as the case may be.

Determinations of the electrode function of the various glasses were made by measuring at room temperature the emf of a cell, consisting of an experimental glass electrode and a well-conditioned Beckman glass electrode, with a Beckman pH meter, Laboratory Model G. The experimental electrodes were made by blowing a bulb on the end of tubing [2] drawn from the experimental glasses and filling the bulb with mercury for the inner connection [10, 11]. The pH response of the electrodes in a solution of pH 1.9 was taken as the zero voltage departure, and the departures over the range of pH 1.9 to 11.9 were noted.

Punctured electrodes were prepared by blowing a bulb of Corning 015 glass [12, 13] on the end of

[2] Tubing was drawn from the experimental glasses by Leonardo Testa of the glassblowing shop at the National Bureau of Standards.

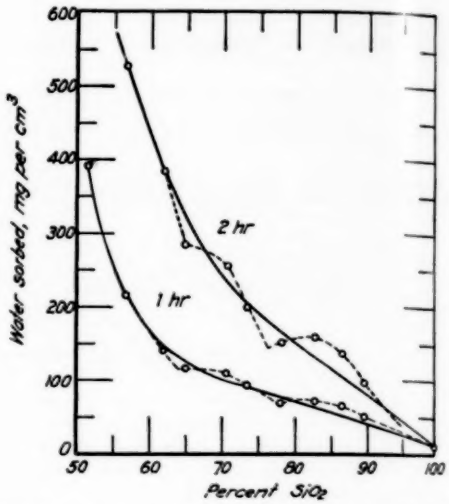

FIGURE 1. *Hygroscopicity-composition curves of* Na_2O-SiO_2 *glasses for 1- and 2-hr exposures.*

TABLE 1. *Hygroscopicity (water sorbed), chemical durability, electrode function, and apparent response to* $[Na^+]$ *for a series of* Na_2O-SiO_2 *glasses compared with Corning 015 and fused silica*

Glasses		Water sorbed after—		Attack (at pH) 6 hr 80° C					Voltage departures at pH values—								Apparent response to $[Na^+]$ [a]
Na_2O	SiO_2	1 hr	2 hr	1.9	4.6	7.1	9.1	11.9	1.9	3.1	4.6	6.4	7.1	9.1	10.1	11.9	
Percent	*Percent* [b]	*mg/cm²*	*mg/cm²*	*Fringes*	*Fringes*	*Fringes*	*Fringes*	*Fringes*	*mv*	*mv*	*mv*	*mv*	*mv*	*mv*	*mv*	*mv*	*mv/pNa*
48.7	51.3	390	1035	(c)	(c)	(c)	(c)	(c)	(d)	(d)	(d)	(d)	(d)	(d)	(d)	(d)	
43.4	56.6	216	527	(c)	(c)	(c)	(c)	(c)	0	49	139	234	274	374	425		339
38.2	61.8	139	383	(c)	(c)	(c)	(c)	(c)	0	47	126	203	235	318	369	458	284
35.2	64.8	115	283	(c)	(c)	(c)	(c)	(c)	0	34	111	189	210	283		391	
29.4	70.6	109	253	>60	72	Pitted	Pitted	Pitted	0	13	51	128	167	254	312	400	209
26.7	73.3	92	190	>22	22	24	30	66	0	7	30	80	65	103	134	181	107
21.9	78.1	60	150	3.6	3.6	3.6	2	6	0	4	10	14	17	23	31	42	25
17.4	82.6	72	157	Swelling >½	Swelling >½	Surface cut, >¼.		3¾	0	4	10	10	10	10	11	4	9
13.6	86.4	65	136	Swelling >0.2.	Swelling >0.2.	Swelling 0.1.		>2½	(f)								
10.5	89.5	50	97	Swelling, D [g].	Swelling, D.	Swelling, D.		<1½	(f)								
Fused silica		11	12	ND	ND	ND			(h)								
Corning 015		61	140	Swelling <0.2.	Swelling <0.2.	Surface cut, D.	Surface cut, <½	1¾<2	0	0	0	0	0	1	1	2	
Corning 015 (punctured).									[i] 0	51	150	252	293	392	440		332
Calomel reference electrode.									[j] 0	71	159	265	307	425	484		

[a] These data calculated from voltage departures between pH 1.9 and pH 10.1.
[b] Composition computed from index of refraction data.
[c] Failed to maintain polish.
[d] No successful electrodes.
[e] Durability data for these glasses were calculated from the attack for 15 min at 80° C.
[f] No electrodes made of these glasses.
[g] D, Detectable; ND, not detectable.
[h] Developed no definite electrode function.
[i] Voltage departure values obtained for a punctured Hg filled electrode of Corning 015 glass.
[j] Theoretical voltage departure of the glass electrode and calomel reference electrode.

Pyrex borosilicate tubing, with the result that fair cracks were formed on cooling due to the difference in expansion of the two glasses.

III. Results and Discussion

1. Hygroscopicity

The data for the water sorbed by this series of glasses after 1- and 2-hr exposure are given in table 1 and plotted in figure 1. Because of the limited data obtained, the results are represented by a smooth curve. However, if lines are drawn through the individual points (dashed lines, fig. 1), breaks in the slope occur near critical compositions of the phase diagram.

An interesting feature of these data is that the glass of approximately 86 percent of silica has the same hygroscopicity as Corning 0.15.

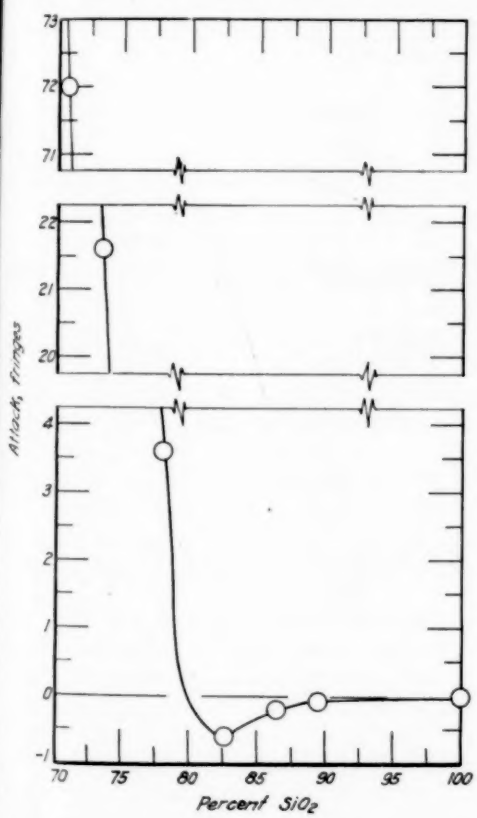

FIGURE 2. *Attack on Na_2O-SiO_2 glasses exposed for 6 hr at 80° C to Britton-Robinson buffer mixture at* pH *4.6.*

2. Durability

Examination of the durability data, table 1 and figure 2, for the 6-hr exposure of the specimens in a solution of pH 4.6 indicates that the more durable glasses for this system occur in the range above 81 percent of silica. Those glasses below 64.8 percent of silica were deliquescent and failed to maintain polished surfaces when exposed to air, so that durability measurements by the interferometer method were impossible. Glasses having a composition of 70.6 and 73.3 percent of silica were less soluble, and results were calculated [1] from a 15-min exposure. Above 80 percent of

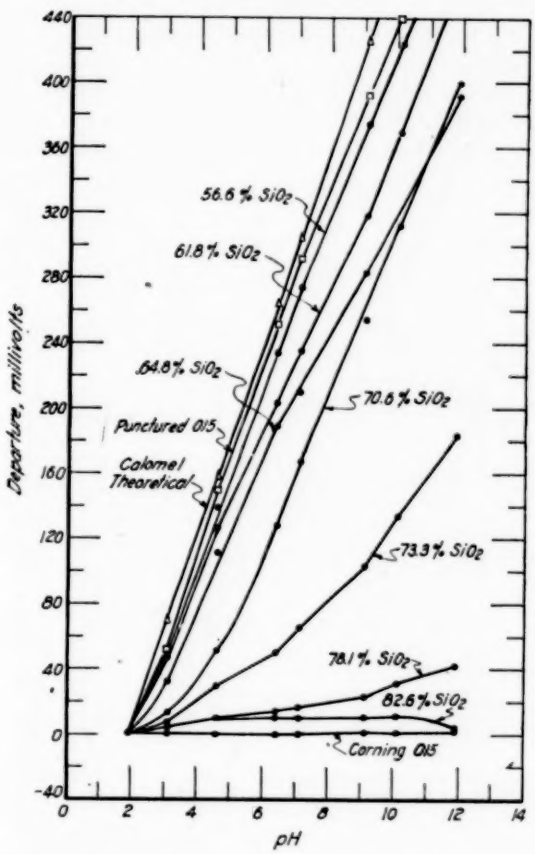

FIGURE 3. *Voltage departures (errors) of electrodes prepared from a series of Na_2O-SiO_2 glasses and Corning 015 glass, by using the Beckman glass electrode as the reference electrode.*

For comparison, the data are plotted for the theoretical voltage departure of a glass electrode from a calomel reference cell in addition to voltage departures shown by a punctured electrode of Corning 015 glass.

silica the durability of the glasses improved, and the glasses resisted solution and tended to swell. The tendency to swell decreased with increasing silica content until it became barely detectable at 89 percent of silica. It is only in the region of swelling, improved durability, and adequate hygroscopicity that one would expect to find successful electrodes. The values of hygroscopicity and durability of the glass of 86 percent of silica are similar to the values obtained on Corning 015 (see table I).

3. Electrode Function

(a) Voltage departure

The data given in table 1 and plotted in figures 3 and 4 show the trends of voltage departures in millivolts for glasses of increased silica content in solutions of various pH values. The poor durability of glasses below 82.6 percent of silica was

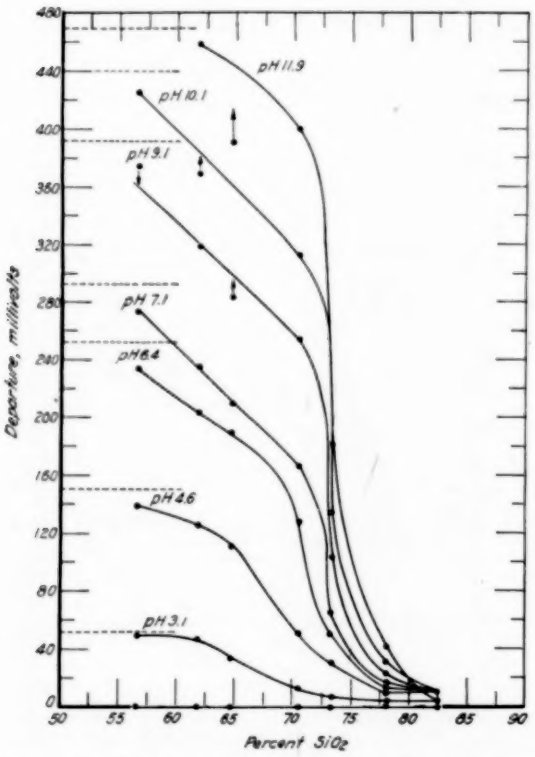

FIGURE 4. *Voltage departures (errors) at various* pH *values for electrodes from* Na_2O-SiO_2 *glasses.*

The dashed lines are the voltage departure values obtained for a "punctured" electrode.

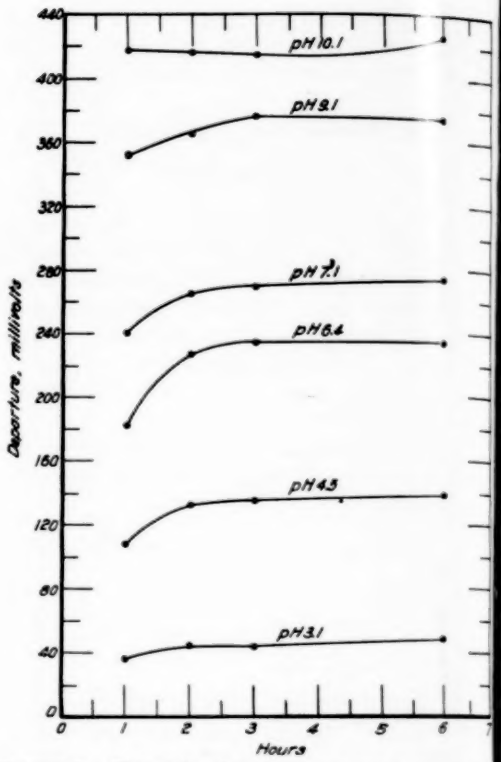

FIGURE 5. *Change in voltage departure over a period of 6 of an electrode prepared from a glass of 43.4 percent* Na_2O *and 56.6 percent of* SiO_2.

accompanied by large voltage departures, and th electrode response of these glasses was erratic These values tended to drift, as is shown in table and figure 5 for an electrode of 56.6 percent silica. At the end of 6 hr, the electrode fail because of hydrolysis of the glass in the buff solution. Voltage departures of electrodes fro glasses of decreasing percentages of silica a proached those of a punctured electrode, as show in figure 3. These values in turn were similar those obtained from a calomel half cell. It obvious that an electrode prepared from a gla absorbing a sufficient amount of water wou necessarily be a punctured electrode.

The response of an electrode prepared from th glass of 82.6 percent of silica approached that the Corning 015. A maximum departure w obtained at pH 4.6, which remained consta until pH 10 and returned toward zero departu at pH 11.9. This latter effect could be attribute

either to improved durability of the glass or to deviation of the reference electrode in this pH range.

TABLE 2. *Voltage departures (errors) at various time intervals for an electrode prepared from a glass containing 43.4 percent of* Na_2O *and 56.6 percent of* SiO_2.

pH	1 hr	2 hr	3 hr	6 hr
1.9	0	0	0	0
3.1	36	44	44	49
5	108	132	135	139
7.4	182	227	234	234
9	240	265	269	274
9.1	352	365	376	374
10.1	417	416	414	425

The values of durability and hygroscopicity for some of the glasses above 82.6 percent of silica indicated that they would produce serviceable electrodes. Extrapolation of the voltage departure curves in figure 4 also indicated that this would be true. Unfortunately, these glasses have high liquidus temperatures and tend to devitrify: hence successful electrodes were not made.

4. Apparent Response to Sodium Ion Activity

Voltage departures from the straight-line relationship exhibited by glass electrodes have generally been interpreted as an equilibrative response to ions other than hydrogen [6]. The data, given in the last column of table 1 and plotted in figure 6, indicate that over the range of pH 1.9 to 10.1 for which a change of pNa of 1.25 units [3] takes place, only a glass of approximately 75 percent of SiO_2 would provide the correct response of 59 mv/pNa. This glass would have poor durability. At compositions where the durability is improved, the response to pNa is too low, whereas glasses of lower silica content have apparent pNa responses that are too high. It is apparent that voltage departures for electrodes prepared from these soda-silica glasses cannot be attributed to response to the sodium ion activity of the buffer solutions.

pH	Britton-Robinson acid mixture volume	0.2 *N* NaOH volume	[Na^+]	pNa
	ml	*ml*		
1.9	100	2.5	0.00488	2.31
10.1	100	78.4	.0878	1.06
				△pNa=1.25

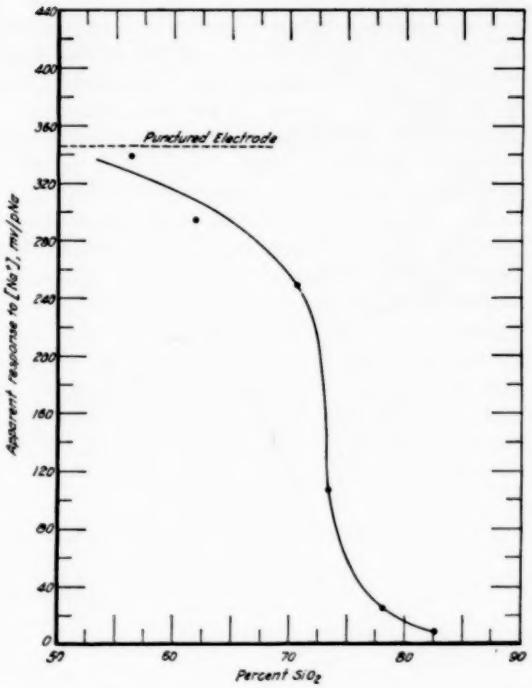

FIGURE 6. *Apparent response to* [Na^+] *of electrodes prepared from* Na_2S-SiO_2 *glasses.*

The values are calculated from voltage departures and [Na^+] for the buffer solutions at pH 1.9 and 10.1.

IV. Summary and Conclusions

A series of glasses in the soda-silica system ranging from 51 percent to near 100 percent of silica were prepared and the durability, hygroscopicity, and electrode function studied. In accordance with the statement that the requirements for a good electrode glass were uniform durability over a long pH range and adequate hygroscopicity, it was predicted that a glass composed of 86 percent of silica and 14 percent of soda would function well as a hydrogen electrode. Unfortunately, this glass has a high liquidus temperature and tends to devitrify, so that satisfactory electrodes were not made. These glasses were hygroscopic, and it is of interest that the

803370—48——3

hydroscopicity data can be plotted in such a manner that changes in slope occur at points that are significant in the phase diagram of the soda-silica system. The glasses could be grouped into three durability classes: Those that were readily soluble, those that had a tendency to swell in acid solutions, and those above 90 percent of silica in which greatly reduced attack was indicated.

The voltage departures of electrodes prepared from the glasses of very high hygroscopicity and poor durability were similar to those of punctured electrodes, which in turn approached the values of a calomel half cell. The large departures of these electrodes could be attributed either to poor durability or to infinite hygroscopicity but not to a pNa response, as it was shown that the departures were not compatible with this latter interpretation.

V. References

[1] Donald Hubbard and Edgar H. Hamilton, J. Research NBS **27,** 143 (1941) RP1409.

[2] Donald Hubbard, Edgar H. Hamilton, and A. N. Finn, J. Research NBS **22,** 339 (1939) RP1187.

[3] Donald Hubbard and Gerald F. Rynders, J. Research NBS **39,** 561 (1947) RP1848.

[4] Donald Hubbard, J. Research NBS **36,** 511 (1946) RP1719.

[5] Donald Hubbard, J. Research NBS **37,** 223 (1946) RP1743.

[6] B. Lengyel and E. Blum, Trans. Faraday Soc. **30,** 461 (1934).

[7] C. A. Faick and A. N. Finn, J. Am. Ceram. Soc. **14,** 518 (1931); BS J. Research **6,** 993 (1931) RP320.

[8] C. A. Faick and B. Fonoroff, J. Research NBS **32,** 67 (1944) RP1575.

[9] H. T. S. Britton, Hydrogen ions, I, 3d ed., 88c, p. 313 (D. Van Nostrand Co., Inc., New York, N. Y., 1943).

[10] F. Haber and Z. Klemensiewicz, Z. physik. Chem. **67,** 385 (1909).

[11] M. R. Thompson, BS J. Research **9,** 833 (1932) RP511.

[12] D. A. MacInnes and M. Dole, J. Am. Chem. Soc. **52,** 29 (1930).

[13] Malcolm Dole, Glass electrode, p. 78 (John Wiley & Sons, Inc., New York, N. Y., 1941).

Washington, May 24, 1948.

U. S. Department of Commerce
National Bureau of Standards

Research Paper RP1924
Volume 41, October 1948

Part of the Journal of Research of the National Bureau of Standards

Effect of Temperature on the Volume of Leather and Collagen in Water

By Charles E. Weir

The coefficients of cubical expansion of 10 tannages of leather and tendon collagen have been measured by using water as the confining liquid. The results, calculated for dry leather of density 1.560 g/ml, show that an average coefficient of 540×10^{-6}/°C applies for collagen and all leathers except chrome-vegetable leather, the coefficient of this tannage being 340×10^{-6}/°C. These averages have a reproducibility indicated by standard deviations of 13×10^{-6}/°C and 37×10^{-6}/°C, respectively. The "shrinkage" or transition temperature is a band rather than a sharp point on the temperature scale. During apparent shrinkage, an increase in real volume of approximately 1 percent occurs. This increase in volume is irreversible, but the thermal expansion below the transition range is nearly completely reversible. The rate of expansion during transition of collagen follows the law of a first-order reaction. The results are interpreted as indicating that the shrinkage does not occur at a characteristic temperature but is a rate process. The transition may be pictured as a change of state possibly coupled with a reaction.

I. Introduction

Although the art of leather manufacture predates historical records, the physical and physicochemical constants, as well as the details of the chemistry of leather and its parent substance, collagen, are largely unknown. Published data for the ordinary physical constants of leather and collagen are practically nonexistent. This lack of data may be attributed directly to the extreme chemical and physical complexity of the system of tanned collagen fibers known as leather. Although it is accepted that leather is possibly not a pure substance and is subject to variations due to differences in the hide itself and introduced by nonuniformity of the tanning processes, it is a matter of practical and theoretical interest to determine either the physical constants or their order of magnitude.

The present experiments were designed primarily to measure the coefficient of cubical expansion of leather with full cognizance that information of a new nature would be obtained in the region of the shrinkage temperature. Using glass dilatometers with water as the confining liquid, it was found that the average coefficient of cubical expansion calculated for dry material is 540×10^{-6}/°C for collagen and all tannages with the exception of chrome-vegetable retan leather, which exhibited a smaller coefficient. This expansion is reversible below the shrinkage or transition temperature. If the leather-water system is heated in the neighborhood of the transition temperature, an irreversible expansion analogous in some respects to a fusion takes place. During this expansion in real volume, the apparent dimensions of the leather decrease, and the temperature at which this process occurs has heretofore been called the shrinkage temperature. The expansion in real volume occurs over a range of temperatures rather than at a sharp point on the temperature scale, and it appears that shrinkage is probably a rate process. The rate of expansion of collagen was found to follow the law of a first-order reaction. At temperatures exceeding the shrinkage temperature, the material formed during transition exhibits reversible expansion, the coefficient of which is essentially of the same order of magnitude as that of the original leather.

II. Apparatus

The dilatometer used is shown in figure 1. Two such dilatometers of the same dimensions were constructed with Pyrex ground glass joints to facilitate cleaning and inserting samples. The stopcock attached to the side arm was used for filling and to permit removal of liquid during the course of the measurement, so that the complete temperature range 25° to 75° C could be covered without using excessively long capillaries. The calibrated capillaries were capped with small ground tips containing a minute hole to permit expansion of the liquid but to retard evaporation of water from the capillary.

The two dilatometers were mounted side by side on a framework, to which was affixed a sheet of graph paper ruled in millimeters. The framework containing the dilatometers was placed opposite a triple-pane insulating window in a temperature-controlled airbath that maintained a temperature in the range 25° to 75° C to within ± 0.001 deg C, as shown by preliminary tests with a Beckman thermometer. Experimental temperatures were measured with the desired accuracy by means of a thermometer graduated to 0.2 deg C, which was hung between the dilatometers so that it could be read through the window.

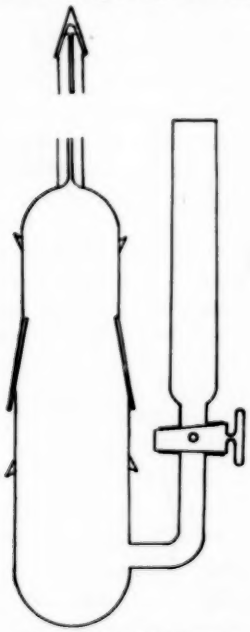

FIGURE 1. *Dilatometer.*

III. Experimental Procedure

1. Preparation of Specimens

Leather used in these experiments was in the form of strips 1 by 3 in. The strips were degreased with chloroform in a Soxhlet extractor for 24 hr washed in running water for 48 hr and then conditioned at $70° \pm 1°$ F and 50 ± 2 percent relative humidity for at least 7 days. Prior to use, the strips were weighed and immersed in distilled water in a suitable vacuum flask. The system was connected to a water pump and evacuated at approximately 30 mm of Hg for at least 48 hr. Sufficient leather was prepared to permit a moisture determination on conditioned strips not used for test.

2. Method of Measurement

The two clean, dry dilatometers were weighed. One dilatometer, hereafter referred to as the blank, was filled with freshly boiled distilled water by using the side arm and stopcock. Trapped and dissolved air was removed by attaching the dilatometer to a water pump by means of the capillary and pumping at a pressure of approximately 30 mm of Hg for several minutes, the stopcock being closed during this process. The water remaining in the side arm was removed by use of alcohol and ether, and this dilatometer was reweighed to obtain the weight of water in the blank.

The second dilatometer was packed with weighed strips of leather that were prepared as described, then filled with water in a similar manner and reweighed. From these measurements, the following necessary data were obtained: (1) the weight of water in the blank, (2) the weight of dry leather in the experimental dilatometer, (3) the weight of water in the experimental dilatometer (this figure includes the weight of the water in the leather obtained from a moisture determination on the conditioned strips).

The dilatometer assembly was placed in the air bath, which was adjusted to the lowest temperature at which both water levels in the capillary tubes were in the range of calibration of the capillaries and after attainment of equilibrium, the readings of the heights of the levels and the temperature were recorded.

The temperature of the air bath was then raised approximately 2 deg C and after attainment of

equilibrium (approximately 3 hr), the temperature and heights of the levels were again recorded. This procedure was repeated until the levels approached the top of the capillaries. At this point, after recording the readings, the stopcocks on the dilatometers were opened, and water was drained from the systems until the levels were again at the bottom of the capillaries. Since this procedure necessitated opening the air bath, it was necessary to permit temperature equilibrium to be reestablished before recording the height of the water levels. From a knowledge of the capillary calibration curves, and the recorded heights of the levels, the volumes of water removed were calculated. A knowledge of the density of water at the temperature of draining permitted calculation of the weight of water removed and consequently a correction of the weights of water in the dilatometers.

3. Calculation of Coefficients of Expansion

From a knowledge of the capillary calibration curves, all readings of heights of water levels were converted into increments of volume based on the initial height of the water level. The volume increment of the water in the dilatometer containing leather was calculated from the volume increment observed in the blank and the ratio of the wieghts of water in the two chambers. Subtraction of the calculated volume increment of the water for the dilatometer containing leather from the volume increment observed in this container, yielded the volume increment of the leather. The volume increments were plotted as ordinates with the corresponding temperatures as abscissas, and the slope of the line through the points was calculated by the method of least squares. The slope of the line, so obtained, was divided by the volume of the leather at the initial temperature to give the coefficient of cubical expansion of the leather.

IV. Results and Discussion

1. Coefficients of Cubical Expansion

The results of the individual measurements of the coefficients of expansion are given in table 1, and the chemical analyses of the leathers are given in table 2.

TABLE 1. *Expansivity of leather and collagen*

Type of material	Volume expansivity	Weight expansivity
TANNAGES ON WHICH DUPLICATE DETERMINATIONS WERE MADE		
	$1/°C$	$(ml/g)/°C$
Chrome	565×10^{-4}	362×10^{-4}
Do	496	320
Chrome-vegetable	398	275
Do	339	217
Vegetable	543	337
Do	502	322
Alum-vegetable	599	383
Do	590	379
TANNAGES ON WHICH SINGLE DETERMINATIONS WERE MADE		
Vegetable-chrome	497×10^{-4}	319×10^{-4}
Iron	592	380
Zirconium-vegetable	473	303
Formaldehyde	532	341
Uranium	532	341
Tendon collagen	538	345

TABLE 2. *Chemical analyses of leathers and collagen used for expansivity measurements*

All figures calculated on dry basis except those for moisture and acidity.

Type of leather	Moisture	Total ash	Grease	Oxide of metal tanning agent	Hide substance	Water-soluble material	Insoluble ash	Acidity
	Percent	*Percent*	*Percent*	*Percent*	*Percent*	*Percent*	*Percent*	pH
Uranium tannage [1]	14.9	14.2			86.5			3.8
Vegetable-zirconium [1]	14.0	5.5	0.2		53.0	5.5	5.4	3.7
Alum-vegetable [1]	12.4	11.4	.4	2.1	62.2	1.8	2.0	3.6
Chrome-vegetable [1]	15.3	5.1	.4		74.4	2.2	3.3	2.7
Alum [1]	11.0	8.1	38.7	1.7	53.7			2.7
Vegetable-chrome [1]	15.1	6.4	0.3	5.0	50.9	3.7	4.5	3.4
Chrome [1]	13.8	4.8	10.4	3.9	73.7			3.2
Vegetable [1]	10.8	1.0	12.1		44.8	9.0	0.2	3.2
Iron [1]	13.4	12.8	5.9	11.9	69.9			3.4
Tendon-collagen [2]	15.7	2.4			98.5			6.0

[1] Analyses made on degreased, washed leather or collagen.
[2] Analyses made on untreated leather.

It is to be noted that the coefficients of expansion agree fairly well, with the exception of the coefficients obtained for chrome-vegetable leathers, which are lower. Statistical analysis of the data obtained from duplicate measurements on four different specimens shown at the top of table 1 yielded the following results:

a. The standard deviation of a single measurement of volume increment is 0.0065 ml, as estimated from the least-squares calculations.

b. The weighted average expansivity of leathers on which duplicate measurements were made, exclusive of chrome-vegetable leathers, is 540×10^{-6}/°C. The standard deviation corresponding to this value is 13×10^{-6}/°C.

c. The weighted average expansivity of chrome-vegetable leather is 340×10^{-6}/°C. The standard deviation corresponding to this value is 37×10^{-6}/°C.

d. The variations of expansivity shown by similar specimens of the same tannage are larger than those anticipated by the experimental errors. Therefore, it is probable that different specimens of the same leather have somewhat different expansivities.

e. The values obtained for chrome-vegetable leather are significantly lower than the average value for the other specimens. The over-all average coefficient of expansion of the samples, including collagen but excluding chrome-vegetable leather, is 540×10^{-6}/°C. The weighted average coefficient of chrome-vegetable leather is 340×10^{-6}/°C.

f. Since there is, in general, no more variation between different leathers than that found between duplicate specimens, there is no necessity for assuming that the expansivity varies appreciably with the tannage, except for chrome-vegetable leather.

Chemical analyses given in table 2 were made in accordance with methods described in Federal Specifications for Leather and Leather Products, KK–L–311, dated March 28, 1945. The analyses were made, in part, on specimens that had been degreased and washed in accordance with the method described for preparation of specimens for expansivity measurements. Such analyses are denoted by footnote 1. Analyses made on samples of leather before any treatment are denoted by footnote 2. All results, except those for moisture and acidity, are calculated on a dry basis.

The volume expansivities given in table 1 are calculated with the assumption that the density of dry leather, irrespective of tannage, is 1.560 g/ml at 70° F. This assumption was made necessary by the lack of data on the density of dry leather. The density figure of 1.560 g/ml was obtained from the data given by Kanagy and Wallace [1].[1] Their figures were calculated to a dry basis and averaged, assuming an average moisture content of 14.60 percent. The figures for the weight expansivities are included in the table, since these figures were measured directly and the volume expansivities involve the assumptions enumerated.

Despite the wide variety of leathers tested, it is seen that the expansivities are very similar and show much less variation than is exhibited by results of most physical tests of leather. In view of this agreement and the fact that variation of density with tannage is most probably a second order effect, the expansivity of 540×10^{-6}/°C is ascribed to leather in general. It must be remembered, however, that this expansivity applies only to leather in water, as evidence has been obtained that a smaller expansivity results if nonpolar liquids are used to confine the leather.

The analyses show a wide range of hide substance content that necessitates the assumption that the collagen itself is the substance reponsible for almost the entire expansion and that salts or tanning materials present contribute little to the expansivity. Since the expansivity is of the magnitude of that of a liquid, and the other materials present are, in the free state, solids, this might be expected.

The volume expansivity obtained from these measurements is not in agreement with a value for the linear expansivity reported by Mitton [2], who found a coefficient of linear expansion of 22×10^{-6}/°C. This value, which was obtained from measurements on dry fibers at elevated temperatures, is of a different order of magnitude than the values for cubical expansion and is typical of a solid. Aside from possible differences due to temperature and environment, the disagreement between the two values is to be expected on the basis of the present concept of the structure of collagen [3].

[1] Figures in brackets indicate the literature references at the end of this paper

Collagen is anisotropic and probably consists of layers of peptide chains oriented parallel to the fiber axis. The layers of chains are assumed to be held together by salt-bonds and hydrogen-bonds. In the direction of the fiber axis it is to be expected that the strong covalent chemical bonds will produce a structure resembling that of a solid and cause a low expansivity. At right angles to the fiber axis the weaker, less well-defined bonds are expected to yield a higher expansivity. Since the volume expansivity represents the sum of the expansivities along the three mutually perpendicular axes, the volume expansivity of collagen will therefore be typical of liquids, the contribution of the expansivity along the peptide chain being of a lesser order of magnitude.

2. Effect of Trapped Air

It has been suggested that reproducibility would be almost impossible because of uncertainties regarding removal of air from the interstices in the leather. The following calculation shows that the effect of trapped air on these measurements is not significant.

The maximum weight of leather used in any measurement was 35 g and may be considered to occupy 35 ml (density=1). Assuming the maximum percentage of voids found by Kanagy and Wallace [1] to be present, i. e., 60 percent, the void space is 21 ml. In the evacuation preparatory to test, a maximum pressure of 30 mm of mercury was used, of which, at 25° C, 24 mm is water vapor and 6 mm is air pressure. Assuming that half the void space is filled by displacement, 10 ml of air will be trapped at 6 mm air pressure. When atmospheric pressure is restored, this air will be compressed to 0.08 ml by relatively air-free water in which it may (and does) dissolve readily. If no solution takes place, this trapped air will undergo an expansion of less than 0.02 ml during a measurement in which the temperature is raised from 25° to 77° C. Since most measurements involve volume increments of 0.4 ml, the air would introduce an error of less than 4 percent in the final volume.

During preparation of dilatometers for test, it was observed that it was not necessary to remove the last traces of visibly trapped air, since small bubbles dissolved readily in the relatively air-free water and did not reform at the highest temperatures attained. The trapped air in the capillary system of the leather will also dissolve, and the resulting error from trapped air is probably negligible.

3. Expansion Curve and Transition

A series of typical expansion curves is shown in figure 2.

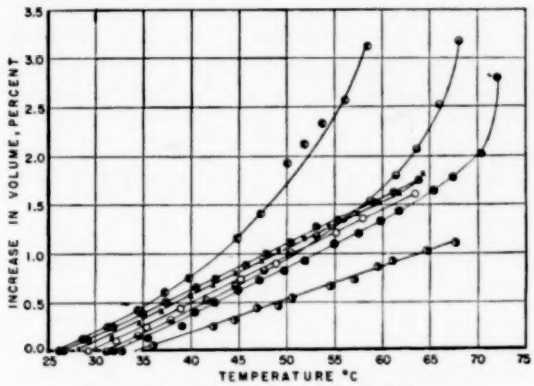

FIGURE 2. *Expansion curves for leather.*

◐, Alum; ⊗, zirconium-vegetable; X, vegetable-chrome; ○, chrome; ◒, alum-vegetable; ●, vegetable; ◑, chrome-vegetable.

In this figure the percentage increase in volume is plotted against the temperature.

The initial portion of each curve is linear and was used for calculation of the coefficients. It will be noted that all the initial linear portions are parallel, save that of the chrome-vegetable leather. Along this portion of the curve, equilibrium was established rapidly, i. e., in 3 hrs. At an elevated temperature, depending on the tannage, a slow process set in that resulted in the excessive expansions seen in three curves. The total volume of leather and fluid in the dilatometer increased, whereas the apparent dimensions of the leather diminished. This discontinuity is identified with the shrinkage temperature, but the changes actually involve an expansion of the real volume of the leather. Although it is not certain that measurements in this region attained equilibrium, because of the slowness of the process involved, it is most probable that there is a progressive increase in volume, as shown by the figure, i. e., the expansion is not a change of state that occurs at a definite temperature, but is rather an analogous change that takes place over an interval of temperatures and may be considered to be a rate process.

The extent of the expansion at this transition has been evaluated roughly and is of the order of 1 percent. That the transition is not a simple fusion is shown by the observation that measurements conducted for long periods of time after transition occurred resulted in almost complete solution of the leather in the form of gelatine. One measurement on alum-vegetable tanned leather showed that two transitions were possible, one probably corresponding to transition of the central band of alum-tanned material and the other corresponding to the transition of the two external vegetable retanned strips. All samples tested showed this increase in volume on transition, with theexception of those for which the transition temperature was too high to be attained.

The increase in volume occurring in the transition process contradicts earlier predictions by Salcedo and Highberger [4], and by Wilson and Porth [5] that contraction should occur during shrinkage. The indication that transition is a process occurring over a temperature interval is at variance with a statement by Wohlisch [6] to the effect that shrinkage takes place above a sharply defined temperature.

Measurements of the shrinkage temperatures of some samples were made in accordance with the method described in Federal Specification for Leather and Leather Products KK–L–311, dated March 28, 1945. These measurements made on alum, alum-vegetable, and vegetable-tanned leathers gave shrinkage temperatures of 73°, 83°, and 68° C, respectively, whereas the transition temperatures noted on the curve as the departure from linearity are 35°, 48°, and 60° C, respectively. This also indicates that the shrinkage temperature is a function of environment and may vary by as much as 38° C, as in the alum-tanned leather.

The linearity of the graphical representation of the results is an argument against the formation of various hydrated leathers. Since there are no breaks in the lines, except for the transition process, if there is a hydrate present, it is stable over the temperature range of 25° to 75°C.

4. Reversibility of Expansion

In figure 3 are shown typical expansion curves in which measurements were made to determine the reversibility of the processes involved in the expansion.

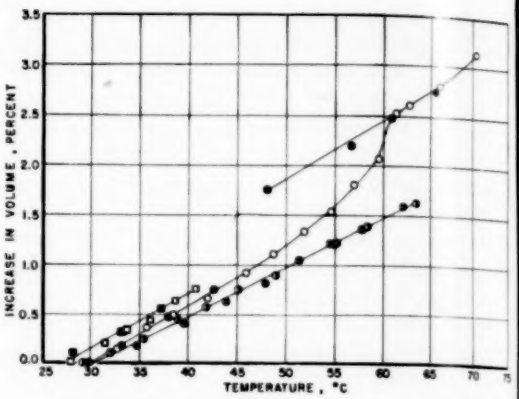

FIGURE 3. *Reversibility of expansion curves.*

□, Tendon collagen, increasing temperature; ■, tendon collagen, decreasing temperature; ○, alum vegetable, increasing temperature; ●, alum vegetable, decreasing temperature; ◑, chrome, increasing temperature; ◐, chrome, decreasing temperature.

These measurements were made by increasing the temperature in 2 deg to 3 deg C steps until the liquid level approached the top of the capillary and then reversing the process and decreasing the temperature stepwise. After this one reversal, the temperature was again raised to the previous maximum, the volume was noted, the capillaries were drained, and the procedure was repeated at higher temperatures. Within the experimental error, the same volume was obtained at the maximum temperature before and after reversal. As shown by the figure, the linear portion of the curve is almost completely reversible. There is some indication from these and other measurements to be reported on the rate of shrinkage, that this reversibility is not complete even at moderate temperatures, but the divergence is very small. In this portion of the curve it appears, therefore, that the final volume is not influenced significantly by the time required for equilibrium to be established.

After passing through the transition, however, the process is not reversible, the contraction curve being displaced from the expansion curve by the increment in volume of the transition. This behavior was verified in every transition observed and represents definite evidence of the irreversibility of the transition process and further evidence that this is not a fusion unless the crystallization process be assumed to be extremely slow. It is very probable that a transition and a reaction with water take place and that even though the

reaction may be reversible, the formation of cross linkages is not because of deformation.

5. Rate of Transition

The measurements made on tendon collagen shown in figure 3 afforded a measurement of the rate of shrinkage. As shown in the figure, the temperature was raised to 41° C and then reduced to 28° C. It was not considered wise to exceed 41° C before reversing the process because of the possibility of transition. After the investigation of the reversal, the next higher temperature reached was 43° C, and after 2.5 hr at this temperature transition set in, and the rate of the process was measured. A graphical representation of the results is shown in figure 4, in which the logarithm of the volume change is plotted against the time.

This sample was essentially at equilibrium at 43° C when the transition ensued, and the increase in volume is measured from this pseudo-equilibrium value. It is noted that a straight line results, indicating a first-order reaction. Deviation from the line is to be expected after long intervals, since water is probably used up in the transition, and only a limited amount of water is available in the dilatometer.

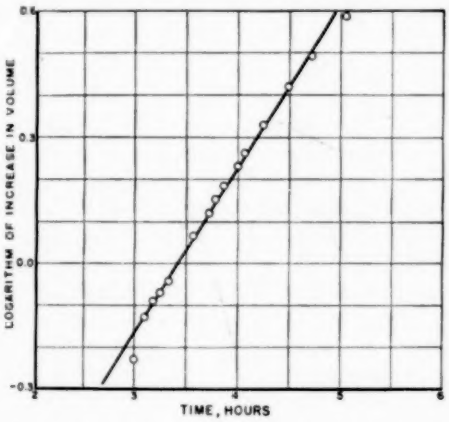

FIGURE 4. *Rate of transition of tendon collagen.*

A calculation of the velocity constant has not been made, since the variation of the constant with temperature may not be ascertained readily in this apparatus. Likewise the original and final volumes are not known, inasmuch as this transition produced an increase in volume sufficiently large to exceed the capacity of the capillary and render further measurements impossible. Further measurements are in progress on the rate of the transition and the temperature dependence of the velocity constant.

The author expresses his appreciation to John Mandel for the statistical analyses of the experimental data.

V. References

[1] Joseph R. Kanagy and Everett L. Wallace, J. Am. Leather Chem. Assn. **38**, 314 (1943).
[2] R. G. Mitton, J. Int. Soc. Leather Trades Chem. **29**, 169 (1945).
[3] George D. McLaughlin and Edwin R. Theis, The chemistry of leather manufacture (Reinhold Publishing Corp., New York, N. Y., 1945).
[4] Ingacio S. Salcedo and John H. Highberger, J. Am. Leather Chem. Assn. **36**, 271 (1941).
[5] John A. Wilson and Irving H. Porth, J. Am. Leather Chem. Assn. **38**, 20 (1943).
[6] W. Wohlisch, Biochem. Z. **247**, 329 (1932).

WASHINGTON, May 6, 1948.

803370—48——4

U. S. Department of Commerce
National Bureau of Standards

Research Paper RP1925
Volume 41, October 1948

Part of the Journal of Research of the National Bureau of Standards

Image Shifts Caused by Rotating a Constant-Deviation Prism in Divergent Light

By James B. Saunders

The use of the constant-deviation prism for producing monochromatic light introduces the problem of image shifts that result from rotating the prism when changing from one spectral line to another. The magnitudes of both the lateral and the axial components of this shift, for a given rotation of the prism, depend upon the position of the axis about which the prism rotates. A position for the axis is known that yields zero lateral shift. The axial shift, however, depends also upon the convergence of the beam and the shape and optical properties of the prism. In this paper a method is presented for locating the positions of the axis of rotation for minimum axial and for minimum total shifts of the foci for both the sagittal and meridian fans of rays.

I. Introduction

The constant-deviation prism, as used in a parallel beam of light emerging from the collimator of a spectroscope or monochromator, has been discussed by Uhler [1, 2],[1] Forsythe [3], and Block [4]. These authors were interested only in the lateral movement of the beam that occurs when the prism is rotated, as in changing from one spectral line to another. They gave no consideration to the case of convergent or divergent light and, therefore, ignored the possibility of axial or lateral changes in the position of the image. Such displacements did not enter their problem, because there is no change in the position of the image if the rays of light within the prism remain parallel. As a result of their studies for the case of collimated light, a unique position of the axis of rotation for which no lateral shift of the beam occurs is known. In this paper it is shown that the same axis serves for noncollimated light as well.

The magnitude of the lateral shift of a converging or diverging beam of light is a measure of the lateral shift of the image. Consequently, the lateral position of the beam and the axial positions of the primary and secondary images, as functions of the angular position of the prism, determine the movements of the image point when the prism is rotated. A simultaneous treatment of these three functions shows that any two of the shifts may be practically eliminated by a proper selection of the axis of rotation.

In most applications of the constant deviation prism a slit-like source (or its equivalent) is used, and one of the astigmatic images either becomes of secondary importance, or its axial movements may be ignored. In this paper a particular application of the constant deviation prism is considered in which one or the other of these images may be ignored. The treatment applies to the recently designed interferograph [5], an instrument for photographing the movements of interference fringes. A constant deviation prism and a single achromatic lens are used to form a monochromatic image of the interference pattern on a photographic film at a fixed distance. The derived equations apply to any triangular constant deviation prism, and particular properties are assigned for an illustration of results.

II. Statement of the Problem

An investigation of the axial image shifts caused by rotating the prism is facilitated by treating the

[1] Figures in brackets indicate the literature references at the end of this paper.

meridian (Southall's terminology [2] used) and sagittal rays separately. The primary and secondary images of a plane that are produced by these two beams usually do not coincide, nor is the shift of the two images equal for a given rotation of the prism about a specified axis. The shape and orientation of the source that illuminates the object plane may, and usually do, contribute differently to the astigmatic effect. Assuming the object to be a point on an interferometer plate that is illuminated by collimated light from a slit-like source in the focal plane of the collimator, a cross section of the beam reflected from this point will approximate a line. Whenever such a beam passes through a prism and a single lens to produce a real image of the point, the astigmatic effect caused by the prism depends upon its orientation with respect to the slit-like source. If the slit-like source is parallel to the refracting edge of the prism, the sagittal rays are more divergent than the meridian rays. The difference in divergence is reversed if the refracting edge is perpendicular to the source. In either case, the less divergent beam produces an image with a comparatively large depth of focus, whereas the depth of focus for the more divergent beam is relatively small. Consequently, the beam that has the greater divergence requires more consideration.

A detailed treatment of this problem of the lateral and axial shifts is too extensive to be given here. However, a presentation of the fundamental equations and their application to a typical, but particular, case furnished the necessary basis for their application to other particular cases. The equations of condition form a system of simultaneous equations, the solution of which gives all the information necessary for a solution in any special application. Either of two slightly different methods of attacking the problem may be followed. One is to require the differential of the shifts with respect to the angle of rotation of the prism to be zero at some specified wavelength of light. Usually this wavelength should be chosen near the middle of the visible spectrum. The second method requires the equality of the image distances for two wavelengths, one near each end of the visible spectrum. The second of these procedures was chosen because it seemed somewhat simpler for this particular presentation.

The following is a sufficient statement of the general problem for its analytical treatment. A source [3] of light is located on the axis and in the left focal plane of the achromatic lens shown in figure 1. The point at which the axial ray emerges from the lens is chosen as the origin of a plane oblique coordinate system with the x-axis coinciding with the axis of the lens. A constant deviation prism is placed with the center of its entrance face initially at the point (G,O) and with its refracting edge normal to the plane of the coordinate axes. Collimated light, from the lens, falls on the first or entrance face of the prism, is internally reflected at the second face, and emerges from the third or exit face at various angles, depending upon the angle of incidence and the geometrical and optical properties of the prism. This discussion is limited to those rays whose angle of emergence, θ, equals the angle of incidence, a condition corresponding to minimum deviation. The total deviation of the rays that emerge under this condition is constant regardless of their wavelengths, and is equal to the angle of the prism as shown in figure 1.

For the initial conditions of the analytical treatment, it is assumed that the angular position, θ_2, of the prism corresponds to the known refractive index for wavelength, λ_2, near the middle of the visible spectrum. The indices for two other wavelengths, λ_1 and λ_3, one near each end of the visible spectrum, must also be known. After the prism has been placed in the above initial position, θ_2, all further movements are limited to rotation about some specified axis that is normal to the plane of coordinates. The position of the prism shown in figure 1 is the result of an arbitrary rotation from the initial position. The angle between the positive x- and y-axes is chosen equal to the internal angle, ω, of the prism that lies opposite the reflecting face so that the emergent ray will be parallel to the y-axis.

The principal emergent ray is intercepted normally by a stationary interferometer plate. This point of interception and reflection (X_3, Y_3) is considered the object point. The principal ray returns from the interferometer along its previous path and continues along the axis of the lens to the conjugate plane of the interferometer. The

[2] The "meridian rays" are those refracted rays of an infinitely narrow homocentric bundle of incident rays that lie in a principal plane of the prism. The "sagittal rays" are those that lie in a plane containing the chief refracted ray and perpendicular to the principal plane.

[3] Such a source can be virtual and formed by a plane, half-silvered mirror that is so orientated that it reflects the light from a real source to the lens.

image point, therefore, remains on the axis of the lens regardless of changes caused in the position of the object pomt by rotating the prism. Any lateral change in the position of the object point is relative to the fixed interferometer and therefore corresponds to a lateral change in the position of the image of the interferometer. Also, a change in the effective object distance caused by rotating the prism produces a corresponding change in the axial or longitudinal position of the image distance. Consequently, the lateral shifts and effective object distances of the object point are a measure of the lateral and longitudinal shifts, respectively, of the image of the interferometer. The correspondence between image and object movements are so well known that this discussion will be limited to movements of the object point alone. The problem then is to locate the position, (X, Y), of the axis of rotation that will result in a minimum shift of the object point as the wavelength of the light, falling normally on the interferometer, changes from λ_1 to λ_3.

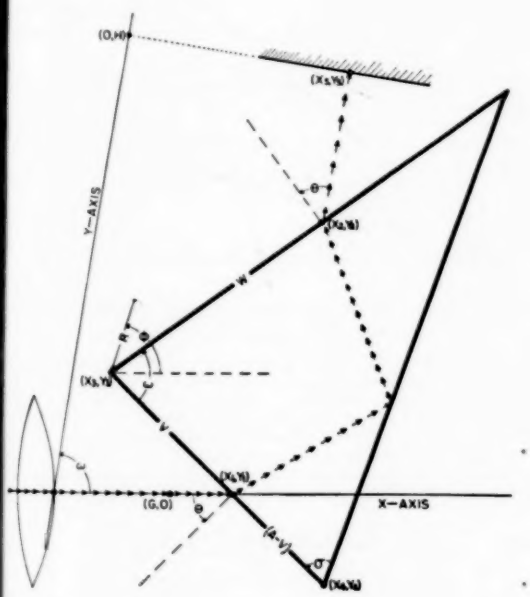

FIGURE 1. *Diagram showing the relative position of optical parts.*

The collimating lens, constant deviation prism, and the interferometer plate are schematically represented. The coordinates of the points that are indicated by dots are represented by the symbols in the adjacent parenthesis. The sum of the segments V and $(A\text{-}V)$ is A, the length of the entrance face of the prism, and is the unit of length on which all the computations are based.

III. Symbols and Abbreviations

The solution of this problem requires a considerable number of symbols. The definition of those that have not already been given or that are not obvious from the figures are listed below.

λ_1, λ_2, and λ_3 are wavelengths of light corresponding to known indices of refraction of the prism. Usually these correspond to the C, D, and F Fraunhofer lines. θ_1, θ_2, and θ_3 are angles of incidence (or angles of emergence) corresponding to wavelengths λ_1, λ_2, and λ_3, respectively. θ_m is the value of θ when $\delta X_5/\delta\theta=0$. A is the length of entrance face of prism. L is the path length of principal ray in prism.

L_2 = value of L for $\lambda=\lambda_2$

P = effective object distance for the sagittal rays

P_ν = value of P for $\lambda=\lambda_\nu$ ($\nu=1$, 2, or 3)

ΔP = absolute magnitude of difference between largest and smallest values of P in the range from θ_1 to θ_3

Q = effective object distance for the meridian rays

R = distance from vertex of angle ω to the axis of rotation

V = distance from (X_3, Y_3) to entrance point of axial or principal ray

$V_2=1/2A$ and is the value of V for $\lambda=\lambda_2$

W = distance from (X_3, Y_3) to exit point of principal ray

W_2 = value of W for $\lambda=\lambda_2$, defined in eq 14′

(X_c, Y_c) = coordinates of the "critical point," defined in the text

(X_i, Y_i) = coordinates of the "intersection point," defined in the text

$X_{5\nu}$ = value of X_5 for $\lambda=\lambda_\nu$ ($\nu=1$, 2, or 3)

ΔX_5 = absolute magnitude of difference between largest and smallest values of X_5 in the range from θ_1 to θ_3.

IV. Derivations

The following relationships are obtained from figure 1:

$$X_1-X_3=V\cos(\theta-\omega)\csc\omega, \tag{1}$$

$$Y_3-Y_1=V\cos\theta\csc\omega, \tag{2}$$

$$X_2-X_3=W\cos\theta\csc\omega \tag{3}$$

$$Y_3 - Y_2 = W\cos(\theta+\omega)\csc\omega, \quad (4)$$

$$X - X_3 = R\sin(\omega-\phi)\csc\omega, \quad (5)$$

$$Y - Y_3 = R\sin\phi\csc\omega, \quad (6)$$

$$X_2 = X_5, \quad (7)$$

$$Y_5 = H - X_5\cos\omega, \quad (8)$$

The principal ray coincides with the x-axis, therefore,

$$Y_1 = 0, \quad (9)$$

and since the prism must rotate as a rigid body, about the axis of rotation,

$$\theta - \theta_2 = \phi - \phi_2, \quad (10)$$

(θ_2 and ϕ_2 being the values for θ and ϕ for the initial conditions mentioned above).

The object distance for the sagittal rays is the sum of the equivalent air path of the principal ray [6] in glass, and the path in air, or

$$P = X_1 + Y_5 - Y_2 - L\cos(\sigma+\tfrac{1}{2}\omega)\csc\theta \quad (11)$$

The corresponding distance for the meridian rays is [6]

$$Q = X_1 + Y_5 - Y_2 - L\cos^2\theta\csc\theta \cos(\sigma+\tfrac{1}{2}\omega)\csc^2(\sigma+\tfrac{1}{2}\omega) \quad (12)$$

The values for L and $(V+W)$, both of which are derived from figure 2 by applying the law of sines to the several triangles formed in the figure, are found to be

$$L = 2V\cos\left(\sigma+\frac{1}{2}\omega\right) - 2A\sin(\sigma)\cos(\sigma+\omega)\csc\left(\sigma+\frac{1}{2}\omega\right), \quad (13)$$

and

$$V+W = 2A\sin\sigma\cos\frac{1}{2}\omega\csc\left(\sigma+\frac{1}{2}\omega\right). \quad (14)$$

The application of Shell's law to this particular problem gives the equation

$$\sin\theta = -n\cos\left(\sigma+\frac{1}{2}\omega\right). \quad (15)$$

from which the values of θ_1, θ_2, and θ_3, corresponding to λ_1, λ_2, and λ_3, respectively, are obtained.

The above equations, 1 to 15, are sufficient to derive the abscissa, X_5, of the object point; the object distance, P, for the sagittal rays; and the object distance, Q, for the meridian rays, in terms of known constants and the parameters θ, X, and Y.

The interferograph uses a slit-like source of light that is parallel to the refracting edge of the prism; consequently, the effect of the meridian rays is negligible in comparison to that of the sagittal rays. The equation for evaluating Q is therefore dropped from further consideration in this discussion. Should it be desirable to study Q, its treatment would be quite similar to that which will be followed here for P.

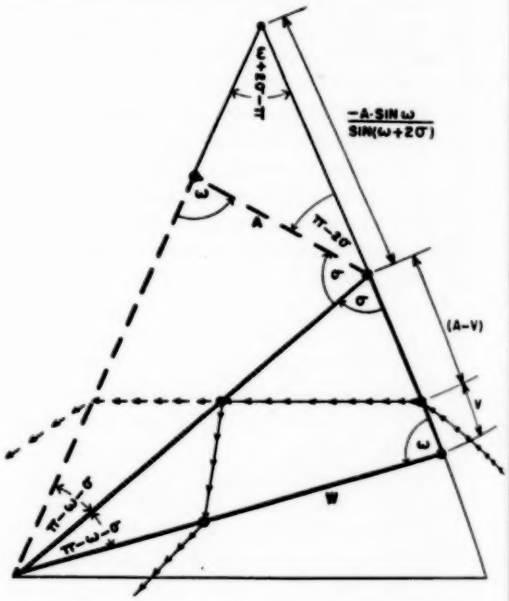

FIGURE 2. *Geometrical correspondence between equivalent isosceles and constant deviation prisms.*

The constant deviation prism is represented by the heavy line enclosure, with its reflecting face opposite the internal angle ω. The mirror image of this prism, as reflected in its reflecting face, is completed with the heavy broken lines. The image of the exit face coincides with the exit face of the corresponding isosceles prism, which is completed with light lines. Consequently, the path in glass for any given ray of light is the same for either prism and depends upon the dimensions and shape of the prism, the position of the entrance point, and the angle of incidence.

V. Illustrative Application

To illustrate the solution of this problem for an important particular case, a constant deviation prism of the Pellin and Broca [7] type is selected that has refractive indices such that θ_1, θ_2, and θ_3 are 54°, 55°, and 56°, respectively. The values of ω and σ are 90° and 75°, respectively. By substituting the angles of this prism into the general equations and eliminating Y_1 and X_2 by means of

eq 7 and 9, they reduce to the corresponding prime numbered equations given below.

$$X_3 = X_1 - V \sin\theta, \tag{1'}$$

$$Y_3 = V \cos\theta, \tag{2'}$$

$$X_2 = X_5 = X_3 + W \cos\theta, \tag{3'}$$

$$Y_2 = Y_3 + W \sin\theta, \tag{4'}$$

$$R \cos\phi = X - X_3, \tag{5'}$$

$$R \sin\phi = Y - Y_3, \tag{6'}$$

$$Y_5 = H, \tag{8'}$$

$$\phi = \theta + \phi_2 - \theta_2, \tag{10'}$$

$$P = X_1 + Y_5 - Y_2 + \frac{1}{2} L \csc\theta, \tag{11'}$$

$$L + V = A\left(1 + \frac{2}{\sqrt{3}}\right) = L_2 + \frac{1}{2} A, \tag{13'}$$

$$W + V = A\left(1 + \frac{1}{\sqrt{3}}\right) = W_2 + \frac{1}{2} A, \tag{14'}$$

$$n = 2 \sin\theta. \tag{15'}$$

On eliminating X_3, Y_3, and W by substitution from eq 1', 2', 3', 4', and 14', the following equations were obtained:

$$X_5 = X_1 - V \sin\theta + \left(W_2 + \frac{1}{2} A - V\right)\cos\theta, \tag{16}$$

$$Y_2 = V(\cos\theta - \sin\theta) + \left(W_2 + \frac{1}{2} A\right)\sin\theta. \tag{17}$$

Similarly, by eliminating X_3, Y_3, and ϕ from eq 1', 2', 5', 6', and 10', it follows that

$$X_1 = V \sin\theta + X - R \cos(\theta + \phi_2 - \theta_2), \tag{18}$$

$$V \cos\theta = Y - R \sin(\theta + \phi_2 - \theta_2). \tag{19}$$

On substituting the value of V from eq 19 into eq 13' and 18, they become

$$L = L_2 + \tfrac{1}{2} A + [R \sin(\theta + \phi_2 - \theta_2) - Y] \sec\theta, \tag{20}$$

$$X_1 = X + Y \tan\theta - R \cos(\phi_2 - \theta_2) \sec\theta \tag{21}$$

The value of V in eq 19 and X_1 in eq 21 are substituted into 16 and 17 to give the following:

$$X_5 = X - Y + R\,[\sin(\theta + \phi_2 - \theta_2) - \cos(\theta + \phi_2 - \theta_2)] + (W_2 + \frac{1}{2} A)\cos\theta, \tag{22}$$

$$Y_2 = (1 - \tan\theta)[Y - R \sin(\theta + \phi_2 - \theta_2)] + (W_2 + \frac{1}{2} A)\sin\theta. \tag{23}$$

By replacing Y_5, L, X_1, and Y_2 in eq 11' by their equivalents in eq 8', 20, 21, and 23, respectively, the equation for P becomes

$$P = X + Y(2 \tan\theta - 1 - \csc 2\theta) + H + (W_2 + \frac{1}{2} A)\sin\theta + \frac{1}{2}(L_2 + \frac{1}{2} A)\csc\theta + R[(1 - 2\tan\theta + \csc 2\theta)\sin(\theta + \phi_2 - \theta_2) - \cos(\theta + \phi_2 - \theta_2)]. \tag{24}$$

According to the above-described initial position of the prism for wavelength λ_2, it follows that for this position $\theta = \theta_2$, $X_1 = G$, and $V = \frac{1}{2} A$. By applying these initial conditions to eq 1', 2', 5', and 6', and by eliminating X_3 and Y_3, solutions are obtained for the initial values of R and ϕ (i. e., R_2 and ϕ_2) in terms of known constants and the coordinates, (X, Y), of the axis of rotation. They are

$$\tan\phi_2 = \frac{2Y - A\cos\theta_2}{2X - 2G + A\sin\theta_2}, \tag{25}$$

$$R^2 = (X - G + \frac{1}{2} A \sin\theta_2)^2 + (Y - \frac{1}{2} A \cos\theta_2)_2. \tag{26}$$

By substituting these values of R and ϕ_2 into eq 22 and 24, and after choosing values for X and Y, the changes in X_5 and P, for any rotation of the prism, are obtained.

Equation 22 may be written in the form

$$X_5 = \alpha + \beta \sin(\theta + \delta), \tag{22'}$$

where $\alpha \equiv X - Y$, and β and δ are related by the expressions $\beta \cos\delta \equiv R\,[\sin(\phi_2 - \theta_2) + \cos(\phi_2 - \theta_2)]$, and $\beta \sin\delta \equiv R\,[\sin(\phi_2 - \theta_2) - \cos(\phi_2 - \theta_2)] + W_2 + \frac{1}{2} A$. By eliminating δ from these equations, an expression relating β and R is obtained. A study of this relationship will show that when $\beta = 0$, the value of R is imaginary, except for the particular case when $\phi_2 = \theta_2 - \frac{1}{4}\pi$. Also, for this particular value of ϕ_2, $R = \frac{1}{\sqrt{2}}(W_2 + \frac{1}{2} A)$. When these values for ϕ_2 and $R(=R_2)$ are substituted into eq 25 and 26, the resultant values for X and Y are found to coincide with the coordinates of the point (X_c, Y_c), found by Bloch [4] and Uhler [2], for which there is no variation in X_5 as the prism is

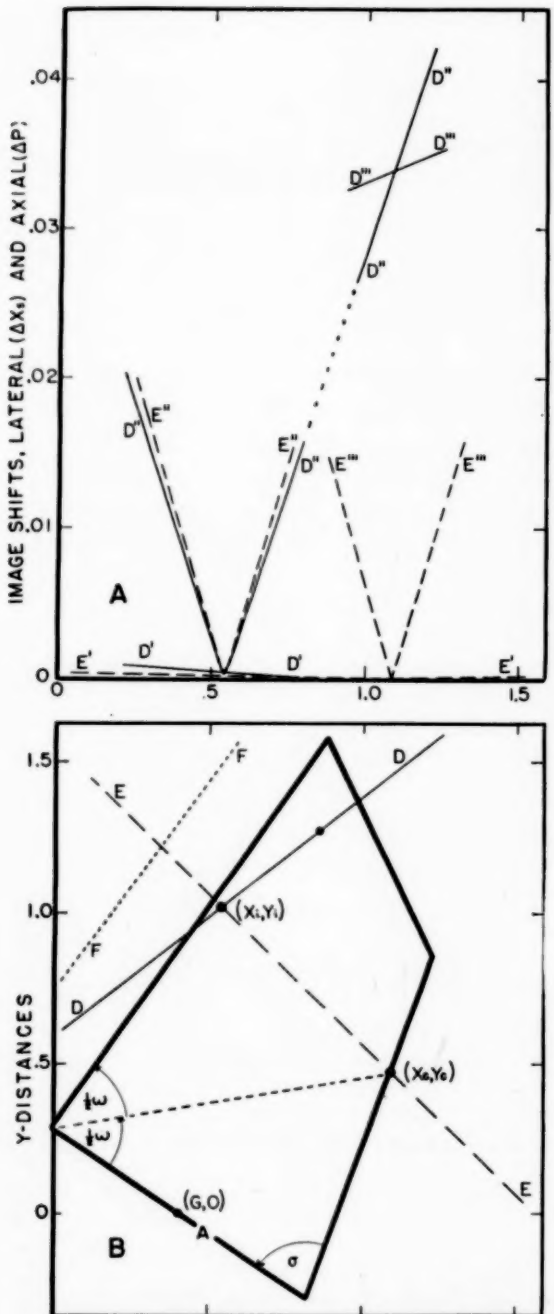

rotated. This point, designated here as the "critical point" (see fig. 3, B), is the intersection of the reflecting face of the prism with the bisector of the opposite angle, ω, when the prism is in the position of initial conditions. For values of β other than zero, the conditions for smallest change in X_s require that a maximum or a minimum of X_s must fall at $\theta=\theta_2$, which is midway between θ_1 and θ_3. This condition is realized by equating the value for X_{s1} to that for X_{s3}, which yields the straight line, $X+Y=X_e+Y_e$, and which is represented by $E-E$ in figure 3, B. If the axis of rotation is located at the critical point, then $X_{s1}=X_{s2}=X_{s3}=$constant for all values of θ. The critical point, therefore, lies on line E–E.

While eq 24 does not exactly represent a simple sine curve, it does so to a close approximation over the limited range of rotations involved in this problem. Consequently, the above discussion relating to the variation in X_s, as shown by eq 22, applies equally well to the variation of P as shown by eq 24. The straight line D-D in figure 3 bears the same relation to P that line E-E does to X_s. The point on D-D that corresponds to the critical point is indicated by the dot above line E-E. The change in P over the range θ_1 to θ_3 and for this point as axis of rotation is not zero but amounts to only a few microns if A is less than 10 cm. The intersection of E-E and D-D (X_i, Y_i) is designated as the "intersection point."

VI. Results

The variation in X_s with θ, in the range from 54° to 56°, is shown in figure 4, A, for several points selected along the line E-E as positions for the axis of rotation. Similarly, in figure 4, B, the same variation is shown for several points selected along the line D-D. The curves are labeled with the abscissas of the corresponding selected points. If the maxima and minima of a curve fall outside this range, as for curves labeled $X=0.525$, 0.531, and 0.560, the value of X_s

FIGURE 3. *Relation of image shifts to position of axis.*

A, Variation of image shifts, as the coordinates of the axis of rotation of the prism are changed; B, initial position of the prism and the relative position of the axis of rotation for minimum image shifts. The abscissa scale is common to both parts of this figure. All scale values are based on the length of the entrance face as the unit. The loci of the axis of rotation for minimum image shifts with respect to the angle of rotation are for the lateral shift, E—E, for the axial shift corresponding to the sagittal rays, D—D, and for the axial shift corresponding to the meridian rays, F—F.

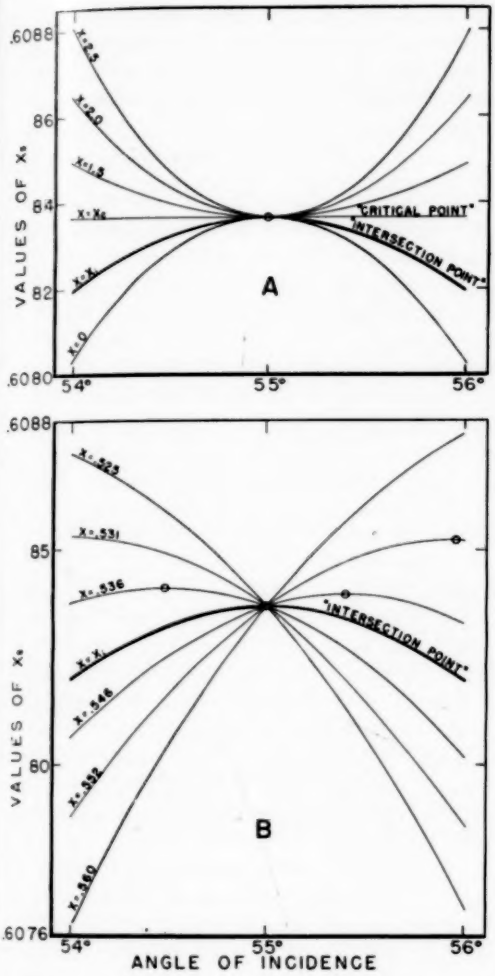

FIGURE 4. *Variation in lateral position of image.*

The change in the lateral position, X_5 of the image, with respect to θ, as the axis of rotation is moved along line *EE* of figure 3, B, is given in figure 4, A. The same change in image position, X_5, as the axis of rotation is moved along line *DD* of figure 3, B, is shown in figure 4, B.

increases or decreases throughout this range as the prism is rotated and the total absolute shift, ΔX_5, equals $|X_{51}-X_{53}|$. If a maximum or a minimum (indicated by circles on some of the curves) falls within this range, say at $\theta=\theta_m$, the variation in X_5 is opposite for the two ranges, θ_1 to θ_m and θ_m to θ_2. If θ_m differs from θ_2, the total absolute shift is the greater of the two values, $|X_{5m}-X_{51}|$ and $|X_{5m}-X_{53}|$. If $\theta_m=\theta_2$ (as for all curves in fig. 4, A) the shift is $\Delta X_5=|X_{5m}-X_{51}|=|X_{5m}-X_{53}|$, since, in this case, $X_{51}=X_{53}$ as was the requirement for the determination of line *E-E*.

The value of ΔX_5 corresponding to all points along *E-E* of figure 3, B, is represented by the broken curve *E'-E'* of figure 3, A; the values for points along the perpendicular (not drawn) to *E-E* at the intersection point are represented by *E''-E''*; and those for points along the perpendicular to *E-E* at the critical point are represented by *E'''-E'''*.

The value of ΔP corresponding to all points along *D-D* of figure 3, B, is represented by the solid line *D'-D'* of figure 3, *A*; the values for points along *E-E* are represented by *D''-D''*; and those for points along the perpendicular to *E-E* at the critical point are represented by *D'''-D'''*.

All lines in figure 3, *A*, are composed of one or more straight sections except *D''-D''* and *E''-E''*. These have curvature only where their abscissas are in the neighborhood of the abscissa of the intersection point, (X_t, Y_t). The nature of this curvature is shown more clearly in figure 5 by a sufficient enlargement of the scales. The corresponding curves are identified by their designations. The curvature is caused by the change in

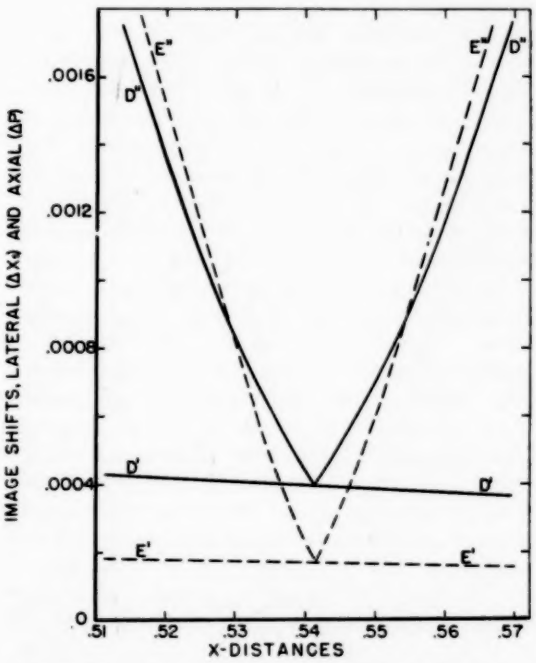

FIGURE 5. *Enlargement of a small part of figure 3, A.*

the range covered by ΔX_5 as θ_m moves through the range from θ_1 to θ_3.

As there is usually some error in placing the prism relative to the chosen axis of rotation, a study of figure 3, *A*, will show that locating the axis of rotation at any point along line *E-E* of figure 3, *B*, and over the range shown by this figure should be about equally good insofar as ΔX_5 is concerned. If the critical point should be chosen for the axis and an error of only $0.01 \times A$ were made in its placement, the resultant value for ΔX_5 could be three times as large as it could be if the axis were accurately placed at the intersecting point. Also, an error in placement at the intersecting point that exceeds $0.02A$ cannot produce a ΔX_5 in excess of the largest ΔX_5 that can be caused by an equal error of placement at the critical point. In the immediate neighborhood of the intersecting point the values for both ΔP and ΔX_5 are small; values for ΔP (curve *D''-D''*) increasing rapidly as the axis moves along *E-E* from this point and remaining almost constant (curve *D'-D'*) as the axis moves along *D-D*; values for ΔX_5 (curve *E''-E''*) increasing rapidly as the axis moves from this point along *D-D* and remaining almost constant (curve *E'-E'*) as the axis moves along *E-E*; and both increasing more or less rapidly for intermediate directions. Consequently, the point of intersection of *D-D* and *E-E* is chosen for the axis of rotation.

In case the meridian focus is dominant, the recommended point for the axis of rotation of the prism would be at the intersection of lines *E-E* and *F-F* (fig. 3, *B*), since *F-F* bears the same relation to the meridian rays that *D-D* does to the sagittal rays.

This enables a designer to produce a monochromator consisting of a prism and a single achromatic lens for which the image distance is equal for three selected wavelengths of light. The treatment described here was used in the design of an instrument for the automatic recording of changes in interference phenomena [5].

A single simple lens may be used with a constant deviation prism to obtain a monochromator having a common focus for two selected wavelengths of light. By equating the right side of eq 22, for X_{51}, to that for X_{53} and the right side of eq 24, for P_1, to that for P_3, two linear equations in X and Y are obtained. The simultaneous solution of X and Y for these equations give the position of the axis of rotation desired. If the lateral shift is unimportant, the focus may be made common to light of three wavelengths.

VII. Conclusions

The above treatment shows that when a constant deviation prism is used with a single lens to form an image of a fixed source or object, the image moves when the prism is rotated to change the color of the light. The magnitude of this image shift is found to depend upon the position of the axis about which the prism is rotated, the optical and geometrical properties of the prism, and the dimensions of the system. A survey of the literature shows that the lateral component of this image shift may be completely eliminated by choosing the axis at a certain point relative to the prism and the optical axis of the lens. In this paper it is shown that the lateral component of the shift will be negligible if the axis is chosen in the neighborhood of the above-mentioned point and on a certain straight line that passes through it. Similarly, it is found that the longitudinal (or axial) component of the shift will also be negligible if the axis is chosen in the neighborhood of another point and on a straight line that passes through it. These two straight lines intersect at a point that is conveniently located for the axis of rotation of the prism.

A fixed focus monochromator for ultraviolet work may be made by using a suitable isotropic crystal for the prism and collimator. This can be accomplished by placing the axis of rotation so that the change in effective object (or image) distance, produced by rotating the prism, is just sufficient to cancel the chromatic aberration of the lens.

VIII. References

[1] H. S. Uhler, Phys. Rev. **29,** 37 (1909).
[2] H. S. Uhler, Astrophys. J. **47,** 65 (1918).
[3] W. E. Forsythe, Astrophys. J. **45,** 278 (1917).
[4] E. Bloch, J. phys. **7** [5], 145 (1917).
[5] J. B. Saunders, J. Research NBS **35,** 157 (1945) RP1668.
[6] Southall's principles and methods of geometrical optics, p. 92 and 93 (The Macmillan Co., New York, N. Y., 1910).
[7] P. Pellin and A. Broca, J. phys. **8** [3], 314 (1899).

WASHINGTON, February 13, 1948.

U. S. Department of Commerce
National Bureau of Standards

Research Paper RP1926
Volume 41, October 1948

Part of the Journal of Research of the National Bureau of Standards

Thimble-Chamber Calibration on Soft X-rays

By Frank H. Day

Condenser *r*-meter thimble chambers of various types have been calibrated against a standard free-air ionization chamber to indicate the wavelength dependance of their readings after exposure to X-rays excited by potentials ranging from 10 to 200 kilovolts. X-ray tubes with low inherent filtration are used. Calibrations are conducted for minimum-filter conditions, and the effect of added filtration on the calibrations is also noted. It has been observed, for instance, that a chamber that reads correctly for filtered radiation of 100-kilovolt quality is in error by a factor of 2.3 for 10-kilovolt X-rays.

I. Introduction

Thimble chambers of the Victoreen type are normally designed for the measurement of relatively hard radiations and are customarily calibrated with X-ray beams that are produced by tubes with an applied voltage of 70 to 200 kv, and which are subjected to some preliminary filtration, at least 2 mm of aluminum or 0.2 mm of copper. Over this range, the chambers yield readings that are practically independent of the radiation quality when calibrated against a free-air chamber. However, in the absence of any other ionization chamber, they are frequently used for measuring very much softer radiations than those for which they are designed or calibrated. Numerous cases have come to our attention where the red Bakelite 25-*r* chamber has been employed to measure radiations produced by potentials as low as 20 or 30 kv, and it has been obvious in many cases that the users have had no reasonable idea as to the magnitude of the errors [1] involved. It therefore appeared to be desirable to investigate the magnitude of these errors and provide some quantitative data thereon.

Measurements cited in this paper with respect to the effect of added filtration on the calibration relate primarily to one 25-*r* chamber. The effect of thimble-chamber type is studied with red Bakelite 25-*r*, 100-*r*, and 250-*r* chambers, as well as the newly designed 250 *r* nylon chamber. When calibrations are made in a given X-ray beam, or in different beams of exactly the same quality, then, as noted below, different chambers of the same type generally require the same corrections.[2] However, chambers of different types require different corrections.

Although the results reported here may be taken as typical, the very magnitude of the corrections required indicates that whenever a thimble chamber is to be used for precise measurement in the very soft X-ray region, it should be specifically calibrated for the exact conditions under which it will be used. This becomes more important, the lower the X-ray excitation potential. The wave form of the excitation potential becomes increasingly more important at the lower potentials also.

It is desirable for thimble-chamber readings to bear a constant relationship to those of a standard free-air chamber over a wide range of X-ray quality. To achieve this, it is necessary that the type of absorption and scattering in the thimble chamber wall be equivalent to that which is observed in air, and that the absorption in the wall thickness be negligible in comparison with the transmission through it, or that the secondary corpuscular radiation within the cavity be enhanced by means of a suitable internal coating of the wall to compensate for radiation lost by absorption in the wall thickness.

The practical attainment of this requirement is not difficult for 50 to 200-kv X-rays emitted by a tube whose inherent filtration is at least 0.2 mm of copper. For example, in the measurement of

[1] By "error" is meant the departure of *r*-meter readings from those of a standard free-air chamber.

[2] "Correction," as here used, is a factor by which *r*-meter readings must be multiplied to make them agree with those of a standard free-air chamber.

radiation from such a tube, the Victoreen 25-r thimble chamber, with its 0.6-mm red bakelite wall, reads only 5 percent low for 50-kv radiation if it reads correctly for 100 to 200-kv radiation.

The problem is much more difficult, however, in the case of long-wavelength X-rays, produced by a tube whose inherent filtration is, say, 1.5 mm of beryllium. X-rays as long as 4 A in wavelength are available in measureable quantity from such a tube, and these are readily absorbed, even in a few centimeters of air. There are applications where it is necessary to determine the exposure at or near the portal of a beryllium-window tube. A properly designed chamber, therefore, should measure 4-A X-rays, (approximately 3-kv quality) with a minimum of correction.

An attempt has been made in this direction,[3] utilizing an ionization chamber having a beryllium wall. The use of an open-air chamber has been reported,[4] utilizing a limiting diaphragm and a mesh-type electrode system consisting of silk threads soaked in India ink to make them electrically conducting. A similar chamber has also been constructed,[5] substituting, in place of the mesh of silk threads, Kodapak I, which is cellulose acetate sheet 0.00088 in. thick containing some plasticizer. Its calibration at the National Bureau of Standards yields scale factors (roentgens per scale division), which vary by less than 8 percent as the X-ray excitation potential is varied from 7.5 to 90 kv and the filtration from the minimum of 1.5 mm of beryllium plus 100 cm of air to this plus 4 mm of aluminum.

II. Experimental Procedure and Results

In this study, the usual substitution method was employed in the calibration of the thimble chambers, the radiation being first measured with a standard guarded-field, free-air ionization chamber and then with the thimble chambers placed in the position of the limiting diaphragm. The filtration between the X-ray tube portal and the ionization chamber is, in all instances, 100 cm of air at approximately 760 mm Hg pressure and 22° C. It is necessarily a part of the minimum filtration, although it is not hereinafter so designated.

[3] J. A. Victoreen, Z. J. Atlee, and E. D. Trout, Am. J. Roent. **53**, 391 (1945).
[4] Edith H. Quimby and Elizabeth F. Focht, Am. J. Roent. **50**, 653 (1943).
[5] Personal communication, H. E. Seemann (Eastman Kodak Co., Rochester, N. Y.).

The standard ionization chamber used in this comparison was the one designed for measuring radiations produced by potentials up to 200 kv. It has an air path of 21.1 cm between the limiting diaphragm and the front edge of the collector plate.[6] Corrections required for the air absorption over this distance vary from about 0.5 percent for 200-kv radiation to 33 percent for 10-kv radiation,[7] and these have been applied in this calibration.

"Constant"[8] potentials, varied in steps between 10 and 200 kv, were employed on each of two tungsten-target X-ray tubes used in the calibration. The first was a thin-walled (1.3 mm) cerium-glass tube, which offers about as little inherent filtration as any glass-window tube. The second was a 200-kv water-cooled tube whose window thickness is only 1.5 mm of beryllium, and which has almost no inherent filtration.

The r-meter readings were observed over approximately the same scale range to avoid any possible scale-factor error and were readily reproduced within ± 1 percent. This is an over-all error, which includes fluctuations in the calibrating equipment of not greater than ± 0.3 percent.

Figure 1 shows thimble-chamber corrections using the beryllium-window tube over the range of 10 to 100 kv, and for filtrations ranging from the minimum of 1.5 mm of beryllium to this plus 6 mm of aluminum of added filtration. For example, it is observed for the minimum filtration, that the correction is 1.52 at 100 kv and increases to 2.3 at 10 kv. It is obvious that when such a large correction is necessary, the calibration of a thimble chamber for use with very soft radiations must be made with considerable care. In fact, some earlier studies[9] indicate the necessity of effecting a special calibration for each specific tube in conjunction with its own specific potential source. The insertion of as little as 1 mm of aluminum in the beam, however, reduces the error from 52 to 3 percent at 100 kv and from 60 to 8 percent at 50 kv.

[6] Lauriston S. Taylor and George Singer, BS J. Research **5**, 507 (1930) RP211.
[7] Frank H. Day and Lauriston S. Taylor, J. Research NBS **40**, 393 (1948) RP1883.
[8] The power supply has a resistance-capacitance filter to reduce the ripple to 0.05 percent per milliampere current drain, and currents used in these calibrations did not exceed 10 ma.
[9] L. S. Taylor, G. Singer, and C. F. Stoneburner, BS J. Research **11**, 289 (1933) RP592.

Similar corrections using the 1.3-mm glass-wall tube are shown in figure 2. Here, for minimum filtration, it is seen that the correction varies from 1.17 at 100 kv to 1.34 at 20 kv. Comparing these corrections with those of the 0.3-mm aluminum curve in figure 1, it is found that they are closely alike over the whole potential range, indicating that the 1.3-mm of cerium glass is equivalent in absorption to approximately 0.3-mm of aluminum.

Calibration curves for the beryllium-window tube and copper filtrations at potentials up to 200 kv are shown in figure 3. It is observed that until approximately 0.22-mm of copper filtration is added to the beam, the errors at low potentials

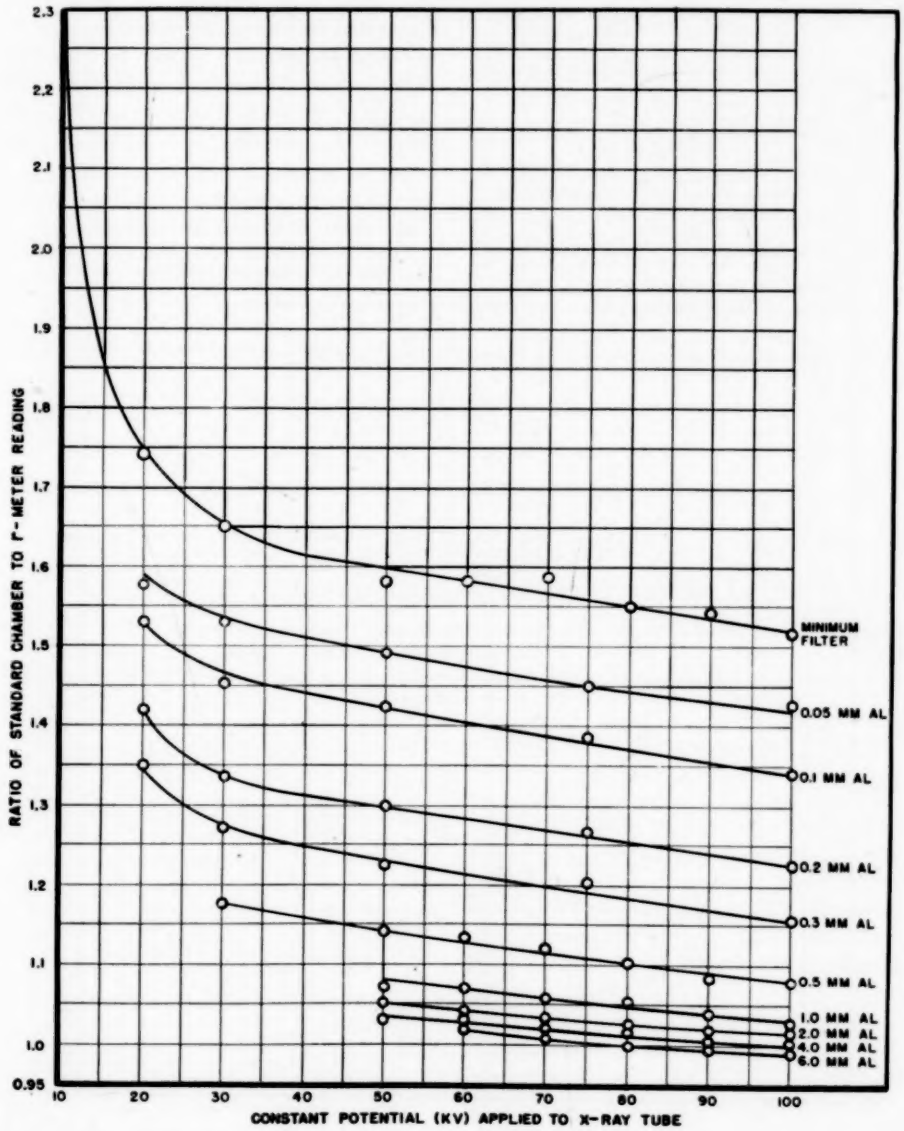

FIGURE 1. *Effect of X-ray excitation potential and added aluminum filtration on the readings of r-meter No. 1193 and 25-r Bakelite thimble chamber, using X-ray tube with 1.5 mm of beryllium inherent filtration.*

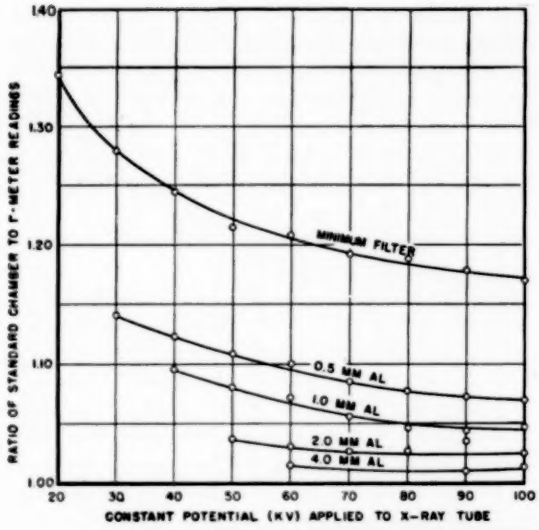

FIGURE 2. *Effect of X-ray excitation potential and added aluminum filtration on the readings of r-meter No. 1193 and 25-r Bakelite thimble chamber, using X-ray tube with 1.3-mm of cerium glass inherent filtration.*

are relatively large, 11 percent, for example, at 50 kv and 0.11-mm of copper filtration. However, for 0.22-mm of copper filtration, the thimble chamber agrees with the standard within ±2 percent over the range of 50 to 200 kv, and additional filtration does not change the calibration curves observably.

In figure 4, calibration curves, for X-rays from the tube with 1.5-mm of beryllium inherent filtration, and no added filtration, show the effect of thimble-chamber type. In this comparison, three types of Bakelite chambers (250-*r*, 100-*r* and 25-*r*) were used in conjunction with *r*-meter No. 1193. Another 25-*r* Bakelite chamber was

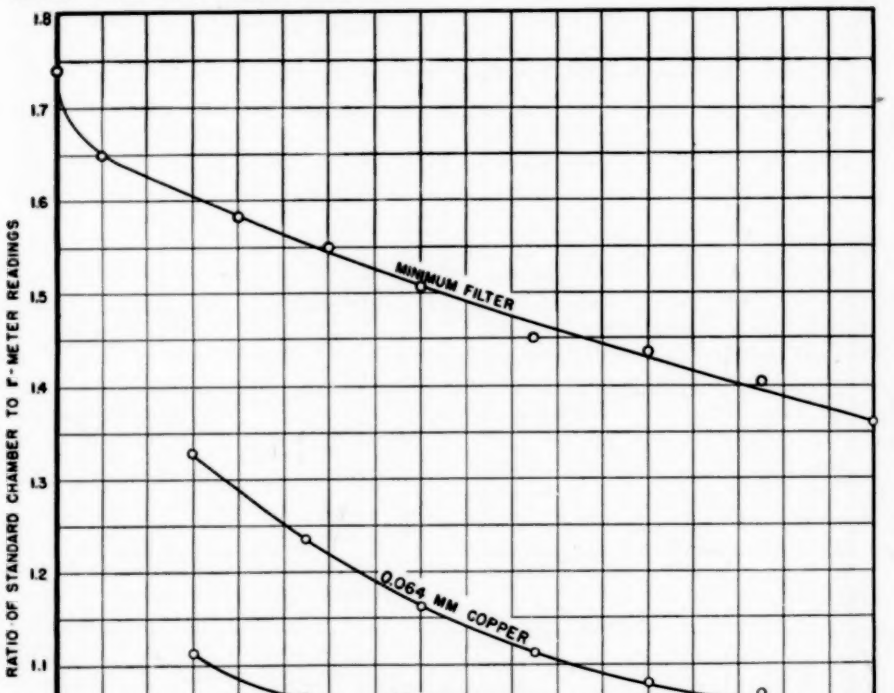

FIGURE 3. *Effect of X-ray excitation potential and added copper filtration on the readings of r-meter No. 1193 and 25-r Bakelite thimble chamber, using X-ray tube with 1.5-mm of beryllium inherent filtration.*

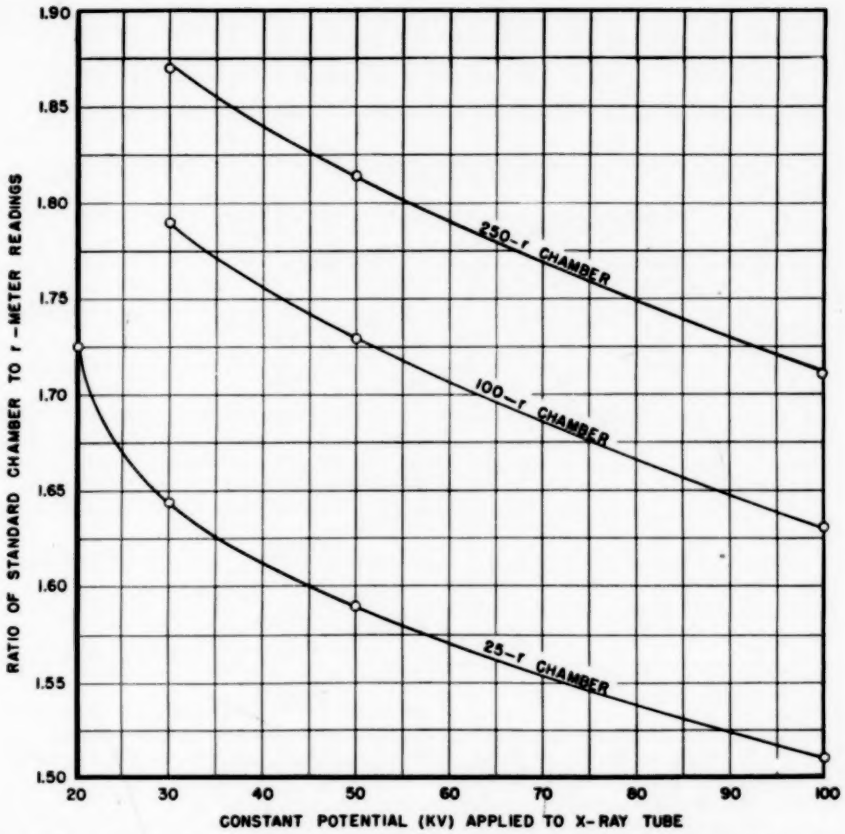

FIGURE 4. *Effect of X-ray excitation potential on the readings of various types of Bakelite thimble chambers, using X-ray tube with 1.5-mm of beryllium inherent filtration and no added filtration.*

The 250-*r*, 100-*r*, and 25-*r* chambers are each used in conjunction with *r*-meter No. 1193. Another 25-*r* chamber used in conjunction with *r*-meter No. 1282, yields readings that are the same within experimental error, as those observed with the 25-*r* chamber, which were read on *r*-meter No. 1193.

used in conjunction with *r*-meter No. 1282. The readings of the two 25-*r* chambers and r-meters are the same, within experimental error, whereas those of the 100-*r* and 250-*r* chambers show substantially greater departure from those of the standard chamber. It is interesting to note that the calibration curves for these chambers run closely parallel to each other. For example, the correction factor to the 100-*r* and 250-*r* chambers are 1.63 and 1.71, respectively, at 100-kv, and 1.79 and 1.87, respectively, at 30-kv, or differences of 0.08 at each potential.

A 250-*r* nylon chamber with a 0.005-in. wall thickness has recently become commercially available, and its calibration is shown in figure 5 using an X-ray tube with 1.5 mm of beryllium inherent filtration. For minimum-filtered radiation, this chamber reads in error by 31.5 to 28 percent over the range of 30 to 100 kv. This is in contrast with an error in the 250-*r* red bakelite chamber readings of 87 to 71 percent in the same excitation potential range, as seen in figure 4.

Table 1 shows the aluminum half-value layers for 10 to 200-kv X-rays with filtration ranging from 1.5 mm of berryllium to this plus 6 mm of aluminum. For minimum filter the very small half-value layers, even at 200 kv, indicate that the great bulk of the absorbed radiation is extremely soft, perhaps in the region of 20 to 30 kv, in terms of the usual measuring techniques. As an example of the effect of X-ray beam quality upon thimble-chamber calibration, it is observed in figure 5 that 6 mm of aluminum are required to reduce the correction factor to a minimum at 150 kv. Table

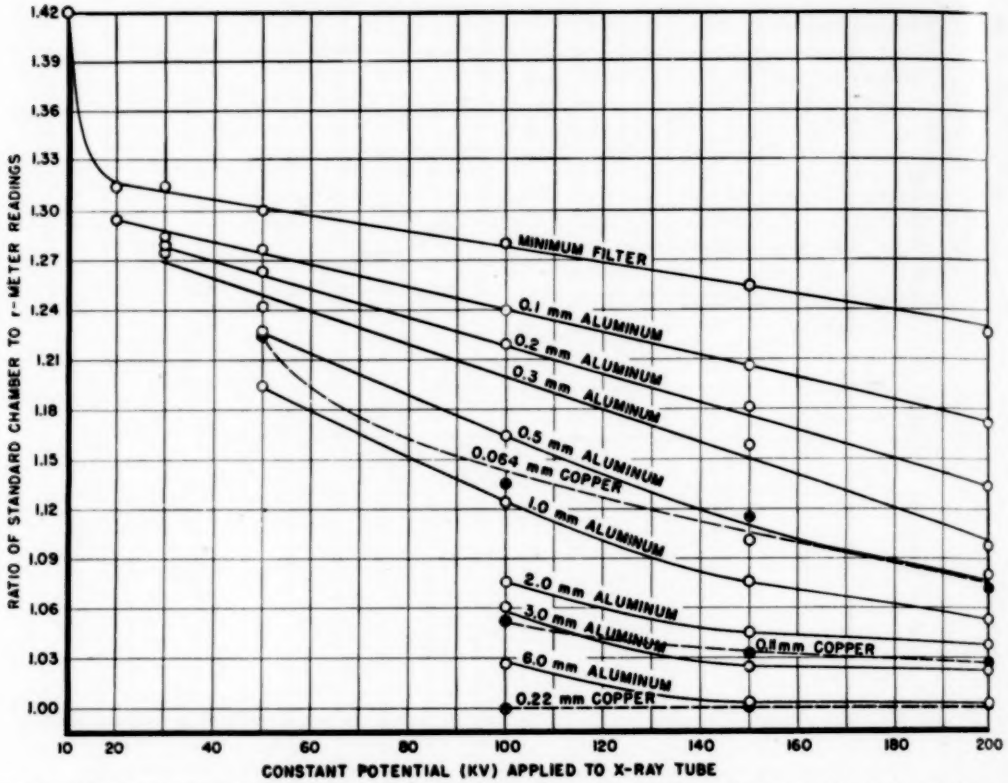

FIGURE 5. *Effect of* X-ray *excitation potential and added filtration on the readings of r-meter No. 2449 and 250-r nylon thimble chamber, using* X-ray *tube with 1.5 mm of beryllium inherent filtration.*

1 indicates that a 150-kv beam, prefiltered by 6 mm of aluminum, has a half-value layer of 7.6 mm of aluminum. This is in contrast with half-value layers ranging from 0.04 to 0.18 mm of aluminum at 10 and 200 kv, respectively, for minimum-filtered beams. In view of the large percentages of soft components in beams from beryllium-window tubes, it is to be expected that chambers used for measuring radiations from such tube, with no added filtration will be very critical as to design characteristics.

TABLE 1. *Aluminum half-value layer determined with free-air ionization chamber as a function of filtration and of X-ray excitation potential*

Constant potential	Half-value layer of aluminum								
	Minimum filter [1]	Added filter							
		0.1 mm Al	0.2 mm Al	0.3 mm Al	0.5 mm Al	1.0 mm Al	2.0 mm Al	3.0 mm Al	6.0 mm Al
kv	mm	mm	mm	mm	mm	mm	mm	mm	mm
10	0.04	0.06	0.10	.....	.....	.....	.....	.....	.....
20	.08	.11	.15	0.18	0.22	.....	.....	.....	.....
30	.09	.14	.19	.27	.35	0.6	0.9	1.2	.....
50	.10	.15	.29	.34	.57	1.0	1.4	1.9	2.8
100	.11	.19	.37	.48	1.0	1.8	2.9	3.6	5.3
150	.14	.29	.64	1.2	2.0	3.2	4.6	5.5	7.6
200	.18	.40	1.3	2.1	3.4	4.6	6.3	7.1	8.8

[1] 1.5 mm of beryllium, plus 100 cm of air.

III. Conclusion

Thimble chambers can be calibrated for use with the very low-potential, lightly filtered radiations, such as produced by beryllium-window X-ray tubes. However, the errors may be as large as 130 percent for radiation produced at 10-kv constant potential.

Considerable care must be exercised in determining the amount and kind of filtration and potential employed in thimble-chamber calibrations for soft X-rays. These factors are relatively unimportant, however, where filtrations above 0.2 mm of copper or about 6 mm of aluminum are used.

WASHINGTON, January 26, 1948.

U. S. Department of Commerce
National Bureau of Standards

Research Paper RP1927
Volume 41, October 1948

Part of the Journal of Research of the National Bureau of Standards

Sources of Error in and Calibration of the *f*-Number of Photographic Lenses

By Francis E. Washer

In problems of photography, where the accuracy of lens marking is critical in determining the proper exposure, the various errors to which these markings are subject is of considerable interest. The present report gives the magnitude of such errors that were found to exist in a representative group of 20 lenses having focal lengths that range from 0.5 to 47.5 in. In addition, the results of calibration of these lenses by a photometric method that permits compensation of light losses resulting from absorption, reflection, and scattering are given. Values of lens transmittance for these lenses are shown. A method of plotting results of nominal, true, and calibrated *f*-numbers is given that permits quick evaluation of the magnitude of the over-all error in terms of fractions of a stop.

I. Introduction

With the advance of photographic technology, a need has developed for more precise information on the light-transmitting characteristics of photographic objectives. In particular, a specific need exists for a more accurate means of marking or calibrating the lenses that employ a variable stop for adjusting the lens speed. The usual method, at present, of calibrating a lens is to inscribe a scale of *f*-numbers on the diaphragm control. These *f*-numbers are based upon certain geometric properties of the lens, and neglecting errors of marking, provide a satisfactory means of varying the speed of the particular lens by definite integral steps. Unfortunately this system of marking takes no cognizance of differences in light-transmitting properties that occur among different types of lenses and, in addition, those differences that result between lenses of the same type when the surfaces of one have been treated to reduce reflection losses.

This problem has been under vigorous attack for the past 10 years and numerous methods [1 to 12][1] have been devised for the rating of lens speed with respect to some standard. These methods differ in such matters as type of light source, comparison lens or standard aperture, and type of light-registering device. The theoretical aspects of the problem have been discussed by McRae [9] and by Gardner [1, 2], who proposed several possible methods for calibration of a lens. In the present article, one of the methods described by Gardner is verified experimentally. The experimental technique is described, and the variations in performance for 20 lenses, having focal lengths that range from 0.5 to 47.5 in., are shown. Attention is given to sources of error in the existing marked *f*-number. Lastly, a process is described for determining the transmittance of a lens from data obtained in the course of calibration.

[1] Figures in brackets indicate the literature references at the end of this paper.

II. Apparatus and Method of Measurement

The apparatus consists essentially of a broad uniform source of white light, a sensitive light-measuring device, and a holder that can be used interchangeably for either mounting the lens under test or one of a series of standard diaphragms each of which has a centrally located circular opening of known diameter. The arrangements of these elements is the same as that suggested by Gardner [1,2]. The relative lens speed is determined by a comparison of the quantity of light flux transmitted by a lens with that transmitted by a circular opening. By making an appropriate series of measurements and by proper interpretation of their significance, the lens can be calibrated in terms of an "ideal" lens having 100-percent transmittance.

1. Procedure for a Lens

A lens in mounted in the holder, and its axis is alined with the center of the broad uniform source and the center of the small circular opening in the baffle covering the sensitive element of the light-measuring device. The front of the lens faces the light source, and the distance separating the rear nodal point of the lens and the baffle covering the light sensitive element is adjusted to equality, with the equivalent focal length, F, of the lens. The opening in the baffle does not usually exceed 1 mm, except for some lenses of very long focal length, in which cases it is kept under $0.01F$. All parts of the equipment are shielded so that only light from the source that passes through the lens can reach the light-sensitive element.

Readings of the light meter are taken at each of the marked stop openings. To minimize error arising from back lash, readings are taken both for the condition of the setting at the marked f-number being made with the diaphragm ring of the lens moving in the closing direction and with the diaphragm ring moving in the opening direction.[2] The readings from these two sets of observations are averaged, and this value is taken as the accepted reading of the light meter at a given marked stop opening.

2. Procedure for the standard diaphragms

The lens is replaced by one of the series of standard diaphragms, which have centrally located circular openings with known diameters. The reading of the light meter is taken, and the distance D, from the diaphragm to the baffle covering the light-sensitive element is measured. This operation is repeated for several of the standard diaphragms so selected that readings of the light meter are obtained throughout the same range of readings that were observed for the various marked apertures of the lens. The brightness of the source and the sensitivity of the light meter are kept unchanged throughout both parts of the experiment. To insure constancy of brightness of the source, a constant voltage transformer is used to maintain a constant voltage for the lamps that illuminate the broad uniform source. To minimize error, two sets of data are taken for both the lens and the series of standard diaphragms, so intermingled that random fluctuations in the brightness of the light source and in the sensitivity of the light meter can be neglected.

Ideally, the diameters of the standard diaphragm openings should be so chosen that the same series of f-numbers are present in both phases of the experiment. Too, the distance, D, should equal the equivalent focal length, F, of the lens. In practice, however, it has proved to be more convenient to let D differ from F and to place more reliance upon the ratio, D/A, where A is the diameter of the circular opening in a standard diaphragm. When a wide variety of lenses are being calibrated, as is the case in this experiment, it is simpler to compute the f-number of the standard diaphragm from the ratio, D/A, and to determine the performance of the conventional series of f-numbers from the curve of light meter reading versus f-number than to attempt to reproduce the conventional set of f-numbers by appropriate selection of values of D and A.

The f-number for a lens is defined by the equation

$$f\text{-number}=\frac{1}{2\sin\alpha}, \tag{1}$$

where α is the angle between the axis and the extreme ray of the circular conical bundle transmitted by the lens. In the case of the standard diaphragm, the relation connecting the measured quantities D and A is

$$\frac{D}{A}=\frac{1}{2\tan\alpha}. \tag{2}$$

Accordingly, the values of the f-numbers for the standard diaphragms can readily be computed from the known values of D/A. A sufficiently accurate determination of the f-number can be made with the aid of a curve, such as is shown in figure 1. To produce this curve, the values of the quantity, f-number $-D/A$, are plotted as a function of D/A. Hence, for a given value of D/A, the increment that must be added thereto to yield the f-number can be easily read from the graph. For values of D/A greater than 15, the values of D/A and f-number are equal for all practical purposes, since their difference is less than 0.1 percent.

[2] Ten lenses (10, and 12 to 20, incl.) were calibrated in this manner. The remaining 10 lenses were calibrated with the diaphragm ring moving in the closing direction only in accordance with the recommendation contained in Report No. 6 of the Subcommittee on Lens Calibration of the Society of Motion Picture Engineers on Nov. 6, 1947.

FIGURE 1.
standar

When
light me
the stan
the resu
nearly e
exactly
from lin
to vary
receiver.
2, shows

FIGURE
Curve 1

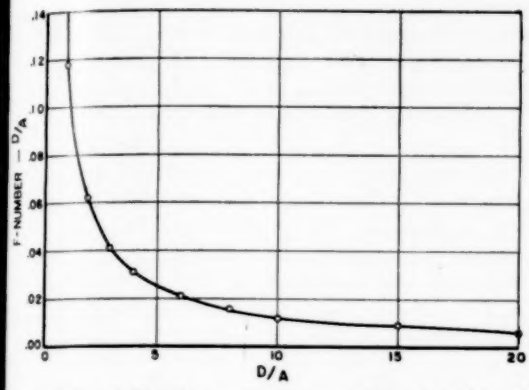

FIGURE 1. *Calibration curve for computing f-number of standard diaphragms when the value of D/A is known.*

III. Results of Measurement

When the values of the scale deflections of the light meter are plotted against the *f*-numbers of the standard diaphragms on logarithmic paper, the resulting curve is a straight line with a slope nearly equal to 2. The fact that the slope is not exactly 2 may be attributed to a slight departure from linearity of the response of the light meter to varying amounts of light indicated on the receiver. This curve, shown as curve 1 in figure 2, shows the relation between the scale deflections of the light meter and the *f*-numbers of an ideal lens.

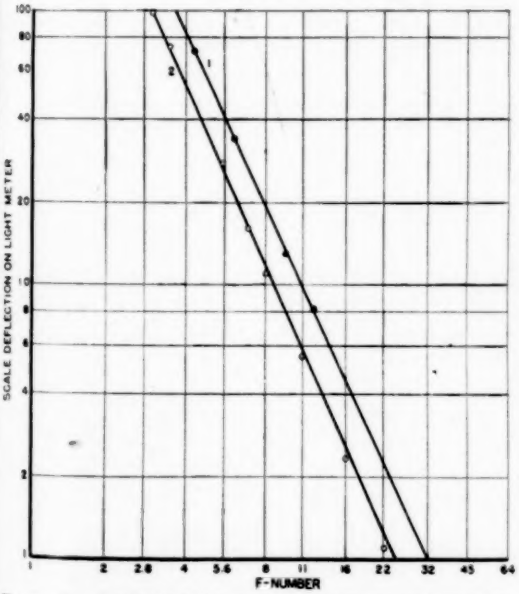

FIGURE 2. *Scale deflection on light meter versus f-number.* Curve 1 is for the standard diaphrams. Curve 2 is for the lens under test.

In a like manner, the values of the scale deflection of the light meter are plotted against the *f*-numbers of the actual lens on the same curve sheet. The resulting curve, designated curve 2 in figure 2, is a straight line parallel to curve 1, but displaced laterally therefrom. This displacement shows in a striking manner the effect of light losses in the actual lens. A fairly close approximation of the relative light transmission of the actual lens at a given *f*-number can be made at once, as it is simply the ratio of the ordinates of curve 1 and curve 2 for the given *f*-number.

It must be mentioned that while curve 1 is always a straight line, this is a consequence of its accurately determined *f*-numbers. On the other hand, the *f*-numbers for curve 2 are read directly from the lens markings and are subject to a variety of errors that will be discussed later in the paper. As a result of these random and systematic errors, the points for curve 2 sometimes do not fall as close to the straight line drawn as could be desired. This is especially noticeable at the small apertures associated with the large *f*-numbers. However, these variations in no way interfere with validity of the final results, but are in fact helpful in tracking down errors in the *f*-numbers.

The values of the calibrated *f*-numbers for the actual lens may be readily obtained from these curves. The calibrated *f*-number is a term used to designate the *f*-number of an ideal lens (i. e., a lens having 100-percent transmittance) transmitting the same amount of light that is transmitted by the actual lens at a given marked *f*-number. The terms *T*-aperture ratio or *T*-stop [3, 7, 8] and equivalent aperture ratio [1, 2] are other designations of this same quantity. To determine the calibrated *f*-number, the value of the scale deflection for a given marked *f*-number of the actual lens is noted, and the value of the *f*-number of the ideal lens, for which the same scale deflection is obtained, is read from curve 1. This has been done for 20 lenses covering a wide range of focal lengths and *f*-numbers. The results are listed in table 1.

The unusual values of marked *f*-numbers, which are listed in the first column, result from assigning a calibrated *f*-number to the maximum stop opening for each lens. The maximum stop

TABLE 1. *Measured value of the calibrated f-number for each value of the marked f-number for each of 20 lenses having focal lengths that range from 0.5 to 47.5 inches*

Lens number	1	2	3	4	5	6	7	8	9	10
Nominal focal length (in.)	0.5	0.5	1.0	1.4	1.6	2.0	2.0	3.0	3.0	3.0
Marked *f*-number	CALIBRATED *f*-NUMBER									
1.9	2.40		2.09							
2.2							2.23			
2.3										
2.5		2.82							2.45	
2.7				3.14	3.14	3.09				
2.8	3.25	3.13	2.86							
3.0							2.79	3.20	2.96	
3.5										3.98
4.0	4.42	4.45	3.92	4.33	4.10	4.36	3.95	4.48	4.07	4.20
4.5										4.85
5.6	5.32	6.32	5.52	5.82	5.46	6.00	5.29	6.22	5.78	6.74
6.8										8.08
7.5										
8.0	7.80	8.78	7.50	8.48	7.37	8.37	7.26	8.72	8.33	10.4
9.5										
11.0	11.0	11.8	9.94	12.5	9.66	11.6	11.2	12.3	11.4	14.1
12.5										
15.0										
16.0	15.4	17.2	13.6	16.8	12.3	16.0	15.7	17.4	17.4	21.3
22.0	21.3			24.2	16.0	21.9	20.4	24.5		33.6
32										
45										
64										
90										
128										

Lens number	11	12	13	14	15	16	17	18	19	20
Nominal focal length (in.)	4.0	7.0	7.5	11.0	13.5	16.5	19.0	24.0	30.0	47.5
Marked *f*-number	CALIBRATED *f*-NUMBER									
1.9										
2.2										
2.3										
2.5										
2.7	2.79									
2.8										
3.0	3.00									
3.5										
4.0										
4.5	4.24		5.60							
5.6										
6.8	5.76		6.86							
7.5		8.00								
8.0					9.72					
9.5	8.33	9.32	9.75	10.1		12.3				
11.0										
12.5	11.1	13.1	13.6	13.9	14.1	13.4	13.6	14.3		
15.0									15.6	
16.0										16.0
22.0	15.4	18.7	18.3	19.7	19.8	19.5	19.2	19.8	19.3	17.3
32		25.2	24.0	28.0	28.4	26.8	25.8	28.2	26.7	23.3
45	27.6	36.7	29.5	37.0	40.0	38.0	37.6	40.9	39.2	34.7
64		49.0			56.9	52.8	50.8	59.9	53.4	48.6
90					76.0	71.8	69.6	86.8	79.0	71.1
128						100.0	98.0	117.0	99.0	97.6
										143.0

opening of a lens quite frequently does not fall in the commonly accepted series of marked *f*-numbers, although the remaining marked *f*-numbers of the lens usually do. The calibrated *f*-numbers, in most instances, are larger than the marked *f*-numbers. This is as expected, because it is known that some of the light incident on the front surface of a lens is lost as a result of reflection back in the object space or by absorption in the glass. The considerable differences in the calibrated *f*-numbers for a given marked *f*-number indicate appreciable differences in the light-transmitting qualities of the various lenses. This is illustrated in figure 3 where the calibrated *f*-numbers are plotted on semilogarithmic paper for 10 lenses. The values are given for the marked

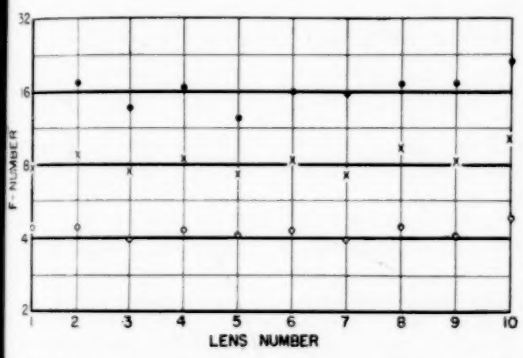

FIGURE 3. *Departure of the calibrated f-number from the marked f-number at f/4, f/8, and 5/16 for 10 lenses.*

The line separations shown are equal to one stop-opening.

f-numbers, 4, 8, and 16. Departures as great as one-third stop-opening are indicated in many instances. As the departures may be in either direction from the marked stop-opening, it is possible to select two lenses such that, on using each for the same scene at the same marked stop-opening, the effective difference in exposure is equal to that produced by a change in excess of one full stop-opening. The fact that some lenses have calibrated *f*-numbers less than the marked stop-opening may seem anomalous in that it indicates a transmittance greater than unity. This is, however, for the most part, an indication of errors in the marked stop-opening and will be discussed in more detail in a later section.

Lens 7 is of especial interest in that the indicated stop-openings are marked in *T*-stops, consequently the values of the calibrated *f*-numbers are quite close to the marked *f*-numbers. Lenses 2, 3, 7, 9, 11, and 20 have coated surfaces to reduce reflection losses. The gain in transmittance is definitely present but is somewhat obscured in table 1, because the marked aperture ratios frequently differ from the true geometric aperture ratio.

The fact that the calibrated *f*-number varies so much from lens to lens for the same nominal *f*-number gives support to the proposition that all lenses should be so marked that differences in light-transmitting properties are negligible for a given *f*-number. This can be done from the curves shown in figure 2 by reversing the procedure used in deriving the information reported in table 1. The deflection of the light meter for a given *f*-number of the ideal lens is noted on curve 1, and the *f*-number of the actual lens, which will yield the same deflection, is read from curve 2. This can also be done by plotting the calibrated *f*-number for a lens listed in table 1 against the marked *f*-number on logarithmic paper. The marked *f*-number for a given calibrated *f*-number can then be read directly from the graph. This has been done for the same 20 lenses, and the results are listed in table 2. This table shows the proper settings in terms of the marked *f*-number, so that each of these lenses will yield uniform performance for each of a series of calibrated *f*-numbers.

TABLE 2. *Settings of the stop-openings in terms of the marked f-number to yield a series of calibrated f-numbers corresponding to 100-percent transmittance for each of 20 lenses having focal lengths that range from 0.5 to 47.5 inches*

Lens number	1	2	3	4	5	6	7	8	9	10
Nominal focal length (in.)	0.5	0.5	1.0	1.4	1.6	2.0	2.0	3.0	3.0	3.0
Calibrated *f*-number	SETTINGS IN TERMS OF MARKED *f*-NUMBER									
2.8	2.33	2.48	2.74	2.38	2.27	2.42	2.81	2.42	2.62	
4.0	3.58	3.60	4.08	3.63	3.83	3.63	4.05	3.56	3.91	3.27
5.7	5.92	5.10	5.80	5.47	5.78	5.33	6.02	5.10	5.50	4.67
8.0	8.10	7.24	8.57	7.56	8.86	7.75	8.63	7.32	7.75	6.26
11.3	11.3	10.5	12.7	10.2	13.8	10.7	11.3	10.3	10.8	8.80
16	16.4	14.9	19.1	15.1	22.0	16.0	16.5	14.6	14.9	12.2
22.6	23.2			20.6	35.3	22.7	24.8	20.5		16.6
32										
45										
64										

Lens number	11	12	13	14	15	16	17	18	19	20
Nominal focal length (in.)	4.0	7.0	7.5	11.0	13.5	16.5	19.0	24.0	30.0	47.5
Calibrated *f*-number	SETTINGS IN TERMS OF MARKED *f*-NUMBER—Continued									
2.8	2.51									
4.0	3.76									
5.7	5.55		4.62							
8.0	7.72	6.80	6.60							
11.3	11.2	9.60	9.23	9.04	8.80	8.60				
16	16.7	13.6	13.4	12.8	12.7	13.1	13.2	12.4	12.8	14.6
22.6	24.7	19.3	20.6	18.2	18.0	18.6	19.2	18.2	18.8	21.4
32	38.1	27.9	36.4	26.2	25.3	26.9	27.4	25.2	26.2	29.0
45		40.5		39.8	35.6	38.2	39.3	35.1	37.3	41.0
64					51.8	56.3	58.6	47.8	53.0	58.2

IV. Sources of Error in the Nominal *f*-Number

In addition to the light losses in the lens arising from absorption and reflection, there are several sources of error that affect the reproducibility in the amount of light reaching the focal plane at a given stop-opening. The first of these is back lash in the iris-diaphragm-stop and results in differences in light transmission, dependent upon the manner in which the diaphragm is set at a given stop-opening. The second error is an actual error in the markings themselves and may arise from errors in aperture, errors in equivalent focal length, or errors in both at the same time. The back lash error varies for each lens, whereas the error in *f*-markings contributes to variations in performance when several different lenses are in use for the same type of work.

1. Error in Setting the Lens at a Given *f*-Number

When the diaphragm is set at a given *f*-number, there is an appreciable difference in the amount of light passed by the lens, dependent upon the direction of movement of the diaphragm control. The error arising from this source has been investigated, and the results are listed in table 3 for several lenses. This backlash error is determined by two methods. In the first method, the lens is mounted on a stand, and the edges of the diaphragm are illuminated from the rear of the lens by a fixed source. Photographs of the stop-opening are made with an auxiliary camera placed in front of the lens. Each stop-opening is photographed for the condition of the setting being made with the diaphragm closing and with the diaphragm opening. Prints are made of these negatives, and the area of each image is measured with a planimeter. Let the area of the image, taken for the condition when the setting is made by closing the diaphragm, be A_c; and the area of the image for the same stop opening, taken for the condition when the setting is made by opening the diaphragm, be A_o. Then the ratio A_c/A_o is accepted as the ratio of the relative illuminations

in the axial region of the focal plane when the lens is used under identical lighting conditions for these two processes of setting the lens at a given *f*-number.

TABLE 3. *Ratios of relative illumination in the axial region of the focal plane for lenses used under identical lighting conditions, settings being made with the diaphragm control moving to close and with the diaphragm control moving to open the lens*

Equivalent focal length	Nominal *f*-number	Ratio of light transmissions diaphragm closing to diaphragm opening		
		Planimeter A_c/A_o	Light meter L_c/L_o	Weighted average
In.				
16.5	9.5	1.01	1.04	1.03
	11	1.01	1.02	1.02
	16	1.02	1.04	1.03
	22	1.02	1.07	1.06
	32	1.05	1.11	1.10
	45	1.13	1.08	1.09
	64	1.11	1.08	1.09
19.0	11	1.00	1.00	1.00
	16	1.06	1.02	1.03
	22	1.05	1.04	1.04
	32	1.07	1.06	1.06
	45	1.10	1.09	1.10
	64	1.24	1.26	1.26
24	11	1.00	1.00	1.00
	16	1.00	1.03	1.02
	22	1.05	1.05	1.05
	32	1.02	1.11	1.09
	45	1.09	1.14	1.13
	64	1.06	1.18	1.16
30	12.5	0.99	1.01	1.00
	16	1.04	1.03	1.03
	22	1.02	1.02	1.02
	32	1.04	1.06	1.05
	45	1.08	1.02	1.03
	64	1.08	1.07	1.07

In the second method, the data taken in section II is treated in such manner as to separate the light meter readings L_c, taken for the condition of the setting being made with the diaphragm closing, and the light meter readings for the same stop opening L_o, taken for the condition of the setting being made with the diaphragm opening. Then the ratio L_c/L_o is accepted as the ratio of the amounts of light passing through the lens for these two conditions and is comparable to A_c/A_o obtained by the first method.

The values of these ratios are tabulated in table 3 for a series of stop-openings for four lenses. The differences by the two methods result mainly from the fact that a greater number of sets of data is used in the determination of L_c/L_o. The third column gives the weighted average with a weight of 4 given to L_c/L_o and a weight of 1 given to A_c/A_o. It is noteworthy that this error arising from backlash varies for 1 to 2 percent at the larger stop-openings to as high as 10 to 26 percent for the smaller stop-openings. It is clear that error from this cause can be avoided by always making the diaphragm setting in the same manner, and preferably in the direction of closing the diaphragm.

There still remains the random error of making the setting, even if care is taken to move the control always in the same direction. This error is, however, small in comparison to backlash error, and it is believed that it should be negligible for the careful worker at the larger stop-openings and perhaps rising to approximately one-fourth of the backlash error for the smaller stop openings.

2. Errors in the Existing Geometrical *f*-Number

(a) At full aperture

The true geometrical *f*-number is obtained by dividing the equivalent focal length of the lens by the diameter of the effective aperture. It is therefore obvious that errors in the value of the equivalent focal length and the effective aperture will be reflected by errors in the *f*-number. Table 4 lists the nominal and measured values of equiv-

TABLE 4. *Comparison of nominal and measured values of equivalent focal length and effective aperture for a representative group of lenses*

Lens number	Equivalent focal length		Difference in equivalent focal length	Effective aperture		Difference in aperture
	Nominal	Measured		Nominal	Measured	
	Mm	*Mm*	*Percent*	*Mm*	*Mm*	*Percent*
1	12.5	12.35	−1.2	6.58	7.07	7.4
2	12.5	12.99	3.5	5.00	5.07	1.4
3	25.4	25.56	1.0	13.37	13.65	2.1
4	35.0	37.50	7.1	12.96	14.06	8.5
5	40.0	42.08	5.2	14.81	14.94	+0.9
6	50.0	51.39	+2.8	18.52	19.62	+5.9
7	50.8	50.62	−0.4	25.40	24.40	−3.9
8	75.0	75.31	.4	26.78	27.36	2.2
9	75.0	75.02	.0	32.61	32.58	−0.1
10	76.2	74.71	−2.0	25.40	24.60	−3.2
11	101.6	99.42	−2.1	39.53	40.64	2.8
12	177.8	180.81	1.8	26.15	26.15	0.0
13	190.5	190.53	0.0	42.34	40.17	−5.1
14	279.4	284.85	2.0	34.92	35.74	2.3
15	342.9	351.60	2.5	45.72	42.21	−7.7
16	419.1	418.14	−0.2	44.12	41.30	−6.4
17	482.6	481.97	−.1	43.87	43.29	−1.3
18	609.6	605.55	−.7	55.42	51.40	−7.2
19	762.0	756.54	−.7	60.96	59.14	−3.0
20	1,206.5	1,207.60	.1			

alent focal length and effective aperture. In those instances, where the nominal focal length was given in inches, conversion has been made to millimeters. The nominal values of effective aperture are computed from the values of nominal focal length and nominal *f*-number. Examination of this table shows that the measured value of the equivalent focal length is within ±2 percent of the nominal focal length for 15 of the 20 lenses. The average departure for the entire 20 lenses is ±1.7 percent. The errors in effective aperture are as high as ±8 percent, with an average for 19 lenses of ±4 percent. Nine of the nineteen lenses show errors in effective aperture in excess of ±3 percent. It is doubtful if the errors in focal length can be brought below ±2 percent during the process of manufacture, but it does seem that the error in aperture at the maximum aperture could also be reduced to ±2 percent.

As a result of these departures of the measured values of the equivalent focal length and effective aperture from their nominal values, appreciable errors in the *f*-number are produced. This is shown in table 5, which lists the nominal and measured *f*-numbers for the same group of lenses. The errors in the *f*-numbers range from −6.8 to +11.1 percent. The effect of these errors in terms of relative transmittance is shown in the last column.

TABLE 5. *Nominal and measured values of the f-number for a representative group of lenses*

Lens number	Nominal focal length	*f*-number		Error in *f*-number	Relative transmittance
		Nominal	Measured		
	mm			*Percent*	
1	12.5	1.9	1.77	−6.8	1.15
2	12.5	2.5	2.62	4.8	0.91
3	25.4	1.9	1.87	−1.6	1.03
4	35.0	2.7	2.67	−1.1	1.02
5	40.0	2.7	2.82	4.4	0.92
6	50.0	2.7	2.62	−3.0	1.06
7	50.8	2.2	2.07	−5.9	1.13
8	75.0	2.8	2.75	−1.8	1.04
9	75.0	2.3	2.30	0.0	1.00
10	76.2	3.0	3.04	1.3	0.97
11	101.6	2.5	2.51	0.4	0.99
12	177.8	6.8	6.91	1.6	97
13	190.5	4.5	4.74	5.3	.90
14	279.4	8.0	7.97	−0.4	1.01
15	342.9	7.5	8.33	11.1	0.81
16	419.1	9.5	10.12	6.5	.88
17	482.6	11.0	11.13	1.2	.98
18	609.6	11.0	11.78	7.1	.87
19	762.0	12.5	12.79	2.3	.96

These values of relative transmittance show that, neglecting losses in the lens, the difference between nominal *f*-number and true geometric *f*-number may alone produce deviations of as much as 19 percent between the expected and actual values of the amount of light passed by the lens. It must be emphasized that these differences are present at maximum stop-opening where the effective aperture is that of a true circular opening and not that of a many-sided opening, which is operative when the aperture is determined by the iris diaphragm. In 6 out of 19 cases, the relative transmittance deviates from unity by 10 percent or more, which may produce significant differences in exposure time in some instances of use.

(b) Errors in the marked *f*-numbers at reduced apertures

It is clear that errors of the type described in the preceding section are also present for all of the marked *f*-numbers. Because the aperture formed by the usual many-leaved iris diaphragm is a polygon, the accuracy of determining the diameter of the effective aperture is somewhat less than that for the full aperture, where the limiting opening is circular. Where the number of leaves is greater than six, two diameters at right angles to one another are measured, and the average is considered to be the diameter of a circular opening of the same area. For those diaphragms having four to six leaves, the area is computed from two or three diameters, and the diameter of the equivalent circle is used in computing the *f*-number. It is believed that the *f*-number obtained in this manner is correct within ±2 percent for the small *f*-numbers and rising to ±5 percent on the average for *f*-numbers greater than 22.

The errors in the *f*-number markings for twelve lenses are shown graphically in figures 4, 5, and 6, where the marked *f*-numbers are plotted as ordinates and the true (measured) *f*-numbers are plotted as abscissae. The dotted line with slope of unity passing through the origin is the line upon which the marked *f*-numbers would lie if there were no error in the markings. The points are plotted on logarithmic paper, so that one may see at a glance what the magnitude of the error is in terms of fractions of a stop-opening. For example, in the case of lens 3, figure 4, the true *f*-number corresponding to the *f*-number marked 16 is 12.9. This error of marking is clearly shown on the graph to exceed one-half stop. For lens 10, figure 5, at

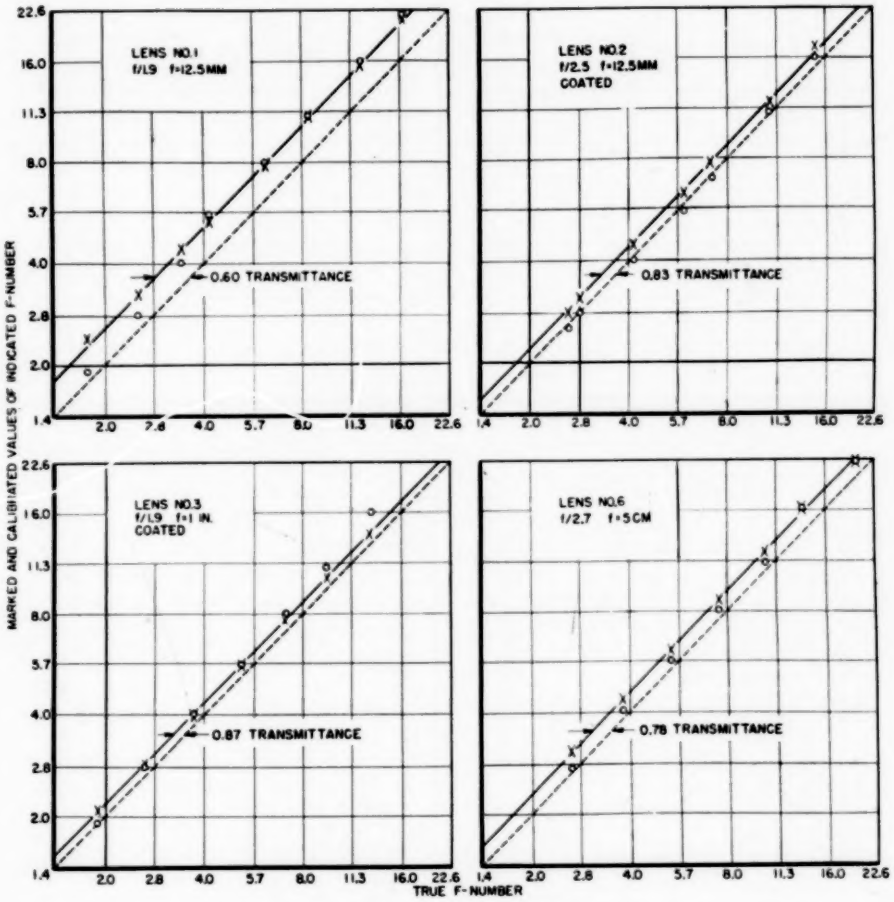

FIGURE 4. *Marked and calibrated values of f-number versus true geometric f-number.*

The circles indicate the marked *f*-numbers, and the crosses indicate the calibrated *f*-numbers. The circles would fall upon the dotted diagonal line if marked and true *f*-numbers were equal. The crosses would fall upon the dotted line if the transmittance were 100 percent. The separation of the dotted- and solid-line curves gives a measure of the transmittance of the lens. The steps in the net equal one stop-opening for ready appraisal of differences in fractions of a stop-opening.

803370—48——5

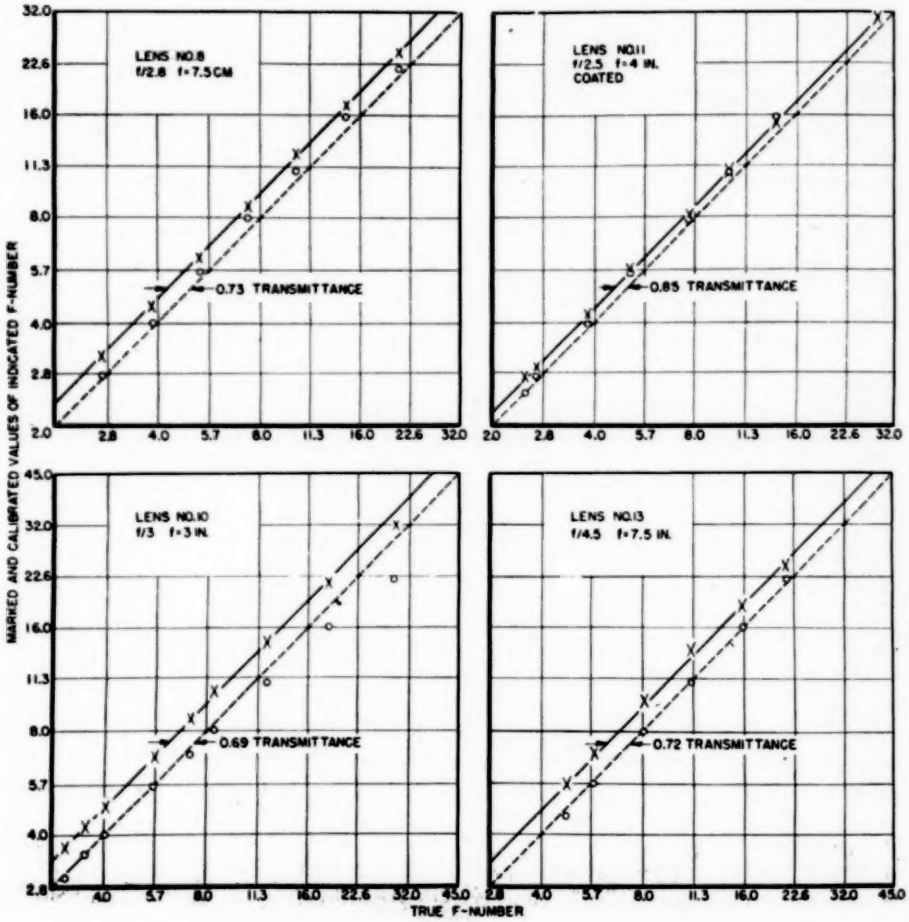

FIGURE 5. *Marked and calibrated values of f-number versus true geometric f-number.*

The circles indicate the marked *f*-numbers, and the crosses indicate the calibrated *f*-numbers. The circles would fall upon the dotted diagonal line if marked and true *f*-numbers were equal. The crosses would fall upon the dotted line if the transmittance were 100 percent. The separation of the dotted- and solid-line curves gives a measure of the transmittance of the lens. The steps in the net equal one stop-opening for ready appraisal of differences in fractions of a stop-opening.

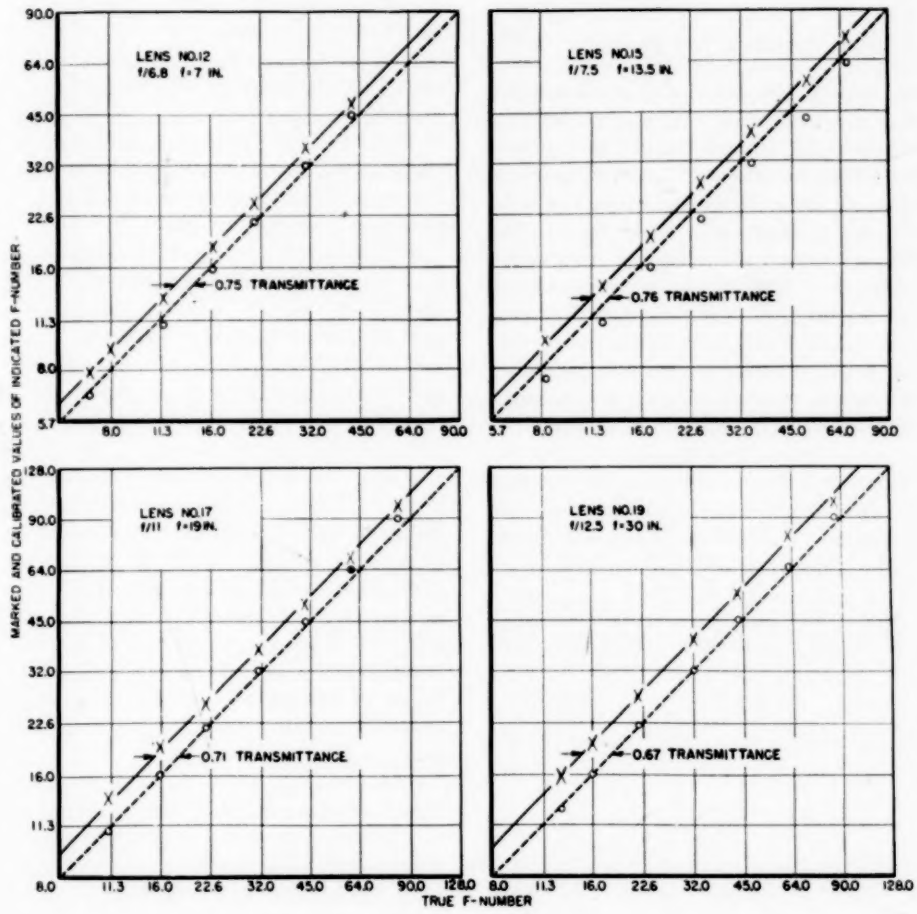

FIGURE 6. *Marked and calibrated values of f-number versus true geometric f-number.*

The circles indicate the marked *f*-numbers, and the crosses indicate the calibrated *f*-numbers. The circles would fall upon the dotted diagonal line if marked and true *f*-numbers were equal. The crosses would fall upon the dotted line if the transmittance were 100 percent. The separation of the dotted- and solid-line curves gives a measure of the transmittance of the lens. The steps in the net equal one stop-opening for ready appraisal of differences in fractions of a stop-opening.

$f/16$, the true f-number is 18.4, or more than one-half stop in the opposite direction. For lens 12, figure 6, the values of marked and true f-number are very close together throughout the range of the markings.

V. Measurement of Transmittance

1. Transmittance at Full Aperture

It is possible, on the basis of the information obtained in the course of this experiment, to determine the light transmittance of the lens itself. It must be emphasized, however, that the transmittance so determined is the ratio of the amount of light passing through the lens to the amount of light incident on the front surface of the lens, and does not differentiate between image-forming and non-image-forming light. There are two ways of making this determination. The first method yields the nominal transmittance, and is simply the square of the ratio of the nominal f-number and the ideal f-number that gives the same deflection on the light meter. Values obtained by this method are listed in table 6, under the heading of nominal transmittance. Since no cognizance is taken of the errors in the nominal f-number, the nominal transmittance is affected by the error in f-number, as well as by reflection and absorption losses in the lens.

TABLE 6. *Nominal and actual values of the transmittance at full aperture for a representative group of lenses*

Lens number	Equivalent focal length	f-number			Transmittance	
		Marked	True	Calibrated	Nominal	Actual
	in.					
1	0.5	1.9	1.77	2.40	0.63	0.54
2	.5	2.5	2.62	2.82	.79	.86
3	1.0	1.9	1.87	2.09	.83	.80
4	1.4	2.7	2.67	3.14	.74	.72
5	1.6	2.7	2.82	3.14	.74	.81
6	2.0	2.7	2.62	3.09	.76	.72
7	2.0	2.2	2.07	2.23	.97	.86
8	3.0	2.8	2.75	3.20	.77	.74
9	3.0	2.3	2.30	2.45	.88	.88
10	3.0	3.0	3.04	3.68	.67	.68
11	4.0	2.5	2.51	2.79	.80	.81
12	7.0	6.8	6.91	8.00	.72	.75
13	7.5	4.5	4.74	5.60	.65	.72
14	11.0	8.0	7.97	10.10	.63	.62
15	13.5	7.5	8.33	9.72	.59	.73
16	16.5	9.5	10.12	12.30	.60	.68
17	19.0	11.0	11.13	13.60	.65	.67
18	24.0	11.0	11.78	14.30	.59	.68
19	30.0	12.5	12.79	15.60	.64	.67

The second method yields the actual transmittance and is the square of the ratio of the measured and calibrated f-numbers. Since this method rules out the error in f-number, the actual transmittance is affected only by reflection and absorption losses in the lens.

It is interesting to consider lenses 16, 17, 18, and 19. These are all of the same type, having 8 glass-air surfaces, but ranging in focal length from 16.5 to 30 ins. The nominal transmittance for these four lenses varies from 0.59 to 0.65, whereas the actual transmittance is almost invariant, changing from 0.67 to 0.68.

The effect of antireflecting coatings on the lens surfaces can be seen in this table. Lenses 2, 3, 7, 9, and 11 are coated, and all have transmittances that exceed 80 percent. Only one, 5, of the uncoated lenses has a transmittance above 80 percent, and the remaining 13 lenses have transmittances ranging from 62 to 75 percent, with one lens (1) falling as low as 54 percent. The antireflecting coatings increase the transmittance by 25 percent or more. Even so, consideration of the actual values of the transmittance shows that 10 percent or more of the incident light is still lost by the coated lens. This is not surprising when it is remembered that antireflecting films usually yield close to 100 percent transmittance for only one wavelength of light. Accordingly, when a broad region of the spectrum is covered, as is the case for white light, the transmittance measured is the average for the whole region.

The fact that the values of transmittance obtained by this procedure are affected in some small amount by the presence of nonimage-forming or scattered light cannot be considered as important. It is improbable that markedly different values would be obtained by the use of collimated light incident on the front surface of the lens during the experiment. In any comparison between the broad source method of measuring transmittance or calibrating a lens and the collimated light method, it is unlikely that light scattered by the lens will produce appreciable difference in the end result. The broad source fills the lens with light, giving rise to a greater amount of scattered light. However, the diaphragm in the focal plane rigidly restricts the measured scattered light to that falling within a small area. The collimator system, at

least for the larger aperture, illuminates the inner surface of the barrel with light at small angles of incidence favorable for reflection. All the light that is scattered and emerges from the lens is evaluated by the detector. It is difficult to say which will give the most weight to scattered light. Certainly for a well-constructed lens, the differences in results obtained by the two methods will be small. For a lens purposely made to reflect the light from the mount, the result is open to question. However such lenses do not constitute a threat, because they would not make satisfactory photographs. The extended source does give a measure of the light (some of which is scattered), which will be incident on a central area of the film when photographing a subject with a reasonably average illumination over the entire field. The collimator method gives a measure of the light available over a central area of the film, plus all scattered light, when photographing a relatively small bright source on a dark ground.

2. Average Transmittance for All Apertures

The value of transmittance obtained in the preceding section is a reliable one for full aperture, but, since a lens is frequently used at reduced stop-opening, it is advantageous to consider a method of determining average transmittance throughout the entire range of stops. This is done by plotting the calibrated *f*-number against the true *f*-numbers as has been done for 12 lenses in figures 4, 5, and 6. The crosses show the relation thus obtained. It is clear that these crosses lie on a straight line, shown as a solid line, parallel to the dotted diagonal line. If the crosses fell on the dotted line, it would indicate a transmittance of 100 percent. As it is, the displacement of the solid line from the dotted line gives at once a measure of the average transmittance for all apertures. This has been computed from the curves, and the value of the average transmittance for all apertures is shown for each of the 12 lenses in the proper figure.

It is worthy of mention that this method of plotting the results of measurement serves the dual purpose of showing the consistency of the method of calibration and the reliability of the measured values of true *f*-number. Errors in either operation would cause the crosses to fall away from the solid-line curve. The fact that these deviations are small indicates that both calibrated and true *f*-numbers have been quite accurately assigned.

VI. Summary

The present system of marking the diaphragms stops, in terms of the geometric *f*-number, is subject to serious deficiencies so far as uniform performance for lenses set at the same marked stop-opening is concerned. Decisions regarding the proper exposure time to use at a selected stop-opening may be in error by ± 10 percent for a lens whose surfaces do not have antireflection coatings, and by even greater amounts for a lens whose surfaces do have antireflection coatings. These errors arise from differences in the reflection and absorption losses in the lens elements themselves, departures of the measured from the nominal focal length, and departures of the measured diaphragm openings from the nominal diaphragm openings.

A method is described whereby a lens can be calibrated by a light meter in terms of an ideal lens, so that the variation in axial illumination in the focal plane need not exceed ± 2 percent in using different lenses set to the same calibrated stop-opening.

VII. References

[1] I. C. Gardner, J. Research NBS **38,** 643 (1947) RP1803.

[2] I. C. Gardner, J. Soc. Motion Picture Engrs. **49,** 96 (1947).

[3] M. G. Townsley, J. Soc. Motion Picture Engrs. **49,** 111 (1947).

[4] F. G. Back, J. Soc. Motion Picture Engrs. **49,** 122 (1947).

[5] L. T. Sachtleben, Method of calibrating lenses, U. S. Patent No. 2,419,421 (Issued April 22, 1947 and assigned to Radio Corporation of America).

[6] A. E. Murray, J. Soc. Motion Picture Engrs. **47,** 142 (1946).

[7] C. R. Daily, J. Soc. Motion Picture Engrs. **46,** 343 (1946).

[8] E. Berlant, J. Soc. Motion Picture Engrs. **46,** 17 (1946).

[9] D. B. McRae, J. Opt. Soc. Am. **33,** 229 (1943).

[10] E. W. Silvertooth, J. Soc. Motion Picture Engrs. **39,** 119 (1942).

[11] D. B. Clarke and G. Laube, J. Soc. Motion Picture Engrs. **36,** 50 (1941).

[12] D. B. Clarke and G. Laube, Method and means for rating the light speed of lenses, U. S. Patent No. 2,334,906 (Issued November 23, 1943, and assigned to Twentiety Century-Fox Film Corp.).

WASHINGTON, May 7, 1948.

U. S. Department of Commerce
National Bureau of Standards

Research Paper RP1928
Volume 41, October 1948

Part of the Journal of Research of the National Bureau of Standards

Mass Spectrometric Investigation of the Thermal Decomposition of Polymers[1]

By Leo A. Wall

The application of the mass spectrometer to the study of the thermal decomposition of polymers is described. The relationships between the structure of polymers and yield of monomers on decomposition are discussed. A quantitative treatment relating the compositions of certain copolymers and the yields of monomers is given. Data are presented showing the composition of the volatile hydrocarbons produced by the thermal decomposition of several vinyl and diene polymers.

I. Introduction

The use of pyrolysis as a tool for investigating the constitution of high polymers has been limited by the difficulty involved in the analysis of the decomposition products. One of the best known examples of its use is the study of natural rubber by Midgley and Henne [1].[2] These investigators subjected 200 lb of natural crepe rubber to distillation in iron vessels in 16-lb batches at atmospheric pressure and 700° C. Analysis of the products disclosed 10 percent of isoprene and 20 percent of dipentene. The theoretical aspects of certain types of polymer pyrolysis have been discussed by Rice and Rice [2].

The recent development of the mass spectrometer as an analytical instrument [3] for hydrocarbon mixtures opened new possibilities for the utilization of pyrolysis as a means for the study of complex molecular structures by the analysis of their characteristic products of decomposition. The technique used in the present investigation consisted in pyrolyzing the polymers under conditions similar to a single-stage molecular distillation. This procedure was adopted to facilitate the removal of primary products before secondary decomposition became appreciable. The fact that a very small sample, 0.001 g, is required increased the utility of the method; it would perhaps be advantageous in the investigation of biological materials.

[1] Supported in part by funds from Reconstruction Finance Corp., Office of Rubber Research.

[2] Figures in brackets indicate the literature references at the end of this paper.

II. Experimental Procedure

The pyrolysis tube or single-stage molecular still (fig. 1) resembles a test tube with a small side arm. The section of 3-mm tube sealed on the top of the tube fits into a break-off device on the spectrometer.

The samples were inserted either as small lumps or as solutions. The preferred method of inserting the sample was to pipette into the side arm 2 ml of a solution of the polymer in a volatile solvent at a concentration of about 0.0005 g/ml. Upon evaporation of solvent, the tube was sealed to a high vacuum system. After evacuation to a pressure of 10^{-5} mm of mercury, the still was sealed off. The volume of each still was 45 ml.

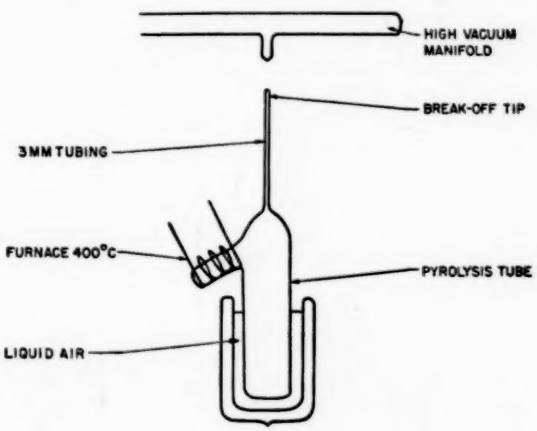

FIGURE 1. *Diagram of pyrolysis apparatus.*

Pyrolysis was induced by heating electrically the side arm containing the polymer, and the body of the tube was immersed in liquid air to condense the products of decomposition. The time of heating was 20 minutes. A temperature of 400° C was used because it produced complete decomposition of most polymers, whereas lower temperatures did not.

After pyrolysis the tube was inserted in the mass spectrometer, the end of the small tubing was broken, and the volatile products were expanded directly into the inlet system (fig. 2). The total

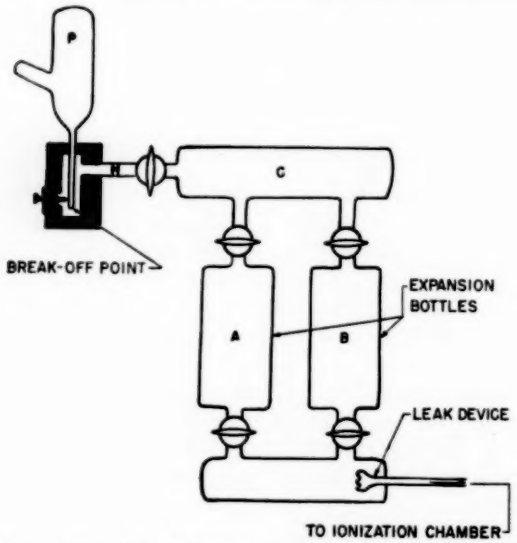

FIGURE 2. *Simplified diagram of mass spectrometer inlet system.*

volume of the inlet system and the sample tube is known. Also, the partial pressure of each component can be determined by means of the known pattern sensitivities. The sensitivity for a compound is the height of a characteristic peak produced when 1-micron pressure of the pure substance is in the inlet system. The gas law is then used to compute the weight of the component produced, from which the percentage yield can be computed.

III. Results of Tests

Tables 1 and 2 show the various volatile hydrocarbons obtained in the pyrolysis experiments. As only products that have about 1 mm or more vapor pressure at room temperature could enter the Consolidated mass spectrometer, these results are given in terms of mole percent of "volatiles". The computed values, particularly where a large number of components occurred, are necessarily approximate. However, the uncertainty in the last significant figure is probably no more than 2 or 3.

TABLE 1. *Volatile products obtained in the pyrolysis of vinyl polymers*

Vinyl polymer	Volatile pyrolysis products [a]	Mole percent
Polyethene[b]	Approximately 30 compounds consisting of n-alkenes, n-alkanes, n-dienes, and cyclics.	
Polyisobutene	Isobutene	78
	Neopentane	10
	Diisobutene	4
	Ethane	2
	C_7H_{14}	1
	C_6H_{12}	0.5
	CH_4	.5
	C_7H_{12}	.4
	C_3H_4	.4
	$C_{10}H_8$	.1
Polystyrene	Styrene	91
	Ethene	3
	Ethylbenzene	1
	Toluene	1
	Benzene	1
	Isopropylbenzene	0.5

[a] The volatile products represent 66 percent of the polyisobutylene and 34 percent of the polystyrene.

[b] In polyethene, it proved impossible to compute an analysis since the products were so varied; however, the ethylene produced was certainly less than 1 percent.

The results vary considerably with the size of sample used. With 0.01 g the yield of isoprene from natural crepe was 18 percent, whereas with 0.001 g it was 2 percent. Apparently the 0.01-g sample produced in the initial phase of the pyrolysis enough permanent gas to decrease the efficiency of the molecular distillation, thereby impeding the removal of the initial products. Dimers, trimers, etc., would thus be further cracked into monomers. More efficient molecular distillation would still further reduce the yield of monomer and produce chiefly degraded polymers within the molecular weight range of 100 to 1,000. The latter figure corresponds approximately to the heaviest hydrocarbon species that can be distilled. Above this molecular weight, molecular cohesion is greater than the carbon-carbon single bond strength [4]. It can thus be seen that although low pressure decreases

side reactions, monomer production is not necessarily improved, as dimers and larger molecules are formed and not subsequently decomposed.

Table 1 shows the analysis of the volatile products formed in the pyrolysis of vinyl polymers. The number and quantities of products other than monomer indicate the extent of various side reactions.

Table 2 presents the analysis of volatile products from some diene polymers. The three isoprene polymers are similar, and the poorer yield of monomer from the natural polymers may be due to the presence of impurities. The presence of cyclopentadiene in the products from the synthetic polymer would be expected, because it is usually present in commercial monomer; it was unexpected, however, in the case of the natural polymers.

Table 3 gives the monomer yields from the various polymers. In the case of three vinyl polymers, the yield is in the inverse order of their heat stabilities [5]. The heat stabilities of the diene polymers might therefore be expected to be in the inverse order of the monomer yields, with the exception of neoprene, which breaks down with the liberation of hydrogen chloride.

TABLE 2. *Volatile products obtained in the pyrolysis of diene polymers*

Diene polymer	Volatile pyrolysis products [a]	Mole percent
Polybutadiene	Butadiene	34
	Vinylcyclohexene	7
	Ethane	18
	Propane	13
	Methane	12
	C_8H_{10}	5
	C_8H_8	5
	C_6H_{10}	2
	C_2H_6	2
	C_6H_6	1
Balata	Isoprene	50
	Dipentene	13
	Methane	13
	Cyclopentadiene	6
	Propene	4
	Ethane	4
	C_8H_{10}	2
	C_6H_{12}	2
	C_7H_{12}	1
	C_6H_{10}	1
	C_6H_{14}	Trace
Natural crepe	Isoprene	57
	Dipentene	13
	Ethane	11
	Cyclopentadiene	7
	C_6H_{10}	7
	CH_4	3
	C_8H_{16}	2
	C_6H_{12}	Trace
Polyisoprene	Isoprene	67
	Dipentene	7
	C_6H_{12}	5
	Methane	4
	Ethane	3
	Cyclopentadiene	3
	C_8H_{16}	3
	C_7H_{12}	2
	C_6H_{10}	2
	Propene	2
	Toluene	1
	C_8H_{10}	0.5
	C_6H_{12}	.1
Methyl rubber	2,3-Dimethylbutadiene-1,3	80
	C_6H_{10}	10
	Ethane	8
	Methane	2
	C_6H_{12}	1
	C_5H_{12}	.1
Polymethylpentadiene	2-methylpentadiene-1,3 + 4-methylpentadiene-1,3	97
	Ethane	3
	Methane	.2
	High-boiling fraction	Trace

[a] The volatile products represent 3, 4, 4, 8, 7, and 26 percent, respectively, of the polymers listed.

Table 3 gives the monomer yields from the various polymers. In the case of three vinyl polymers, the yield is in the inverse order of their heat stabilities [5]. The heat stabilities of the diene polymers might therefore be expected to be in the inverse order of the monomer yields, with the exception of neoprene, which breaks down with the liberation of hydrogen chloride.

TABLE 3. *Monomer yields in pyrolysis of polymers*

	Polymer	Monomer yield
		Percent
Diene polymers	Polybutadiene	1
	Natural crepe	2
	Balata	2
	Polyisoprene (synthetic)	5
	Methyl rubber	6
	Polymethylpentadiene	26
	Neoprene [a]	2
Vinyl polymers	Polyethene	0
	Polystyrene	33
	Polyisobutene	50

[a] The production of HCl accounted for 68 percent of the chlorine in neoprene.

IV. Discussion of Results

1. Polymers From Single Monomers

Thermal decomposition of polymers may be considered to occur through three types of reactions analogous to those leading to the formation of the polymer. The initial reaction is very likely the random breaking of some of the weakest bonds, which in hydrocarbons are the carbon-carbon single bonds. A single break would form two radicals, which could easily disintegrate into small molecules and a small terminal radical. Other random breaks could form diradicals that

803370—48——6

could decompose only into small molecules, so that the over-all result would be similar to that when a single break is considered. Thus, the second type of reaction would be the formation of small molecules, sometimes chiefly monomer and terminal radicals. Finally, the small radicals would either acquire a hydrogen from other molecules, thus forming other radicals, or terminate by combining with each other or disproportionating. For high molecular-weight polymers, the quantity of products formed in the last step would be insignificant. However, if the large radicals prefer to pick off hydrogen atoms from other molecules thereby producing different radicals that are also capable of removing hydrogen or splitting into molecules and still other radicals, then there will be produced a variety of products other than monomer.

Whatever mechanism of thermal decomposition is considered, only products formed from the fragments of the chain ends would depend on the molecular weight and distribution. This effect would be appreciable only for rather low molecular weight polymers. Bachman et al. [6] report that the pyrolytic yield of styrene from low molecular weight polystyrene decreases with decreasing molecular weight of the polymer.

A simplified scheme for the thermal depolymerization of the vinyl polymers, except for the case where the C—Y bond is weaker than the C—C bond, may be postulated as follows:

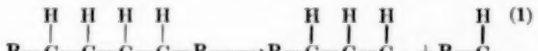
(1)

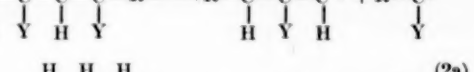
(2a)

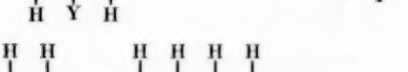
(2b)

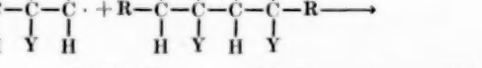
(2c)

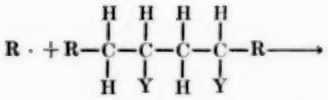
(3a)

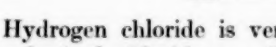

Hydrogen chloride is very easily stripped from polyvinyl chloride, so that the above reaction scheme is not applicable in this and similar cases, where the bonds to the substituted side groups are weaker than the C—C bonds in the chain.

In a chain with head-to-tail structure, all of the C-C bonds are identical, and even with other arrangements the bonds are certainly changed very little. With a head-to-tail structure, it can be seen by inspection that there are two ways of splitting out monomers. It can also be seen that head-to-head and tail-to-tail structure decreases the number of ways and hence the probability of obtaining monomer. Therefore, the conditions favoring monomer are large molecular weight, head-to-tail structure, and a monomer that is both heat stable and unreactive. The complexity of the experimental results indicate that even under molecular distillation conditions the evaporation of products is slow compared to the reactions such as those postulated above. Most of the products obtained, however, can be formed as a consequence of the assumed scheme.

The relative rates of reaction 2a and 2b should then determine the results of pyrolysis. Reaction 2b depends on the reactivity of the radicals formed in the initial break. The activation engergies for the removal of a hydrogen by radicals should increase in the following order:

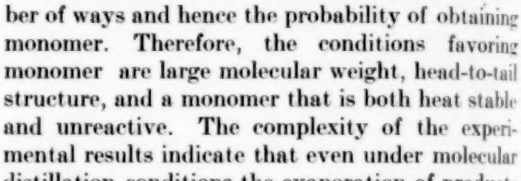

Kharasch [7] has found this order of reactivity for the removal of chlorine atoms from carbon tetrachloride. For the type of radicals on the right, there is no theoretical basis for readily predicting the exact order of reactivity; however, it is certain that they are quite unreactive compared to RCH_2. Also, the radical RCF_2 should have difficulty in removing fluorine from nearby chains. Polytetrafluoroethyelene [8], then, presumably de-

composes chiefly in accordance with reaction 2a. In general, all polymers giving appreciable yields of monomer on pyrolysis are capable of producing such relatively unreactive radicals through an initial scission of the chain. Since most of the common polymers are formed from mono or asymmetrically disubstituted monomers, the initial break produces two types of radicals, a reactive one and an unreactive one. The former rapidly picks up a hydrogen. It is then logical to conclude that the unreactive type of radical is the most abundant species of radical in the decomposing polymer and produces the major portion of monomer according to reaction 2a.

Although radical reactivity seems to be the determining factor, it is linked with steric effects, since groups that stabilize the radical also cause increased steric hindrance. The bonds in the chain are consequently weaker, and decomposition will occur at lower temperatures. Thus reaction 2a is favored simultaneously by both steric and radical factors.

The results on polyisobutylene and polystyrene are interesting in this light. The styrene radical would ordinarily be assumed more unreactive than the tertiary butyl radical; however, polyisobutylene, in which there is known to be a large steric effect [9], produces the largest yield of monomer.

It is known that carbon-carbon bond strengths become weaker as one proceeds from primary to tertiary bonds [10]. This effect is probably independent of steric hindrance but not of the reactivity of the radicals formed by bond scission. Also, bonds adjacent or alpha to double and triple bonds are relatively stronger, whereas beta bonds are weaker.

A scheme similar to that for the vinyl decomposition can be postulated for the dienes. However, diene decomposition differs from that for the vinyls primarily because all of the bonds in the chain are not identical. Hence splitting will not be at random. The bonds in the beta position to the double bonds are presumed to be the weakest, and breaking of these bonds favors monomer production. Thus the effect on monomer yield of the weakness of these bonds in the dienes compensates for the dependence on the manner of splitting. Scission of any other bonds would lead to products other than monomer, dimer, etc., whereas in vinyls it does not matter which bond of the chain breaks first. In the diene case also, the radical reactivity effect appears to account for the differences found among such polymers. However, because of the double bonds in the chain, the dienes can react in many more ways than the vinyl polymers, and hence comparisons between the two types of polymers are not significant.

2. Copolymers

In all thermal decompositions there are competing reactions that the structure of the polymer either does or does not favor. This comes about through the operation of two effects: (1) probability, or the number of ways a certain result is obtained, and (2) bond strengths. The arrangement of substituent groups decides the first, and their nature decides the second. In copolymers, the study of these effects leads to some interesting conclusions.

For instance, in GR-S we have essentially styrene units isolated between butadiene units:

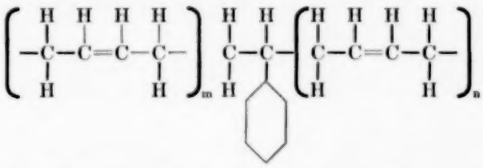

In this arrangement styrene can be obtained in only one way instead of the two possible in polystyrene. Hence the probability of obtaining styrene is halved. Theoretically, one should expect from GR-S, assuming that all styrene units were isolated, only half of the percentage of styrene yield possible on the basis of the polystyrene results. Thus, if by a given method the yield of styrene is 33 percent by weight from polystyrene, GR-S, which contains 23.5 percent by weight of styrene, should yield $23.5 \times 0.33 \times 1/2 = 3.9$ percent. The experimental yield was 3 percent.

In the case of the copolymer of methyl methacrylate with styrene, we find that, considering a head-to-tail structure and complete alternation,

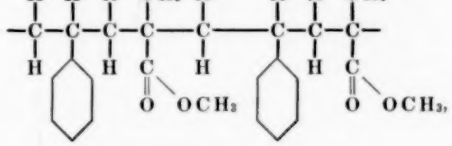

there are two ways of obtaining monomers. Hence, we would expect the same yields of mono-

mer as from the simple polymers. This has been found to be true by Bachman, et al. [6], who recovered 66 percent of the styrene from such a copolymer, whereas under the same conditions polystyrene yielded 60 to 65 percent of its styrene. In the case of a symmetrical disubstituted ethene polymerized with a monosubstituted or asymmetrically disubstituted ethene, we should again have a copolymer that has only one way of splitting out monomer if the monomer units considered are isolated from one another.

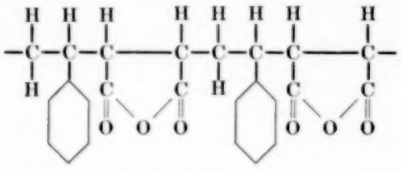

Bachman also depolymerized the copolymer of styrene and maleic anhydride. His yield would be expected to be $1/2 \times 60$, or 30 percent, of styrene recovered. Instead, he obtained 11 percent; however, the polymer loses carbon dioxide readily, so that side reactions may easily occur and thereby reduce the yield of styrene.

The above results confirm the assumed head-to-tail arrangement for polystyrene and polymethylmethacrylate. The low experimental yields from the copolymers imply an increased susceptibility to side reactions and cannot be attributed to head-to-head and tail-to-tail arrangements in the simple polymers.

Table 4 presents the comparative yields of styrene from various copolymers compared to the yield from polystyrene. It can be seen that the yield depends on the nature of the copolymer as well as the conditions of pyrolysis. In order to use pyrolysis as an analytical technique, one would need to know how the monomer units, were distributed in the copolymer which can be obtained from copolymer theory; or if one knew the amounts of different monomers in the polymer the yields would indicate their arrangement.

TABLE 4. *Comparison of styrene yields from polymer and copolymers*

	Polymer	Styrene yield *
		Percent
This work	Polystyrene	33
	GR-S	14
Bachman's work	Polystyrene	60 to 65
	Polystyrene-methylmethacrylate	66
	Polystyrene-maleicanhydride	11 to 12

* Styrene yield $= \frac{\text{styrene recovered}}{\text{styrene in polymer}} 100$.

Assuming that the effect of side reactions on the yield of a given monomer remains constant in going from simple polymer to copolymers, and that the C—C bonds in the vinyl chain and sequences are of equal strength for a given monomer, then the pyrolysis yield of monomer from the copolymer formed at low conversion can be calculated if one knows the yield from the simple polymer, the monomer reactivity ratios (r_A and r_B) [11, 12], and the composition of the monomer charge. The probability of regenerating monomer A, for example, styrene, from the simple polymer can be considered unity. The probability of obtaining monomer A from sequences BAB consisting of say butadiene-styrene-butadiene units is 1/2, from $BAAB$ sequences 3/4, and from $BA_1A_2 \ldots A_iB$ is $(2i-1)/2i$.

It has been shown [13] that the probability of a given sequence containing i monomer units is

$$P_{BA}i_B = P_{BA}P_{AB}P_{AA}^{i-1}, \tag{4}$$

where P_{BA} is the probability of a radical ending in monomer B reacting with monomer A in the process of copolymerization. Probabilities P_{AB} and P_{AA} are similarly defined. They can be calculated from the following expressions:

$$P_{BA} = \frac{A}{A + r_B B}, \tag{5}$$

$$P_{AB} = \frac{B}{r_A A + B}, \tag{6}$$

$$P_{AA} = \frac{r_A A}{r_A A + B}, \tag{7}$$

where A and B are the concentrations of the monomer in the mixture from which the polymer under consideration was formed.

The probability of obtaining monomer A from any copolymer is simply the sum of the products of the probabilities of the various sequences and the probabilities of obtaining the monomer from the sequence. Hence

$$P_A \text{ from copolymer} = \sum_{i=1}^{i=\infty} \frac{2i-1}{2i} P_{BA}i_B = P_{BAB} \sum_{i=1}^{i=\infty} \frac{2i-1}{2i} P_{AA}^{i-1}. \tag{8}$$

The yield of $A(Y_A)$ from copolymer would then be given by

$$Y_A = N_A P_{BAB} \sum_{i=1}^{i=\infty} \frac{2i-1}{2i} P_{AA}^{i-1} \qquad (9)$$

or

$$Y_A = N_A \left[P_{BA} + \frac{P_{BAB}}{2P_{AA}} \ln P_{AB} \right], \qquad (10)$$

where N_A is the yield of A from its simple polymer under the same conditions used to decompose the copolymer of A with B. By means of eq 5, 6, and 7, the function can be written in terms of monomer concentrations, A and B, used in making the copolymer.

$$Y_A = N_A \frac{A}{A + r_B B} \left[1 + \frac{B}{2r_A A} \ln \frac{B}{r_A A + B} \right] \qquad (11)$$

These equations are valid, of course, only for polymers formed at low degrees of conversions or where the relative monomer concentrations are constant during polymerization. Monomer A can be any stable mono or asymmetrically disubstituted ethylene and B any diene or symmetrically disubstituted ethylene. Deviations from the predicted results may be an indication of the extent to which the initial assumptions are not true.

Figure 3 is a plot of eq 11 applied to styrene-butadiene copolymer where N_A is taken to be 33. A 33-percent yield of styrene was obtained on the depolymerization of polystrene by our technique.

Figure 4 is a theoretical plot of yield against polymer composition. The straight line would apply if the copolymer were simply a mixture of polystyrene and polybutadiene, whereas the curved line would apply for a pure copolymer formed at low degrees of conversion.

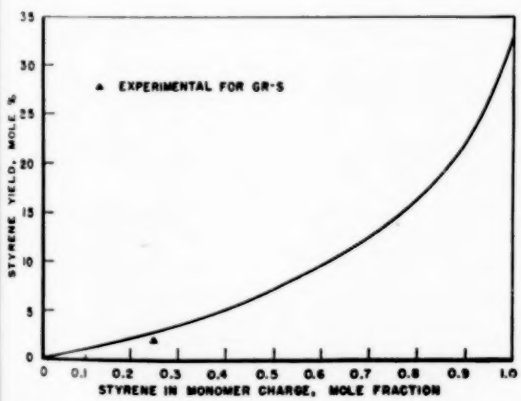

FIGURE 3. *Styrene yield versus monomer composition.*

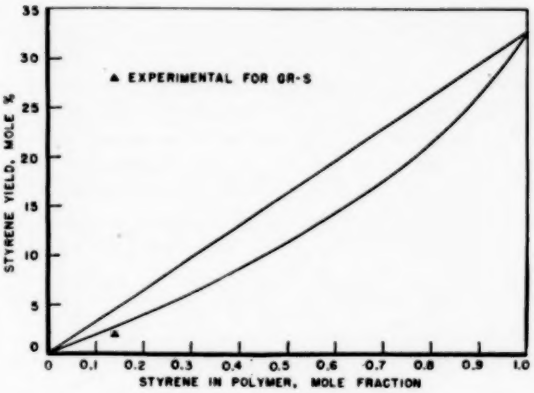

FIGURE 1. *Styrene yield versus polymer composition.*

The above-mentioned considerations, using monomer yield as a criterion for structural variations, should, of course, be correlated with yield of other products. Nevertheless, monomer yield alone can furnish information on the arrangement of the units, the number and types of sequences in certain copolymers, or composition. As the mass spectrometer is calibrated for more compounds, this technique should become increasingly valuable and perhaps become at least a supplementary analytical tool for the study of polymers.

V. Conclusions

The thermal decomposition of polymers can be studied by the use of the mass spectrometer to identify the volatile products. Small samples (0.001 g) are sufficient, and the experimental procedure is relatively simple. Qualitative estimates can be made rapidly, but precise analyses require considerable study of the mass spectrometric records. The chief limitations are that mass spectrometric data must be obtained for a large number of pure compounds, and that the studies are restricted to the volatile decomposition products; that is, those having a vapor pressure at room temperature of 1 mm of mercury or more.

Important structural arrangements in the polymer can be deduced from the nature of the

pyrolysis products, but minor ones are frequently obscured because of the many secondary products formed. In general, it appears that monomers, from which relatively unreactive radicals are derived, have a higher degree of resonance stabilization and form polymers that decompose to a large extent into monomer. Polymers formed from such monomers appear more susceptible to thermal degradation. Polymers that have weakly held side groups, as well as fluorine substituted polymers, would form exceptions to this generalization.

Monomer yield alone can be used as a criterion of structure for certain copolymers and can be estimated from a knowledge of the relative reactivity of the monomers, the conditions of polymerization, and the results obtained with simple polymers.

The author thanks A. K. Brewer, F. O. Rice, and Robert Simha for their direction, encouragement, and suggestions. Acknowledgment is also made to Robert Reese, Lee Parham, and Vernon H. Dibeler for operating the mass spectrometer, and to Howard W. Bond for advice on problems of technique.

VI. References

[1] T. Midgley and A. L. Henne, J. Am. Chem. Soc. **51,** 1215 (1929).
[2] F. O. Rice and K. K. Rice, The aliphatic free radicals (Johns Hopkins Press, Baltimore, Md., 1935).
[3] H. W. Washburn, H. F. Wiley, and S. M. Rock, Ind. Eng. Chem., Anal. Ed. **15,** 541 (1943).
[4] W. H. Carothers and J. W. Hill, J. Am. Chem. Soc. **54,** 1557 (1932).
[5] R. B. Seymour, Ind. Eng. Chem. **40,** 524 (1948).
[6] G. B. Bachman, H. Hellman, K. R. Robinson, R. W. Finhold, E. J. Kahler, L. J. Filar, L. V. Heisey, L. L. Lewis, and D. D. Micucci, J. Org. Chem. **12,** 108 (1947).
[7] M. S. Kharasch, S. Kane, and H. C. Brown, J. Am. Chem. Soc. **64,** 1621 (1942).
[8] E. E. Lewis and M. A. Naylor, J. Am. Chem. Soc. **69,** 1968 (1947).
[9] A. G. Evans and M. Polanyi, J. Chem. Soc. 252 (1947).
[10] E. C. Baughan, M. G. Evans, and M. Polanyi, Trans. Faraday Soc. **37,** 377 (1941).
[11] F. R. Mayo and F. M. Lewis, J. Am. Chem. Soc. **66,** 1594 (1944).
[12] R. Simha and H. Branson, J. Chem. Phys. **12,** 253 (1944).
[13] T. Alfrey and G. Goldfinger, J. Chem. Phys. **12,** 205 (1944).

WASHINGTON, November 21, 1947.

U. S. Department of Commerce
National Bureau of Standards

Research Paper RP1929
Volume 41, October 1948

Part of the Journal of Research of the National Bureau of Standards

Purification, Purity, and Freezing Points of 30 Hydrocarbons of the API-Standard and API-NBS Series[1]

By Anton J. Streiff,[2] Janice C. Zimmerman,[2] Laurel F. Soule,[2] Marie T. Butt,[2] Vincent A. Sedlak,[2] Charles B. Willingham, and Frederick D. Rossini

This report describes the purification and determination of freezing points and purity of 30 hydrocarbons of the API-Standard and API-NBS series, including eight paraffins, six cycloparaffins, three aromatics, twelve olefins, and one acetylene.

I. Introduction

Previous reports described the purification and determination of freezing points and purity of 84 hydrocarbon compounds of the API-Standard and API-NBS series, which were produced as part of the cooperative program on Standard Samples of hydrocarbons of the National Bureau of Standards and the American Petroleum Institute [1, 2, 3, 4].[3]

This report describes the purification and determination of freezing points and purity of an additional 30 hydrocarbon compounds under this cooperative program, including 8 paraffin hydrocarbons, 5 alkylcyclopentanes, 11 monoolefins, 3 diethylbenzenes, ethylcyclobutane, 1-butyne and cyclohexene. Four of these additional 30 compounds are second and purer lots of compounds, the first lots of which were described in the earlier reports.

The final lots of the material labeled API-Standard are sealed "in vacuum" in glass ampoules and made available as NBS Standard Samples of hydrocarbons, by the American Petroleum Institute and the National Bureau of Standards. The material labeled API-NBS is made available in appropriate small lots, through the American Petroleum Institute Research Project 44 at the National Bureau of Standards, on loan to qualified investigators for the measurement of needed properties.

II. Materials

The starting materials were supplied as follows:

By the API Research Project 45 on the synthesis and properties of hydrocarbons of low molecular weight at the Ohio State University, Columbus, Ohio, under the supervision of C. E. Boord:

Ethylcyclobutane.
cis-1,3-Dimethylcyclopentane.
trans-1,3-Dimethylcyclopentane (B).[4]
n-Butylcyclopentane.
1-Hexene (one-half).
trans-2-Hexene.
trans-3-Hexene.
3-Methyl-1-pentene.
2-Methyl-2-pentene.
2-Ethyl-1-butene (one-half).
1-Heptene.
1,3-Diethylbenzene (one-third).
1-Butyne (Ethylacetylene).

By the Hydrocarbon Laboratory at the Pennsylvania State College, State College, Pa., under the supervision of F. C. Whitmore:

2,3,3-Trimethylhexane.
2,2,4-Trimethylhexane.
2,3,3-Trimethylhexane.
2,3,5-Trimethylhexane.
3,3,4-Trimethylhexane.
cis,cis,cis-1,2,3-Trimethylcyclopentane.
cis,trans,cis-1,2,3-Trimethylcyclopentane.

[1] This investigation was performed at the National Bureau of Standards as part of the work of the American Petroleum Institute Research Project 6 on the Analysis, purification, and properties of hydrocarbons.

[2] Research associate on the American Petroleum Institute Research Project 6 at the National Bureau of Standards.

[3] Figures in brackets indicate the literature references at the end of this paper.

[4] In this paper (B) following the name of a compound indicates that for the API-NBS series, it is a second (and usually slightly purer) sample of the given compound, the first sample of which will be labeled (A).

TABLE 1. *Information on the purification of 30 API–Standard and API–NBS hydrocarbons*

Compound [a]	Laboratory [b] providing starting material	Hydrocarbon charged for distillation		Distillation [f]								Volume of selected sample	
		Volume	Purity	Kind [c]	Azeotrope-forming substance [d]	Amount of hydrocarbon in the azeotropic distillate [e]	Distilling column number [f]	Number of theoretical plates [f] (approx.)	Reflux ratio [f] (approx.)	Rate of collection of distillate	Results plotted in figure	API-Standard	API-NBS
Paraffins													
		liters	mole %			% by volume				ml/hour		ml	ml
2,2-Dimethylpropane (Neopentane)	Univ. Oil Prod.	2.00		Reg.			1	150	150/1	2.0	1	475	
2,2-Dimethylpropane (Neopentane)	Calif. Res. Corp.	0.98		Reg.			1	150	150/1	2.0	2	[g]500	250
2,2,3-Trimethylbutane (B)	General Motors	0.40	99.60±0.05				h				3		260
2,2,4-Trimethylpentane (B)	APIRP6 [i]	0.30	99.83±0.05				h				4		180
2,2,3-Trimethylpentane	Penn State	2.71		Reg.			12	135	165/1	4.5	5		
		1.81		Azeo.	Cell.	66	3A	200	160/1	4.5	6	990	366
2,2,4-Trimethylpentane	Penn State	3.00		Azeo.	Cell.	72	13	150	155/1	8.0	7		
		2.44		Reg.			12	135	165/1	4.5	8		
		1.83		Azeo.	Cell.	71	15A	200	160/1	4.5	9	985	195
2,3,3-Trimethylpentane	Penn State	2.24		Reg.			12	135	165/1	4.5	10		
		1.61		Azeo.	Cell.	60	4	200	160/1	4.5	11	785	156
2,3,5-Trimethylpentane	Penn State	2.12		Reg.			12	135	165/1	4.5	12		
		1.67		Azeo.	Me. Cell.	62	11A	200	160/1	4.5	13	1015	225
3,3,4-Trimethylpentane	Penn State	2.44		Reg.			12	135	165/1	4.5	14		
		1.54		Azeo.	Cell.	30	15A	200	160/1	4.5	15	1040	215
Cycloparaffins													
Ethylcyclobutane	APIRP45	2.48	93.62±0.06	Reg.			12	135	165/1	4.5	16		294
cis-1,3-Dimethylcyclopentane	APIRP45	[j]5.34		Reg.			4	200	160/1	4.5	17		
		[k]5.49		Reg.			15A	200	160/1	4.5	18		
		2.61	96.42±0.30	Azeo.	Ethanol	62	4	200	160/1	4.5	19		
		1.66	98.72±0.27	Azeo.	Ethanol	60	2A	200	160/1	4.5	20	585	160
trans-1,3-Dimethylcyclopentane (B)	APIRP45	[j]5.34		Reg.			4	200	160/1	4.5	17		
		[z]5.88		Reg.			15A	200	160/1	4.5	21		
		2.67	92.5±0.4	Azeo.	Ethanol	63	3A	200	160/1	4.5	22		
		1.73	99.2±0.10	Azeo.	Ethanol	62	2A	200	160/1	4.5	23	[g]1050	270
cis,cis,cis-1,2,3-Trimethylcyclopentane	Penn State	1.24	98.90±0.10	Reg.			4	200	160/1	4.5	24		
		0.90	99.22±0.08	Azeo.	Me. Cell.	66	15A	200	160/1	4.5	25	460	100
cis,trans,cis-1,2,3-Trimethylcyclopentane	Penn State	0.14	98.48±0.12	Azeo.	Me. Cell.	76	1A	150	150/1	2.0	26		
		0.06	99.79±0.04	[m] Azeo.	Me. Cell.	77	4	200	160/1	4.5	27	175	50
		[m]0.29	99.88±0.04										
n-Butylcyclopentane	APIRP45	6.05	99.85±0.03	Reg.			14	125	125/1	12.5	28		
		1.90	99.92±0.03	Azeo.	Cell.	40	11A	200	160/1	4.5	29	1158	345

[a] See footnote a of table 2.

[b] The abbreviations represent the following laboratories: APIRP45; American Petroleum Institute Research Project 45 at the Ohio State University, Columbus, Ohio. Penn State; Hydrocarbon Laboratory at the Pennsylvania State College, State College, Pa. NACA; National Advisory Committee for Aeronautics, Flight Propulsion Research Laboratory, Cleveland, Ohio. General Motors; General Motors Corporation, Detroit, Mich. NBS Auto Sec.; Automotive Section, National Bureau of Standards, Washington, D. C. Calif. Res. Corp.; California Research Corporation, Richmond, Calif. Phillips; Phillips Petroleum Company, Bartlesville, Okla. Univ. Oil Prod.; Universal Oil Products Co., Riverside, Ill. APIRP6; American Petroleum Institute Research Project 6 at the National Bureau of Standards, Washington, D. C.

[c] The abbreviations are: Azeo , azeotropic; Reg., regular.

[d] The abbreviations are: Cell., Cellosolve (ethylene glycol monoethyl ether); Me. Cell., methyl Cellosolve (ethylene glycol monomethyl ether); Me. Carb., methyl Carbitol (diethylene glycol monomethyl ether).

[e] Approximate value obtained from the actual volume of hydrocarbon recovered by extracting the azeotrope—forming substance with water in separatory funnels.

[f] See reference [5] for further details.

[g] This is a second and improved API-Standard sample of this hydrocarbon.

[h] This material was given its final purification by B. J. Mair by the method of adsorption. See references [6, 7].

[i] Obtained by purchase of commercially available material from the Rohm & Haas Co., Philadelphia, Pa.

[j] One of two similar charges. Both *cis* and *trans* -1,3-dimethylcyclopentane were obtained from this material (see fig. 17).

[k] This charge consisted of material having substantially the same composition, from each of the two previous distillations (see footnote j), together with material from the first distillation of the concentrate of the *trans* isomer (see footnote z and fig. 21).

[l] This charge consisted of material having substantially the same composition from each of the two previous distillations (see footnote j).

[m] This is a second lot of *cis, trans, cis*-1,2,3-trimethylcyclopentane supplied by the Pennsylvania State College.

[n] This material was divided into seven charges for purification by adsorption (see footnote h and fig. 31).

[o] This is a second lot of 1,3-diethylbenzene supplied by the API Research Project 45.

TABLE 1—Continued

Compound [a]	Laboratory [b] providing starting material	Hydrocarbon charged for distillation: Volume	Hydrocarbon charged for distillation: Purity	Distillation [f]: Kind [c]	Distillation [f]: Azeotrope-forming substance [d]	Distillation [f]: Amount of hydrocarbon in the azeotropic distillate [e]	Distillation [f]: Distilling column number [f]	Distillation [f]: Number of theoretical plates [f] (approx.)	Distillation [f]: Reflux ratio [f] (approx.)	Distillation [f]: Rate of collection of distillate	Distillation [f]: Results plotted in figure	Volume of selected sample: API-Standard	Volume of selected sample: API-NBS
Aromatics													
		liters	mole %			% by volume				ml/hour		ml.	ml.
1,2-Diethylbenzene	NACA	3.60	97.6±0.06	Reg.			4	200	160/1	4.5	30		
		[n]3.29					h				31	750	170
1,3-Diethylbenzene (B)	NACA	2.40	98.7±0.10	Azeo.	Me. Carb.	73	8	130	145/1	8.5	32		
		1.08	99.15±0.08	Reg.			12	135	165/1	4.5	33	1080	175
	API-RP45	[o]0.93	99.15±0.08										
1,4-Diethylbenzene	NACA	3.56	99.40±0.05	Reg.			9	135	165/1	4.5	34		
		1.88		Azeo.	Me. Carb.	66	11A	200	160/1	4.5	35		
		[p]2.42					h				36	1110	245
Olefins													
1-Pentene (B)	Phillips	4.65		Reg.			3A	200	160/1	4.5	37	[q]1240	470
1-Hexene	API-RP45	3.19	98.4±0.2	Reg.			9	135	165/1	4.5	38		
		1.81	99.80±0.08	Reg.			4	200	160/1	4.5	39	[r]695	545
	API-RP6 [g]	6.13	80.6±0.5	Reg.			13	130	155/1	8.0	40		
		3.16	99.44±0.12	Azeo.	Ethanol	77	9	135	165/1	4.5	41	[r]780	
trans-2-Hexene	API-RP45	[s]3.45	97.5±0.2	Reg.			11A	200	160/1	4.5	42		
		[t]2.44	99.8±0.11	Reg.			2A	200	160/1	4.5	43	1030	350
trans-3-Hexene	API-RP45	6.50	98.7±0.1	Reg.			13	130	155/1	8.0	44		
		1.71	99.67±0.03	Reg.			11A	200	160/1	4.5	45	1020	200
3-Methyl-1-pentene	API-RP45	[u]5.00		Reg.			9	135	165/1	4.5	46		
		[v]2.44		Reg.			11A	200	160/1	4.5	47	1000	175
2-Methyl-2-pentene	API-RP45	3.13	99.80±0.03	Reg.			4	200	160/1	4.5	48	1120	335
3-Methyl-cis-2-pentene	General Motors	[w]6.00		Reg.			8	130	145/1	8.5	49		
		[x]3.80		Reg.			2A	200	160/1	4.5	50		
		2.16	99.62±0.08	Azeo.	Ethanol	76	12A	200	160/1	4.5	51	1045	250
2-Ethyl-1-butene	API-RP45	2.85	97.2±0.2	Reg.			12	135	165/1	4.5	52		
		1.77	99.4±0.06	Azeo.	Ethanol	78	3A	200	160/1	4.5	53	[aa]620	[bb]140
	API-RP6 [g]	6.47	70. ± 5.	Reg.			10	135	165/1	4.5	54		
		1.59	99.32± 0.06	Azeo.	Ethanol	79	4	200	160/1	4.5	55	[aa]515	[bb]140
1-Heptene	API-RP45	2.89	97.8±0.3	Reg.			12	135	165/1	4.5	56		
		1.96	99.47±0.10	Reg.			4	200	160/1	4.5	57	925	220
2,4,4-Trimethyl-1-pentene	NBS Auto Sec.	[cc]6.00		Reg.			14	125	125/1	12.5	58		
		[dd]6.04	99.24±0.08	Reg.			13	130	155/1	8.0	59		
		2.80	99.67±0.06	Azeo.	Me. Cel.	79	15A	200	160/1	4.5	60	1160	350
2,4,4-Trimethyl-2-pentene	NBS Auto Sec.	[cc]6.00		Reg.			14	125	125/1	12.5	58		
		[dd]4.54		Reg.			10	135	165/1	4.5	61		
		2.73		Azeo.	Ethanol	50	11A	200	160/1	4.5	62	1140	320
Cyclohexene	API-RP6 [y]	6.20	99.13±0.06	Reg.			10	135	165/1	4.5	63	2250	735
Acetylenes													
1-Butyne	API-RP45	2.95		Reg.			1	150	150/1	2.0	64	1125	265

[a] This material was divided into five charges for purification by adsorption (see footnote h and fig. 36). It consisted of 0.80 l. from the first distillation in column 9 (see fig. 34) and 1.62 l. from the second distillation in column 11A (see fig. 35).

[b] Obtained by purchase of commercially available material from the Connecticut Hard Rubber Co., New Haven, Conn.

[c] The total volume of the API-Standard sample was 1,475 ml.

[d] One of two similar charges.

[e] This charge consisted of material having substantially the same composition, from each of the two previous distillations (see footnote s).

[f] One of two charges of similar material, one of which was 5.00 l. and the other 2.80 l.

[g] This charge consisted of material, having substantially the same composition, from each of the two previous distillations (see footnote u).

[h] One of three charges of similar material, two of which were 6.00 l. each, and the third of which was 5.30 l.

[i] This charge consisted of material, having substantially the same composition, from each of the three previous distillations (see footnote w).

[j] Obtained by purchase of commercially available material from the Eastman Kodak Co., Rochester, N. Y.

[aa] The total volume of the API-Standard sample was 1,135 ml.

[bb] The total volume of the API-NBS sample was 280 ml.

[cc] One of four similar charges. Both 2,4,4-trimethyl-1-pentene and 2,4,4-trimethyl-2-pentene were obtained from this material (see fig. 58).

[dd] This charge consisted of material, having substantially the same composition, from each of the four previous distillations (see footnote cc).

By the National Advisory Committee for Aeronautics, through its Flight Propulsion Research Laboratory at Cleveland, Ohio:

1,2-Diethylbenzene.
1,3-Diethylbenzene (B) (two-thirds).
1,4-Diethylbenzene.

By the General Motors Corporation Research Laboratories, Detroit, Mich., through T. A. Boyd and W. G. Lovell:

2,2,3-Trimethylbutane (B).
3-Methyl-*cis*-2-pentene.

By the Hydrocarbons Research Laboratory, Automotive Section, National Bureau of Standards, through F. L. Howard and D. B. Brooks:

"Diisobutylene" (2,4,4-Trimethyl-1-pentene+ 2,4,4-Trimethyl-2-pentene)

By the California Research Corporation, Richmond, Calif., through A. Kremser:

2,2-Dimethylpropane (Neopentane).

By the Phillips Petroleum Co., Bartlesville, Okla., through F. E. Frey:

1-Pentene (B).

By the Universal Oil Products Co., Riverside, Ill., through V. Haensel:

2,2-Dimethylpropane (Neopentane)

By the API Research Project 6 at the National Bureau of Standards, by purchase:

2,2,4-Trimethylpentane (B).	2-Ethyl-1-butene (one-half).
1-Hexene (one-half).	Cyclohexene.

Table 1 summarizes the amounts of the starting materials and gives some additional information as to source and purity.

[1] See footnote 4.

III. Purification

The procedure followed in the process of purification and determination of purity was the same as that described in the previous reports [2, 3, 4], except that in the purification of 2,2,3-trimethylbutane, 2,2,4-trimethylpentane, 1,2-diethylbenzene, and 1,4-diethylbenzene, use was made of the process of adsorption.

In addition to the name of the laboratory supplying the starting materials, table 1 and its footnotes give complete information for each distillation for each of the compounds.

Details of the distillation apparatus and operations are described in reference [5], and details of the adsorption apparatus and operations are given in references [6] and [7].

Figures 1 to 64, inclusive, show graphically the results of the distillation and adsorption operations listed in table 1. These figures give, as appropriate, as a function of volume of hydrocarbon in the distillate or filtrate, the refractive index (n_d at 25° C, to ± 0.0001), the boiling point of the distillate (at the controlled pressure of 724.5 mm Hg, to ± 0.01 deg C), the freezing point of selected fractions of hydrocarbon distillate (in air at 1 atm, usually, with a precision near ± 0.003 deg C), and the purity of the hydrocarbon distillate. The letters *W*, *X*, *Y*, *Z*, indicate the disposition of the material as follows: *W*, returned to the laboratory suppling the material; *X*, blended for redistillation; *Y*, used for the API-Standard material; *Z*, used for the API-NBS material.

As demonstrated in the previous reports [2, 3, 4], the blending of fractions of distillate for the preparation of material of the highest purity can be done safely only on the basis of the freezing points of selected fractions. This is similarly true for the blending of fractions of filtrate from the adsorption process.

IV. Freezing Points, Cryoscopic Constants, and Purity

Table 2 gives the following information for each of the 30 compounds, except as otherwise indi-

Footnotes for table 2.

[a] (B) following the name of a compound indicates that for the API-NBS series, it is a second (and usually slightly purer) sample of the given compound, the first sample of which will be labeled (A).

[b] F indicates freezing, and M indicates melting. See reference [8] for experimental details and the definition of the cryoscopic constant.

[c] The values in this column, except as otherwise indicated, were calculated as described in reference [8], using the values of the cryoscopic constants and freezing points for zero impurity given in the preceding columns.

[d] Not determined in this investigation. From the x tables of the American Petroleum Institute Research Project 44, [9].

[e] This is a second and improved API-Standard sample of this hydrocarbon.

[f] Estimated by analogy with isomers subjected to similar purification.

[g] This cryoscopic constant was determined by the procedure given on page 371 of reference [8].

TABLE 2. *Freezing points and purity of 30 API–Standard and API–NBS hydrocarbons*

Compound[a]	Kind of time-temperature observations used to determine the freezing point[b]	Freezing point of the actual selected sample in air at 1 atm.		Freezing point for zero impurity in air at 1 atm.	Cryoscopic constant[b] A	Calculated amount of impurity in the actual selected sample[c]	
		API–Standard	API–NBS			API–Standard	API–NBS
Paraffins							
		°C	°C	°C	deg^{-1}	mole %	mole %
2,2-Dimethylpropane (Neopentane)	F	-16.65	—	-16.550 ± 0.020	[d](0.00595)	0.06±0.02	—
2,2-Dimethylpropane (Neopentane)	F	-16.587	-16.580	-16.550 ± 0.020	[d](0.00595)	[e]0.022±0.012	0.018±0.012
2,2,3-Trimethylbutane (B)	F	-	-24.950	-24.930 ± 0.020	[d](0.00430)	—	[f]0.09±0.08
2,2,4-Trimethylpentane (B)	M	-	-107.393	-107.365±0.013	[d](0.0403)	—	0.11±0.05
2,2,5-Trimethylhexane	-	-	-	—	—	[f](0.30±0.20)	[f](0.25±0.20)
2,2,4-Trimethylhexane	M	-	-	-120.0±0.3	0.06	0.30±0.20	0.25±0.20
2,3,3-Trimethylhexane	M	-116.829	-116.815	-116.800±0.020	0.0447	0.13±0.06	0.07±0.06
2,3,5-Trimethylhexane	—	—	—	—	—	[f](0.30±0.20)	[f](0.25±0.20)
3,3,4-Trimethylhexane	M	-101.27	-101.24	-101.20±0.03	0.033	0.23±0.10	0.15±0.10
Cycloparaffins							
Ethylcyclobutane	M	-	-142.770	-142.750±0.015	0.0378	—	0.08±0.06
cis-1,3-Dimethylcyclopentane	M	-134.04	-133.980	-133.90±0.05	0.0461	0.65±0.23	0.41±0.23
trans-1,3-Dimethylcyclopentane (B)	M	-133.714	-133.706	-133.690±0.015	[d](0.04596)	[e]0.11±0.07	0.07±0.06
cis, cis, cis-1,2,3-Trimethylcyclopentane	F and M	-116.471	-116.458	-116.430±0.025	0.0245	0.10±0.06	0.07±0.06
cis, trans, cis-1,2,3-Trimethylcyclopentane	M	-112.736	-112.727	-112.705± 0.012	0.0365	0.11±0.04	0.08±0.04
n-Butylcyclopentane	M	-107.393	-107.392	-107.385±0.010	0.0424	0.034±0.025	0.030±0.025
Aromatics							
1,2-Diethylbenzene	F	-31.257	-31.250	-31.240±0.010	0.0299	0.05±0.03	0.03±0.03
1,3-Diethylbenzene (B)	M	-83.938	-83.933	-83.920±0.010	0.0369	0.07±0.04	0.05±0.04
1,4-Diethylbenzene	F	-42.878	-42.860	-42.850±0.010	0.0240	0.07±0.07	0.023±0.020
Olefins							
1-Pentene (B)	M	-165.264	-165.250	-165.220±0.020	[d](0.06000)	[e]0.26±0.12	0.18±0.12
1-Hexene	M	-139.826	-139.826	-139.800±0.015	0.0509	0.14±0.08	0.13±0.08
trans-2-Hexene	M	-133.001	-132.998	-132.970±0.020	0.0564	0.17±0.11	0.16±0.11
trans-3-Hexene	F and M	-113.441	-113.439	-113.430±0.015	0.055	0.06±0.03	0.05±0.03
3-Methyl-1-pentene	F and M	-153.1	-153.1	-153.0±0.1	[g]0.03	0.30±0.20	0.25±0.20
2-Methyl-2-pentene	F and M	-135.088	-135.078	-135.070±0.015	0.0508	0.09±0.05	0.04±0.03
3-Methyl-cis-2-pentene	M	-138.474	-138.466	-138.445±0.015	0.0509	0.15±0.08	0.11±0.08
2-Ethyl-1-butene	F and M	-131.551	-131.540	-131.530±0.010	0.0454	0.10±0.04	0.08±0.04
1-Heptene	M	-119.075	-119.067	-119.035±0.020	0.0509	0.20±0.10	0.16±0.10
2,4,4-Trimethyl-1-pentene	F and M	-93.508	-93.496	-93.480±0.010	[d](0.0330)	0.09±0.03	0.05±0.03
2,4,4-Trimethyl-2-pentene	F and M	-106.356	-106.353	-106.330±0.015	[d](0.0300)	0.08±0.05	0.07±0.05
Cyclohexene	M	-103.517	-103.516	-103.500±0.015	[d](0.01376)	0.025±0.020	0.022±0.020
Acetylenes							
1-Butyne (Ethylacetylene)	F and M	-125.756	-125.749	-125.720±0.020	[g]0.035	0.13±0.07	0.10±0.07

cated: the kind of time-temperature curves, whether freezing or melting, used to determine the freezing point [8]; the freezing point of the actual sample, in air at 1 atm [8], for both the API-Standard and API-NBS lots; the calculated value of the freezing point for zero impurity [8]; the value of the cryoscopic constant, determined from the lowering of the freezing point on the addition of a known amount of an appropriate impurity [8]; and the resulting calculated amount of impurity in the API-Standard and the API-NBS materials.

Grateful acknowledgment is made to the other organizations and individuals listed in section II of this report for their contributions of materials for use in this work.

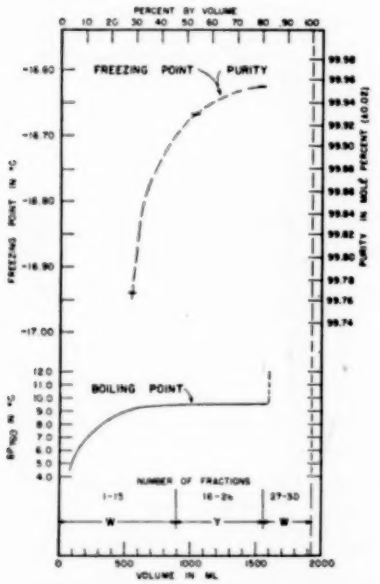

FIGURE 1. *Results of the first and only distillation of the first lot of 2,2-dimethylpropane (neopentane).*

This material had not been fractionated by the supplier. Regular distillation at atmospheric pressure in Still 1 (5/2/45 to 5/25/45).

V. References

[1] NBS Tech. News Bul., No. 350 (June, 1946).
[2] A. J. Streiff, E. T. Murphy, V. A. Sedlak, C. B. Willingham, and F. D. Rossini, J. Research NBS **37,** 331 (1946) RP1752.
[3] A. J. Streiff, E. T. Murphy, J. C. Cahill, H. F. Flanagan, V. A. Sedlak, C. B. Willingham, and F. D. Rossini, J. Research NBS **38,** 53 (1947) RP1760.
[4] A. J. Streiff, E. T. Murphy, J. C. Zimmerman, L. F. Soule, V. A. Sedlak, C. B. Willingham, and F. D. Rossini, J. Research NBS **39,** 321 (1947) RP1833.
[5] C. B. Willingham and F. D. Rossini, J. Research NBS **37,** 15 (1946) RP1724.
[6] B. J. Mair, A. L. Gaboriault, and F. D. Rossini, Ind. Eng. Chem. **39,** 1072 (1947).
[7] Purification of five hydrocarbons by adsorption. API Research Project 6. National Bureau of Standards. A. J. Streiff, B. J. Mair, and F. D. Rossini. Unpublished.
[8] A. R. Glasgow, Jr., A. J. Streiff, and F. D. Rossini, J. Research NBS **35,** 355 (1945) RP1676.
[9] American Petroleum Institute Research Project 44 at the National Bureau of Standards. Selected values of properties of hydrocarbons. Tables 1z, 2z, 3z, 5z, 6z, 7z, and 8z.

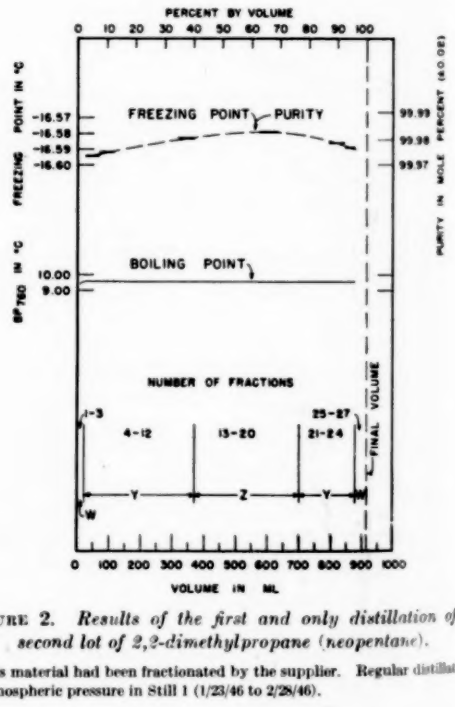

FIGURE 2. *Results of the first and only distillation of a second lot of 2,2-dimethylpropane (neopentane).*

This material had been fractionated by the supplier. Regular distillation at atmospheric pressure in Still 1 (1/23/46 to 2/28/46).

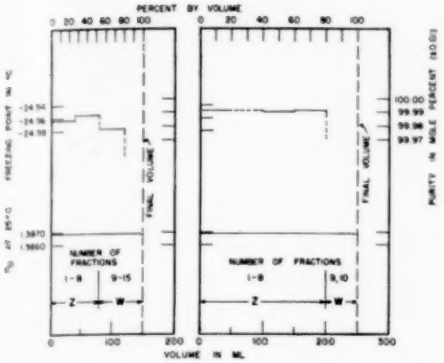

FIGURE 3. *Results of the purification by adsorption of 2,2,3-trimethylbutane.*

Adsorption in Column 10 (4/16/47); column 10 (5/8/47).

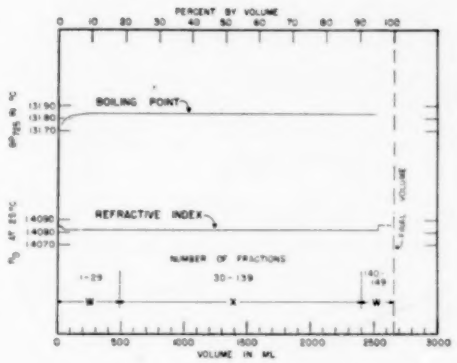

FIGURE 5. *Results of the first distillation of 2,2,3-trimethylhexane.*

Regular distillation at 725 mm Hg in Still 12 (10/7/46 to 11/1/46).

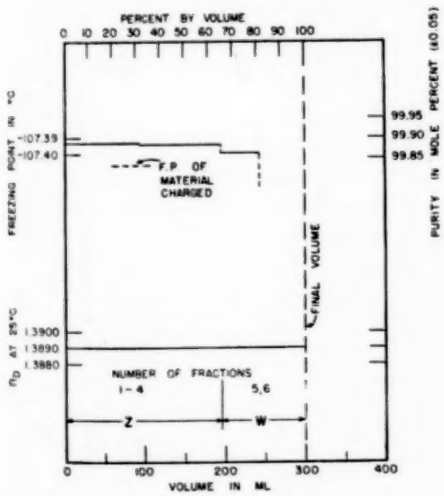

FIGURE 4. *Results of the purification by adsorption of 2,2,4-trimethylpentane.*

Adsorption in Column 10 (4/8/47).

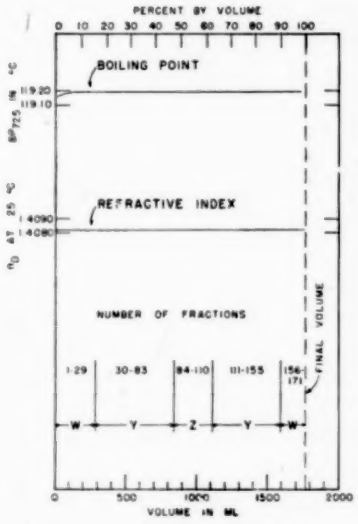

FIGURE 6. *Results of the second and final distillation of 2,2,3-trimethylhexane.*

Azeotropic distillation with ethylene glycol monoethyl ether at 725 mm Hg in Still 3A (7/24/47 to 8/25/47).

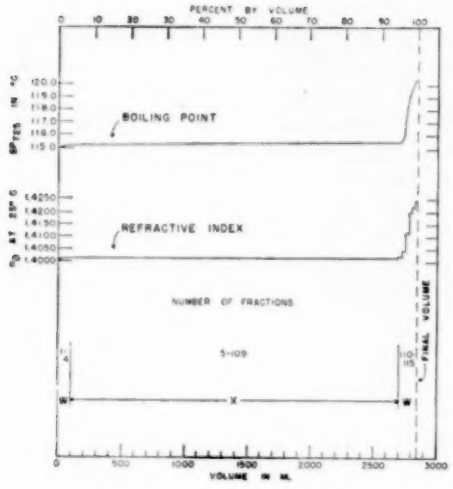

FIGURE 7. *Results of the first distillation of 2,2,4-trimethylhexane.*

Azeotropic distillation with ethylene glycol monoethyl ether at 725 mm Hg in Still 13 (10/21/44 to 11/15/44).

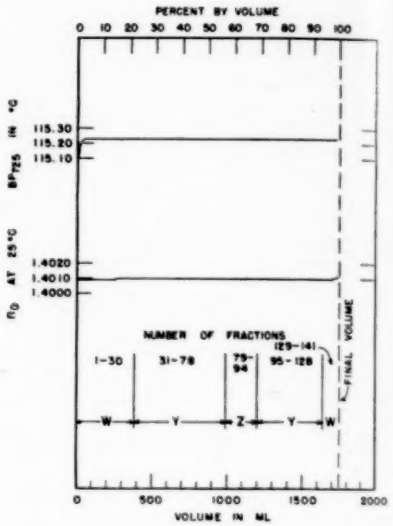

FIGURE 9. *Results of the third and final distillation of 2,2,4-trimethylhexane.*

Azeotropic distillation with ethylene glycol monoethyl ether at 725 mm Hg in Still 15A (1/8/47 to 2/3/47).

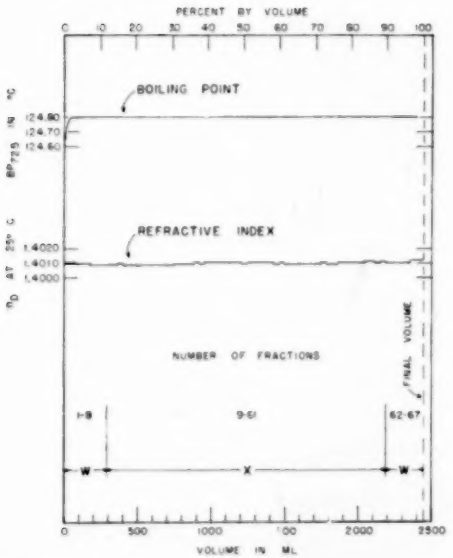

FIGURE 8. *Results of the second distillation of 2,2,4-trimethylhexane.*

Regular distillation at 725 mm Hg in Still 12 (9/5/45 to 9/29/45).

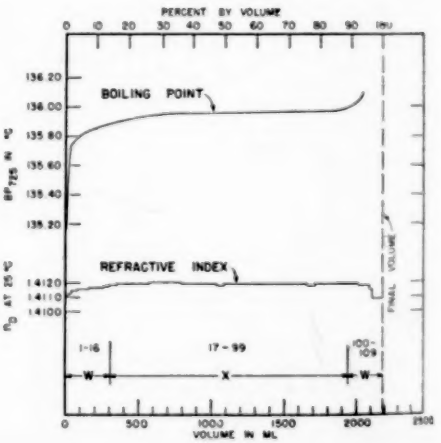

FIGURE 10. *Results of the first distillation of 2,3,3-trimethylhexane.*

Regular distillation at 725 mm Hg in Still 12 (8/21/46 to 9/11/46).

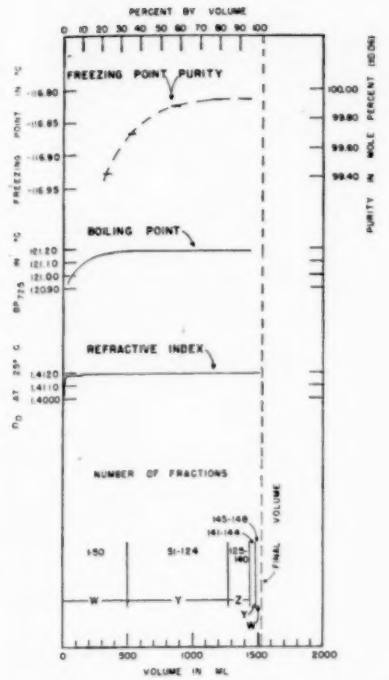

FIGURE 11. *Results of the second and final distillation of 2,3,3-trimethylhexane.*

Azeotropic distillation with ethylene glycol monoethyl ether at 725 mm Hg in Still 4 (12/27/46 to 1/22/47).

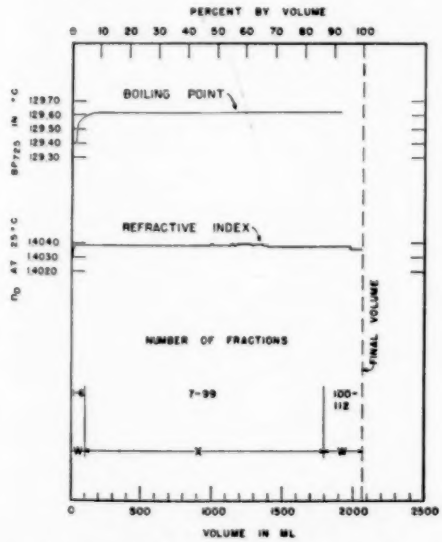
PERCENT BY VOLUME
0 10 20 30 40 50 60 70 80 90 100
BOILING POINT
REFRACTIVE INDEX
NUMBER OF FRACTIONS
FINAL VOLUME
VOLUME IN ML
0 500 1000 1500 2000 2500

FIGURE 12. *Results of the first distillation of 2,3,5-trimethylhexane.*

Regular distillation at 725 mm Hg in Still 12 (7/29/46 to 8/19/46).

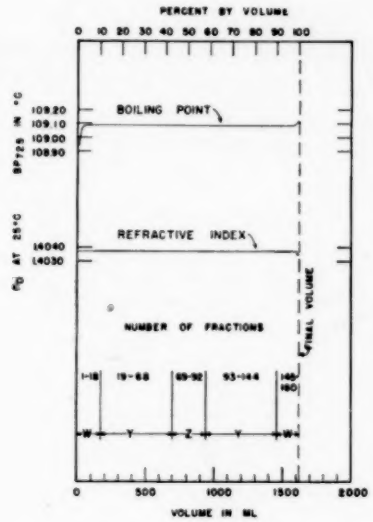

FIGURE 13. *Results of the second and final distillation of 2,3,5-trimethylhexane.*

Azeotropic distillation with ethylene glycol monomethyl ether at 725 mm Hg in Still 11A (10/24/46 to 11/24/46).

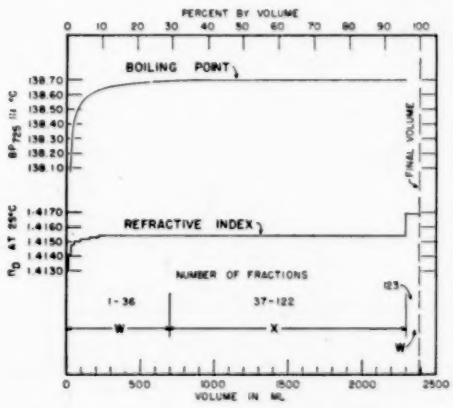
PERCENT BY VOLUME
0 10 20 30 40 50 60 70 80 90 100
BOILING POINT
REFRACTIVE INDEX
NUMBER OF FRACTIONS
FINAL VOLUME
VOLUME IN ML
0 500 1000 1500 2000 2500

FIGURE 14. *Results of the first distillation of 3,3,4-trimethylhexane.*

Regular distillation at 725 mm Hg in Still 12 (9/12/46 to 10/4/46).

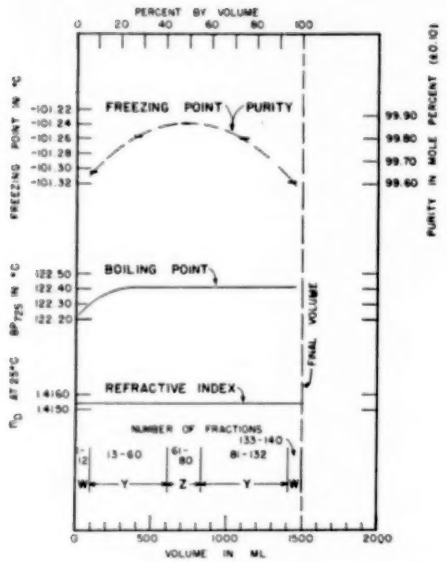

FIGURE 15. *Results of the second and final distillation of 3,3,4-trimethylhexane.*

Azeotropic distillation with ethylene glycol monoethyl ether at 725 mm Hg in Still 15A (8/19/47 to 9/8/47).

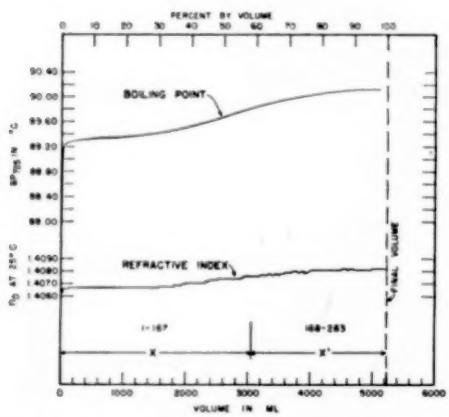

FIGURE 17. *Results of the first distillation of cis and trans-1,3-dimethylcyclopentane.*

Regular distillation at 725 mm Hg in Still 4 (10/1/46 to 11/20/46). One or two distillations of similar material. See footnote j of table 1. Fractions 2 to 167 (marked "x") were redistilled to obtain *trans*-1,3-dimethylcyclopentane (see fig. 21 and footnote z of table 1). Fractions 168 to 283 (marked "x'") were redistilled to obtain *cis*-1,3-dimethylcyclopentane (see fig. 18 and footnote k of table 1).

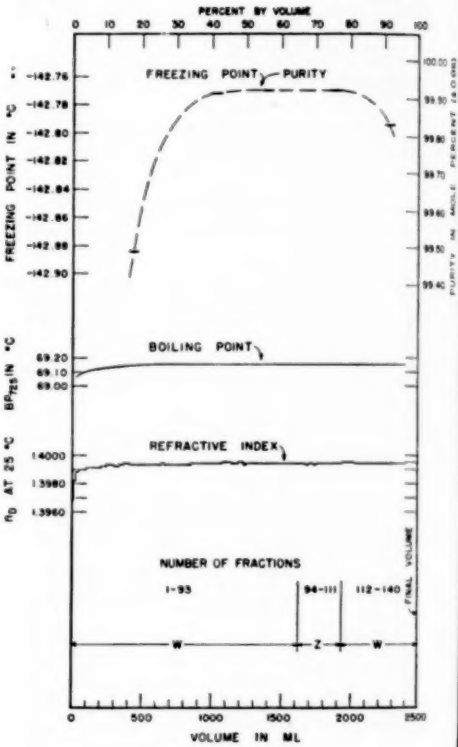

FIGURE 16. *Results of the first and only distillation of ethylcyclobutane.*

Regular distillation at 725 mm Hg in Still 12 (7/3/46 to 7/27/46).

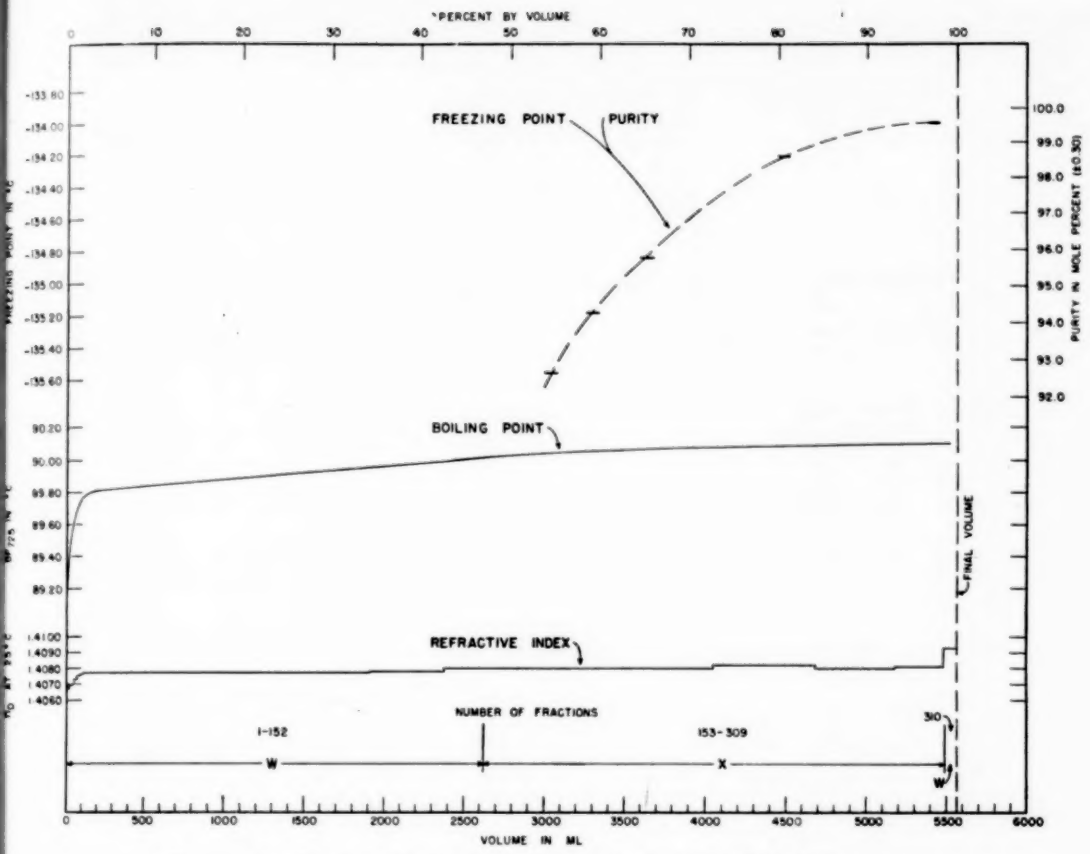

FIGURE 18. *Results of the second distillation of cis -1,3-dimethylcyclopentane.*
Regular distillation at 725 mm Hg in Still 15A (4/25/47 to 6/17/47). See footnote k of table 1.

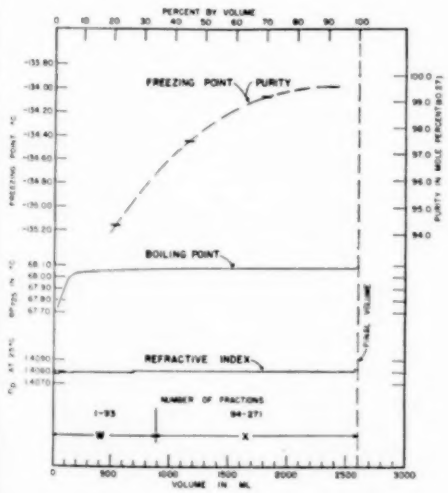

FIGURE 19. *Results of the third distillation of cis -1,3-dimethylcyclopentane.*

Azeotropic distillation with ethanol at 725 mm Hg in Still 4 (6/26/47 to 8/13/47).

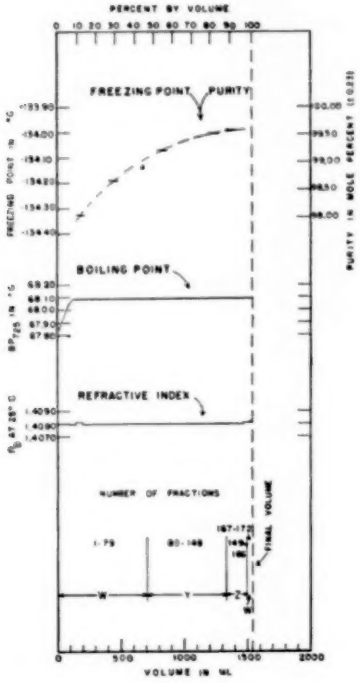

FIGURE 20. *Results of the fourth and final distillation of cis-1,3-dimethylcyclopentane.*

Azeotropic distillation with ethanol at 725 mm Hg in Still 2A (8/14/47 to 9/22/47).

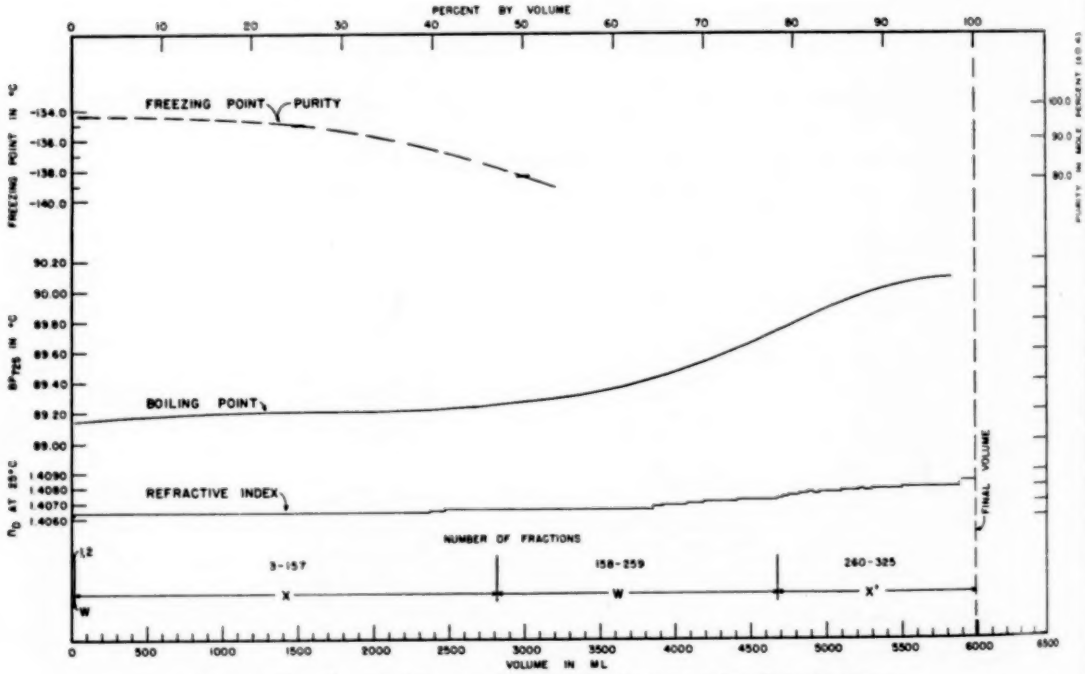

FIGURE 21. *Results of the second distillation of trans-1,3-dimethylcyclopentane.*

Regular distillation at 725 mm Hg in Still 15A (2/4/47 to 4/3/47). See footnote z of table 1. The part marked "x'" was used as part of the charge for the concentrate of *cis* isomer. (See footnote k of table 1, and fig. 18.)

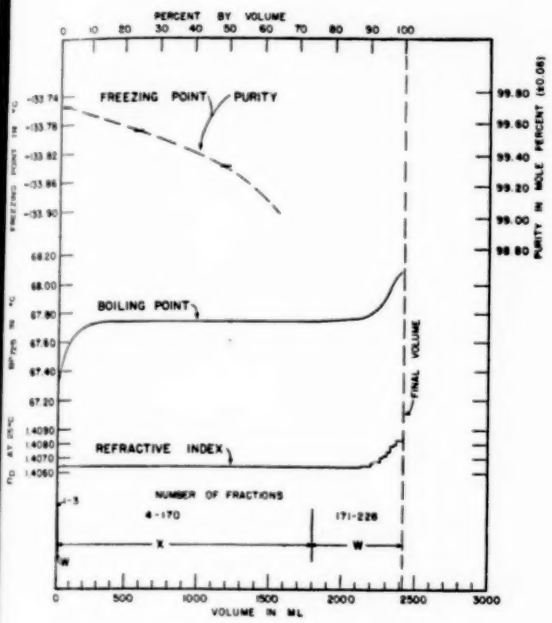

FIGURE 22. *Results of the third distillation of trans-1,3-dimethylcyclopentane.*

Azeotropic distillation with ethanol at 725 mm Hg in Still 3A (4/17/47 to 5/26/47).

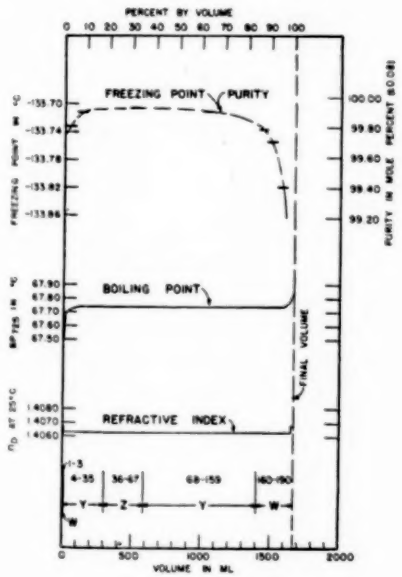

FIGURE 23. *Results of the fourth and final distillation of trans-1,3-dimethylcyclopentane.*

Azeotropic distillation with ethanol at 725 mm Hg in Still 2A (7/9/47 to 8/13/47).

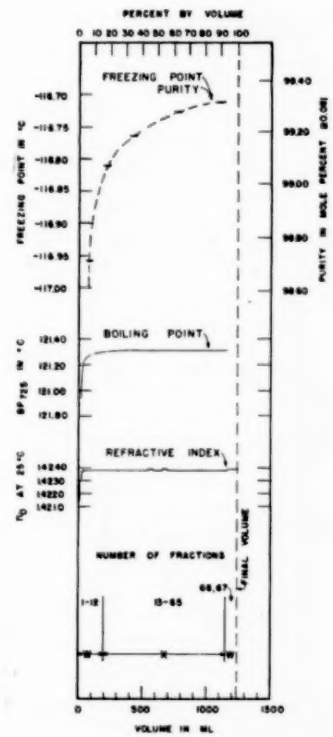

FIGURE 24. *Results of the first distillation of cis,cis,cis-1,2,3-trimethylcyclopentane.*

Regular distillation at 725 mm Hg in Still 4 (11/22/46 to 12/5/46).

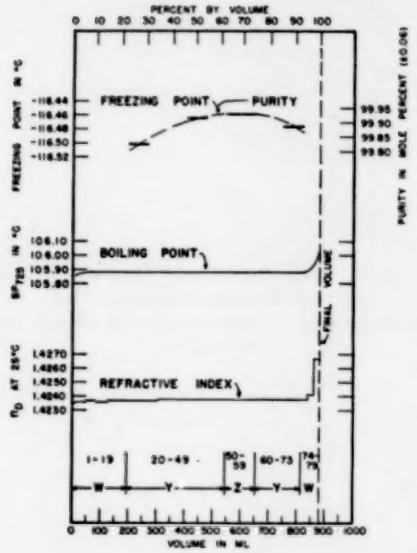

FIGURE 25. *Results of the second and final distillation of cis,cis,cis-1,2,3-trimethylcyclopentane.*

Azeotropic distillation with ethylene glycol monomethyl ether at 725 mm Hg in Still 15A (12/24/46 to 1/8/47).

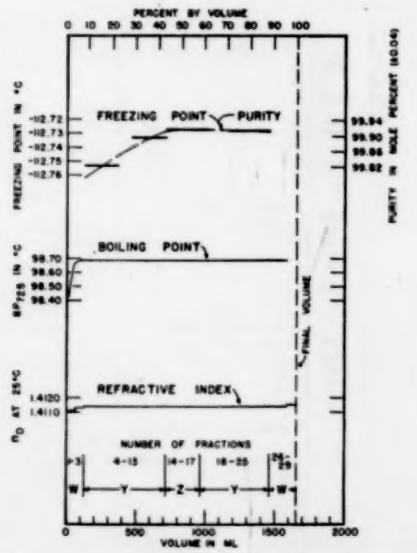

FIGURE 27. *Results of the second and final distillation of cis,trans,cis-1,2,3-trimethylcyclopentane.*

Azeotropic distillation with ethylene glycol monomethyl ether at 725 mm Hg in Still 4 (2/4/47 to 2/11/47). (See footnote m of table 1.)

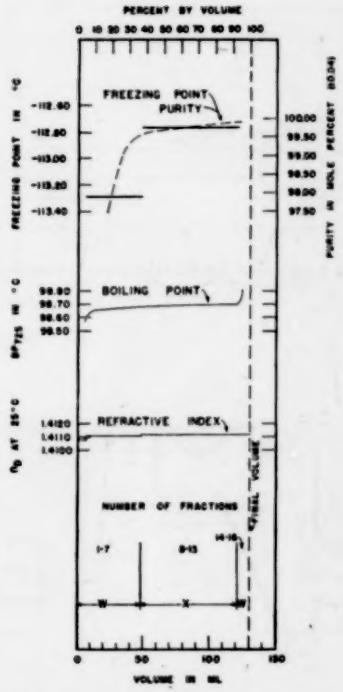

FIGURE 26. *Results of the first distillation of cis,trans, cis-1,2,3-trimethylcyclopentane.*

Azeotropic distillation with ethylene glycol monomethyl ether at 725 mm Hg in Still 1A (12/26/46 to 1/3/47).

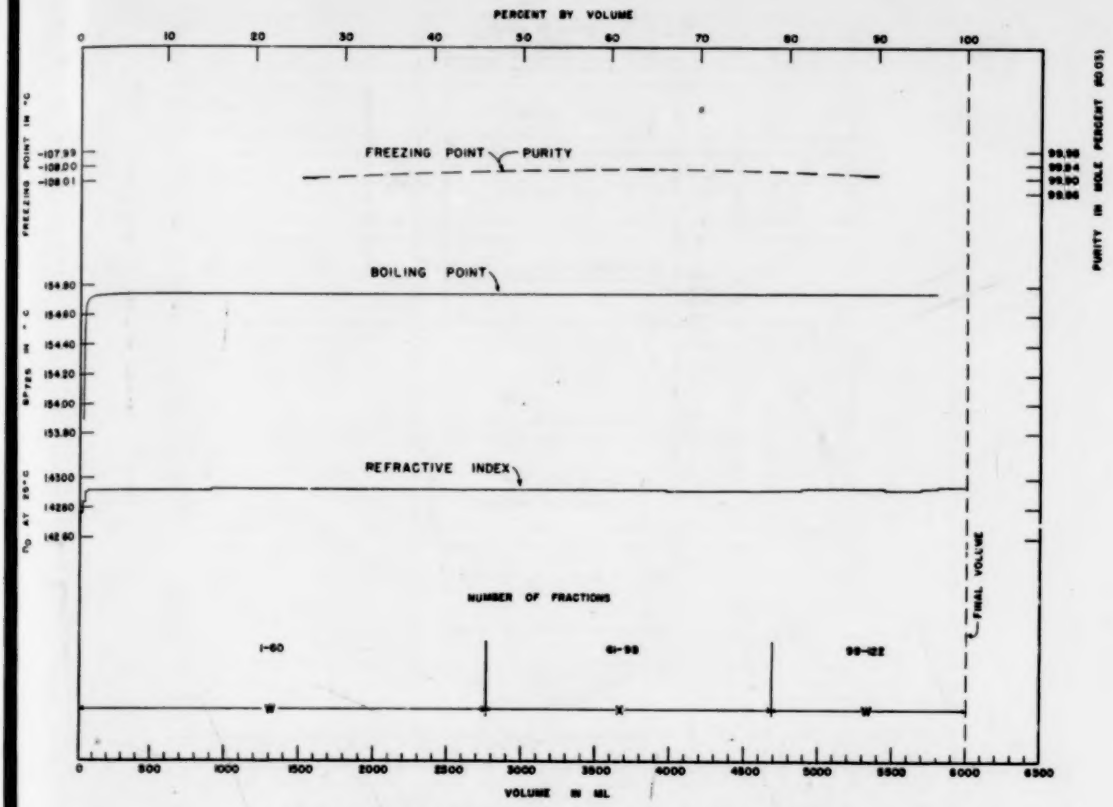

FIGURE 28. *Results of the first distillation of n-butylcyclopentane.*

Regular distillation at 725 mm Hg in Still 14 (12/16/46 to 1/7/47).

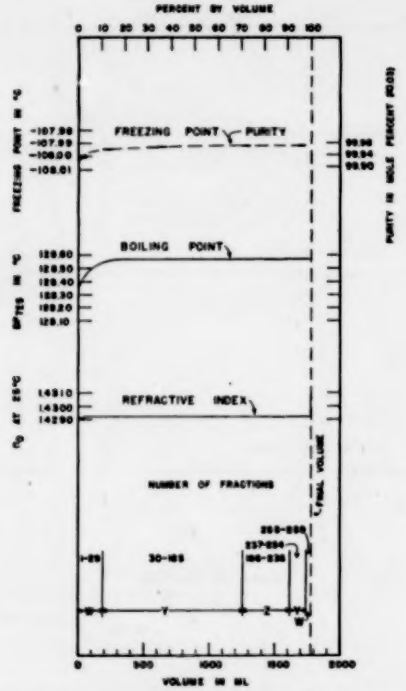

FIGURE 29. *Results of the second and final distillation of n-butylcyclopentane.*
Azeotropic distillation with ethylene glycol monoethyl ether at 725 mm Hg in Still 11A (2/25/47 to 4/14/47).

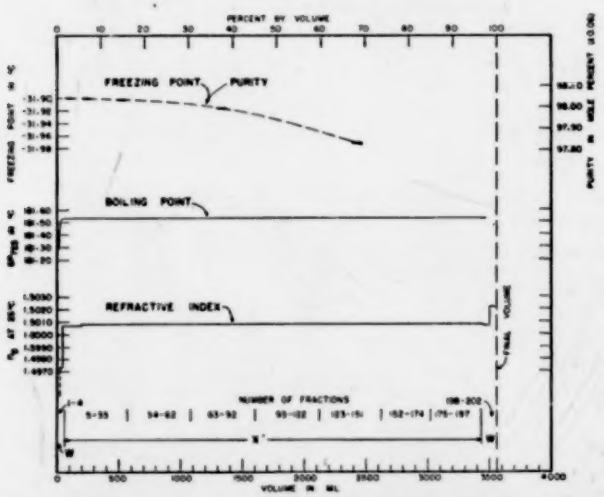

FIGURE 30. *Results of the first distillation of 1,2-diethylbenzene.*
Regular distillation at 725 mm Hg in Still 4 (4/2/47 to 5/8/47). The part of the distillate marked "X" received its final purification by adsorption. (See fig. 31 and footnote n of table 1.)

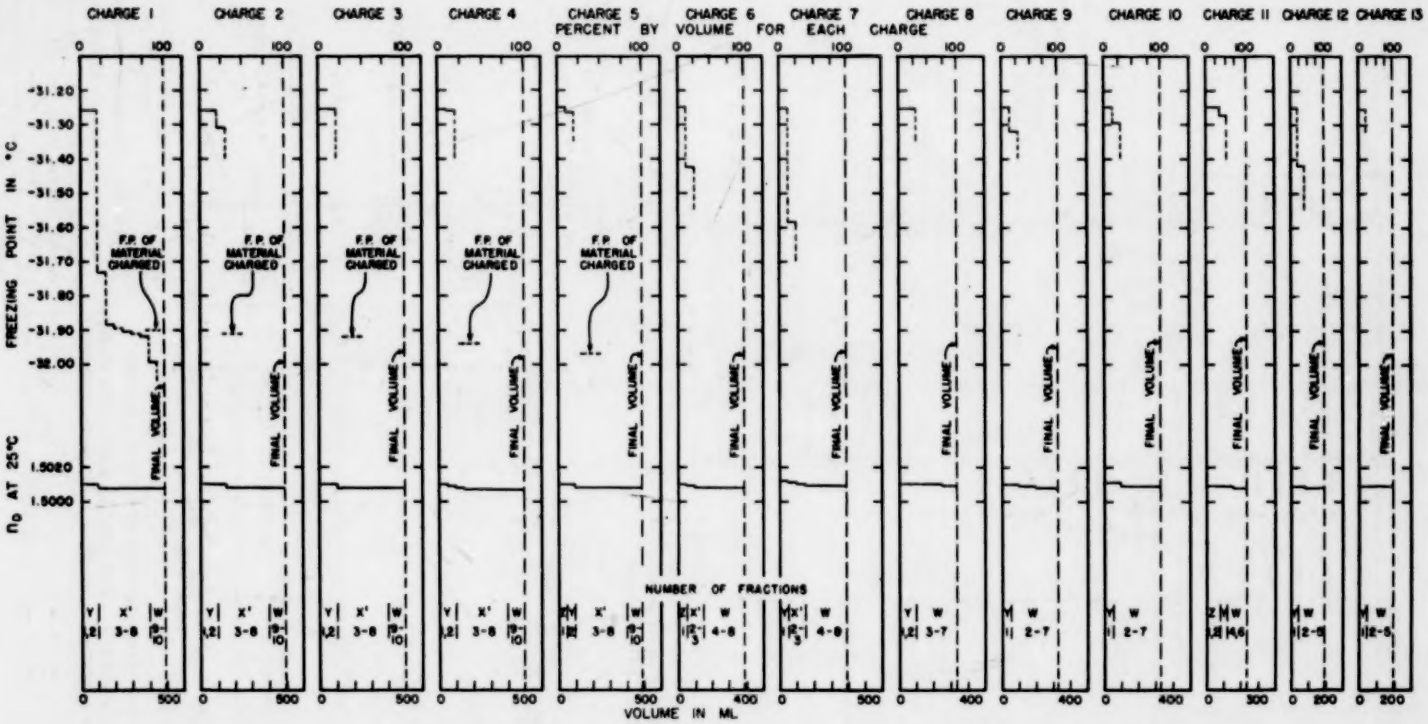

FIGURE 31. *Results of the final purification of 1,2-diethylbenzene by adsorption.*

See legend for figure 30 and footnote n of table 1. The part of the filtrate from each of the first 7 charges marked "X" was blended together for subsequent charges 8 to 13.

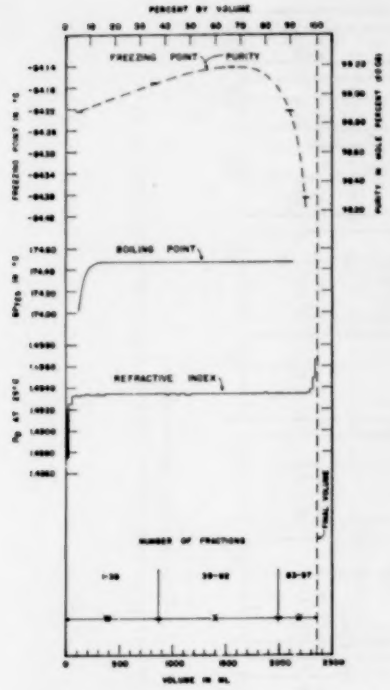

FIGURE 32. *Results of the first distillation of 1,3-diethyl-benzene.*

Azeotropic distillation with diethylene glycol monomethyl ether at 725 mm Hg in Still 8 (11/9/44 to 11/28/44).

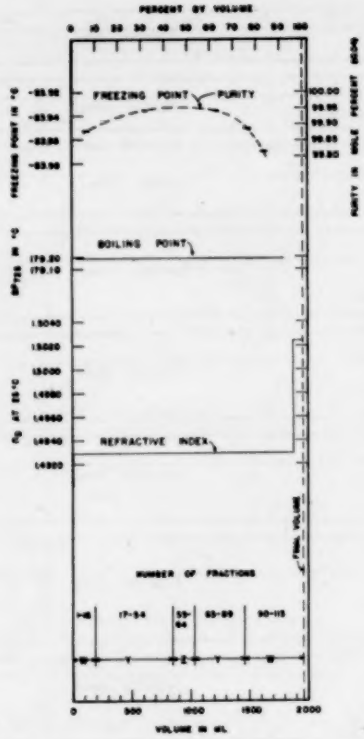

FIGURE 33. *Results of the second and final distillation of 1,3-diethylbenzene.*

Regular distillation at 725 mm Hg in Still 12 (10/26/45 to 11/16/45). See footnote a of table 1.

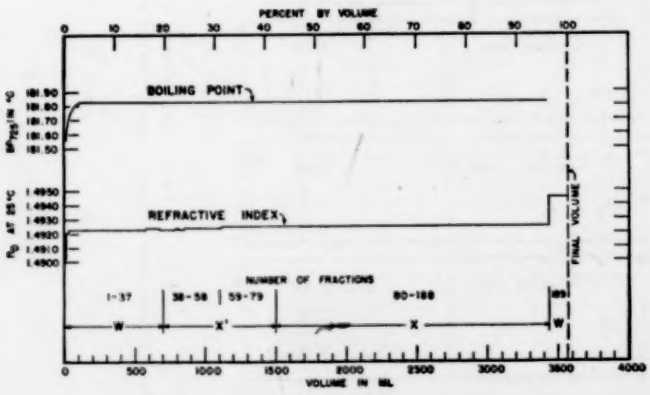

FIGURE 34. *Results of the first distillation of 1,4-diethylbenzene.*

Regular distillation at 725 mm Hg in Still 9 (1/6/47 to 2/10/47). The distillate marked "X'" was given its final purification by adsorption. (See results in columns 13 and 11 in fig. 36.)

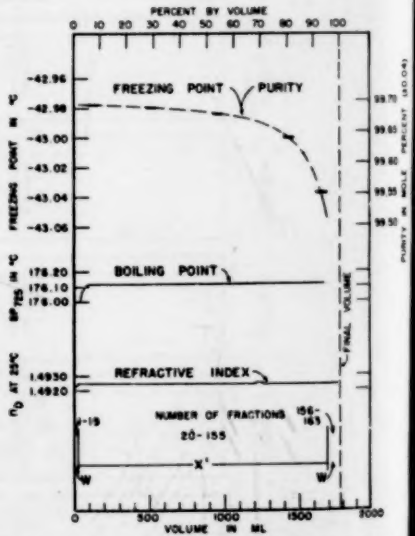

FIGURE 35. *Results of the second distillation of 1,4-diethylbenzene.*

Azeotropic distillation with diethylene glycol monomethyl ether at 725 mm Hg in Still 11A (4/17/47 to 5/19/47). The part of the distillate marked "X'" was blended and divided into three similar charges for final purification by adsorption. (See results in columns 1, 2, and 3 in fig. 36.)

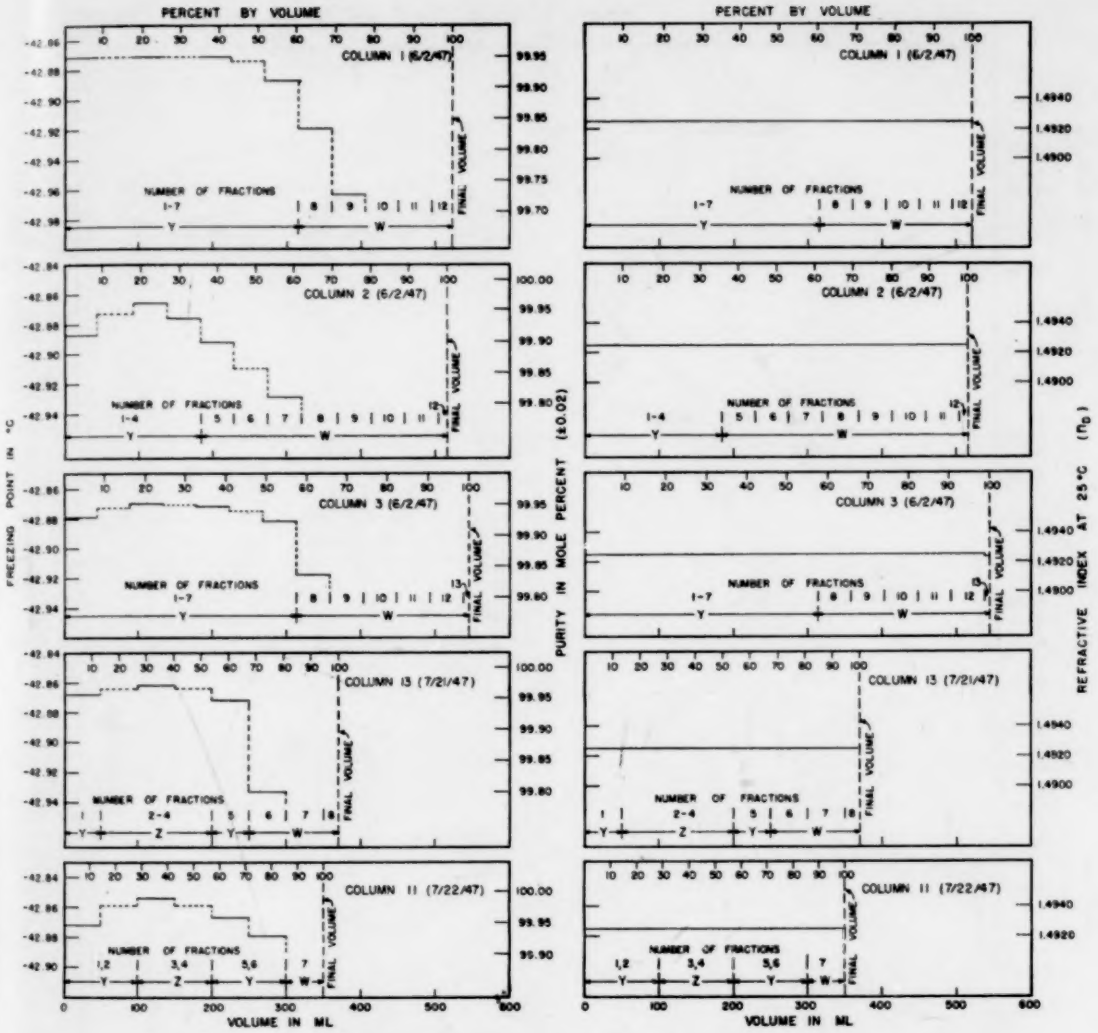

FIGURE 36. *Results of the final purification of 1,4-diethylbenzene by adsorption.*

See legends for figures 34 and 35 and footnote p of table 1.

803370—48——7

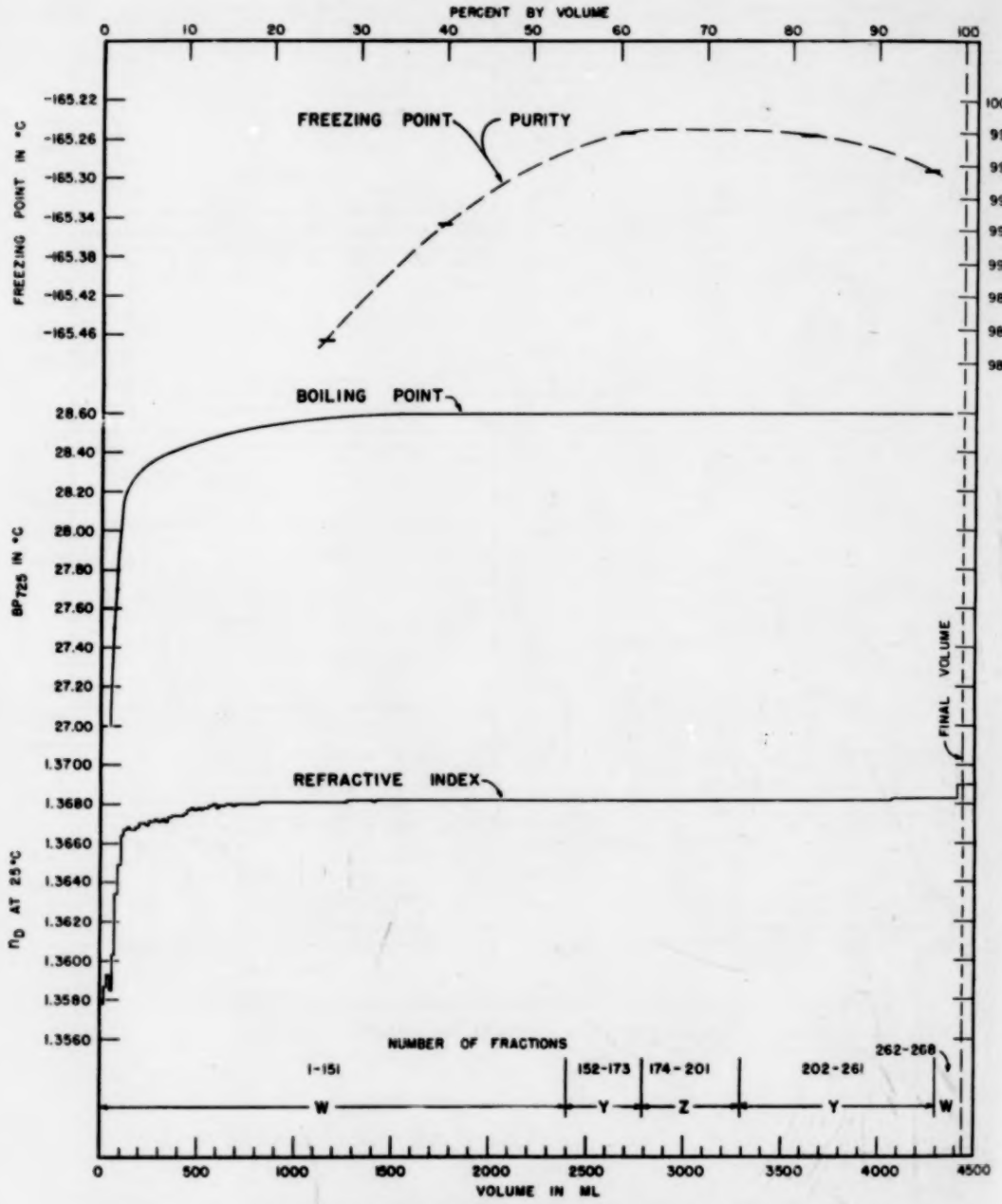

FIGURE 37. *Results of the first and only distillation of 1-pentene.*

Regular distillation at 725 mm Hg in Still 3A (1/21/47 to 3/24/47).

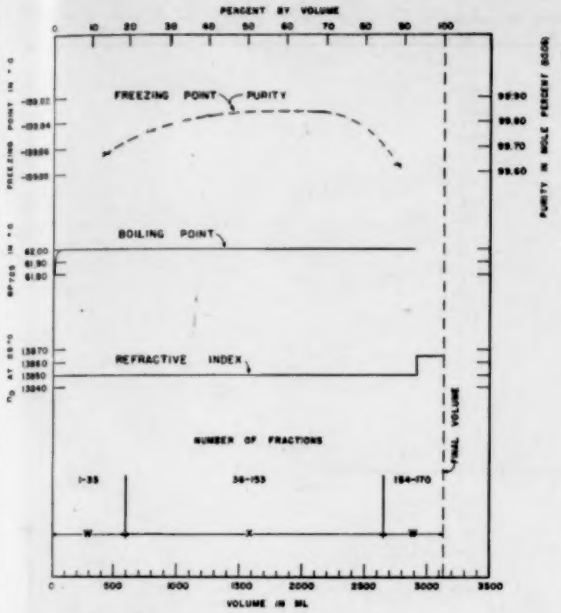

FIGURE 38. *Results of the first distillation of the first lot of 1-hexene.*

Regular distillation at 725 mm Hg in Still 9 (9/30/46 to 11/1/46).

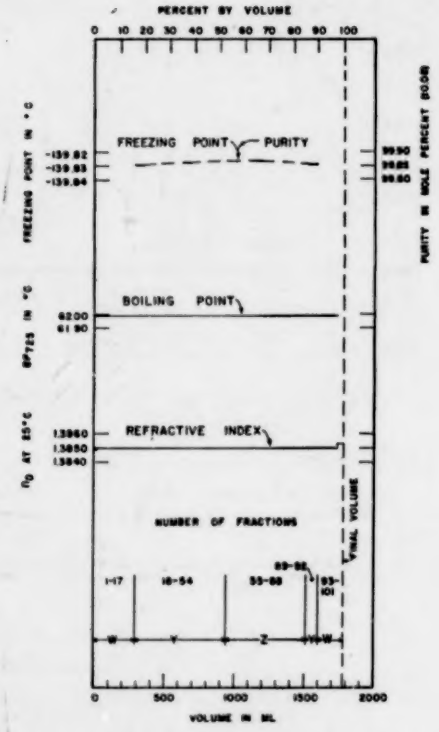

FIGURE 39. *Results of the second and final distillation of the first lot of 1-hexene.*

Regular distillation at 725 mm Hg in Still 4 (2/13/47 to 3/4/47). See footnote r of table 1.

803370—48——8

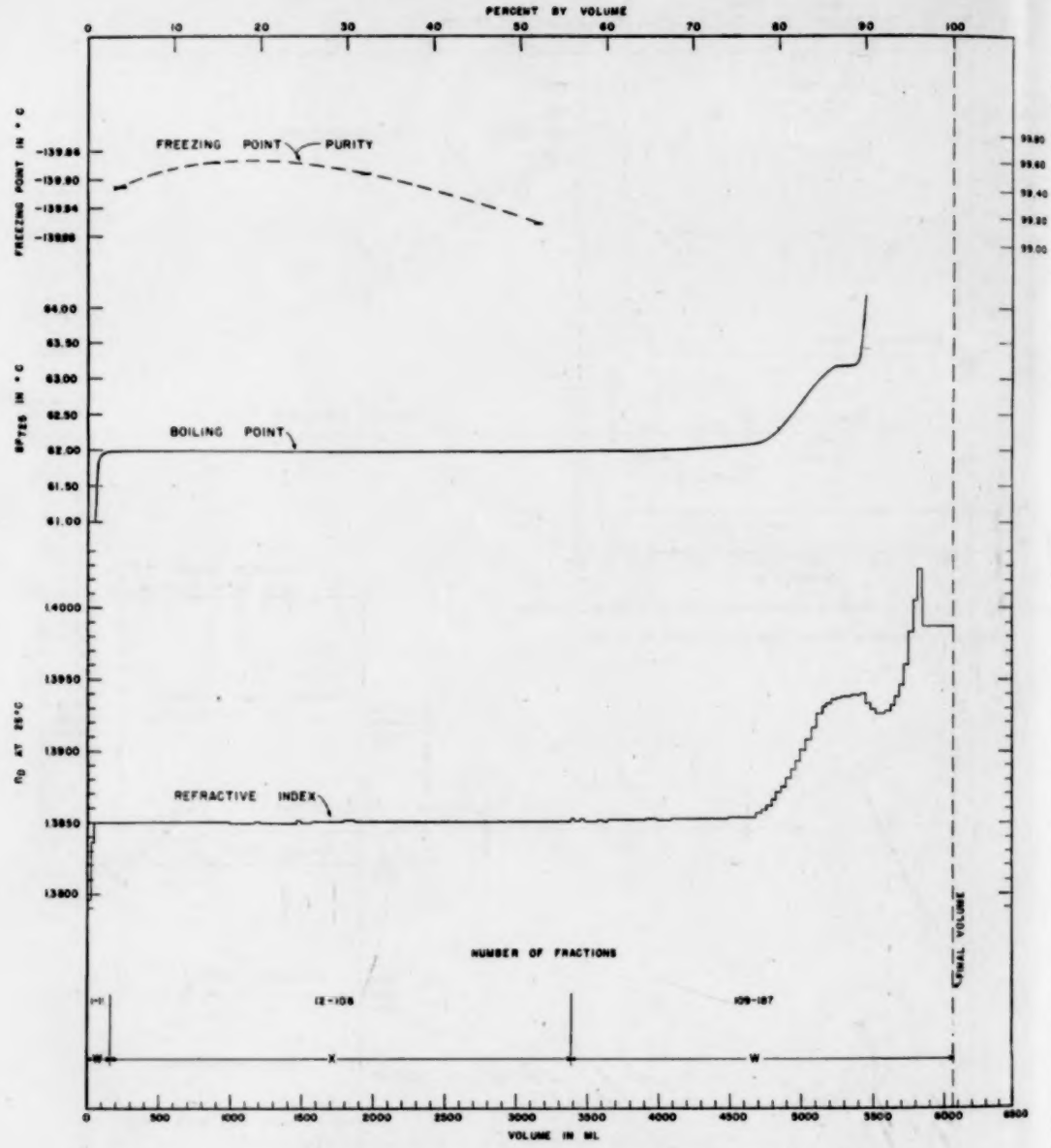

FIGURE 40. *Results of the first distillation of a second lot of 1-hexene.*

Regular distillation at 725 mm Hg in Still 13 (12/9/46 to 1/20/47)

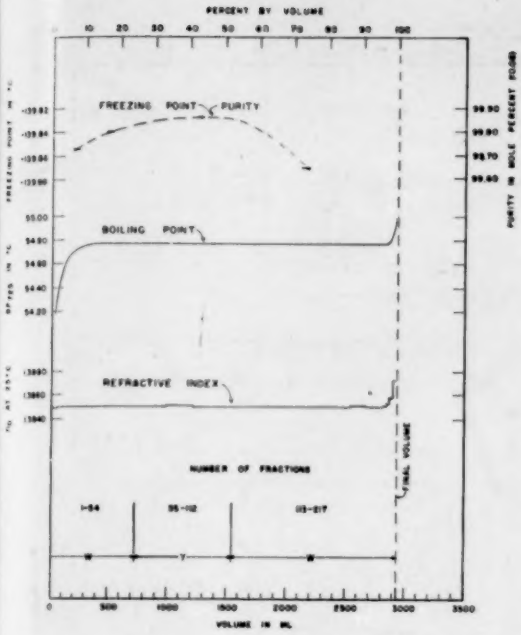

FIGURE 41. *Results of the second and final distillation of the second lot of 1-hexene.*

Azeotropic distillation with ethanol at 725 mm Hg in Still 9 (2/11/47 to 3/3/47). See footnote r of table 1.

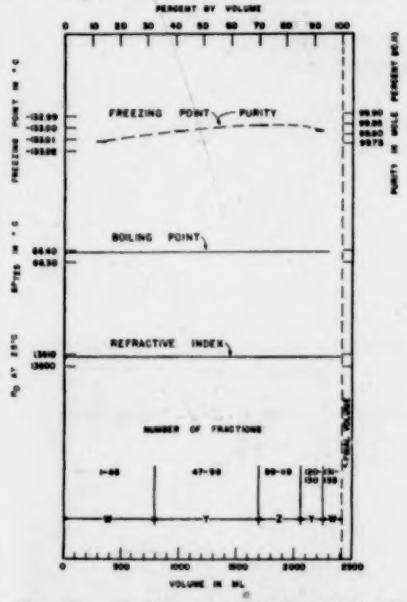

FIGURE 43. *Results of the second and final distillation of trans-2-hexene.*

Regular distillation at 725 mm Hg in Still 2A (3/13/47 to 4/7/47). See footnotes s and t of table 1.

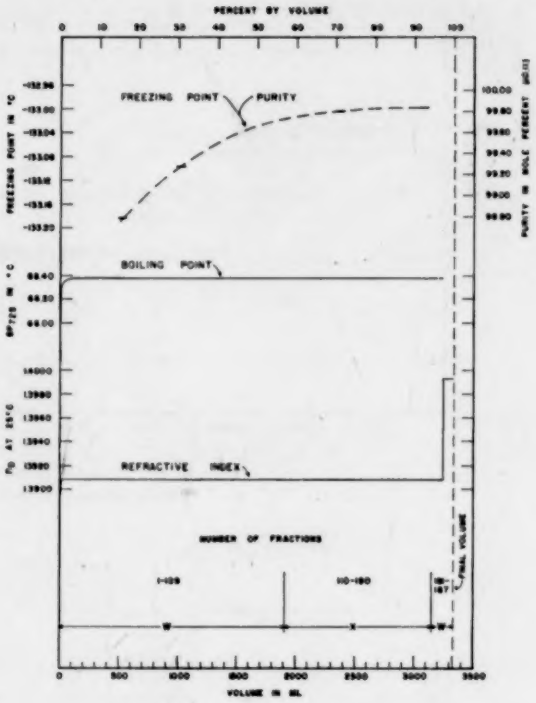

FIGURE 42. *Results of the first distillation of trans-2-hexene.*

Regular distillation at 725 mm Hg in Still 11A (12/17/46 to 1/20/47). One of two distillations of similar material.

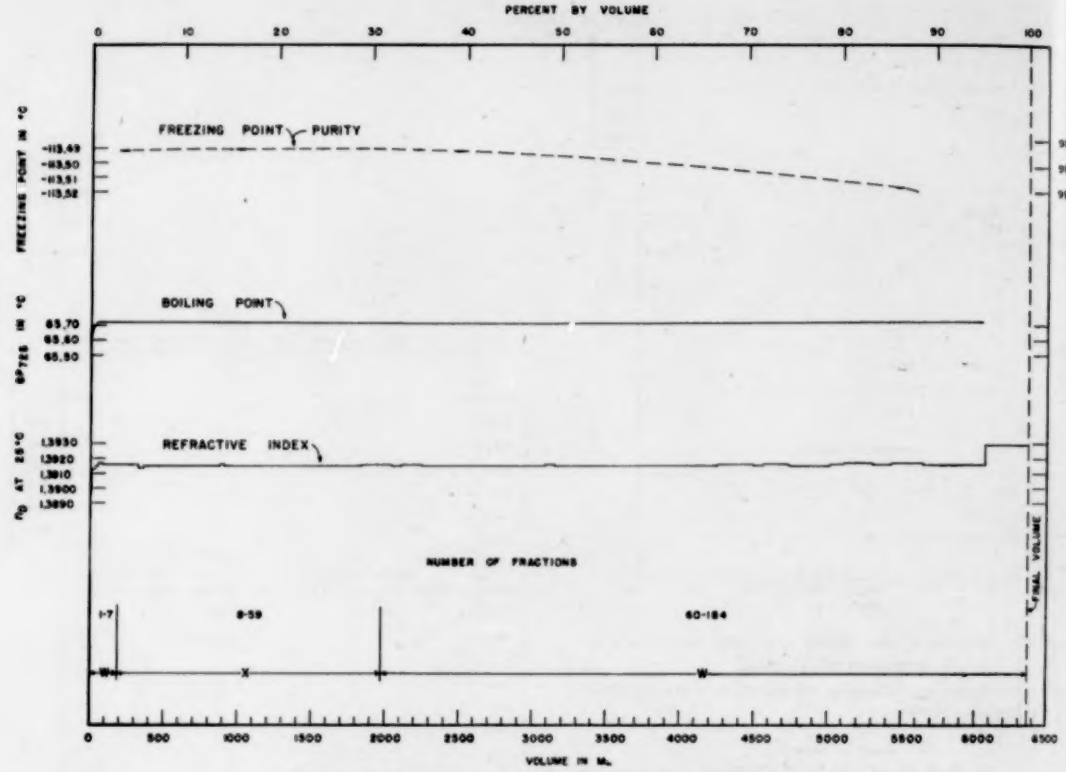

FIGURE 44. *Results of the first distillation of trans-3-hexene.*
Regular distillation at 725 mm Hg in Still 13 (7/29/46 to 9/3/46).

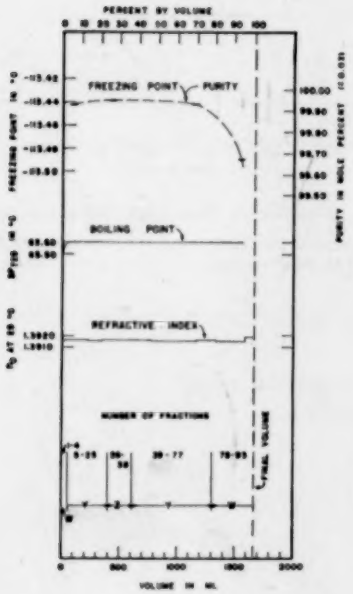

FIGURE 45. *Results of the second and final distillation of trans-3-hexene.*

Regular distillation at 725 mm Hg in Still 11A (11/27/46 to 12/16/46).

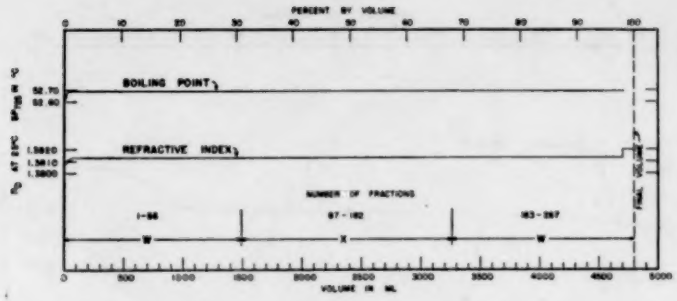

FIGURE 46. *Results of the first distillation of 3-methyl-1-pentene.*

Regular distillation at 725 mm Hg in Still 9 (11/4/46 to 12/30/46). One of two distillations of similar material. See footnote u of table 1.

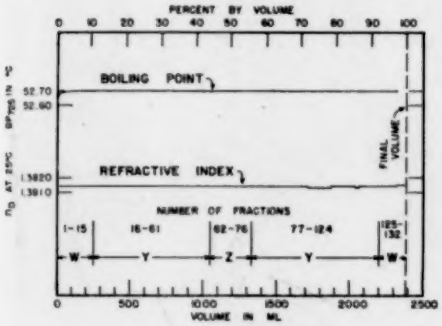

FIGURE 47. *Results of the second and final distillation of 3-methyl-1-pentene.*

Regular distillation at 725 mm Hg in Still 11A (5/20/47 to 6/16/47).

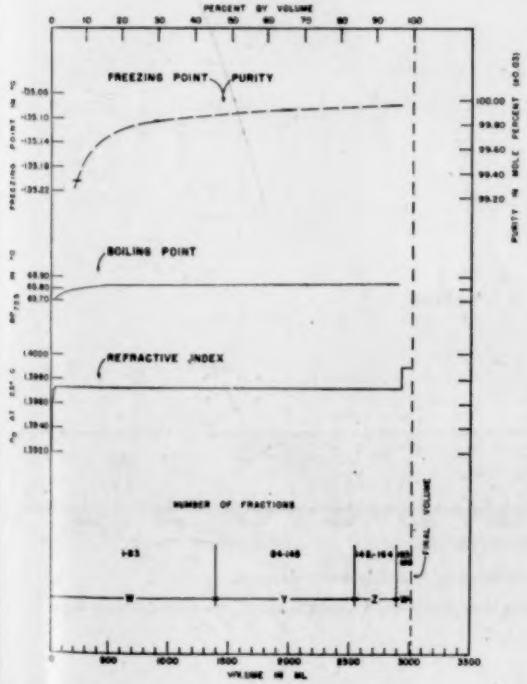

FIGURE 48. *Results of the first and only distillation of 2-methyl-2-pentene.*

Regular distillation at 725 mm Hg in Still 4 (5/28/47 to 6/26/47).

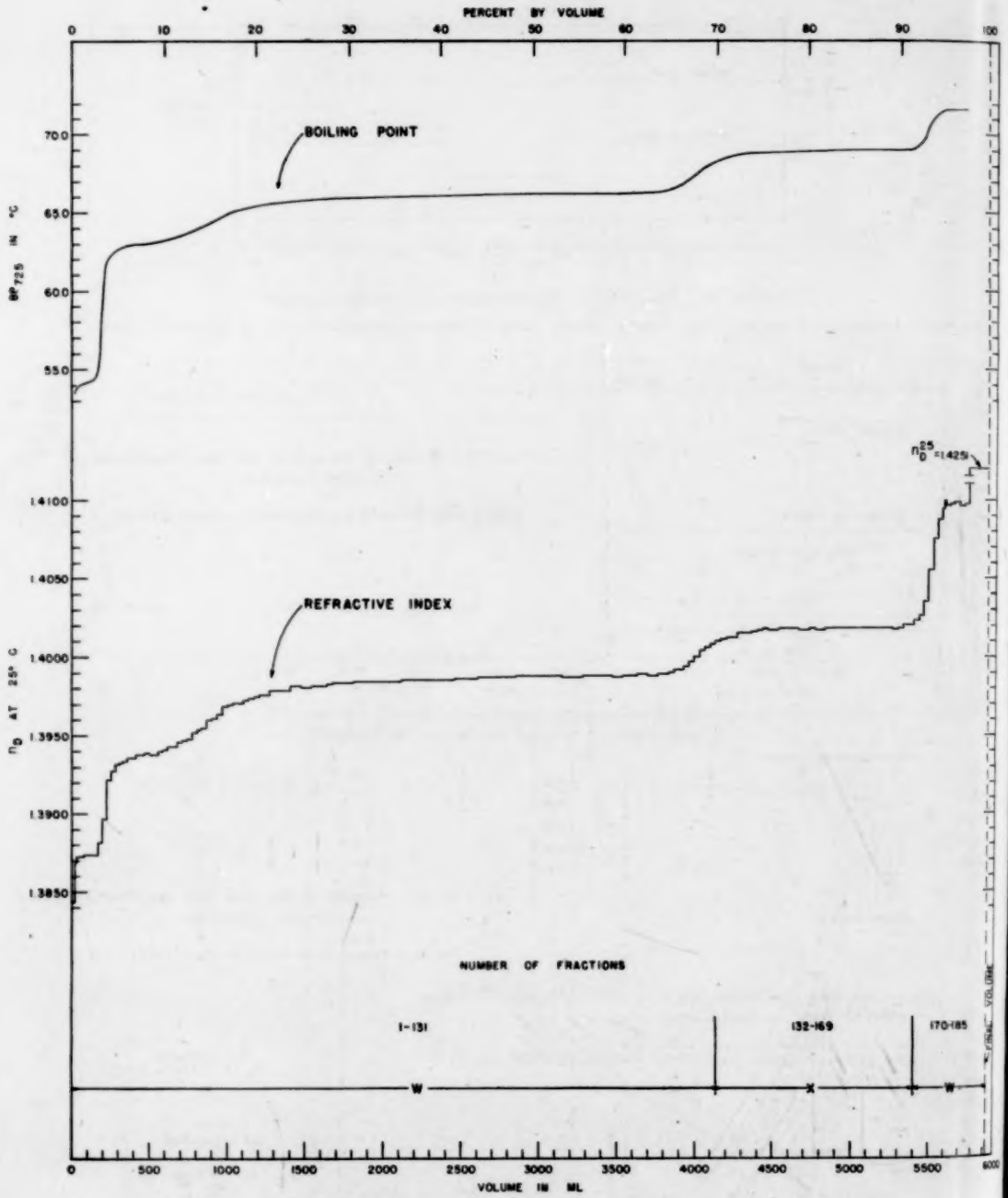

FIGURE 49. *Results of the first distillation of 3-methyl-cis-2-pentene.*

Regular distillation at 725 mm Hg in Still 8 (12/12/45 to 1/21/46). One of three distillations of similar material. See footnote w of table 1.

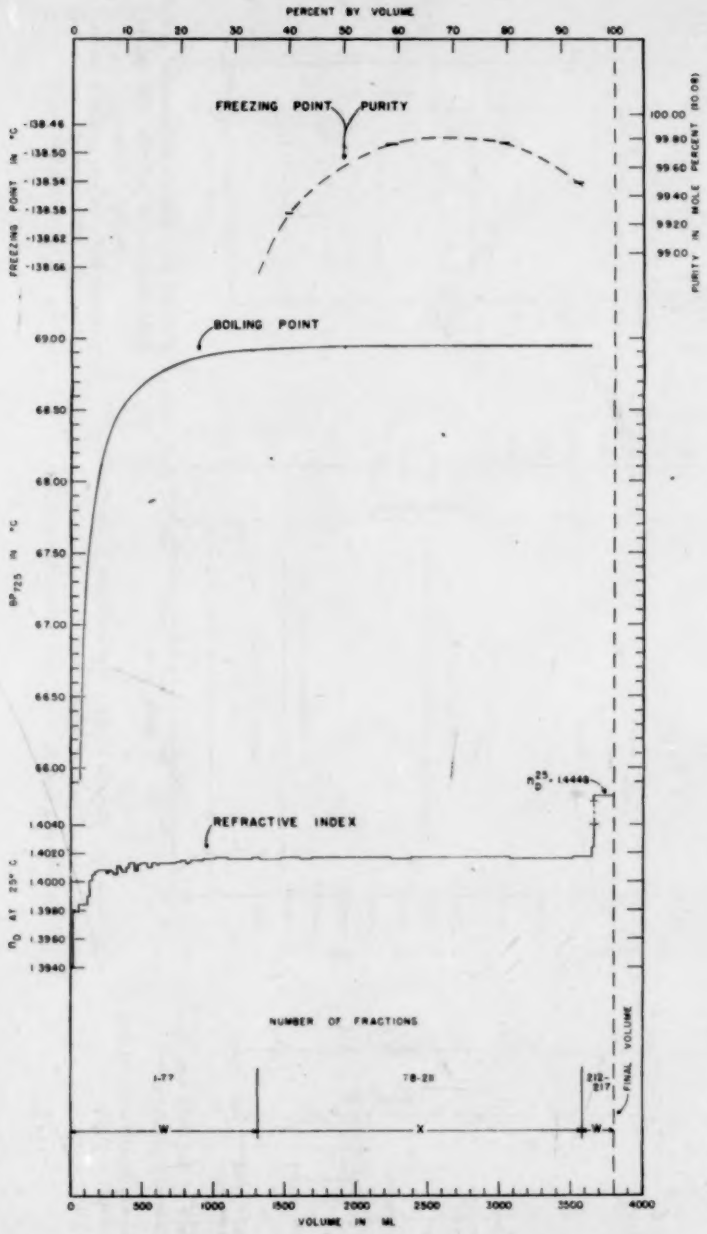

FIGURE 50. *Results of the second distillation of 3-methyl-cis-2-pentene.*
Regular distillation at 725 mm Hg in Still 2A (4/8/47 to 5/19/47). See footnotes w and x to table 1.

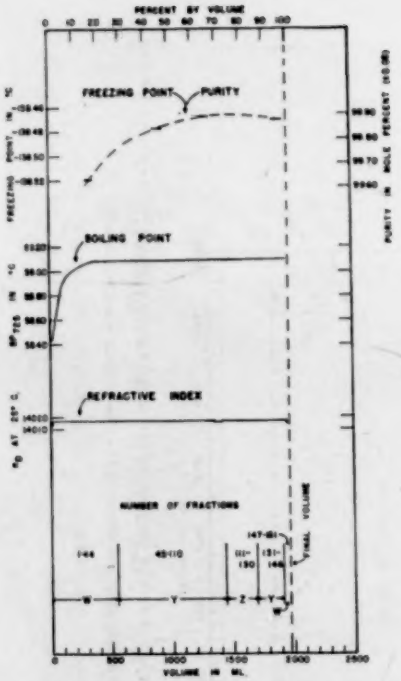

FIGURE 51. *Results of the third and final distillation of 3-methyl-cis-2-pentene.*

Azeotropic distillation with ethanol at 725 mm Hg in Still 12A (6/20/47 to 7/17/47).

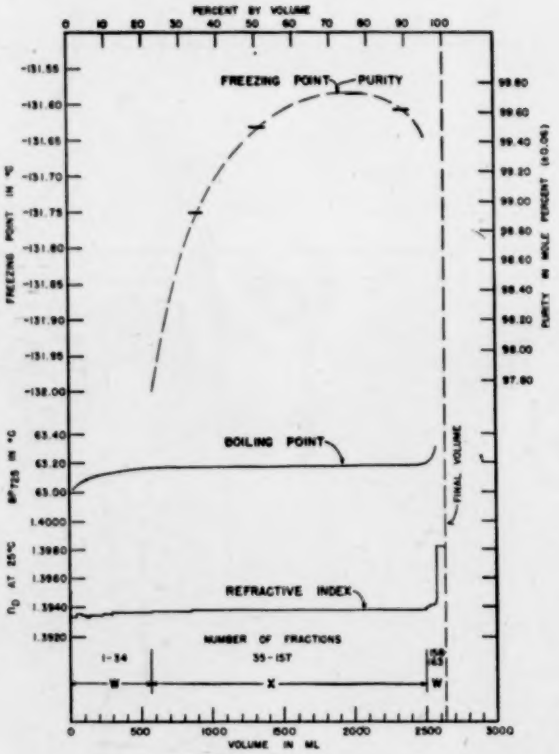

FIGURE 52. *Results of the first distillation of the first lot of 2-ethyl-1-butene.*

Regular distillation at 725 mm Hg in Still 12 (2/7/46 to 3/11/46).

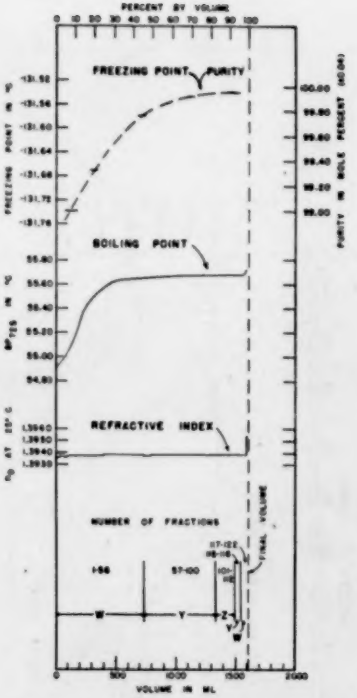

FIGURE 53. *Results of the second and final distillation of the first lot of 2-ethyl-1-butene.*

Azeotropic distillation with ethanol at 725 mm Hg in Still 3A (3/25/47 to 4/17/47). See footnotes aa and bb to table 1.

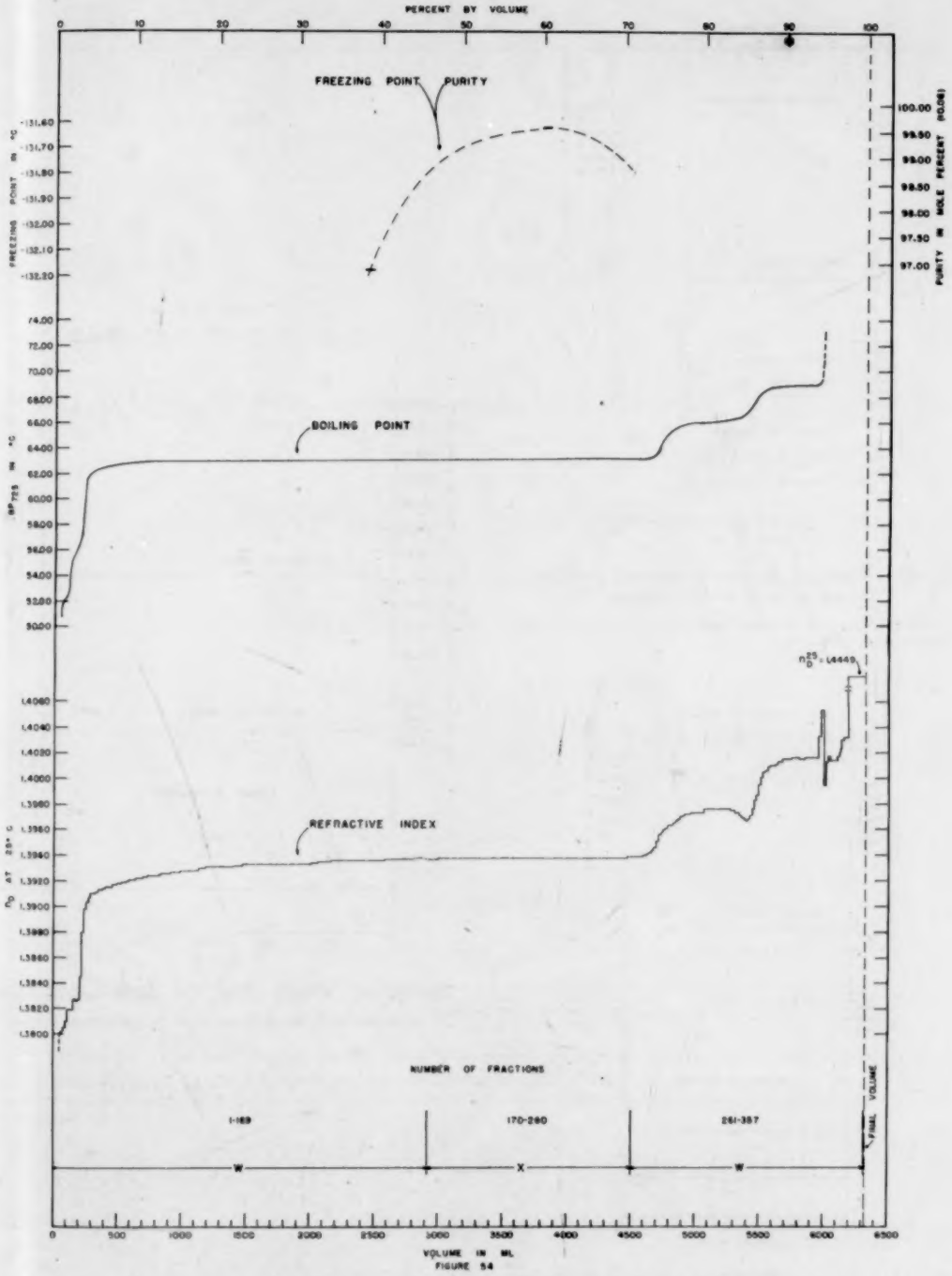

FIGURE 54. *Results of the first distillation of the second lot of 2-ethyl-1-butene.*

Regular distillation at 725 mm Hg in Still 10 (12/20/46 to 2/27/47).

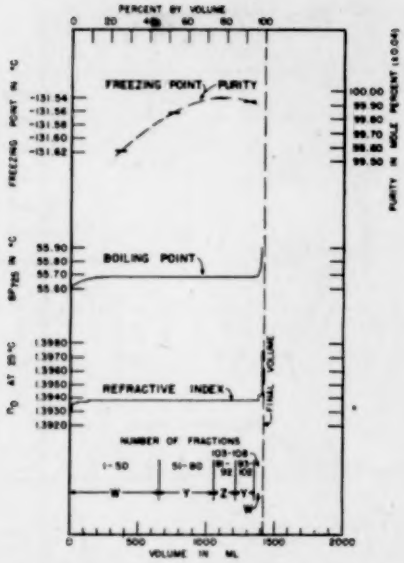

FIGURE 55. *Results of the second and final distillation of the second lot of 2-ethyl-1-butene.*

Azeotropic distillation with ethanol at 725 mm Hg in Still 4 (5/8/47 to 5/28/47.) See footnotes aa and bb to table 1.

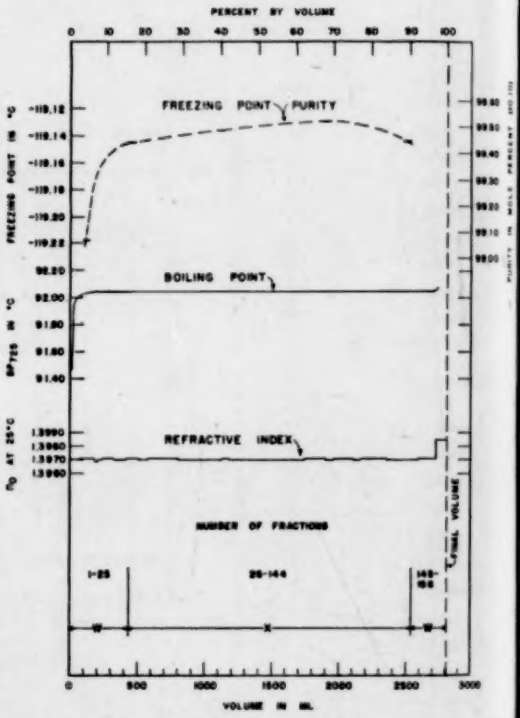

FIGURE 56. *Results of the first distillation of 1-heptene.*

Regular distillation at 725 mm Hg in Still 12 (4/30/46 to 5/31/46).

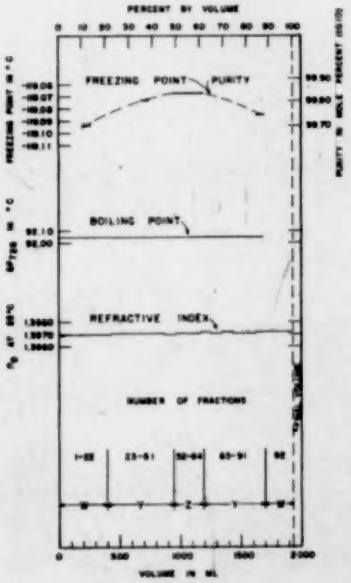

FIGURE 57. *Results of the second and final distillation of 1-heptene.*

Regular distillation at 725 mm Hg in Still 4 (12/6/46 to 12/26/46).

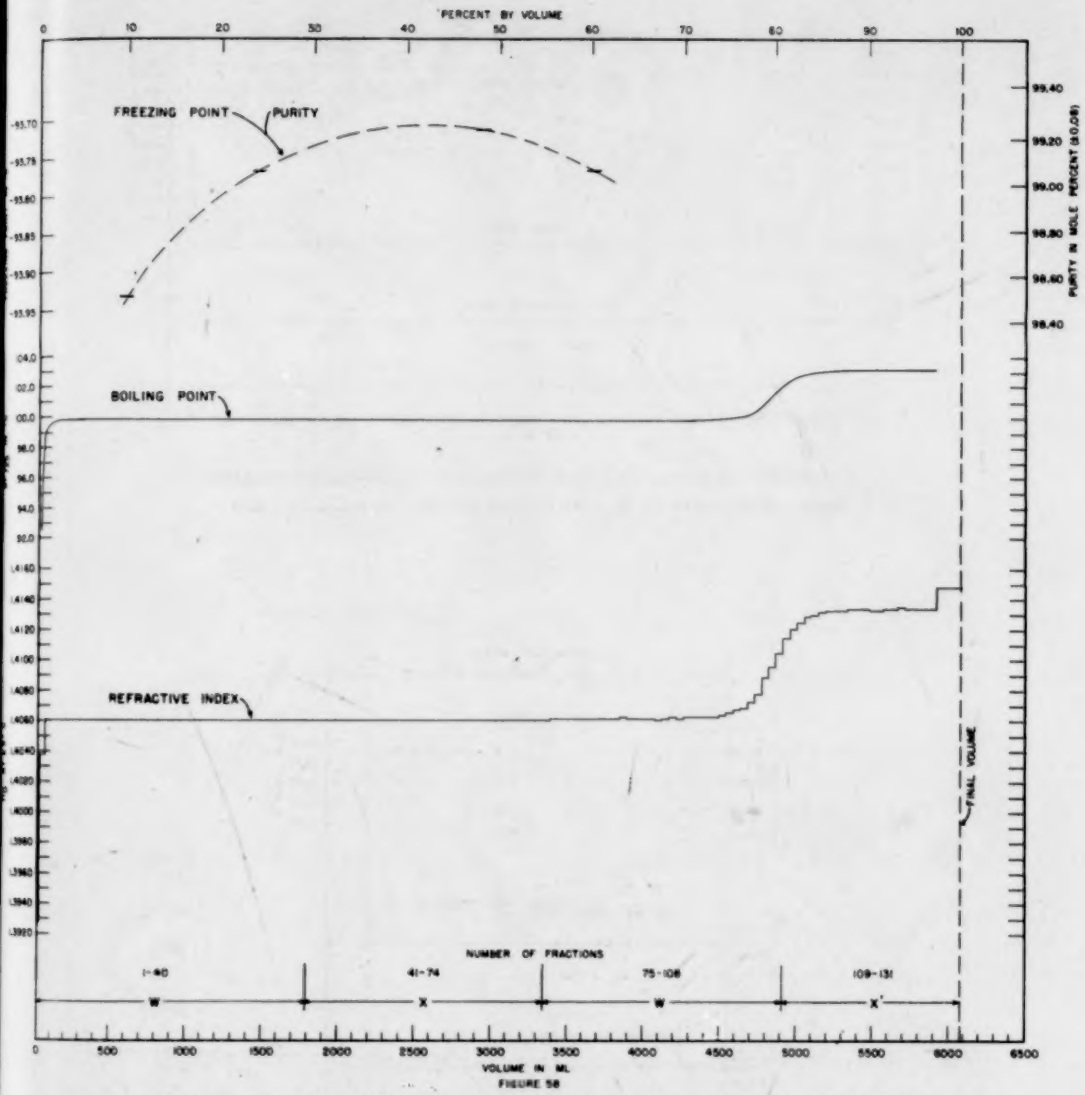

FIGURE 58

FIGURE 58. *Results of the first distribution of 2,4,4-trimethyl-1-pentene and 2,4,4-trimethyl-2-pentene.*

Regular distillation at 725 mm Hg in Still 14 (12/19/45 to 1/12/46). One of four distillations of similar material. See footnote cc of table 1. Fractions 41 to 74 (marked "x") were redistilled to obtain 2,4,4-trimethyl-1-pentene (see fig. 59). Fractions 109 to 131 (marked "x'") were redistilled to obtain 2,4,4-trimethyl-2-pentene (see fig. 61).

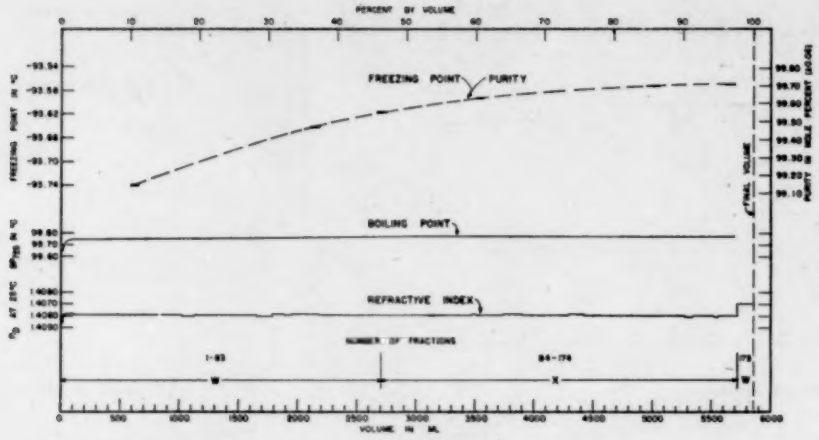

FIGURE 59. *Results of the second distillation of 2,4,4-trimethyl-1-pentene.*

Regular distillation at 725 mm Hg in Still 13 (4/16/46 to 5/20/46). See footnote dd to table 1

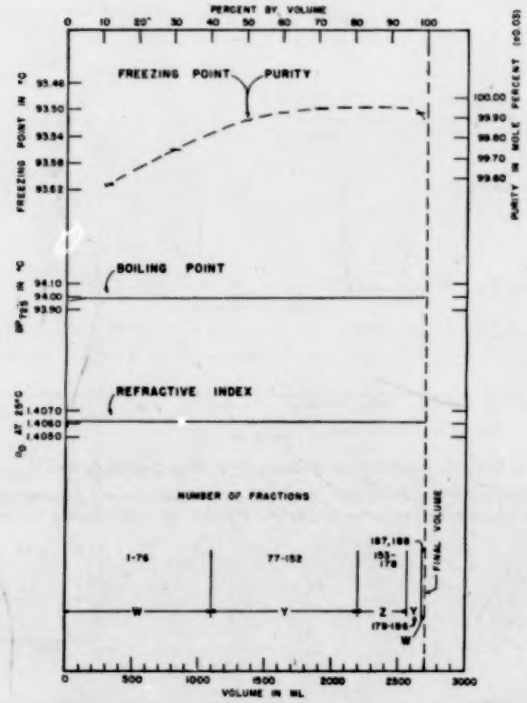

FIGURE 60. *Results of the third and final distillation of 2,4,4-trimethyl-1-pentene.*

Azeotropic distillation with ethylene glycol monomethyl ether at 725 mm Hg in Still 15A (6/26/47 to 7/30/47).

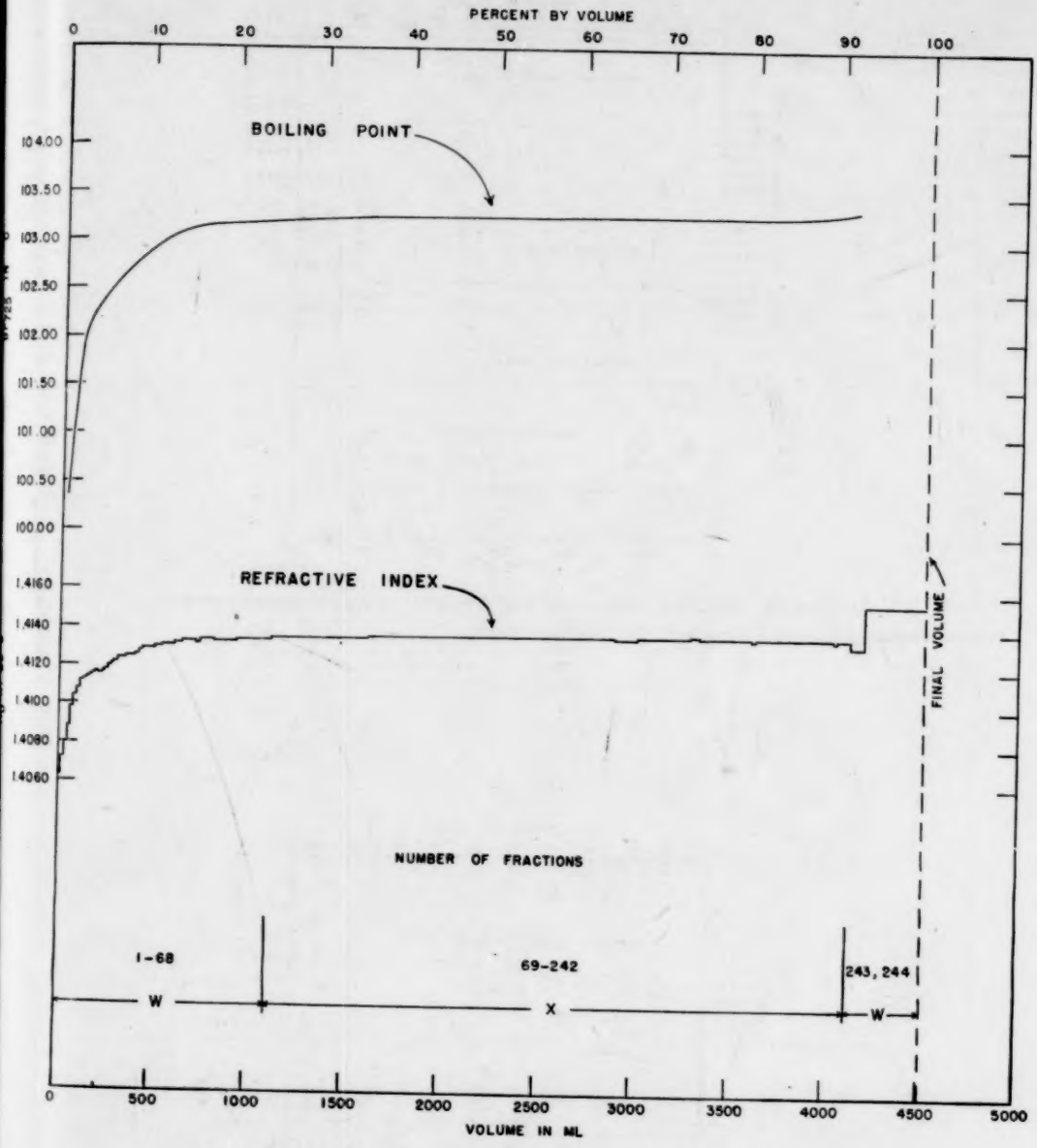

FIGURE 61. *Results of the second distillation of 2,4,4-trimethyl-2-pentene.*

Regular distillation at 725 mm Hg in Still 10 (4/16/46 to 5/31/46). See footnote dd to table 1.

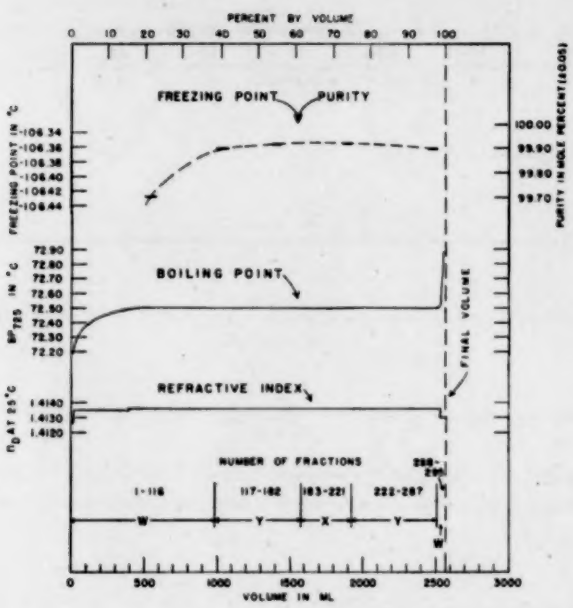

FIGURE 62. *Results of the third and final distillation of 2,4,4-trimethyl-2-pentene.*

Azeotropic distillation with ethanol at 725 mm Hg in Still 11A (6/17/47 to 8/8/47).

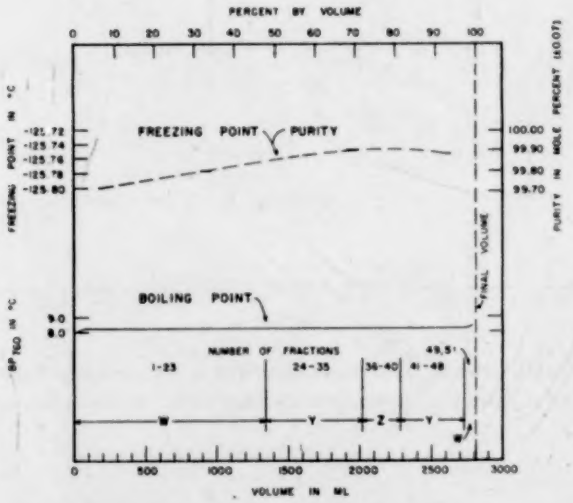

FIGURE 64. *Results of the first and only distillation of 1-butyne.*

Regular distillation at atmospheric pressure in Still 1 (9/6/45 to 11/a/45).

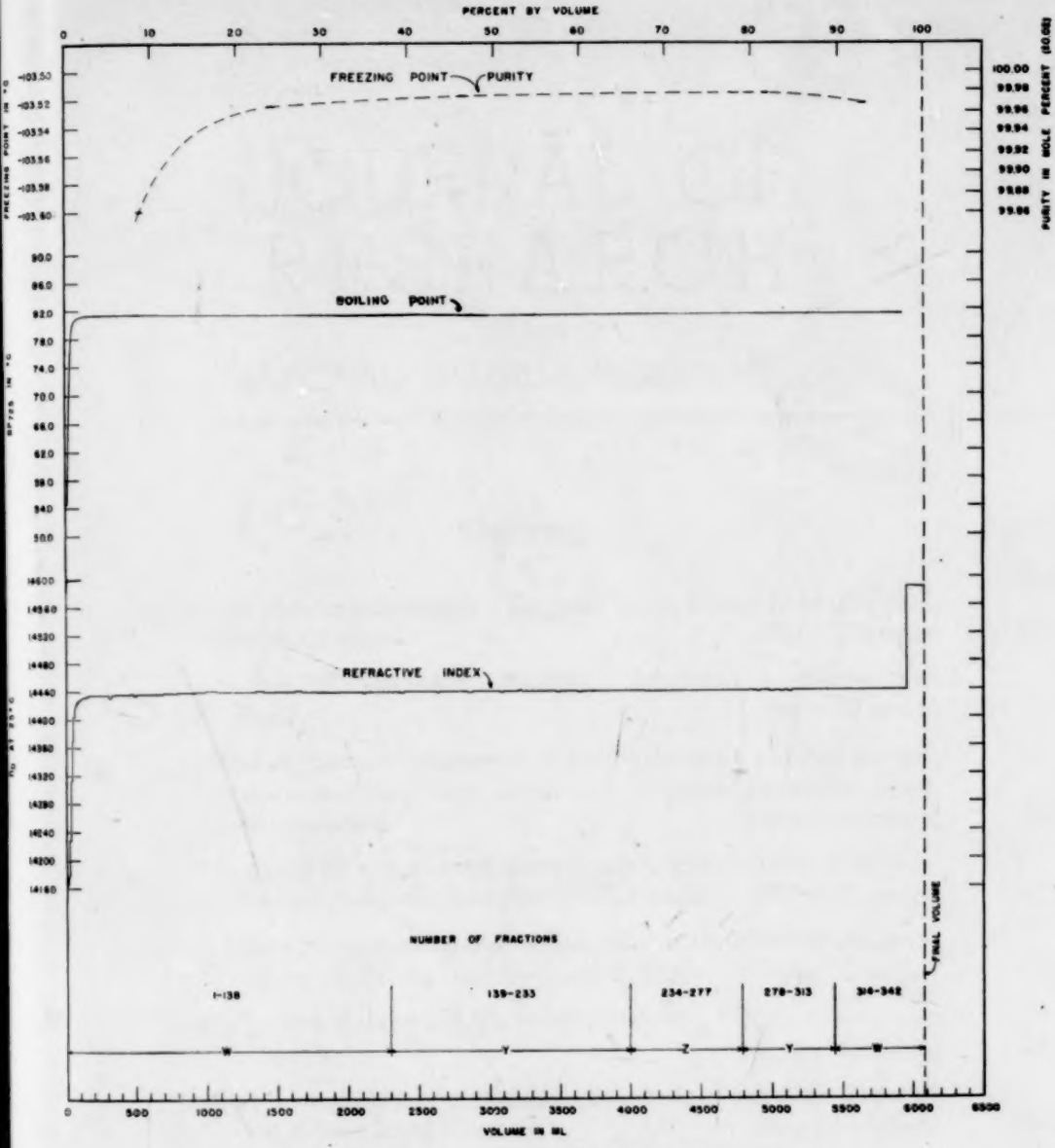

FIGURE 63. *Results of the first and only distillation of cyclohexene.*

Regular distillation at 725 mm Hg in Still 10 (10/16/46 to 12/19/46).

WASHINGTON, May 21, 1948.